

**The application of “PNP” aminodiphosphine complexes in the
oxidation of *n*-octane and styrene**

by

Dunesha Naicker

Submitted in fulfillment of the academic requirements for the degree of
Doctor of Philosophy in the
School of Chemistry,
University of KwaZulu-Natal,
Durban,
South Africa

February 2015

As the candidate’s supervisor I have approved this dissertation for submission.

Signed: _____ Date: _____
Prof. Holger B. Friedrich (Supervisor)

Abstract

The oxidation of hydrocarbons provides a cost effective method of converting cheap starting material to bulk chemicals and more importantly in the synthetic transformation to fine chemicals. Transition metals effectively catalyze these oxidation reactions. However, the use of a good ligand system is imperative in controlling the activity of the metal complexes. Aminodiphosphine or "PNP" ligands have been used extensively in ethylene oligomerisation with chromium as the active metal.

In this study six PNP ligands were synthesized and the substituent on the nitrogen atom was varied by making use of alkyl substituents such a cyclohexyl, *iso*-propyl and pentyl, as well as phenyl and substituted phenyl (chlorophenyl and methoxy phenyl) substituents. The ligands were complexed to the transition metals Co, Rh, Ir and Ru. These new bidentate complexes were fully characterized by NMR analysis, IR spectroscopy, HRMS and melting point determination. X-ray quality crystals were grown for eight of the metal complexes (all novel, R% < 10).

These complexes were then compared in the oxidation of styrene and *n*-octane. This includes the comparison of two structural types of "PNP" cobalt complexes having the cyclohexyl, *iso*-propyl and pentyl substituents on the nitrogen atom. In the oxidation of *n*-octane, the complex with the flexible ligand backbone showed higher activity. The ketones were the dominant product with highest selectivity to 2-octanone (34%). In the oxidation of styrene under optimum conditions, the complexes bearing the rigid ligand backbone were most active with good yields to benzaldehyde (25%).

In the oxidation of styrene, of the six Ir and Rh complexes investigated, the Ir complexes were slightly more active than the Rh complexes, with the complex bearing the chlorophenyl substituent on the nitrogen atom being the most active (88% conversion). Higher yields to benzaldehyde than styrene oxide were obtained. In the oxidation of *n*-octane, the ketones were the dominant product formed over both the Ir and Rh catalysts. For both studies the catalysts were recovered and reused over 3 cycles.

Ruthenium catalysts bearing the alkyl substituents were also applied in both oxidation studies. In the oxidation of styrene, > 80% conversion was obtained with a greater yield to benzaldehyde. In the oxidation of *n*-octane, the alcohols were the dominant product with good selectivity to 2 and 3-octanol (> 23%).

Preface

The experimental work described in this dissertation was carried out in the School of Chemistry, University of KwaZulu-Natal, Westville Campus, Durban, from June 2012 to February 2015, under the supervision of Prof. H. B. Friedrich.

These studies represent original work by the author and have not otherwise been submitted in any form or degree or diploma to any tertiary institution. Where use has been made of the work of others it is duly acknowledged in the text.

Dunesha Naicker

B. Sc (Honours) (UKZN-Westville Campus)

M.Sc (UKZN-Westville Campus)

Declaration - Plagiarism

I, _____ declare that

1. The research reported in this thesis, except where otherwise indicated is my original research.
2. This thesis has not been submitted for any degree or examination at any other university.
3. This thesis does not contain other persons' data, pictures, graphs or other information, unless specifically acknowledged as being sourced from other person.
4. This thesis does not contain other persons' writing, unless specifically acknowledged as being sourced from other researchers. Where other written sources have been quoted, then:
 - a. Their words have been re-written but the general information attributed to them has been referenced.
 - b. Where their exact words have been used, then their writing has been placed in italics and inside quotation marks, and referenced.
5. This thesis does not contain text, graphics or tables copied and pasted from the Internet, unless specifically acknowledged, and the source being detailed in the thesis and in the References sections.

Signed: _____

Date_____

Dunesha Naicker

Declaration – Publications

Publication 1: Cobalt aminodiphosphine complexes as catalysts in the oxidation of *n*-octane.

Dunesha Naicker, Holger B Friedrich* and Bernard Omondi

Published in RSC Advances. DOI:10.1039/C5RA07365K

Publication 2: Oxidation of styrene by TBHP using cobalt “PNP” aminodiphosphine complexes as highly effective catalysts.

Dunesha Naicker, Holger B Friedrich* and Venkata Dasireddy

In preparation for publication in Catalysis Communications.

Publication 3: Iridium and rhodium “PNP” aminodiphosphine complexes used as catalysts in the oxidation of styrene.

Dunesha Naicker, Holger B Friedrich* and Pramod B Pansuriya

Submitted for publication in RSC Advances

Publication 4: Iridium and rhodium “PNP” aminodiphosphine complexes used as catalysts in the oxidation of *n*-octane.

Dunesha Naicker, Holger B Friedrich* and Pramod B Pansuriya

Publication 5: Ruthenium “spider” complexes used as catalysts in the oxidation of *n*-octane and styrene.

Dunesha Naicker, Holger B Friedrich* and Pramod B Pansuriya

Submitted for publication in Chemistry Open.

Contribution by authors

Holger Friedrich acted as research advisor.

Bernard Omondi and Pramod Pansuriya assisted with the elucidation and interpretation of the single crystals.

I did all the experimental work as well as data collection and interpretation.

Signed: _____

Date _____

Dunesha Naicker

Conference Contributions

Part of the work discussed in this dissertation has been presented as a poster and oral in the following conferences:

Catalysis Society of South Africa (CATSA) 2012

Poster presentation: C-H activation of *n*-octane by cobalt aminodiphosphine PNP complexes.

D. Naicker and H.B Friedrich

Inorganic 2013

Oral presentation: The synthesis and characterization of “PNP” aminodiphosphine cobalt complexes and their application in the C-H activation of *n*-octane.

D. Naicker and H.B Friedrich

Catalysis Society of South Africa (CATSA) 2013

Poster presentation: The oxidation of *n*-octane by cobalt aminodiphosphine PNP complexes.

D. Naicker and H.B Friedrich

Catalysis Society of South Africa (CATSA) 2014

Oral presentation: “PNP” complexes of group 9 transition metals in the oxidation of styrene.

D. Naicker and H.B Friedrich

This thesis is dedicated to my Lordships, Shree Krishna and Shrimathi Radharani and to my parents, Mr and Mrs Naicker.

Acknowledgments

I thank God for His richest blessings, grace and for being my light in times of despair, “*for without your grace, nothing is possible*”.

My sincere thanks to my supervisor, Prof. Holger B. Friedrich for his exceptional guidance and supervision through out my postgraduate career.

I gratefully acknowledge NRF and THRIP for their financial support.

In addition, I thank the following people: Mr Dilip Jagjivan for his assistance with the NMR, Ms. Crescentia Mkosi for her efficient handling of the financial matters, Ms Unathi for help with instrumentation analysis, Mr Gregory Moodley for ensuring the availability of chemicals and solvents, Mr Miler Nundkumar for assistance with the gases.

My sincere and deepest gratitude to Dr Pramod Pansuriya, for his generosity and assistance with characterization. Dr Bernard Owaga for his assistance with crystal structures of chapter 2. Philani Mpungose for help with catalytic work. Furthermore, I take this opportunity to thank the members of the Catalysis Research Group at UKZN for their valuable input during the group meetings.

I would like to thank my dearest friends, Dr Dasireddy, Ziyaad, Shanil, Sharmini, Drushan, Nonjabulo, Dr Valand, Delon, Deveshni, Jo Anne and Kogilan for their unwavering friendship and support.

My heartfelt and endless gratitude to my parents, Mr and Mrs Naicker, for their understanding and effortless support and to my sisters, Perushni and Sushmita, for their love, care and patience.

List of Figures

Figure 1.1. Diagram of the active site of MMO derived from <i>Methylococcus capsulatus</i> (Bath).	5
Figure 1.2. The Py ₃ Ph ₂ ligand used by Chavez et al. in the oxidation of cyclohexane.	10
Figure 1.3. Tripodal 4N ligands used in the oxidation of cyclohexane and adamantan.	10
Figure 1.4. Chemical properties of C-H bonds.	15
Figure 1.5. The oxidation of isoeugenol by Cobalt SMDPT complexes in the formation of vanillin.	18
Figure 1.6. Ir Vaska complexes used in the oxidation studies.	20
Figure 1.7. Half sandwich compound used by Burlington et al. in the oxidation of styrene.	20
Figure 1.8. The ligands (1) used in this study containing the different substituents on the nitrogen atom.	22
Figure 1.9. Ligands (2) containing the ethylene spacer group between the N and P atoms, as well as different alkyl substituents on the nitrogen atom used in this study.	22
Figure 2.1. Representation of complexes 1 and 2 ; R = cyclohexyl for 1a or 2a ; n-pentyl for 1b or 2b and iso-propyl for 1c or 2c .	32
Figure 2.2. The molecular structures of complexes 2a and 2c showing part of the atom-numbering scheme. Displacement ellipsoids are drawn at 50% probability level and H atoms have been omitted for clarity.	38
Figure 2.3. Selectivity of the blank reaction (no catalyst) to products of oxidation at a ratio of 1:5 of substrate to oxidant at 80 °C in acetonitrile.	39
Figure 2.4. Conversion of <i>n</i> -octane by catalysts 1 and 2 at a ratio of 1:5 of substrate to oxidant at 80 °C in acetonitrile.	39
Figure 2.5. Selectivity of catalyst 1 to the products of oxidation at a ratio of 1:5 of substrate to oxidant at 80 °C in acetonitrile.	40
Figure 2.6. Selectivity of catalyst 2 to the products of oxidation at a ratio of 1:5 of substrate to oxidant at 80 °C in acetonitrile.	41
Figure 3.1. Complexes of type 1 and 2 used in this study as catalysts in the oxidation of styrene. (R= cyclohexyl (a); iso-propyl (b) and pentyl (c)).	47
Figure 3.2. Conversion of styrene and yield to benzaldehyde and styrene oxide.	48
Figure 3.3. Conversion of styrene over time and yield to benzaldehyde and styrene	50

oxide.	
Figure 3.4. Conversion of styrene over time and yield to benzaldehyde and styrene oxide over catalysts 1a and 2a .	51
Figure 4.1. General structure of the complexes used as catalysts in the oxidation of styrene. (M=Ir (1) and Rh (2); R= cyclohexyl (a), iso-propyl (b), pentyl (c), phenyl (d), chlorophenyl (e) and methoxyphenyl (f); Cp* = η^5 -pentamethylcyclopentadienyl).	56
Figure 4.2. 2D ^{103}Rh and ^{31}P NMR spectrum of compound 2c .	64
Figure 4.3. Structure of complexes 1f and 2f with labeling scheme. The phenyl groups of P(2) are removed/omitted for clarity.	65
Figure 4.4. Crystal packing of complexes 1f and 2f (010) along the <i>c</i> -axis.	66
Figure 4.5. Conversion of styrene over catalysts 1 and 2 in MeCN.	70
Figure 4.6. Yield to benzaldehyde and styrene oxide over catalysts 1 and 2 in MeCN.	71
Figure 4.7. ^{31}P NMR of the fresh and recovered catalysts 1c and 2c .	72
Figure 4.8. Conversion of styrene by recovered catalysts over 1c and 2c over three cycles in MeCN.	72
Figure 5.1. General structure of the complexes used as catalysts in the oxidation of <i>n</i> -octane. (M = Ir (1) and Rh (2); R = cyclohexyl (a), <i>iso</i> -propyl (b), pentyl (c), phenyl (d), chlorophenyl (e) and methoxyphenyl (f); Cp* = η^5 -pentamethylcyclopentadienyl).	78
Figure 5.2. Structure of compounds 1c , 2c and 2d with labeling scheme. The phenyl groups of P(2) are removed/omitted for clarity.	82
Figure 5.3. Crystal packing of compound 1c , 2c and 2d along the <i>c</i> -axis	85
Figure 5.4. Optimization of the substrate:oxidant ratio in the oxidation of <i>n</i> -octane.	88
Figure 5.5. Optimization of temperature in the oxidation of <i>n</i> -octane.	89
Figure 5.6. Screening of the iridium (1) and rhodium (2) catalysts with the different substituents on the nitrogen atom (a-f).	89
Figure 5.7. Selectivity to the products of oxidation of <i>n</i> -octane by the Ir (1) catalysts.	90
Figure 5.8. Selectivity to the products of oxidation of <i>n</i> -octane by the Rh (2) catalysts.	91
Figure 5.9. Recyclability testing of catalysts 1c and 2c in the oxidation of <i>n</i> -octane.	93
Figure 5.10. Recyclability testing of catalysts 1c - selectivity to the products of oxidation.	93
Figure 5.11. Recyclability testing of catalysts 2c - selectivity to the products of	94

oxidation.

Figure 5.12. ^{31}P NMR of the fresh and recovered catalysts 1c and 2c .	94
Figure 6.1. Ruthenium complexes bearing the PNP ligand backbone used in this study (R = cyclohexyl (a); <i>iso</i> -propyl (b) and pentyl (c)).	102
Figure 6.2. Structure of compound a with selected atom labeling scheme. The phenyl groups of P1, P2, P1a and P2a are removed/omitted for clarity.	107
Figure 6.3. Crystal packing of compound a along the <i>c</i> -axis.	109
Figure 6.4. Selectivity to the products of oxidation of the blank reaction (no catalyst) at a substrate:oxidant molar ratio of 1:5.	111
Figure 6.5. Conversion of <i>n</i> -octane by catalysts a-c .	112
Figure 6.6. Selectivity to products of oxidation of <i>n</i> -octane by catalysts a-c .	112
Figure 6.7. Conversion of styrene and reaction rate using catalyst a at room temperature, 50 °C and 80 °C.	114
Figure 6.8. Selectivity to benzaldehyde at room temperature, 50 °C and 80 °C.	114
Figure 6.9. UV spectrum of catalyst b with oxidant and without oxidant.	116
Figure 6.10. ^{31}P NMR of fresh and recovered catalyst a after styrene oxidation.	116

List of Tables

Table 2.1. Crystal data and structure refinement for complexes 2a and 2c .	35
Table 2.2. Comaprison of the $\nu_{\text{P-N}}$ band shifts of complexes 1 and their respective ligands.	37
Table 2.3. Selected bond lengths (\AA) and angles ($^{\circ}$) for complexes 2a and 2c .	37
Table 2.4. Selectivity parameters in the oxidation of <i>n</i> -octane by catalysts 1 and 2 .	41
Table 3.1. Oxidation of styrene using H_2O_2 at 50 $^{\circ}\text{C}$ and 80 $^{\circ}\text{C}$.	49
Table 3.2. Screening of catalysts 1 and 2 at optimized conditions.	51
Table 4.1. Single crystal structural information of complexes 1f and 2f .	62
Table 4.2. Selected bond lengths (\AA) and bond angles ($^{\circ}$) of complexes 1f and 2f .	66
Table 4.3. Non-classical hydrogen C—H...O bonding and C—H...F interactions of complexes 1f and 2f .	67
Table 4.4. C-H...Cg interactions of complexes 1f and 2f .	67
Table 4.5. $\pi \dots \pi$ interactions of complexes 1f and 2f .	68
Table 4.6. Turnover number for catalysts 1 and 2 towards benzaldehyde and styrene oxide.	71
Table 5.1. Single crystal structural information of complexes 1c and 2c and 2d .	80
Table 5.2. Selected bond lengths (\AA) and bond angles ($^{\circ}$) of complexes 1c , 2c and 2d .	83
Table 5.3. Non-classical hydrogen C—H...X interactions of complexes 1c , 2c and 2d .	86
Table 5.4. X-Y...Cg interactions of complexes 1c , 2c and 2d .	86
Table 5.5. $\pi \dots \pi$ interactions of complexes 2c and 2d .	87
Table 5.6. Selectivity parameters by Ir and Rh catalysts in the oxidation of <i>n</i> -octane.	92
Table 6.1. Single crystal structural information of complexes a .	105
Table 6.2. Selected bond lengths (\AA) and bond angles ($^{\circ}$) of complex a .	108
Table 6.3. Non-classical hydrogen C—H...O, C—H...Cl and C—H...Cg interactions of the complex [110].	109
Table 6.4. $\pi \dots \pi$ interactions of the complex.	110
Table 6.5. Selectivity parameters in the oxidation of <i>n</i> -octane by catalysts a-c .	113
Table 6.6. Catalytic results of catalysts a-c under optimum conditions.	115

List of Schemes

Scheme 1.1. Oxidation of alkanes by cytochrome P450.	4
Scheme 1.2. The difference between activation by transition metals (A) and that occurring via radical or electrophilic routes (B).	7
Scheme 1.3. The relationship between bond strength and selectivity as well as reactivity, where primary C–H bonds exhibit greatest selectivity and lowest reactivity in comparison to their tertiary counterparts.	8
Scheme 1.4. Proposed mechanisms of olefin oxidation to form epoxides (a and b) and ketones and aldehyde (c and d).	17
Scheme 3.1. Proposed mechanism for the oxidation of styrene by catalysts 1 and 2 , (L=Ligand).	52
Scheme 4.1. Proposed mechanism for the oxidation of styrene by complexes 1 and 2 .	74

Abbreviations

ATR	= Attenuated total reflection
asym.	= Asymmetric
bza	= Benzaldehyde
C-H	= Carbon-Hydrogen bond
Calcd	= Calculated
Cp	= Cyclopentadiene
Cp*	= η^5 - pentamethylcyclopentadienyl
Cy	=cyclohexyl
d	= Doublet
DCE	= 1,2 Dichloroethane
DCM	= Dichloromethane
eqn	= Equation
ESI	= Electron spray ionization
Et ₃ N	= Triethylamine
EtOH	= Ethanol
FID	=Flame ionization detector
FT-IR	= Fourier Transform-Infrared
g	= Gram
GC	= Gas Chromatography
H ₂ O ₂	= Hydrogen peroxide
HRMS	= High resolution mass spectroscopy
Hz	= Hertz
J	= Coupling constant
Kcal/mol	= Kilocalories per mole
L	= Ligand
l	= Liter
M	= Metal
m	= Multiplet
<i>m</i>	= Medium
mCPBA	= metachloroperoxybenzoic acid
MHz	= Megahertz
MeCN	= Acetonitrile
MeOH	= Methanol
min	= Minute

ml	= Milliliter (10^{-3} liter)
mmol	= Millimolar
MMO	= Methane monooxygenase
mol	= Moles
Mp	= Melting point
mV	= Millivolts
MW	= Molecular weight
N	= Nitrogen
NMO	= <i>N</i> -methylmorpholine <i>N</i> oxide
NMR	= Nuclear magnetic resonance
ODH	= Oxidative Dehydrogenation
P	= Phosphorous
Ph	= Phenyl
PhIO	= Iodosyl benzene
PNP	= Aminodiphosphine
ppm	= Parts per million
por	= Porphyrin
qui	= Quintet
rt	= Room temperature
s	= Strong
sym.	= Symmetric
t	= Triplet
TBA	= <i>tert</i> - butyl ethylene
TBHP	= <i>Tert</i> -butyl hydroperoxide
<i>t</i> -BuOH	= <i>Tert</i> -butanol
<i>t</i> -BuOOH	= <i>Tert</i> -butyl hydroperoxide
THF	= Tetrahydrofuran
TGA	= Thermal gravimetric analysis
TOF	= Turnover frequency
TON	= Turnover number
w	= weak
XRD	= X-ray diffraction
μl	= Microliter (10^{-6} liter)

Contents

Title	i
Abstract	ii
Preface	iii
Declaration-Plagiarism	iv
Declaration-Publications	v
Conference contributions	vi
Acknowledgments	viii
List of figures	ix
List of tables	xii
List of schemes	xiii
Abbreviations	xiv
Contents	xvi

Chapter One.....	1
Literature review	
Oxidation: The route to some value added products	
1.1 Introduction	1
1.2 Alkane oxidation	2
1.2.1 Factors affecting alkane oxidation.....	6
1.2.2 Oxidation of alkanes by group nine transition metals	8
1.2.2.1 Cobalt	9
1.2.2.2 Rhodium	11
1.2.2.3 Iridium	12
1.3 Styrene epoxidation	13
1.3.1 Mechanism of olefin oxidation.....	15
1.3.2 Oxidation of styrene by group nine transition metals	17
1.3.2.1 Co, Rh and Ir	18
1.4 Conclusion.....	20
1.5 Aim of study.....	21
1.6 References	26

Chapter Two	31
Cobalt “PNP” aminodiphosphine complexes as catalysts in the oxidation of <i>n</i>-octane	
2.1 Abstract.....	31
2.2 Introduction	31
2.3 Experimental.....	33
2.3.1 Synthesis and characterization of the compounds.....	33
2.3.2 Crystal structure analysis.....	34
2.3.3 Oxidation of <i>n</i> -octane	36
2.4 Results and Discussion.....	36
2.4.1 Synthesis and characterization of the compounds.....	36
2.4.2 Description of the X-ray crystal structures.....	37
2.4.3 Oxidation of <i>n</i> -octane	38
2.5 Conclusion.....	43
2.6 References	43
Chapter Three.....	46
Oxidation of styrene by TBHP using cobalt “PNP” aminodiphosphine complexes as highly effective catalysts	
3.1 Abstract.....	46
3.2 Introduction	46
3.3 Experimental.....	47
3.3.1 Oxidation of styrene	47
3.4 Results and discussion.....	48
3.5 Conclusion.....	53
3.6 References	53
Chapter 4.....	55
Iridium and rhodium “PNP” aminodiphosphine complexes used as catalysts in the oxidation of styrene	
4.1 Abstract.....	55
4.2 Introduction	55
4.3 Experimental.....	57
4.3.1 Synthesis and characterization of compounds.....	57
4.3.2 Crystal structure analysis.....	61
4.3.3 Oxidation of styrene	61
4.4 Results and Discussion.....	63

4.4.1 Synthesis and characterization of the compounds.....	63
4.4.2 Description of crystal structures.....	64
4.4.3 Oxidation of styrene	69
4.5 Conclusion.....	74
4.6 References	75
Chapter Five.....	77
Iridium and rhodium “PNP” aminodiphosphine complexes used as catalysts in the oxidation of <i>n</i>-octane	
5.1 Abstract.....	77
5.2 Introduction	77
5.3 Experimental.....	79
5.3.1 Crystal structure analysis.....	79
5.3.2 Oxidation of <i>n</i> -octane	81
5.4 Results and discussion.....	81
5.4.1 Description of crystal structures.....	81
5.4.2 Oxidation of <i>n</i> -octane	88
5.5 Conclusion.....	95
5.6 References	96
Chapter Six.....	100
Ruthenium “spider” complexes used as catalysts in the oxidation of <i>n</i>-octane and styrene	
6.1 Abstract.....	100
6.2 Introduction	100
6.3 Experimental.....	102
6.3.1 Synthesis and characterization of the compounds.....	102
6.3.2 Crystal structure analysis.....	104
6.3.3 Oxidation studies	106
6.4 Results and discussion	106
6.4.1 Synthesis and characterization of the compounds.....	106
6.4.2 Description of crystal structures.....	107
6.4.3 Oxidation of <i>n</i> -octane	110
6.4.4 Oxidation of styrene	113
6.5 Conclusion.....	116
6.6 References	117

Chapter Seven.....	120
Summary	
Appendix A.....	123
Appendix B.....	151
Appendix C.....	219
Appendix D.....	247

Chapter One

Literature review

Oxidation: The route to some value added products

1.1 Introduction

One of the major processes in converting organic compounds into useful chemicals such as diols, epoxides, alcohols and carbonyl compounds is catalytic oxidation.¹⁻⁴ For example, large scale chemicals such as ethylene oxide, styrene and maleic anhydride are produced via the oxidative route, where the latter is made via the heterogeneous oxidation of butane with vanadyl phosphate as the catalyst.⁵ There is a great demand for more effective and enhanced catalytic routes.⁵ In homogenous catalysis, the development of an efficient method for the selective oxidation of C-H bonds of either a single substrate or within a group of substrates continues to be a challenging task, as this could lead to the development of new industrial methods.⁶⁻¹² The C-H bonds are unstable to reactive oxygen compounds leading to free radical chain reaction by the attack by oxygen-centered species, which often makes controlling of the selectivity rather difficult.^{5,8} This often leads to low selectivity, which is characteristic of oxidation of hydrocarbons on a large industrial scale.⁵ This calls for the development of efficient precious metal catalysts, since the metal, in most cases, serves to generate the reactive oxygen radical which initiates the radical chain oxidation reaction.^{5,13} The activation of C-H bonds by transition metals dates back to 1800's and was revolutionized by Shilov in 1972 with the selective alkane functionalization of methane to methanol and methyl chloride using a platinum catalyst.¹⁴ Transition metal complexes are used as catalysts in a variety of organic reactions and have been identified as homogenous catalysts showing high reproducibility and activity, homogeneity and selectivity under mild conditions.¹⁰ However, problems such as separation, contamination of reaction products and corrosion are amongst many faced by homogenous catalysts.¹⁰ These catalysts are of particular significance as most of the industrial oxidations take place in the presence of a homogenous catalyst.¹⁰

At this point it is wise to make the distinction between activation and functionalization. As Crabtree simply puts it, activation is the point when the substrate binds to the metal center, followed by the cleavage of the bond via oxidative addition.¹⁵ Functionalization refers to the alteration of the substrate and regeneration of the metal species, which results in a catalytic cycle.¹⁵ This usually occurs through an intermediate step, however, functionalization has

proved to be more tedious than activation.¹⁶ The principal behind activation is to replace the strong C-H bond by a functionalized weaker bond.³

This review highlights the oxidation of alkanes (linear and cycloalkanes) and olefins, in particular styrene, by group 9 transition metals. Attention is drawn to substrates and transition metals discussed in the dissertation.

1.2 Alkane oxidation

Saturated hydrocarbons are relatively abundant, cheap and are the main components of natural gas and oil.^{7,17,18} In addition, they serve as carbon raw materials in the production of value added chemicals.¹⁷ However, their broad synthetic uses are limited due to their inertness. Current petrochemical technologies make use of power consuming processes that operate at high temperatures and pressures and utilize a number of steps, such as dehydrogenation, cracking, or reforming.^{17,19,20} The ongoing challenge is the development of atom efficient and mild, selective, direct oxidation of unsaturated sp³ C-H bonds into a mixture of alkyl peroxides, alcohols and ketones which are then transformed to more valuable ketones and aldehydes, that could lead to a paradigm shift in the petrochemical industry.^{7,9,11,15,21-23} This would make way for a system that is environmentally cleaner and economically superior.¹⁹

At elevated temperatures, alkanes react quite easily, as in combustion.²⁴ However, these reactions are uncontrollable and lead to the formation of unwanted products such as water and carbon dioxide.²⁴

Heterogeneous catalytic activation of alkanes is on the rise, with the increase in the number of gas to liquid plants worldwide.²⁵⁻²⁷ Processes such as cracking and oxidative dehydrogenation are one of the major sources of olefins.²⁸ “Oxidative dehydrogenation (ODH) involves the removal of hydrogen from the reactant molecules, by oxygen of the feed, to form the corresponding olefins without parallel or consecutive oxidation reactions giving carbon monoxide or dioxide as non-selective products.”²⁹ Studies have been undertaken with vanadium-based catalysts (VMgO) in the ODH of shorter alkanes giving rise to the corresponding olefins and dienes.^{25-28,30}

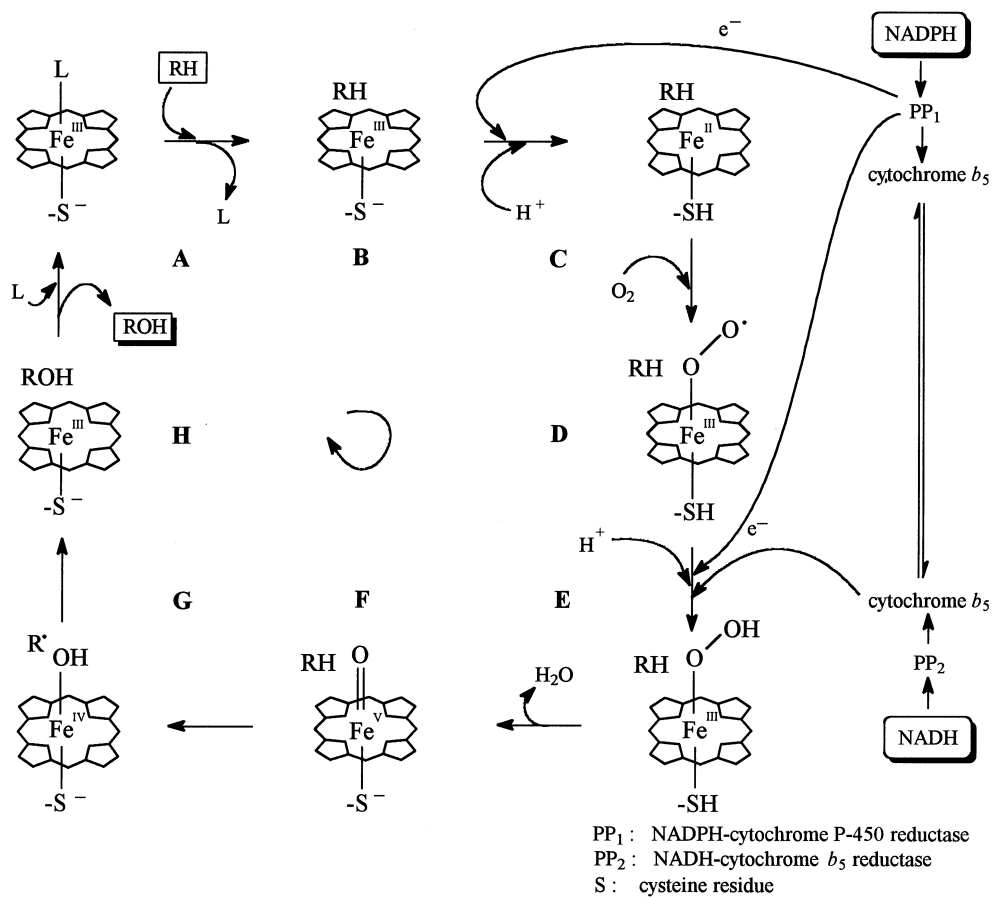
The ODH of alkanes has been of interest to many researchers due to the following reasons suggested by Cavani and co-workers.²⁸

- i. Ethylene is the preferred product over propylene (product in demand), which is observed in cracking, and thus it does not satisfy the market demand for the desired olefins.
- ii. The oxygen in ODH counteracts catalyst deactivation which is brought upon in coking. Furthermore in degydrogenation, thermodynamic constraints limit alkane conversion.
- iii. ODH is exothermic which improves energy efficiency, whilst cracking and dehydrogenation are endothermic.

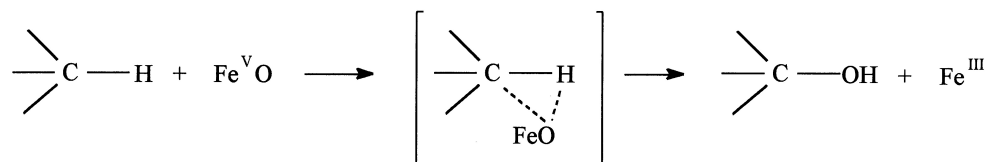
Cracking is defined as “the treatment of hydrocarbons over solid catalysts at temperatures above about 300 °C for the production of hydrocarbon materials of lower average molecular weight”.³¹ Conventional processes such as steam cracking, fluid cracking, deep catalytic cracking and thermal catalytic cracking (which is more environmentally friendly) lead to the formation of plastic materials, synthetic fibers and rubbers.³² Studies carried out over mixed metal oxides MoO₃-CeO₂ impregnated on silica-alumina surface in the thermal catalytic cracking of *n*-hexane resulted in the formation of light olefins, whilst the unsupported catalyst causes the formation of aromatics.³² In the petroleum industry, cracking has become a useful application, for the conversion of heavy oils, and the acid treated solid catalysts usually include clays (montmorillonite) and solid oxides (combination of alumina and silica).^{31,33}

Enzymatic alkane activation has been widely explored, since they are able to selectively catalyze the oxidation of alkanes at physiological temperatures and pressures. Numerous studies have been undertaken in trying to understand the efficiency and selectivity, as well as the mechanistic pathways of enzymatic paraffin activation.^{3,16,24} Cytochrome P450 or P450-I, which consist of an iron oxo species and a delocalized oxidizing group over the thiolate and porphyrin ligands is capable of selectively controlling the oxidation of alkanes by making use of dioxygen and molecular hydrogen.^{34,35} The oxidation of alkanes by cytochrome P450 by dioxygen includes eight steps (Scheme 1.1).³ First, the low-spin cytochrome P450 A is converted to the high spin form B. This is followed by reduction, after which the coordination of dioxygen to iron(II) occurs. Thereafter, the formation of an oxenoid, F, occurs via reduction of the complex and elimination of a water molecule, which is followed by the cleavage of the C-H bond in the substrate molecule. Cleavage may occur by two mechanisms, the oxenoid and the “rebound” radical mechanism. The former includes direct

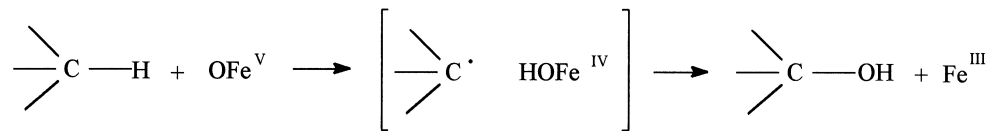
insertion of the oxygen atom, whilst the latter is a more widely accepted scheme. This involves a radical C-H bond cleavage with recombination in the cage.³



The oxenoid mechanism:



The "rebound" radical mechanism:



Scheme 1.1. Oxidation of alkanes by cytochrome P450.³

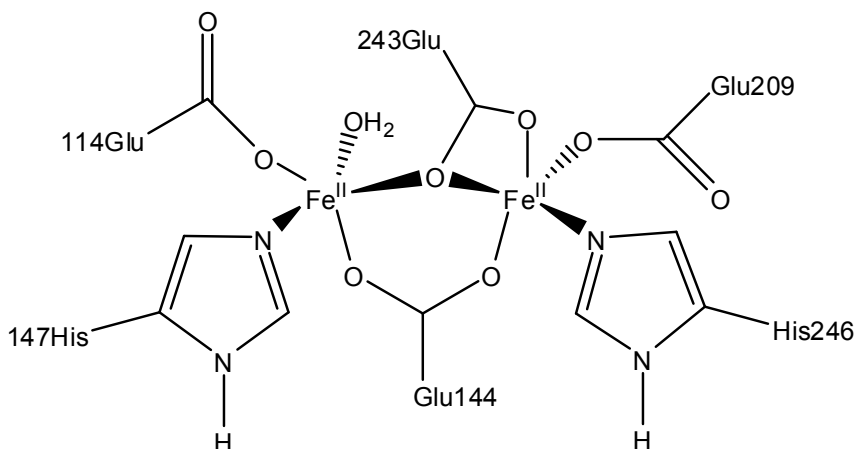


Figure 1.1. Diagram of the active site of MMO derived from *Methylococcus capsulatus* (Bath).³⁶



Methane monoxygenase (MMO) makes use of its non-heme diiron active site in the catalytic oxidation of methane to methanol (Fig.1.1). This six-coordinate octahedral compound, consists of bridged iron ions by hydroxide ion, water and carboxylate.³⁶ In its reduced state, MMOH selectively oxidizes methane to methanol through the different conformations of the molecule (eqn 1).^{15,36} The monooxygenase pathway operates by utilizing two equivalents of NAD(P)H (2 electrons of oxidation power), one splits the O–O bond of oxygen, where one O atom is reduced to water, whilst the remaining O atom is incorporated into the substrate.^{15,36}

There has been a rapid development of catalytic systems, which are inspired by biological enzymes, MMO and cytochrome P450.^{8,37-45} These include metallophoryins and Schiff base systems.^{10,11,46-52} Early work reported by Cook et al. shows sterically crowded Mn and Fe porphyrins as effective catalysts for hydroxylation of alkanes, where the regioselectivities are comparable to those of some isoenzymes of cytochrome P450.⁵⁰ More recently White and co-workers reported site selective C-H activation by iron complexes.⁵³⁻⁵⁷ Doro and co workers have designed manganese 5-(pentafluorophenyl)-10,15-20-tri(2,6-dichlorophenyl)porphyrin and grafted them onto aminopropylated silica in the catalytic oxidation of cyclohexane using iodosyl benzene (PhIO) and hydrogen peroxide as oxidants. Greater selectivity to cyclohexanol and cyclohexanone was observed.⁴⁶ Studies on polymer supported Cu(II) Schiff base complexes in the oxidation of ethyl benzene, propyl benzene and adamantane showed good product selectivity to the ketone product when using hydrogen peroxide as an oxidant.⁴⁸ Manganese salen compounds immobilized on montmorillonite were also used in the biomimetic oxidation of cyclooctane and cyclohexane with sodium periodate

(NaIO₄) as the oxidant. Conversions of 74% (cyclooctane) and 35% (cyclohexane) were achieved with higher yields to the ketone than the alcohol.⁴⁹

1.2.1 Factors affecting alkane oxidation

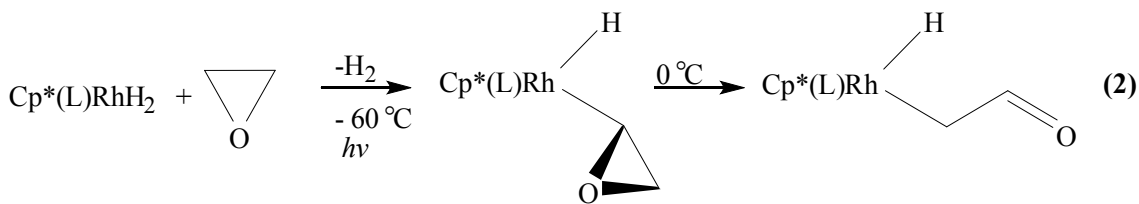
The contributing factor to the lack of reactivity in alkanes stems from their high bond energies. For example, methane has a C-H bond energy of 104 kcal.mol⁻¹, whilst primary and secondary C-H bond energies range from 90-98 kcal.mol⁻¹.^{12,18,20,58} This results in alkanes being inert due to the strong and localized C-C and C-H bonds, which hold the constituent atoms together.²⁴ These saturated hydrocarbons lack a high energy filled orbital or low energy empty orbital that can readily participate in a chemical reaction.²⁴

Apart from the inertness of alkanes, other factors contribute to the lack of reactivity of paraffin's. These include:

- i. Selectivity
- ii. Activity
- iii. Thermodynamics

There has been a massive effort in trying to achieve selective C-H bond activation over the past 30 years.^{6,7,12,17,19,21,22,37,59-68} The much desired terminal carbon functionalization is one of the main goals.¹⁴ Selectivity poses a problem, due to the intermediate products being more reactive than the alkane itself.¹⁴ This results in the formation of unwanted products. For example methanol has a C-H bond energy that is 10 kcal.mol⁻¹ less than methane.¹⁴ This will require methanol to be removed as soon it is produced, else over oxidation to carbon dioxide will occur.^{14-16,58} To overcome this drawback, a pathway that does not involve C-H bond homolysis should be employed. This may involve dioxygen as the oxidant, but due to its unstable triplet state selective functionalization often cannot be achieved as a radical pathway is most likely to occur.⁵⁸ However, the use of transition metals with stable oxidation states can lead to non radical pathways, even when the oxidant is dioxygen.⁵⁸

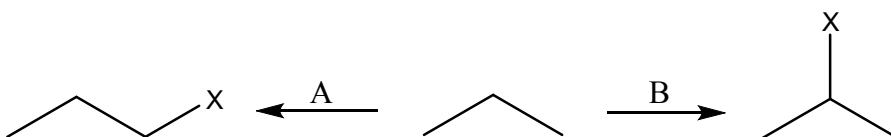
Organometallic C-H bond activation has further proved promising, as in equation 2 where activation of the C-H bond is preferred over the more reactive epoxide.²⁴



Selectivity for the sp^2 (benzylic) over sp^3 hybridized C–H bonds occurs when:⁶⁹

- η^3 coordination stabilises the benzylic product.
- Steric hindrance disfavors the formation of the metal-aryl product.

The preferential oxidation of one carbon atom over another is a highly desirable task.²³ This is most noted when trying to activate longer chain alkanes ($> \text{C}_3$), as there is a preferential activation for the secondary and tertiary carbons over the primary carbon.⁵⁸ This is due to the homolytic bond energies that decrease as one moves from the primary to the tertiary carbon (primary C–H > secondary C–H > tertiary C–H). Since activation of the terminal position is highly desirable for commodity chemicals, discovering ways to overcome this problem are important.⁵⁸ The preference for the least substituted alkyl is noted, giving rise to functionalized linear alkanes when activation occurs using low valent late transition metals (Scheme 1.2).¹⁵

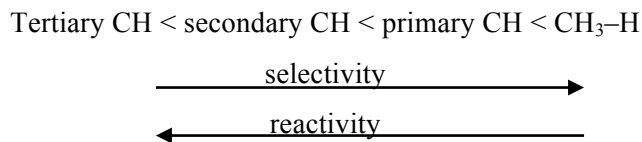


Scheme 1.2. The difference between activation by transition metals (A) and that occurring via radical or electrophilic routes (B).¹⁵

Labinger and Bercaw state that the valuable reactions are those that occur at a reasonable rate.²⁴ Kinetic factors determine the selectivity in alkane functionalization, where the least reactive primary bonds are highly selective to activation (Scheme 1.3).¹⁶ MacLeod et al. have employed that by making use of bulky substituents, the regioselectivity is influenced or the preference of functionalization of one carbon atom over the other.²³ However, in terms of activity, the reaction proceeds much slower, as noted in the activation of *n*-octane.⁷⁰

Thermodynamics is the major obstacle in alkane activation, typically, since most of their reactions, such as dehydrogenation to alkenes or carbonylation, are endothermic.^{16,24} There is also the preferential activation of stronger aromatic C–H bonds over weaker sp^3 hybridized bonds.⁶⁹ This has been attributed to greater differences in the M–C bond strength.⁶⁹ To overcome this, the insertion of an electronegative element, such as an oxidant, will lead to an

exothermic reaction by at least 30 kcal.mol⁻¹, as in alkane hydroxylation.¹⁶ This will lead to high value commodity chemicals such as alcohols, aldehydes and acids. However, most metal centers are sensitive to oxidants and O₂.²⁴

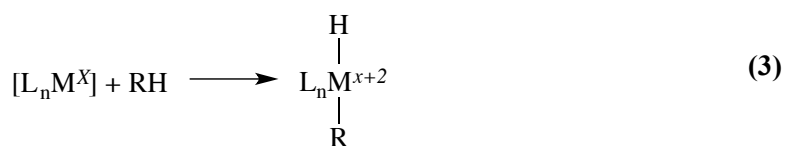


Scheme 1.3. The relationship between bond strength and selectivity as well as reactivity, where primary C-H bonds exhibit greatest selectivity and lowest reactivity in comparison to their tertiary counterparts.¹⁶

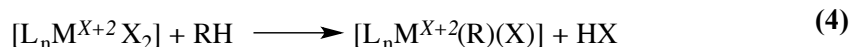
1.2.2 Oxidation of alkanes by group nine transition metals

Labinger and Bercaw have provided a useful review explaining the five fundamental classes in the activation of alkanes by organometallic complexes.²⁴ These include:

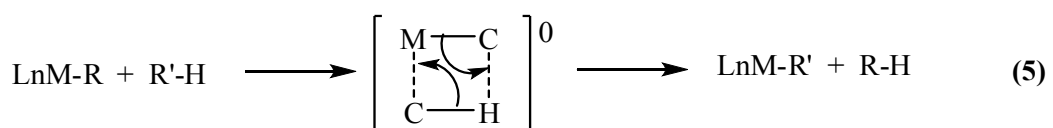
- i. *Oxidative addition* of alkanes to low valent, electron rich complexes such as Re, Fe, Ru, Os, Rh, Ir, and Pt (eqn 3).²⁴



- ii. *Electrophilic addition*, which proceeds directly to the functionalized alkane (eqn 4).^{21,24}



- iii. *Sigma bond metathesis* - Addition of the alkane across a bond to an electropositive metal, which forms an intermediate that ultimately results in a new hydrocarbon and a new metal alkyl species (eqn 5).^{15,21,24}



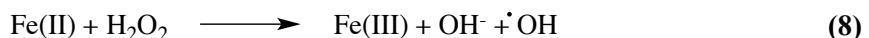
iv. *Metalloradical activation* - Abstraction of hydrogen from an alkane by the metal center (eqn 6).^{21,24}



v. *1,2-addition* - involves alkane addition across a metal double bonded to a non metal (eqn 7).^{21,24}



In spite of the many challenges that chemists faced in activating the C-H bonds of hydrocarbons, initial alkane oxidation by Fenton in 1898 was achieved using iron salts and hydrogen peroxide.^{3,16,71} Fenton chemistry or the Haber-Weiss chemistry occurs via OH• radicals, which are generated through the oxidation of iron (+2 oxidation state to +3). These radicals attack the alkane forming carbon radicals which react with oxygen and eventually form the respective alcohol or ketone (eqns (8-10)).¹⁶



Using this Fenton mechanism as a platform, much improvement and elaboration has been made with other transition metals and different oxidants.^{1,9,11,17,22,23,59}

Henceforth, this chapter will draw particular attention to group nine transition metals (Co, Rh and Ir) and their application in the catalytic oxidation of alkanes.

1.2.2.1 Cobalt

Early studies carried out by Saussine and co workers⁷², showed that cobalt(III) alkylperoxy complexes were used in the stoichiometric hydroxylation of cyclohexane, adamantane, *cis*-decalin and *n*-octane.⁷² Highest yield was to cyclohexanone (24%) in the oxidation of cyclohexane. With the hydroxylation of adamantane, a good yield of 26% to adamantine-1-ol was reported, however, with *n*-octane as the substrate, the highest yield of 12% to 2-octanone was achieved. Using the oxidant *tert*-butyl hydroperoxide in the oxidation of cyclohexane, very high conversion of 100% was achieved with a good yield to cyclohexanol (39%).⁷² Chavez et al. synthesized three cobalt peroxide complexes using a strong field pentadentate ligand (Py₃Ph₂) (Fig. 1.2).⁷³ The complexes were used as catalysts in the oxidation of cyclohexane to cyclohexanol and cyclohexanone and cyclohexyl chloride. The reaction

occurs via the production of *tert* butoxy and cyclohexyl radical. A maximum yield of 59% to the stated products was achieved at an optimum temperature of 50 °C.⁷³

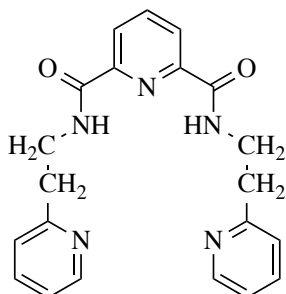


Figure 1.2. The Py₃Ph₂ ligand used by Chavez et al.⁷³ in the oxidation of cyclohexane.

Kanjina and Trakarnpruk⁷⁴ have synthesized cobalt substituted polyoxometalates for the catalytic oxidation of cyclohexane using hydrogen peroxide as the oxidant. The reaction proceeds via a radical mechanism with good selectivity to both the respective ketone (> 33%) and alcohol (> 58%) products.⁷⁴ Tripodal 4N ligands (Fig. 1.3) complexed to cobalt for the oxidation of cyclohexane and adamantane were synthesized by Tordin et al.¹³ Using *m*-CPBA as the oxidant, the catalytic runs were carried out in a mixture of two solvents, DCM and MeCN (1:3 and 3:1 vv). Higher conversion was obtained in the 1:3 vv of MeCN:DCM with good selectivity to cyclohexanol (177 TON) and 1-adamantanol (68 TON).¹³ This system has proved to be more efficient than that of a nickel substituted tripodal ligand.⁶²

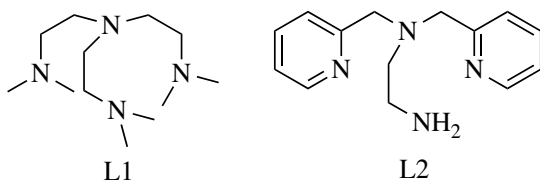


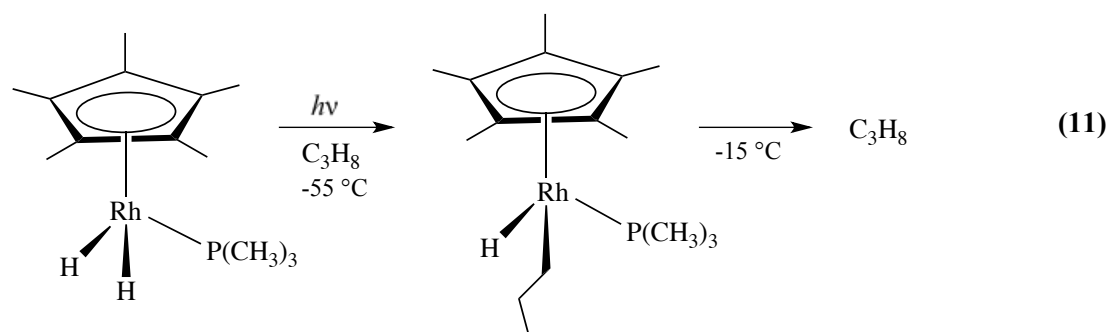
Figure 1.3. Tripodal 4N ligands used in the oxidation of cyclohexane and adamantane.¹³

Nam et al. have used metal perchlorate salts of first row transition metals in the oxidation of cyclohexane and its derivatives using *m*-CPBA as the oxidant.⁴⁴ Good yields to the primary oxidation products were obtained with cobalt salts exhibiting highest catalytic activity and good yields.⁴⁴ Sandwich type tungstophosphate anions, [M₄(H₂O)₂(PW₉O₃₄)₂]¹⁰⁻ where M= Co⁺², Mn⁺² and Fe⁺³ were also employed in the oxidation of cyclohexane and cyclooctane with H₂O₂ as the oxidant. The cobalt complex gave conversions of cyclohexane of 83% and 91% with highest selectivity to cyclohexanone > 60%. Similar conversions of cyclooctane were also obtained, but with a much higher selectivity to the ketone, cyclooctanone (83%). In

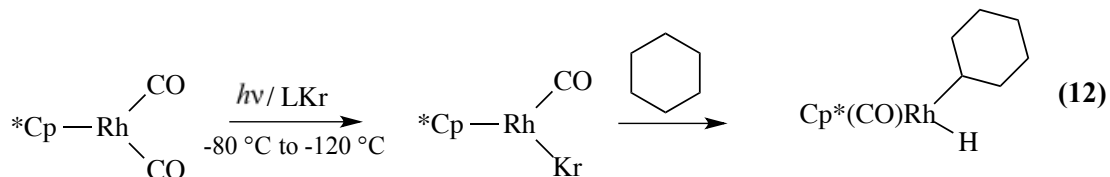
comparison to the manganese and iron salts, the iron salts displayed highest activity, however, the cobalt salts were most selective to the ketone product.⁷⁵

1.2.2.2 Rhodium

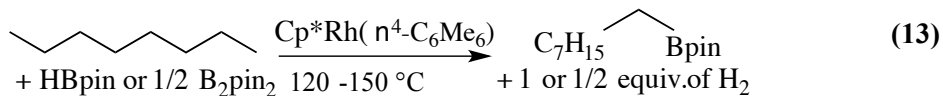
The activation of alkane C-H bonds by rhodium and iridium (Section 1.2.2.3) complexes has not been thoroughly explored. Most studies are based on intramolecular oxidative addition reactions (Section 1.2.2). The earliest studies were carried out by Jones and Feher in 1982 where they synthesized and irradiated the complex $[C_5(CH_3)_5]Rh[P(CH_3)_3]H_2$ in liquid propane at -55 °C to produce the corresponding *n*-propyl complex (eqn 11).⁷⁶



Periana and Bergman have also exposed rhodium cyclopentadienyl complexes to UV radiation in solutions of various alkanes, resulting in the loss of the hydride and formation of the C-H insertion product. These results show that the rate constants of the rhodium complexes are much higher than those of the corresponding iridium complexes.⁷⁷ Bengali et al. have synthesized $CpRh(CO)_2$ and $Cp^*Rh(CO)_2$ and used these in the C-H activation of cyclohexane after irradiation in liquid xenon and liquid krypton, forming the corresponding cyclohexyl metal complexes as shown in eqn 12 for the Cp^* example.⁷⁸



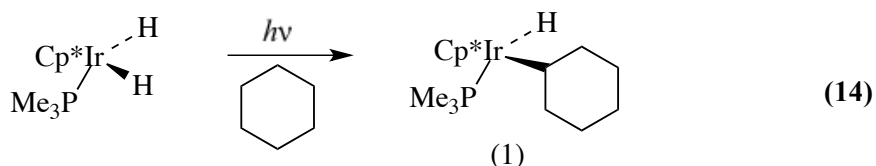
More recently, Hartwig et al. have synthesized a bisboryl complex which reacts with pinacolborane, HBpin, to form a $Cp^*Rh(H)(Bpin)_3$ complex (eqn 13).⁷⁹ The resulting complex is heated at 125 °C in octane to form octylboranate ester in good yield.⁷⁹



The only catalytic system reported to date is that by Nomura and Uemura,⁸⁰ who used rhodium salts such as Rh₃O, [Rh(acac)₃], [RhCl(CO)₂]₂, [RhCl(PPh₃)₃] and [Rh₂(OAc)₄] in the oxidation of cyclohexane using peracetic acid, H₂O₂, TBHP and *m*-CPBA as oxidants. Rh₃O proceeds rather efficiently with up to a 62.2 % yield to the products and a TON of 1911. Among the different alkanes tested, the conversion of *n*-octane was least efficient, with a TON of 93.⁸⁰

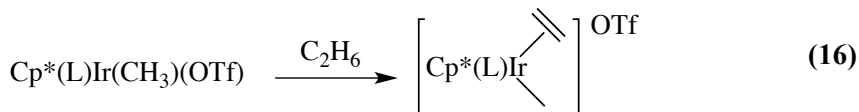
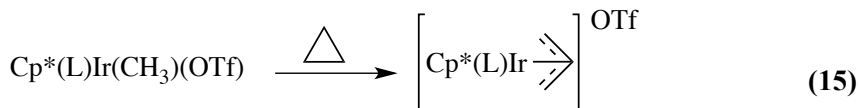
1.2.2.3 Iridium

One of the earliest examples of intermolecular alkane C-H activation was that reported by Janowicz and Bergman in 1982.⁸¹ Irradiation of a dihydrido iridium complex in cyclohexane results in extrusion of the dihydrogen and formation of the new product (**1**) in good yield (eqn 14).⁸¹



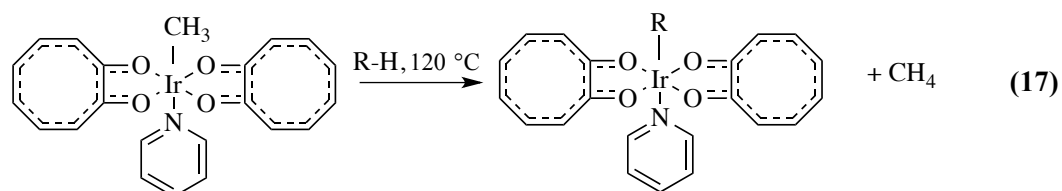
A year later the same authors determined the relative rates at which C-H activation occurs for different alkanes using the same complex as in eqn 14 and they noticed that those C-H bonds with high bond energies react very rapidly.⁸² Hoyano and Graham also report the irradiation of (η -C₅Me₅)Ir(CO)₂ in neopentane and cyclohexane, forming new hydriodneopentyl and cyclohexyl iridium compounds.⁸³

Burger and Bergman report the activation of cyclopropane (eqn 15) and ethane (eqn 16) using Cp^{*}(PMe₃)Ir(OTF)₂ to give a cationic allyl and a hydrido(ethylene)complex respectively.⁸⁴



Golden and co workers have synthesized cationic iridium complexes ($[\text{Cp}^*(\text{PMe}_3)\text{IrH}(\text{L}')]^+$ where $\text{L}' = \text{C}_2\text{H}_4$, CO, and THF) and reacted them with various alkanes at low temperatures (-20 °C) using hydrogen-deuterium exchange leading to an iridium dihyridoalkyl intermediate.⁸⁵

New oxygen donor ligands complexed to iridium $[\text{Ir}(\text{trop-O,O})_3]$ (trop = tropolonato) where heated to 120 °C in cyclohexane to give the corresponding cyclohexyl iridium complex and these complexes reacted 50 times faster than the acac (acteylacetonate) analogue (eqn 17).^{86,87}



1.3 Styrene epoxidation

There is an abundant supply of cheap, unsaturated materials from oils, which are used as fuels for cars and airplanes.⁸⁸ Oxidizing these olefins is an economical way of turning the mineral oil into higher value added chemicals such as ketones, aldehydes and epoxides.^{88,89} Olefin epoxidation is one of the main routes that lead to epoxide production on a laboratory and industrial scale, since in a single step, two C-O bonds are created with stereoselective control and high regioselectivity.⁹⁰⁻⁹³ One of the leading methods for the industrial direct alkene oxidation uses of oxygen, peracids and peroxides.⁹⁰

Epoxides have a widespread application in chemical and pharmaceutical industries and are readily converted to alcohols, aldehydes and polyethers.⁹¹ In the oxidation of styrene, styrene oxide is quite difficult to produce, whilst benzaldehyde and phenylacetaldehyde are usually the dominant products.^{90,91} Styrene oxide is an important intermediate in the synthesis of

pharmaceuticals and fine chemicals, whilst benzaldehyde is a valuable chemical and has widespread application in the agro chemical and the perfume and dye industries.⁹⁴⁻⁹⁹

The oxidation of alkenes is efficiently catalyzed by transition metal complexes, e.g in the Wacker process in which a Pd-Cu catalyst system effectively catalyze the oxidation of ethylene to acetaldehyde in H₂O (eqn 18 - 20).^{89,100}



Transition metals have received much attention because they are required for the functionalization of lower alkenes, which are used as by products in the production of gasoline.¹⁰¹ They are also used in understanding reactions of biological importance and are required for partial selective oxidation.¹⁰¹ In the oxidation of styrene, transition metals have been extensively studied, where the choice of oxidant and catalyst can modify the course of the reaction.^{91,95,100-103}

Much work has been done on Schiff base complexes and heterogenizing them on various supports; however, selectivity in homogenous systems is rather good.^{97,102,104-111} Schiff base complexes receive more attention due to their ability to mimic enzyme catalyzed oxidation reactions.¹⁰⁶ Yang et al. have immobilized copper and oxo-vanadium Schiff base complexes on SBA-15 and used them as catalysts in the oxidation of styrene with air and hydrogen peroxide as oxidants.¹⁰⁷ Immobilization of the same metals on amino-modified graphene oxide by Li et al. gave higher conversions and good selectivity to styrene oxide in comparison to the SBA supported catalysts.⁹⁷ Higher yields to benzaldehyde were obtained using the homogenous system, however, with the heterogeneous system, good selectivity to styrene oxide and recoverability was found.¹⁰⁷

Copper and nickel salen complexes covalently linked to Keggin type polyoxometalates showed better activity in styrene oxidation with hydrogen peroxide as an oxidant compared to the homogenous system.^{105,111} However, better selectivity to the epoxide was obtained with the unbound Cu(II) salen complexes.¹⁰⁵ Electron rich Cu Schiff base complexes derived from aldehydes showed good activity giving TONs of 300 using *tert*-butyl hydroperoxide as an oxidant.¹⁰² Polymer bound Mn(II) Schiff base complexes gave TONs of 3-31 at different catalyst:oxidant (PhIO) molar ratios.¹⁰⁶ However, Mn Schiff based complexes encapsulated in

zeolite Y were highly active catalysts, with better yield to benzaldehyde observed in the homogenous system than the heterogeneous system.¹⁰⁹ Iron-salen complexes immobilized on a clay support, as catalysts in the oxidation of styrene, gave benzaldehyde yields of 10-30 % and low TONs (7-20).¹⁰⁸

1.3.1 Mechanism of olefin oxidation

Chen and White illustrate that secondary C-H bonds have a chemoselective advantage in oxidation studies due to increased steric accessibility as compared to tertiary C-H bonds (Fig. 1.4).⁵⁵ Furthermore, secondary C-H bonds can undergo both electronic activation and deactivation due to their intermediate electronic properties.⁵⁵ High site selectivity can be achieved during functionalization due to a variety of stereoelectronic effects present in these secondary C-H bonds.⁵⁵

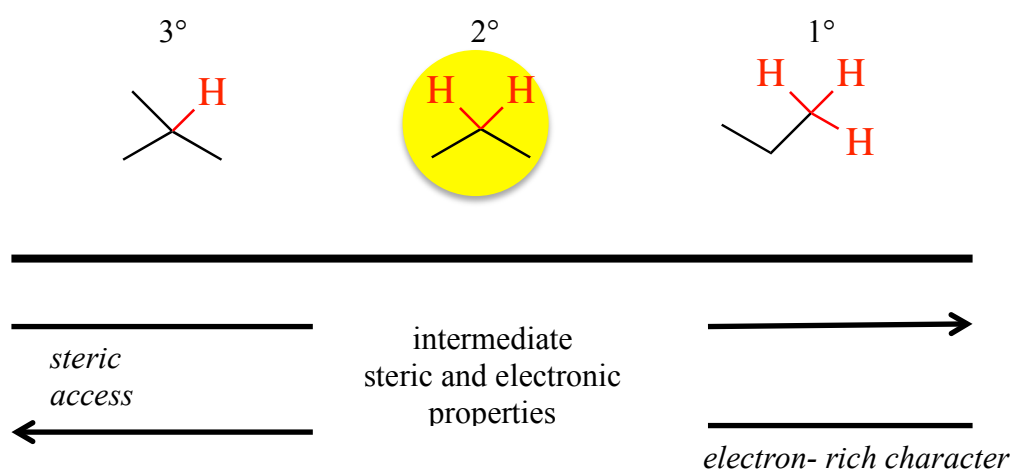


Figure 1.4. Chemical properties of C-H bonds.⁵⁵

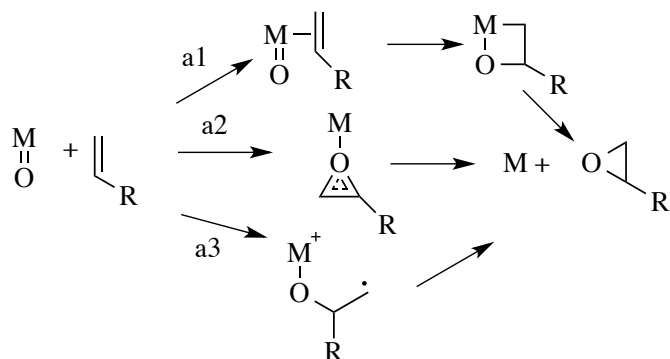
Bruin et al. explain the three mechanistic classes of olefin-oxidation catalyzed by transition metals:⁸⁸

- Autoxidation: This occurs through a radical chain mechanism, which is initiated at the metal center and then propagates far from the metal species.
- No metal-olefin interaction: This occurs through the transfer of oxygen from the oxidant to the olefin.
- Metal-olefin interaction: In this case oxygenation occurs with the olefin that is coordinated to the metal center. This is most prominent in late transition metals as well as in Wacker oxidation.

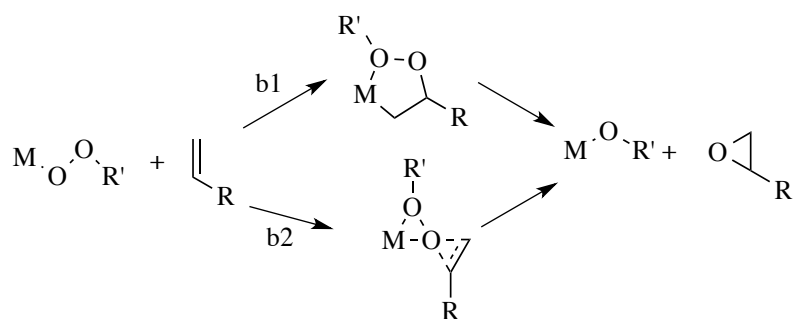
The formation of the epoxide can occur via a metal-oxo species (a) or via a metal-hydroperoxy or metal-alkylperoxy species (b) (Scheme 1.4). In the former, epoxidation at the metal can occur via metalla-oxetanes (a1) or via direct transfer (a2 or a3). For early transition metals that have high oxidation states, epoxidation proceeds via a process, b, with the olefin insertion into the metal-oxygen bond (b1) or through b2, where oxygen transfer occurs via the nucleophilic attack of the olefin at the peroxide. The formation of the ketone or aldehyde occurs via metal induced nucleophilic attack (c) or via a metal (hydro) peroxy species (d). The former (c), involves the typical Wacker type catalysis with the intermolecular (c1) or intramolecular (c2) nucleophilic attack of the hydroxide at the coordinated alkene. For late transition metals, oxidation proceeds via the activation of both the oxidant and the alkene (d2). The electrophilic nature of the alkene increase upon coordination and deprotonation increases the nucleophilic nature of the peroxide.

Epoxidation

a) via metal-oxo species

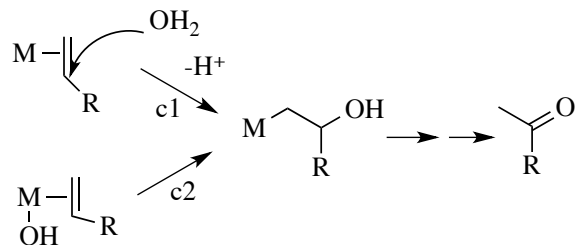


b) via metal-hydroperoxy or metal alkyl-peroxy species

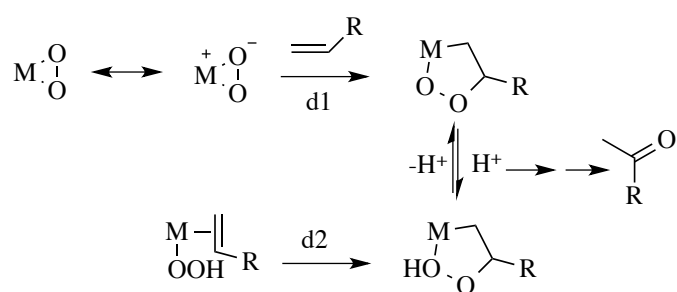


Ketone/ aldehyde formation

c) via metal-induced nucleophilic attack



d) via metal-(hydro)peroxy species



Scheme 1.4. Proposed mechanisms of olefin oxidation to form epoxides (a and b) and ketones and aldehyde (c and d).⁸⁸

1.3.2 Oxidation of styrene by group nine transition metals

Extensive research has been done on second and third row transition metals, which are used as catalysts forming the active oxo species, which are capable of performing oxidative cleavage.^{112,113} Ruthenium based complexes have gained much interest over the years in various fields such as photomolecular devices, probes for biological macromolecules and artificial photosynthesis due to their wide range of chemical accessible oxidation states (Ru^{+2} to Ru^{+8}), which make them versatile as energy transfer and electron transfer compounds.^{114,115}

One of the key steps in oxidation reactions is the formation of an intermediate ruthenium-oxo species through the mediation of a suitable oxidant.¹¹⁶⁻¹²¹ Ruthenium catalysts have been widely explored in epoxidation reactions using different oxidants and ligand systems.^{93,112-134}

In this review, attention is drawn to the group 9 transition metals, Co, Rh and Ir, in the oxidation of styrene, since they are the focus of this thesis.

1.3.2.1 Co, Rh and Ir

One of the earliest studies that was carried out was with cobalt salen complexes in the oxidation of styrene by Zombeck et al. in 1982.¹³⁵ The reaction was performed in different solvent systems and was greatly enhanced when $\text{RhCl}(\text{PPh}_3)_3$ was added.¹³⁵ Drago et al. synthesized [bis(salicylidene- γ -iminopropyl)methylamine cobalt(II), CoSMDPT, complexes for the oxidation of isoeugenol in the formation vanillin and acetophenone.¹³⁶ High TONs of 562 were obtained.¹³⁶

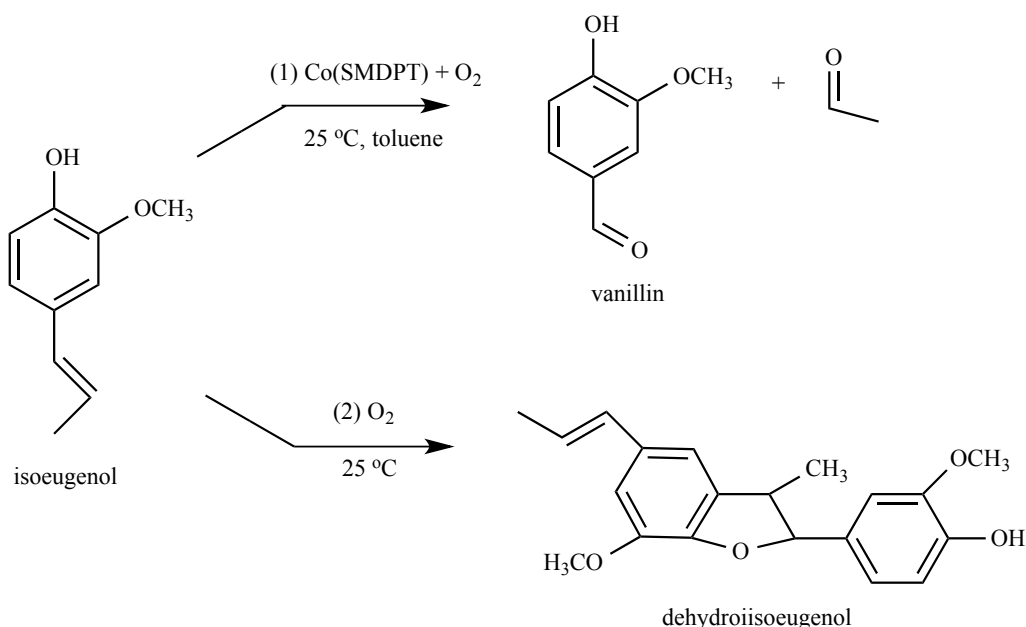


Figure 1.5. The oxidation of isoeugenol by cobalt SMDPT complexes in the formation of vanillin.¹³⁶

Cobalt salts, CoBr_2 , CoCl_2 , $\text{Co}(\text{acac})_3$, $\text{Co}(\text{OAC})_2 \cdot 4\text{H}_2\text{O}$ and CoF_2 were used as catalysts in the oxidation of methyl styrene in a $t\text{-BuOH}$ solvent system with O_2 as the oxidant.¹³⁷ The highest conversion (91%) was obtained using CoCl_2 as a catalyst. When the same salt was used as a catalyst in the oxidation of styrene, a 30 % conversion was obtained with high yields to benzoic acid.¹³⁷

Catalytically active Co(III) ions occupying sites in molecular sieves (AlPO-36, microporous aluminophosphate number 36) were highly active catalysts in the oxidation of styrene, with 46% conversion and good selectivity to the epoxide (34%) and diol (59%).¹³⁸ Tang et al. also reported the epoxidation of styrene using cobalt containing molecular sieves, Co-Faujasite zeolite and Co- MCM-41.¹³⁹ Depending on the solvent system, high conversions were obtained using acetylacetone (69%), with lower expoxide selectivity (30%). Co

encapsulated in zeolite Y gave conversions of 63% with a higher selectivity to benzaldehyde (59%).¹⁴⁰ In a DMF (*N,N* dimethylformamide) and DMA (*N,N* dimethylacetamide) solvent system, lower conversions (44%; 45%) were found, but better selectivity to the epoxide (60%; 74%).¹³⁹ Mesoporous silica (MCM-41) functionalized with Co(II) salen showed conversions of 56.5% and a TOF of 36 in the oxidation of styrene with hydrogen peroxide as an oxidant.¹⁴¹ The homogenous Co(II) salen complex system showed lower conversion (41.7%) and TOF (15).¹⁴¹

When CoO is used as a catalyst with TBHP as an oxidant, 47% conversion is obtained with highest selectivity to styrene oxide (73%) and low selectivity to benzaldehyde (0.1%).¹⁴² Cobalt substituted Keggin-type polyoxometalates impregnated on a Schiff base modified SBA-15 were also used as effective catalysts in styrene oxidation with hydrogen peroxide as an oxidant under mild conditions.¹⁴³ A 41% conversion was obtained with a 39% yield to benzaldehyde.¹⁴³ The non-impregnated catalyst showed a 54 % conversion with a 37 % selectivity to benzaldehyde.¹⁴³ A similar study of Co^{2+} adsorbed onto functionalized SBA-15 showed conversions of 92% with high epoxide selectivity (63 %) when oxygen was used as an oxidant.¹⁴⁴ The selectivity to the epoxide increased when TBHP was used as an oxidant (70%) and was slightly lower when air and hydrogen peroxide were used.¹⁴⁴ Schiff base polymer-cobalt complexes used in the oxidation of styrene with TBHP as an oxidant were also highly selective catalysts to styrene oxide (72%).¹⁴⁵

Both Rh and Ir complexes have been studied extensively in the oxidation of alkenes⁸⁸, however, very limited research is carried out using styrene as a substrate. One of the earliest studies was carried out by Takao and co workers using $\text{RhCl}(\text{PPh}_3)_3$ and RhCl_3 as catalysts in the oxidation of styrene under oxygen atmosphere.¹⁴⁶ When $\text{RhCl}(\text{PPh}_3)_3$ was used high yields to benzaldehyde were obtained at 80 °C with dioxane as a solvent. Trace conversion was noted when the solvent system was changed to ethanol, pyridine or acetic acid. However, RhCl_3 used a catalyst gave much higher yield to benzaldehyde and styrene oxide in toluene as compared to when $\text{RhCl}(\text{PPh}_3)_3$ was used.¹⁴⁶ A similar study was carried out by the same authors on iridium Vaska complexes $\text{IrXCO}(\text{PPh}_3)_3$ where X = Cl, Br and I.¹⁴⁷ The activity of the catalysts increases in the order: Cl < I < Br. They have postulated that the oxidation using these Vaska complexes proceeds via the coordination of both the oxygen and triphenylphosphine as in Fig 1.6.¹⁴⁷

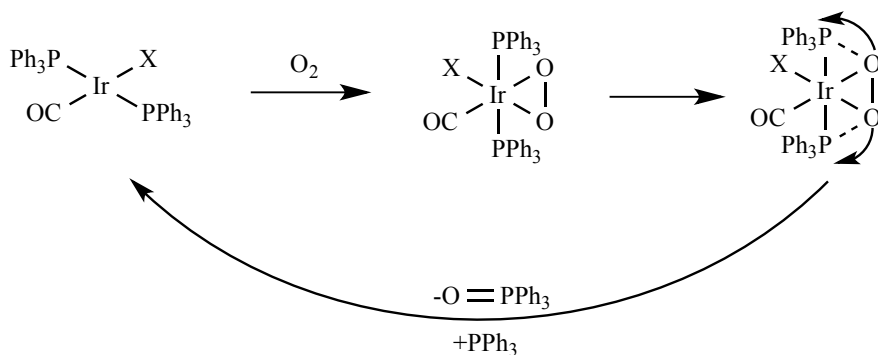


Figure 1.6. Ir Vaska complexes used in the oxidation studies.¹⁴⁷

Farrar et al. have shown that the coordination of oxygen and styrene is essential for the epoxidation reaction catalyzed by $[(\text{RhCl}(\text{C}_2\text{H}_4)_2)_2]$.¹⁴⁸ Bis(pyridylimino)isoindolato-iridium complexes gave a 55% conversion over a 48 h period with a 50 % yield to styrene oxide.¹⁴⁹

More recently Burlington et al. used an half sandwich Ir complex (Fig 1.7) in the oxidation of styrene with PhIO as an oxidant and they obtained low yields to benzaldehyde (11%) and phenylacetaldehyde (11%).¹⁵⁰

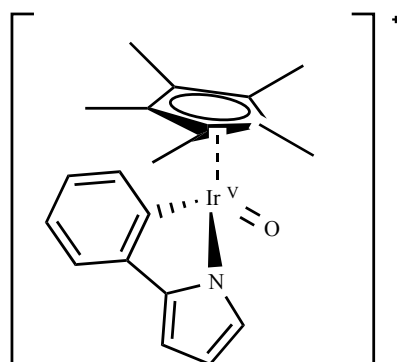


Figure 1.7. Half sandwich compound used by Burlington et al. in the oxidation of styrene.¹⁵⁰

1.4 Conclusion

Oxidation chemistry has enthralled scientists for many years and will continue to do so for the years to come. The scope and magnitude in this field of study is unlimited. The challenge is to develop a system that provides good selectivity to the desired products, but at the same time give a mechanistic insight as to how the reaction proceeds. This review has shown that there is a potential to develop the chemistry of group 9 transition metals in the oxidation of alkanes and alkenes. Much work has been done on Co systems, however, this is not the case for systems containing Rh and Ir. With new ligand systems on the rise, there is enormous

potential to develop this chemistry by fine-tuning the catalytic reactions in order to obtain products of high added value.

1.5 Aim of study

The development of metal-based homogenous catalysts capable of oxidizing hydrocarbons under mild conditions continues to be a challenge for chemists around the world. There is a major need for the formation of alcohols (or oxygenates) by the hydroxylation of alkanes because the current commercial solid metal oxide catalysts are not sufficiently active for the functionalization of unsaturated C-H bonds and require high temperatures and pressures which often lead to low selectivity.¹⁹

Many transition metal complexes used as homogenous catalysts have shown high homogeneity, selectivity, reproducibility and activity, as well as the ability to catalyze reactions under mild conditions.¹⁵¹ However, the appropriate choice of ligand plays an important role, as this can fine tune the activity of the metal and alter the catalytic behavior. In this study we have used aminodiphosphine ligands (PNP) in the oxidation of *n*-octane and styrene. This ligand system has been widely explored in ethylene oligomerisation with chromium as the active metal.¹⁵²⁻¹⁵⁸ These bi-dentate or multidentate ligands are part of a system that displays high activity, variability and stability.¹⁵⁹⁻¹⁶¹ Modification of the ligand backbone, by using different donor substituents (such as soft (N) and hard (P) donors) or central anionic atoms, tailors the activity of the metals, allowing the reactions of the metal ions to be selective, due to the high demand the ligands place on the stereochemistry of the complex.^{162,163}

In this study, the substituent on the nitrogen atom has been varied so as to vary the basicity of the ligand backbone (Fig 1.8). This was done with the intention of observing if these groups have an effect on the catalytic activity and selectivity to the products of oxidation. Alkyl substituents such cyclohexyl (**a**) (cyclic), *iso*-propyl (**b**) (branched) and *n*-pentyl (**c**) (straight chained) as well as phenyl (**d**) based substituents and substituted phenyl (chlorophenyl (**e**) and methoxyphenyl (**f**)) are used. In order to add flexibility to the ligand backbone, ethylene spacer groups between the N and P atoms are used (Fig 1.9). Again, the R group was varied by making use of different alkyl substituents on the nitrogen atom.

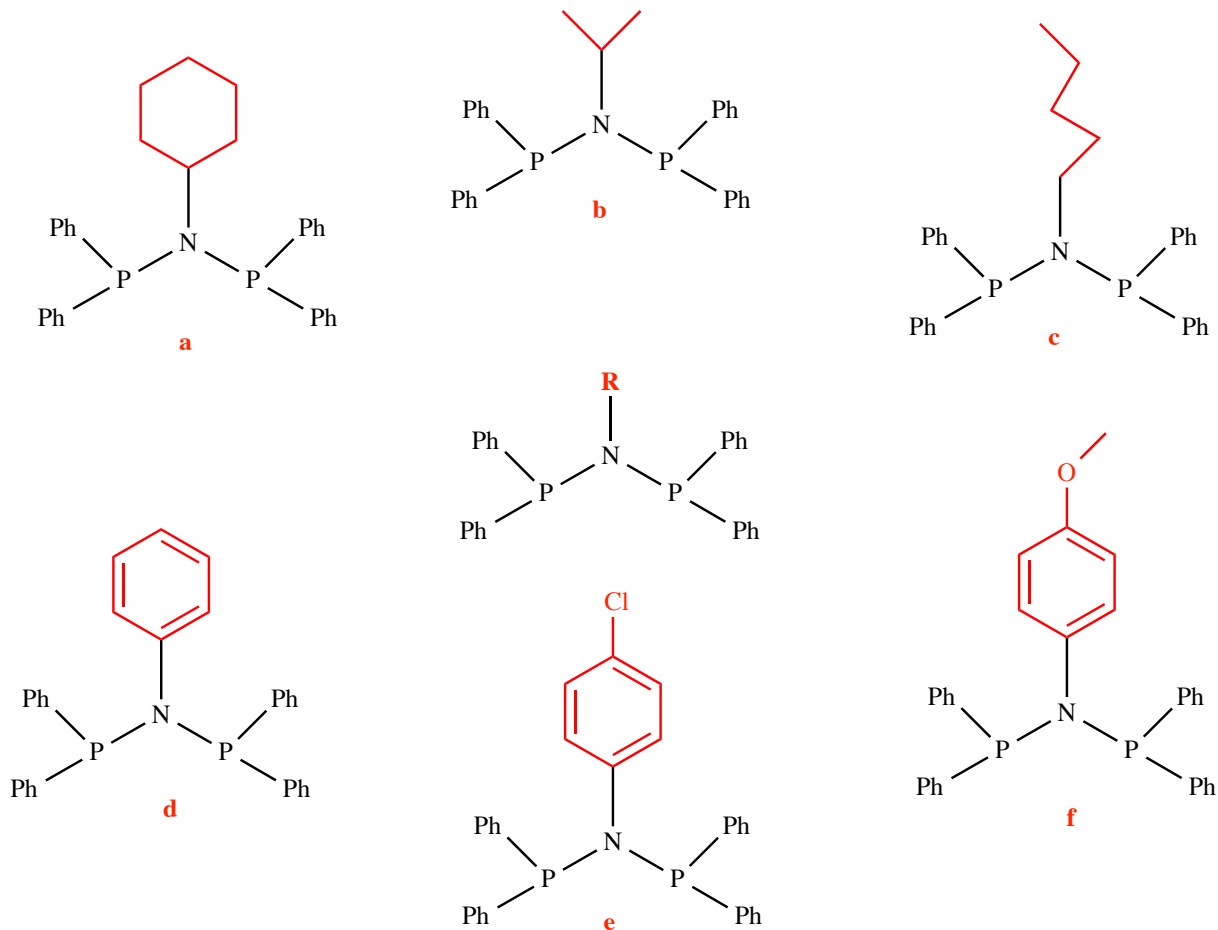


Figure 1.8. The ligands (**1**) used in this study containing the different substituents on the nitrogen atom.

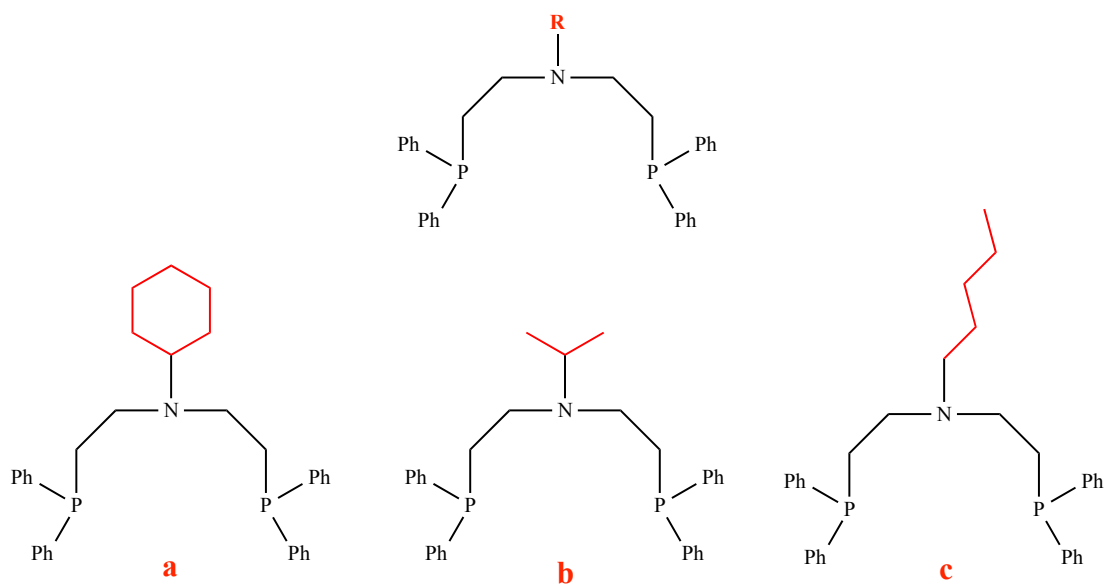


Figure 1.9. Ligands (**2**) containing the ethylene spacer group between the N and P atoms, as well as different alkyl substituents on the nitrogen atom used in this study .

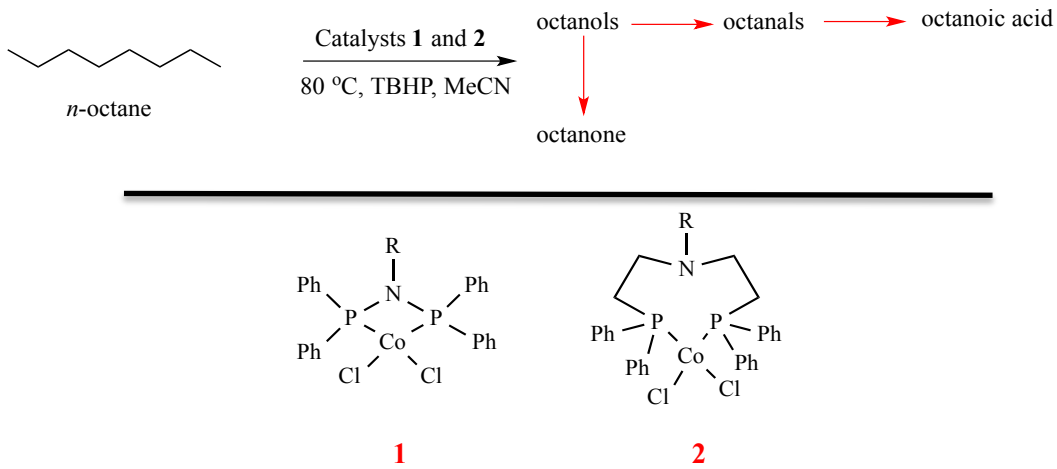
These ligands have been complexed to the transition metals Co, Rh, Ir and Ru and were used as catalyst in the oxidation of *n*-octane and styrene. Cobalt was chosen as one of the transition metals since it is relatively cheap, widespread and easily available. Furthermore, with the success of first row transition metals, such as iron and copper, in oxygenation reactions using biological enzymes, cobalt serves as a promising candidate in the C-H activation of alkanes and alkenes.

The oxidation of both *n*-octane and styrene using iridium and rhodium complexes has not been thoroughly explored. Very few cases have been reported and most work was undertaken in the 1980's. To gain scientific insight, it was most decided that complexes of these metals bearing the "PNP" ligand backbone, be investigated in the oxidation of these respective substrates.

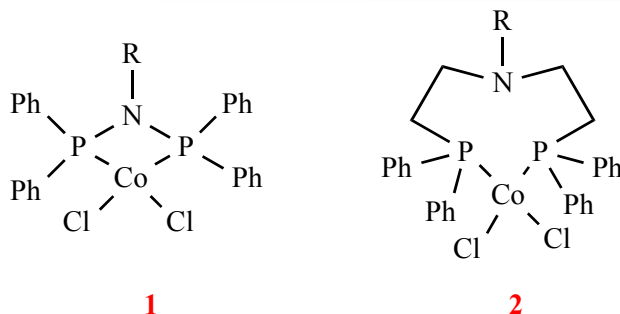
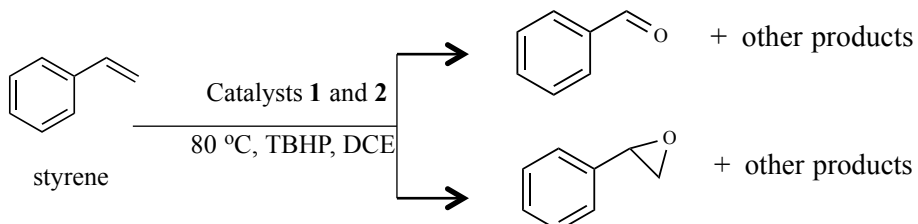
Ruthenium oxidation catalysis has been thoroughly explored with a variety of ligand systems. However, when using a phosphine-based ligand, the catalyst is highly susceptible to ligand degradation. This study presents new work using the aminodiphosphine ligand system, under mild conditions, in the oxidation of *n*-octane and styrene, in the hope of recovering the catalyst without ligand degradation.

In each of these studies, the solvent, oxidant and reaction temperature were varied so as to determine the optimum conditions for best selectivity and conversion to the desired products. Below is a graphical summary of the content of each chapter.

Chapter 2 – Cobalt “PNP” aminodiphosphine complexes as catalysts in the oxidation of *n*-octane

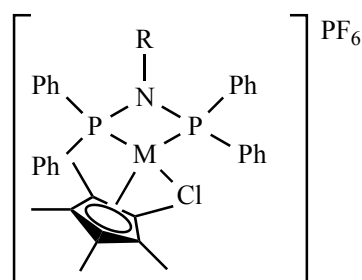
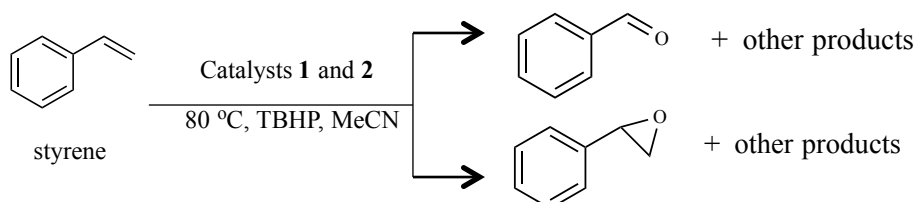


Chapter 3 – Oxidation of styrene by TBHP using cobalt “PNP” aminodiphosphine complexes as highly effective catalysts



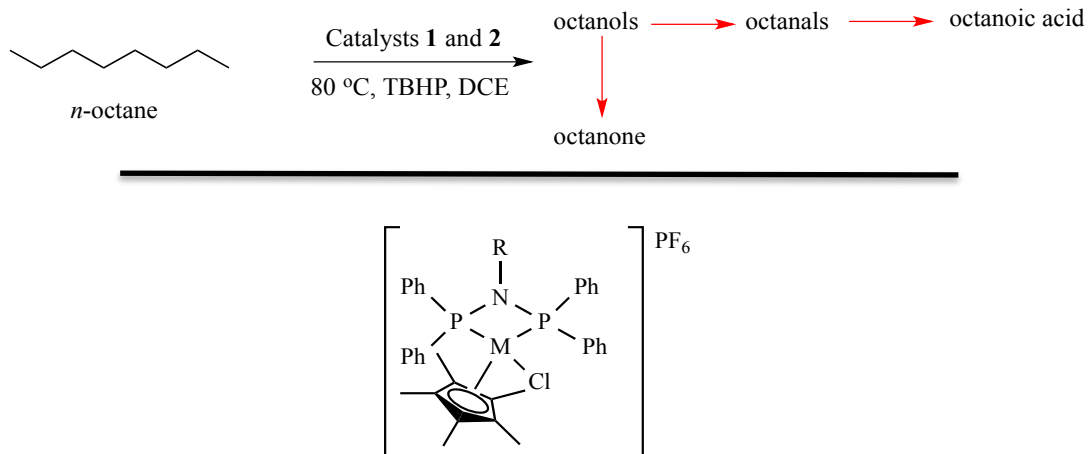
R= cyclohexyl (**a**), *iso*-propyl (**b**) and pentyl (**c**)

Chapter 4 – Ir and Rh “PNP” aminodiphosphine complexes as catalysts in the oxidation of styrene



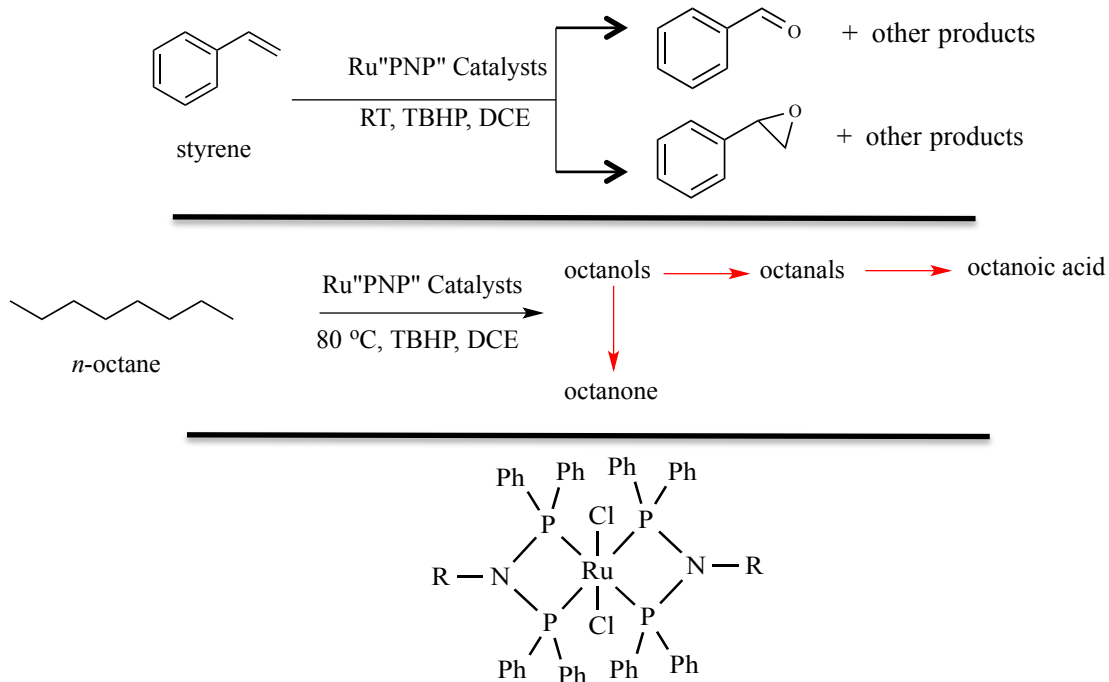
R = cyclohexyl (**a**); pentyl (**b**); *iso*-propyl (**c**); phenyl (**d**); chlorophenyl (**e**); methoxyphenyl (**f**).
M = Ir (**1**) and Rh (**2**)

**Chapter 5 – Ir and Rh “PNP” aminodiphosphine complexes
as catalysts in the oxidation of *n*-octane**



R = cyclohexyl (**a**); pentyl (**b**); *iso*-propyl (**c**); phenyl (**d**); chlorophenyl (**e**); methoxyphenyl (**f**).
M = Ir (**1**) and Rh (**2**)

**Chapter 6 – Ru “spider” complexes as catalysts in the
oxidation of *n*-octane and styrene**



R = cyclohexyl (**a**); pentyl (**b**); *iso*-propyl (**c**);

1.6 References

- [1] Amini, M.; Haghdoost, M. M.; Bagherzadeh, M. *Coord. Chem. Rev.* **2013**, *257*, 1093-1121.
- [2] Mizuno, N.; Kamata, K. *Coord. Chem. Rev.* **2011**, *255*, 2358-2370.
- [3] Shilov, A. E.; Shul'pin, G. B. *Chem. Rev.* **1997**, *97*, 2879-2932.
- [4] Punniyamurthy, T.; Velusamy, S.; Iqbal, J. *Chem. Rev.* **2005**, *105*, 2329-2363.
- [5] van Leeuwen, P. W. N. M. *Homogeneous Catalysis: Understanding the Art*; Kluwer Academic Publishers: Dordrecht, **2004**, p 299.
- [6] He, Y.; Gorden, J. D.; Goldsmith, C. R. *Inorg. Chem.* **2012**, *51*, 12651-12660.
- [7] Kirillova, M. V.; Kirillov, A. M.; Mandelli, D.; Carvalho, W. A.; Pombeiro, A. J. L.; Shul'pin, G. B. *J. Catal.* **2010**, *272*, 9-17.
- [8] Curci, R.; D'Accolti, L.; Fusco, C. *Acc. Chem. Res.* **2005**, *39*, 1-9.
- [9] Kirillov, A. M.; Shul'pin, G. B. *Coord. Chem. Rev.* **2013**, *257*, 732-754.
- [10] Gupta, K. C.; Kumar Sutar, A.; Lin, C-C. *Coord. Chem. Rev.* **2009**, *253*, 1926-1946.
- [11] Smith, J. R.L.; Iamamoto, Y.; Vinhado, F. S. *J. Mol. Catal. A: Chem.* **2006**, *252*, 23-30.
- [12] Jia, C.; Kitamura, T.; Fujiwara, Y. *Acc. Chem. Res.* **2001**, *34*, 633-639.
- [13] Tordin, E.; List, M.; Monkowius, U.; Schindler, S.; Knör, G. *Inorg. Chimi. Acta* **2013**, *402*, 90-96.
- [14] Goldman, A., S.; Goldberg, K., I. *Organometallic C-H Bond Activation: An Introduction; Activation and Functionalization of C-H Bonds*. American Chemical Society **2004**, 885, p 1-43.
- [15] Crabtree, R. H. *J. Organomet. Chem.* **2004**, *689*, 4083-4091.
- [16] Crabtree, R. H. *J. Chem. Soc. Dalton Trans.* **2001**, 2437-2450.
- [17] Kirillov, A. M.; Kirillova, M. V.; Pombeiro, A. J. L. *Coord. Chem. Rev.* **2012**, *256*, 2741-2759.
- [18] Bergman, R. G. *Science* **1984**, *223*, 902-908.
- [19] Conley, B. L.; Tenn I, W. J.; Young, K. J. H.; Ganesh, S. K.; Meier, S. K.; Ziatdinov, V. R.; Mironov, O.; Oxgaard, J.; Gonzales, J.; Goddard III, W. A.; Periana, R. A. *J. Mol. Catal. A: Chem.* **2006**, *251*, 8-23.
- [20] Silva, A. C.; Fernández, T. L.; Carvalho, N. M. F.; Herbst, M. H.; Bordinhão, J.; Jr, A. H.; Wardell, J. L.; Oestreicher, E. G.; Antunes, O. A. C. *Appl. Catal. A: Gen.* **2007**, *317*, 154-160.
- [21] Sivaramakrishna, A.; Suman, P.; Veerashekhar Goud, E.; Janardan, S.; Sravani, C.; Sandeep, T.; Vijayakrishna, K.; Clayton, H. S. *J. Coord. Chem.* **2013**, *66*, 2091-2109.
- [22] Shul'pin, G. B.; Kudinov, A. R.; Shul'pina, L. S.; Petrovskaya, E. A. *J. Organomet. Chem.* **2006**, *691*, 837-845.
- [23] Mac Leod, T. C. O.; Kirillova, M., V.; Pombeiro, A. J. L.; Schiavon, M. A.; Assis, M. D. *Appl. Catal. A: Gen.* **2010**, *372*, 191-198.
- [24] Labinger, J. A.; Bercaw, J. E. *Nature* **2002**, *417*, 507-514.
- [25] El Khalifa, E. A.; Friedrich, H. B. *Appl. Catal. A: Gen.* **2010**, *373*, 122-131.
- [26] Friedrich, H. B.; Mahomed, A. S. *Appl. Catal. A: Gen.* **2008**, *347*, 11-22.
- [27] Friedrich, H. B.; Govender, N.; Mathebula, M. R. *Appl. Catal. A: Gen.* **2006**, *297*, 81-89.
- [28] Cavani, F.; Ballarini, N.; Cericola, A. *Catal. Today* **2007**, *127*, 113-131.
- [29] Meunier, F. C.; Yasmeen, A.; Ross, J. R. H. *Catal. Today* **1997**, *37*, 33-42.
- [30] Comite, A.; Sorrentino, A.; Capannelli, G.; Di Serio, M.; Tesser, R.; Santacesaria, E. *J. Mol. Catal. A: Chem.* **2003**, *198*, 151-165.
- [31] Emmett, P. H. *Catalysis*; Reinhold Pub. Corp., **1958**, 6.
- [32] Al-Yassir, N.; Le Van Mao, R. *Appl. Catal. A: Gen.* **2006**, *305*, 130-139.
- [33] Corma, A.; Orchillés, A. V. *Micro. Mesopor. Mat.* **2000**, *35-36*, 21-30.
- [34] Rittle, J.; Green, M. T. *Science* **2010**, *330*, 933-937.
- [35] Wu, L.-L.; Yang, C.-L.; Lo, F.-C.; Chiang, C.-H.; Chang, C.-W.; Ng, K. Y.; Chou, H.-H.; Hung, H.-Y.; Chan, S. I.; Yu, S. S. F. *Chem. A Eur. J.* **2011**, *17*, 4774-4787.

- [36] Westerheide, L.; Pascaly, M.; Krebs, B. *Curr. Opin.Chem.Biol.* **2000**, *4*, 235-241.
- [37] Shul'pin, G. B.; Süss-Fink, G.; Shul'pina J. *Mol. Catal. A: Chem.* **2001**, *170*, 17-34.
- [38] Yiu, S.; Man, W.; Lau, T. *J. Am. Chem. Soc.* 2008, *130*, 10821-10827.
- [39] Nizova, G. V.; Krebs, B.; Süss-Fink, G.; Schindler, S.; Westerheide, L.; Cuervo, G. L.; Shul'pin, G. B. *Tetrahedron* 2002, *58*, 9231-9237.
- [40] Shul'pin, G. B.; Stoeckli-Evans, H.; Mandelli, D.; Kozlov, Y. N.; Vallina, A. T.; Woitiski, C. B.; Jimenez, R. S.; Carvalho, W. A. *J. Mol. Catal. A: Chem.* 2004, *219*, 255-264.
- [41] Katsuki, T. *Coord. Chem. Rev.* **1995**, *140*, 189-214.
- [42] Balamurugan, M.; Mayilmurugan, R.; Suresh, E.; Palaniandavar, M. *Dalton Trans.* **2011**, *40*, 9413-9424.
- [43] Barton, D. H. R.; Doller, D. *Acc. Chem. Res.* **1992**, *25*, 504-512.
- [44] Nam, W.; Ryu, J. Y.; Kim, I.; Kim, C. *Tetrahedron Lett.* 2002, *43*, 5487-5490.
- [45] Kille, S.; Zilly, F. E.; Acevedo, J. P.; Reetz, M. T. *Nat. Chem.* 2011, *3*, 738-743.
- [46] Doro, F. G.; Smith, J. R. L.; Ferreira, A. G.; Assis, M. D. *J. Mol. Catal. A: Chem.* **2000**, *164*, 97-108.
- [47] Cagnina, A.; Campestrini, S.; Di Furia, F.; Ghiotti, P. *J. Mol. Catal. A: Chem.* **1998**, *130*, 221-231.
- [48] Islam, S. M.; Roy, A. S.; Mondal, P.; Mubarak, M.; Mondal, S.; Hossain, D.; Banerjee, S.; Santra, S. C. *J. Mol. Catal. A: Chem.* **2011**, *336*, 106-114.
- [49] Bahramian, B.; Mirkhani, V.; Mogahadam, M.; Tangestaninejad, S. *Catal. Commun.* **2006**, *7*, 289-296.
- [50] Cook, B. R.; Reinert, T. J.; Suslick, K. S. *J. Am. Chem. Soc.* **1986**, *108*, 7281-7286.
- [51] Vinhado, F. S.; Gandini, M. E. F.; Iamamoto, Y.; Silva, A. M. G.; Simões, M. M. Q.; Neves, M. G. P. M. S.; Tomé, A. C.; Rebelo, S. L. H.; Pereira, A. M. V. M.; Cavaleiro, J. A. S. *J. Mol. Catal. A: Chem.* **2005**, *239*, 138-143.
- [52] Lu, H.; Zhang, X. P. *Chem. Soc. Rev.* **2011**, *40*, 1899-1909.
- [53] Gormisky, P. E.; White, M. C. *J. Am. Chem. Soc.* **2013**, *135*, 14052-14055.
- [54] Bigi, M. A.; Reed, S. A.; White, M. C. *J. Am. Chem. Soc.* **2012**, *134*, 9721.
- [55] Chen, M. S.; White, M. C. *Science* **2010**, *327*, 566-571.
- [56] White, M. C. *Synlett* **2012**, *23*, 2746-2748.
- [57] Vermeulen, N. A.; Chen, M. S.; White, M. C. *Tetrahedron* **2009**, *65*, 3078-3084.
- [58] Sen, A. *Acc. Chem. Res.* **1998**, *31*, 550-557.
- [59] Kirillov, A. M.; Kirillova, M. V.; Shul'pina, L. S.; Figiel, P. Ç. J.; Gruenwald, K. R.; Guedes da Silva, M. F. T. C.; Haukka, M.; Pombeiro, A. J. L.; Shul'pin, G. B. *J. Mol. Catal. A: Chem.* **2011**, *350*, 26-34.
- [60] Kirillova, M. V.; Kozlov, Y. N.; Shul'pina, L. C.; Lyakin, O. Y.; Kirillov, A. M.; Talsi, E. P.; Pombeiro, A. J. L.; Shul'pin, G. B. *J. Catal.* **2009**, *268*, 26-38.
- [61] Nagataki, T.; Ishii, K.; Tachi, Y.; Itoh, S. *Dalton Trans.* **2007**, 1120-1128.
- [62] Nagataki, T.; Tachi, Y.; Itoh, S. *Chem. Commun.* **2006**, 4016-4018.
- [63] Shul'pin, G. B. *C.R. Chimie* **2003**, *6*, 163-178.
- [64] Shul'pin, G. B. *Mini-Rev: Org. Chem.* **2009**, *6*, 95-104.
- [65] Shul'pin, G. B.; Golfeto, C. C.; Süss-Fink, G.; Shul'pina, L. S.; Mandelli, D. *Tetrahedron Lett.* **2005**, *46*, 4563-4567.
- [66] Shul'pin, G. B.; Kozlov, Y.; Shul'pina, L. S.; Kudinov, A. R.; Mandelli, D. *Inorg. Chem. Commun.* **2009**, *48*, 10480-10482.
- [67] Shul'pin, G. B.; Kozlov, Y. N.; Shul'pina, L. S.; Petrovskiy, P. V. *Appl. Organomet. Chem.* **2010**, *24*, 464-472.
- [68] Shul'pina, L. S.; Kirillova, M. V.; Pombeiro, A., J.L.; Shul'pin, G. B. *Tetrahedron* **2009**, *65*, 2424-2429.
- [69] Zhu, Y. J.; Fan, L.; Chen, C. H.; Finnell, S. R.; Foxman, B. M.; Ozerov, O. V. *Organometallics* **2007**, *26*, 6701-6703.
- [70] Liu, F.; Pak, E. B.; Singh, B.; Jensen, C. M.; Goldman, A. S. *J. Am. Chem. Soc.* **1999**, *121*, 4086-4087.

- [71] Dunford, H. B. *Coord. Chem. Rev.* **2002**, *233–234*, 311-318.
- [72] Saussine, L.; Brazi, E.; Robine, A.; Mimoun, H.; Fischer, J.; Weiss, R. *J. Am. Chem. Soc.* **1985**, *107*, 3534-3540.
- [73] Chavez, F. A.; Nguyen, C. V.; Olmstead, M. M.; Mascharak, P. K. *Inorg. Chem.* **1996**, *35*, 6282-6291.
- [74] Kanjina, W.; Trakarnpruk, W. *J. Met. Mats. Min.* **2010**, *20*, 29-34.
- [75] Santos, I. C. M. S.; Gamelas, J. A. F.; Balula, M. S. S.; Simões, M. M. Q.; Neves, M. G. P. M. S.; Cavaleiro, J. A. S.; Cavaleiro, A. M. V. *J. Mol. Catal. A: Chem.* **2007**, *262*, 41-47.
- [76] Jones, W. D.; Feher, F. J. *Organometallics* **1983**, *2*, 562-565.
- [77] Periana, R. A.; Bergman, R. G. *Organometallics* **1984**, *3*, 508-510.
- [78] Bengali, A. A.; Arndsten, B. A.; Burger, P. M.; Schultz, R. H.; Weiller, B. H.; Kyle, K. R.; Moore, C. B.; Bergman, R. G. *Pure Appl. Chem* **1995**, *67*, 218-288.
- [79] Hartwig, J. F.; Cook, K. S.; Hapke, M.; Incarvito, C. D.; Fan, Y.; Webster, C. E.; Hall, M. B. *J. Am. Chem. Soc.* **2005**, *127*, 2538-2552.
- [80] Nomura, K.; Uemura, S. *J. Chem. Soc. Chem. Commun.* **1994**, 129-130.
- [81] Janowicz, A. H.; Bergman, R. G. *J. Am. Chem. Soc.* **1982**, *104*, 352-354.
- [82] Janowicz, A. H.; Bergman, R. G. *J. Am. Chem. Soc.* **1983**, *105*, 3929-3939.
- [83] Hoyano, J. K.; Graham, W. A. G. *J. Am. Chem. Soc.* **1982**, *104*, 3723-3725.
- [84] Burger, P.; Bergman, R. G. *J. Am. Chem. Soc.* **1993**, *115*, 10462-10463.
- [85] Golden, J. T.; Andersen, R. A.; Bergman, R. G. *J. Am. Chem. Soc.* **2001**, *123*, 5837-5838.
- [86] Bhalla, G.; Periana, R. A. *Angew. Chem.* **2005**, *117*, 1564-1567.
- [87] Tenn, W. J.; Young, K. J. H.; Bhalla, G.; Oxgaard, J.; Goddard, W. A.; Periana, R. A. *J. Am. Chem. Soc.* **2005**, *127*, 14172-14173.
- [88] Bruin, d. B.; Budzelaar, P. H. M.; Gal, A. W. *Angew. Chem. Int. Ed.* **2004**, *43*, 4142-4157.
- [89] Chiappe, C.; Sanzone, A.; Dyson, P. J. *Green Chem.* **2011**, *13*, 1437-1441.
- [90] Grigoropoulou, G.; Clark, J. H.; Elings, J. A. *Green Chem.* **2003**, *5*, 1-7.
- [91] Saha, D.; Maity, T.; Dey, T.; Koner, S. *Polyhedron* **2012**, *35*, 55-61.
- [92] Ahmad, A. L.; Kohestani, B.; Bhatia, S.; Ooi, S. B. *Int. J. App. Cer. Tech.* **2012**, *9*, 588-598.
- [93] Gallo, E.; Caselli, A.; Ragaini, F.; Fantauzzi, S.; Masciocchi, N.; Sironi, A.; Cenini, S. *Inorg. Chem.* **2005**, *44*, 2039-2049.
- [94] Patel, A.; Pathan, S. *Ind. Eng. Chem. Res.* **2011**, *51*, 732-740.
- [95] P Patil, N. S.; Jha, R.; Uphade, B. S.; Bhargava, S. K.; Choudhary, V. R. *Appl. Catal. A-Gen.* **2004**, *275*, 87-93.
- [96] Karandikar, P.; Agashe, M.; Vijayamohanan, K.; Chandwadkar, A. J. *Appl. Catal. A-Gen.* **2004**, *257*, 133-143.
- [97] Li, Z.; Wu, S.; Ding, H.; Lu, H.; Liu, J.; Huo, Q.; Guan, J.; Kan, Q. *New J. Chem.* **2013**, *37*, 4220-4229.
- [98] Shit, S.; Yadava, U.; Saha, D.; Fröhlich, R. *J. Coord. Chem.* **2012**, *66*, 66-76.
- [99] Ding, Y.; Gao, Q.; Li, G.; Zhang, H.; Wang, J.; Yan, L.; Suo, J. *J. Mol. Catal. A: Chem.* **2004**, *218*, 161-170.
- [100] Jiang, G.; Chen, J.; Thu, H.-Y.; Huang, J.-S.; Zhu, N.; Che, C.-M. *Angew. Chem. Int. Ed.* **2008**, *47*, 6638-6642.
- [101] Joergensen, K. A. *Chem. Rev.* **1989**, *89*, 431-458.
- [102] Rayati, S.; Zakavi, S.; Koliae, M.; Wojtczak, A.; Kozakiewicz, A. *Inorg. Chem. Commun.* **2010**, *13*, 203-207.
- [103] Kanmani, A. S.; Vancheesan, S. *Stud. Surf. Sci. and Catal.* **1998**, *113*, 285-292.
- [104] Vasconcellos-Dias, M.; Nunes, C. D.; Vaz, P. D.; Ferreira, P.; Brandão, P.; Félix, V.; Calhorda, M. J. *J. Catal.* **2008**, *256*, 301-311.
- [105] Mirkhani, V.; Moghadam, M.; Tangestaninejad, S.; Mohammadpoor-Baltork, I.; Rasouli, N. *Catal. Commun.* **2008**, *9*, 2411-2416.
- [106] Du, X.-D.; Yu, X.-D. *J. Polym. Sci. Pol. Chem.* **1997**, *35*, 3249-3254.

- [107] Yang, Y.; Zhang, Y.; Hao, S.; Guan, J.; Ding, H.; Shang, F.; Qiu, P.; Kan, Q. *Appl. Catal. A: Gen.* **2010**, *381*, 274-281.
- [108] Dhakshinamoorthy, A.; Pitchumani, K. *Tetrahedron* **2006**, *62*, 9911-9918.
- [109] Silva, M.; Freire, C.; de Castro, B.; Figueiredo, J. L. *J. Mol. Catal. A: Chem.* **2006**, *258*, 327-333.
- [110] Bai, R.; Fu, X.; Bao, H.; Ren, W. *Catal. Commun.* **2008**, *9*, 1588-1594.
- [111] Mirkhani, V.; Moghadam, M.; Tangestaninejad, S.; Mohammadpoor-Baltork, I.; Shams, E.; Rasouli, N. *Appl. Catal. A: Gen.* **2008**, *334*, 106-111.
- [112] Spannring, P.; Bruijninckx, P. C. A.; Weckhuysen, B. M.; Klein Gebbink, R. J. M. *Catal. Sci. Tech.* **2014**, *4*, 2182-2209.
- [113] Jahromi, B. T.; Kharat, A. N.; Zamanian, S. *Chinese Chem. Lett.* **2014**, In press.
- [114] Moghadam, M.; Mirkhani, V.; Tangestaninejad, S.; Mohammadpoor-Baltork, I.; Kargar, H.; Sheikhshoaei, I.; Hatefi, M. *J. Iran. Chem. Soc.* **2011**, *8*, 1019-1029.
- [115] Chatterjee, D.; Basak, S.; Riahi, A.; Muzart, J. *J. Mol. Catal. A: Chem.* **2006**, *255*, 283-289.
- [116] Dakkach, M.; López, M. I.; Romero, I.; Rodríguez, M.; Atlamsani, A.; Parella, T.; Fontrodona, X.; Llobet, A. *Inorg. Chem.* **2010**, *49*, 7072-7079.
- [117] Dakkach, M.; Fontrodona, X.; Parella, T.; Atlamsani, A.; Romero, I.; Rodriguez, M. *Dalton Trans.* **2014**, *43*, 9916-9923.
- [118] Dakkach, M.; Atlamsani, A.; Parella, T.; Fontrodona, X.; Romero, I.; Rodriguez, M. *Inorg. Chem.* **2013**, *52*, 5077-5087.
- [119] Cheng, W.-C.; Fung, W.-H.; Che, C.-M. *J. Mol. Catal. A: Chem.* **1996**, *113*, 311-319.
- [120] Mahalingam, V.; Karvembu, R.; Chinnusamy, V.; Natarajan, K. *Spectrochim. Acta A* **2006**, *64*, 886-890.
- [121] Nishiyama, H.; Motoyama, Y. *Chem. Commun.* **1997**, 1863-1864.
- [122] Agarwala, H.; Ehret, F.; Chowdhury, A. D.; Maji, S.; Mobin, S. M.; Kaim, W.; Lahiri, G. K. *Dalton Trans.* **2013**, *42*, 3721-3734.
- [123] Aneetha, H.; Padmaja, J.; Zacharias, P. S. *Polyhedron* **1996**, *15*, 2445-2451.
- [124] Antony, R.; Tembe, G. L.; Ravindranathan, M.; Ram, R. N. *Euro. Polym. J.* **2000**, *36*, 1579-1589.
- [125] Barf, G. A.; van den Hoek, D.; Sheldon, R. A. *Tetrahedron* **1996**, *52*, 12971-12978.
- [126] Bressan, M.; Morville, A. *Inorg. Chem.* **1989**, *28*, 950-953.
- [127] Benet-Buchholz, J.; Comba, P.; Llobet, A.; Roeser, S.; Vadivelu, P.; Wadeohl, H.; Wiesner, S. *Dalton Trans.* **2009**, 5910-5923.
- [128] Chatterjee, D.; Basak, S.; Mitra, A.; Sengupta, A.; Le Bras, J.; Muzart, J. *Catal. Commun.* **2005**, *6*, 459.
- [129] Chowdhury, A. D.; Das, A.; K, I.; Mobin, S. M.; Lahiri, G. K. *Inorg. Chem.* **2011**, *50*, 1775-1785.
- [130] Klawonn, M.; Tse, M. K.; Bhor, S.; Döbler, C.; Beller, M. *J. Mol. Catal. A: Chem.* **2004**, *218*, 13-19.
- [131] Kogan, V.; Quintal, M. M.; Neumann, R. *Org. Lett.* **2005**, *7*, 5039-5042.
- [132] Robbins, M. H.; Drago, R. S. *J. Chem. Soc. Dalton Trans.* **1996**, 105-110.
- [133] Sala, X.; Rodríguez, A. M.; Rodríguez, M.; Romero, I.; Parella, T.; von Zelewsky, A.; Llobet, A.; Benet-Buchholz, J. *J. Org. Chem.* **2006**, *71*, 9283-9290.
- [134] Stoop, R. M.; Bachmann, S.; Valentini, M.; Mezzetti, A. *Organometallics* **2000**, *19*, 4117-4126.
- [135] Zombeck, A.; Hamilton, D. E.; Drago, R. S. *J. Am. Chem. Soc.* **1982**, *104*, 6782-6784.
- [136] Drago, R. S.; Corden, B. B.; Barnes, C. W. *J. Am. Chem. Soc.* **1986**, *108*, 2453-2454.
- [137] Lin, Y. H.; Williams, I. D.; Li, P. *Appl. Catal. A: Gen.* **1997**, *150*, 221-229.
- [138] Raja, R.; Sankar, G.; Meurig Thomas, J. *Chem. Commun.* **1999**, 829-830.
- [139] Tang, Q.; Zhang, Q.; Wu, H.; Wang, Y. *J. Catal.* **2005**, *230*, 384-397.
- [140] Yang, Y.; Ding, H.; Hao, S.; Zhang, Y.; Kan, Q. *Appl. Organomet. Chem.* **2011**, *25*, 262-269.
- [141] Luo, Y.; Lin, J. *Micropor. Mesopor. Mat.* **2005**, *86*, 23-30.

- [142] Choudhary, V. R.; Jha, R.; Jana, P. *Catal. Commun.* **2008**, *10*, 205-207.
- [143] Hu, J.; Li, K.; Li, W.; Ma, F.; Guo, Y. *Appl.Catal. A: Gen.* **2009**, *364*, 211-220.
- [144] Cui, H.; Zhang, Y.; Zhao, L.; Zhu, Y. *Catal. Commun.* **2011**, *12*, 417-420.
- [145] Demetgül, C.; Delikanlı, A.; Sarıbüyük, O. Y.; Karakaplan, M.; Serin, S. *Des. Monomers Polym.* **2012**, *15*, 75-91.
- [146] Takao, K.; Wayaku, M.; Fujiwara, Y.; Imanaka, T.; Teranishi, S. *B. Chem.Soc. of Jpn* **1970**, *43*, 3898-3900.
- [147] Takao, K.; Fujiwara, Y.; Imanaka, T.; Teranishi, S. *B. Chem.Soc. of Jpn* **1970**, *43*, 1153-1157.
- [148] Farrar, J.; Holland, D.; Milner, D. *J. J. Chem. Soc. Dalton Trans.* **1975**, 815-821.
- [149] Camerano, J. A.; Sämann, C.; Wadeohl, H.; Gade, L. H. *Organometallics* **2011**, *30*, 379-382.
- [150] Turlington, C. R.; Harrison, D. P.; White, P. S.; Brookhart, M.; Templeton, J. L. *Inorg. Chem.* **2013**, *52*, 11351-11360.
- [151] Gupta, M.; Hagen, C.; Flesher, R. J.; Kaska, W. C.; Jensen, C. M. *Chem. Commun.* **1996**, 2083-2084.
- [152] Teo, S.; Weng, Z.; Hor, T. S. A. *Organometallics* **2008**, *27*, 4188-4192.
- [153] Blann, K.; Bollmann, A.; de Bod, H.; Dixon, J. T.; Killian, E.; Nongodlwana, P.; Maumela, M. C.; Maumela, H.; McConnel, A. E.; Morgan, D. H.; Overette, M. J.; Pretorius, M.; Kuhlmann, S.; Wasserscheid, P. *J. Catal.* **2007**, *249*, 244-249.
- [154] Blann, K.; Bollmann, A.; Dixon, J. T.; Hess, F. M.; Killian, E.; Maumela, H.; Morgan, D. H.; Neveling, A.; Otto, S.; Overett, M. *J. Chem. Comm.* **2005**, 620-621
- [155] Bollmann, A.; Blann, K.; Dixon, J. T.; Hess, F. M.; Killian, E.; Maumela, H.; McGuiness, D. S.; Morgan, D. H.; Neveling, A.; Otton, S.; Overette, M.; Slawin, A. M. Z.; Wasserscheid, P.; Kihlmann, S. *J. Am. Chem. Soc.* **2004**, *126*, 14712-14713.
- [156] Overett, M. J.; Blann, K.; Bollmann, A.; Dixon, J. T.; Hess, F.; Killian, E.; Maumela, H.; Morgan, D. H.; Neveling, A.; Otto, S. *Chem. Comm.* **2005**, 622-624.
- [157] Bowen, L. E.; Haddow, M. F.; Orpen, A. G.; Wass, D. F. *Dalton Trans.* **2007**, 1160-1168.
- [158] Bowen, L. E.; Charernsuk, M.; Hey, T. W.; McMullin, C. L.; Orpen, A. G.; Wass, D. F. *Dalton Trans.* **2010**, *39*, 560-567.
- [159] Benito-Garagorri, D.; Alves, L. G. a.; Puchberger, M.; Mereiter, K.; Veiros, L. F.; Calhorda, M. J.; Carvalho, M. D.; Ferreira, L. P.; Godinho, M.; Kirchner, K. *Organometallics* **2009**, *28*, 6902-6914.
- [160] Benito-Garagorri, D.; Kirchner, K. *Acc. Chem. Res.* **2008**, *41*, 201-213.
- [161] van der Boom, M. E.; Milstein, D. *Chem. Rev.* **2003**, *103*, 1759-1792.
- [162] Xu, X.; Xi, Z.; Chen, W.; Wang, D. *J. Coord. Chem.* **2007**, *60*, 2297-2308.
- [163] Albrecht, M.; van Koten, G. *Angew. Chem. Int. Ed.* **2001**, *40*, 3750-3781.

Chapter Two

Cobalt “PNP” aminodiphosphine complexes as catalysts in the oxidation of *n*-octane

2.1 Abstract

Two types of cobalt aminodiphosphine complexes have been synthesized and characterized by IR spectroscopy, elemental analyses and single crystal X-ray diffraction. These are $[\text{Ph}_2\text{PN}(\text{R})\text{PPh}_2]\text{CoCl}_2$, **1** and $[\text{Ph}_2\text{P}(\text{CH}_2)_2\text{N}(\text{R})(\text{CH}_2)_2\text{PPh}_2]\text{CoCl}_2$, **2** where R= C₆H₁₁ (**a**); C₅H₁₁ (**b**); C₃H₇ (**c**). The functional groups on the nitrogen atom (R) were varied from a cyclohexyl ring, to *n*-pentyl alkyl chain, to an *iso*-propyl branched substituent. Complexes **2a** and **2c** were analyzed using single crystal X-ray diffraction. The geometry around the metal centers in **2a** and **2c** were distorted tetrahedral. All complexes showed good activity as catalysts for the oxidation of *n*-octane using *tert*-butyl hydroperoxide (TBHP) as the oxidant. The complex bearing the flexible ligand backbone with the cyclohexyl substituent on the nitrogen atom was the most active and showed high selectivity towards ketones with 2-octanone being the dominant product.

Keywords: Cobalt aminodiphosphine complexes; oxidation; *n*-octane; *Tert*-butyl hydroperoxide

2.2 Introduction

The conversion of paraffins or saturated hydrocarbons to more valuable products has drawn the interests of many scientists over the last twenty years.¹⁻³ This is due to the central problem, where general, selective, efficient and catalytic functionalisation reactions of unactivated paraffin C–H bonds remains unsolved.¹⁻¹⁰

The need for paraffin activation has practical implications in the replacement of current petrochemical feedstocks (olefins) by economical and easily accessible alkanes, which can result in more efficient strategies for fine chemical synthesis and the proficient use of energy.¹¹⁻¹³ However, the conversion of alkanes to desired functionalized products suffers many shortcomings. These include the chemical inertness of the alkanes, the preferential activation of substrates containing sp² hybridized C–H bonds over sp³ hybridized C–H bonds and cases where the intermediate products are more reactive than the alkane which may react more effortlessly with the metal center.^{2,3,14-18}

Taking into account such shortcomings, a well-suited ligand system is needed. One such system could include the aminodiphosphine or PNP ligands. These bi-dentate or multidentate ligands have been used extensively in ethylene oligomerization with chromium as the active metal.¹⁹⁻²⁵ These ligands are ideally suited for catalytic

applications in that they are part of a system that displays high activity, stability and variability.²⁶⁻²⁸ Modification of the ligand backbone, by using different donor substituents or central anionic atoms, tailors the activity of the metals, allowing the reactions of the metal ions to be selective, due to the high demand ligands place on the stereochemistry of the complex.^{29,30}

In this work, a new approach has been undertaken in using cobalt aminodiphosphine complexes in the C–H activation of *n*-octane. Transition metal-mediated oxidative functionalization of hydrocarbons into useful organic compounds has become an area of immense interest and has led to great advancements in large-scale industrial and synthetic organic processes.³¹⁻³⁴ The development of synthetic models has been biologically inspired by a number of enzymes such as methane monooxygenase and cytochrome P450, which makes use of a reactive iron-oxo species in the oxidation of a number of alkanes.^{13,35-39} With the success of first row transition metals, such as iron and copper in the aforementioned enzymes, cobalt serves as promising candidate in the C–H activation of alkanes.^{40,41} White and co workers have reported site selective C–H activation by a non-heme iron complex in trying to mimic enzymatic activation.^{3,17,42-44} More recently Tordin and coworkers have used cobalt complexes with tripodal 4N ligands in the oxidation of alkanes, while SNS cobalt complexes have also been studied in the oxidation of *n*-octane.^{40,45} Phosphine based ligands have not been widely explored due to ligand degradation or loss of ligand from the metal complex.⁴⁶ However, Wong and co-workers have used ruthenium based phosphine complexes in the oxidation of *n*-octane and reported low conversions.^{47,48} These catalytic oxidation processes are carried out using a variety of oxidants, namely, PhIO, NaOCl, H₂O₂, alkyl hydroperoxides, percarboxylic acids and molecular oxygen.^{33,49-52}

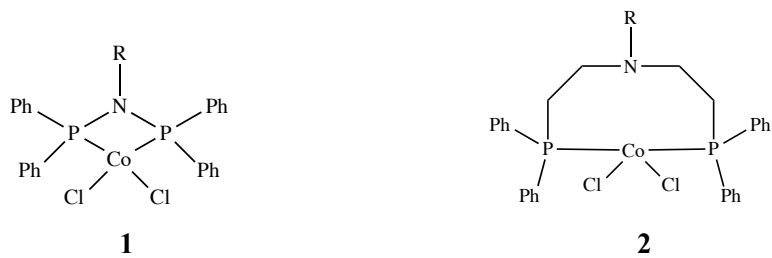


Figure 2.1. Representation of complexes **1** and **2**; R = cyclohexyl for **1a** or **2a**; *n*-pentyl for **1b** or **2b** and *iso*-propyl for **1c** or **2c**.

We herein report the synthesis and characterization of two sets of cobalt aminodiphosphine complexes (**1** and **2**) and their application in the catalytic oxidation of *n*-octane in acetonitrile using *tert*-butyl hydroperoxide (TBHP) as the oxidant (Fig. 2.1). The rigidity (**1**) and flexibility (**2**) of the ligand backbone was varied to asses whether this will influence the catalytic activity. The substituent on the nitrogen atom was also varied making use of three different types of functional groups, a ringed (cyclohexyl), straight chained (*n*-pentyl) and a branched (*iso*-propyl) substituent, with the intention of observing if these groups have an effect on the catalytic activity and selectivity to the products of oxidation. To our knowledge the complexes used in this study are new. Furthermore,

limited studies have been carried out in the activation of *n*-alkanes, as compared to cycloalkanes, due to their low activity and tendency to undergo over oxidation. However, valorization of medium length chain *n*-alkanes is of special importance since these are the building blocks in the chemical industry and provide a cheaper alternate feedstock.⁵³⁻⁵⁵

2.3 Experimental

2.3.1 Synthesis and characterization of compounds

All experiments were performed using standard Schlenk techniques under inert conditions in moisture free glassware with anhydrous solvents. All solvents were analytical grade. To render the reaction glassware moisture free, it was heated with a heat gun followed by cycles of vacuum and nitrogen pressure. Diethyl ether and hexane were distilled from sodium benzophenoneketyl under nitrogen. Dichloromethane was distilled from P₂O₅, and ethanol from magnesium turnings. Deuterated solvents were used as received and stored in a desiccator. The NMR spectra were recorded at 400 MHz (¹H), 100 MHz (¹³C) and 162 MHz (³¹P) using a Bruker Ultrashield 400 MHz spectrometer. ¹H NMR and ¹³C{¹H} NMR chemical shifts are reported in parts per million (ppm) downfield from tetramethylsilane. ¹H NMR and ¹³C{¹H} NMR signals were referenced to the residual hydrogen signal of CDCl₃ (7.26 ppm) and (77.16 ppm) respectively. ³¹P NMR chemical shifts were reported in parts per million (ppm) from triphenylphosphine (-17.6 ppm). The FT-IR spectra were recorded using a Perkin Elmer Universal Attenuated Total Reflection (ATR) Sampling Accessory attached to the FT-IR series 100. Elemental analyses were carried out on a Thermo-Scientific Flash 2000 CHNS/O analyzer. All PNP (**1** and **2**) ligands were synthesized with modification of literature procedure.^{20,56}

Synthesis of [Ph₂PN(Cy)PPh₂]CoCl₂ (1a**).** The synthesis was adapted from a reported procedure in literature.⁵⁷ To a 100 ml two necked round bottom flask, 10 ml of ethanol was added and purged with nitrogen for 10 minutes. Thereafter, [Ph₂PN(Cy)PPh₂] (0.62 mmol, 0.29 g) and CoCl₂.6H₂O (0.63 mmol, 0.15 g) were added. The solution was slowly stirred at room temperature. The round bottom flask was equipped with a condenser and the solution was brought to reflux at 77 °C. After 15 minutes under reflux the solution changed color from blue to green. After 24 hours diethyl ether was added to allow precipitation of the complex. The solvent was decanted and the complex was washed with diethyl ether (3 x 10 ml) and dried under high vacuum. Crystals were grown from diethyl ether and dichloromethane through vapour diffusion. Yield: 59%, 0.22 g. Decomposes >192°C. IRv_{max} (ATR)/cm⁻¹: 997 (m), (P-N); 1067 (m) (cyclohexyl ring vibrations); 1433 (m) (aromatic ring); 2852 (s) (CH₂). Anal. (%) Calcd for C₃₀H₃₁Cl₂CoNP₂: C: 60.3%; H: 5.2%; N: 2.3%. Found: C: 60.3%; H: 5.2%; N: 2.3%.

Synthesis of [Ph₂PN(C₅H₁₁)PPh₂]CoCl₂ (1b**).** Synthesized according to the procedure described for **1a** except that [Ph₂PN(C₅H₁₁)PPh₂] (0.62 mmol, 0.290 g) was used. Yield: 45%, 0.16 g. Decomposes >227 °C. IRv_{max}

(ATR)/cm⁻¹: 998 (*s*), (P-N); 1434 (*m*) (aromatic ring); 2945 (*s*) (CH₂). Anal. (%) Calcd for C₂₉H₃₁Cl₂CoNP₂: C: 59.5%; H: 5.3%; N: 2.4%. Found: C: 58.6%; H: 6.0%; N: 2.2%.

Synthesis of [Ph₂PN(C₃H₇)PPh₂]CoCl₂ (1c). Synthesized according to the procedure described for **1a** except that [Ph₂PN(C₃H₇)PPh₂] (0.62 mmol, 0.27 g) was used. Yield: 61%, 0.21 g. Decomposes >165 °C. IR ν_{max} (ATR)/cm⁻¹: 998 (*s*), (P-N); 1434 (*m*) (aromatic ring); 2933 (*s*) (CH₂). Anal. (%) Calcd for C₂₇H₂₇Cl₂CoNP₂: C: 58.2%; H: 4.9%; N: 2.5%. Found: C: 58.0%; H: 5.2%; N: 2.4%.

Synthesis of [Ph₂PC₂H₄N(Cy)C₂H₄PPh₂]CoCl₂ (2a). Synthesized according to the procedure described for **1a** except that [Ph₂PC₂H₄N(Cy)C₂H₄PPh₂] (0.62 mmol, 0.32 g) was used. Yield: 81 %, 0.33 g. Melting point: 251-252 °C. IR ν_{max} (ATR)/cm⁻¹: 1030 (*m*) (cyclohexyl ring vibrations); 1434 (*m*) (aromatic ring); 2931 (*s*) (CH₂). Anal. (%) Calcd. for C₃₄H₃₉Cl₂CoNP₂: C: 62.5%; H: 6.02%; N: 2.14%. Found: C: 61.8%; H: 6.08%; N: 2.08%.

Synthesis of [Ph₂PC₂H₄N(C₅H₁₁)C₂H₄PPh₂]CoCl₂ (2b). Synthesized according to the procedure described for **1a** except that [Ph₂PC₂H₄N(C₅H₁₁)C₂H₄PPh₂] (0.62 mmol, 0.32 g) was used. Yield: 82 %, 0.26 g. Melting point: 190-192 °C. IR ν_{max} (ATR)/cm⁻¹: 1434 (*m*) (aromatic ring); 2952 (*s*) (CH₂). Anal. (%) Calcd. for C₃₄H₃₉Cl₂CoNP₂: C: 61.8%; H: 6.13%; N: 2.18%. Found: C: 62.1%; H: 6.18%; N: 2.18%.

Synthesis of [Ph₂PC₂H₄N(C₃H₇)C₂H₄PPh₂]CoCl₂ (2c). Synthesized according to the procedure described for **1a** except that [Ph₂PC₂H₄N(C₃H₇)C₂H₄PPh₂] (0.62 mmol, 0.31 g) was used. Yield: 40 %, 0.15 g. Melting point: 250-253 °C. IR ν_{max} (ATR)/cm⁻¹: 1435 (*m*) (aromatic ring); 2869 (*s*) (CH₂); 2964 (*s*) (CH). Anal. (%) Calcd. for C₃₁H₃₅Cl₂CoNP₂: C: 60.7%; H: 5.75%; N: 2.28%. Found: C: 60.4%; H: 5.83%; N: 2.19%.

2.3.2 Crystal structure analysis

Crystals of compounds **2a** and **2c** were grown by the vapour diffusion of diethyl ether into a solution of the complexes in dichloromethane at room temperature to give blue crystals for **2a** and **2c**. The crystals of the complexes were each selected and glued onto the tip of glass fibers separately. (More information is available in Appendix A).

The crystals were then mounted in a stream of cold nitrogen at 100(1) K and centered in the X-ray beam by using a video camera. Crystal evaluation and data collection were performed on a Bruker Smart *APEXII* diffractometer with Mo K α radiation ($\lambda = 0.71073 \text{ \AA}$) and a diffractometer to crystal distance of 4.00 cm. The initial cell matrix was obtained from three series of scans at different starting angles. Each series consisted of 12 frames collected at intervals of 0.5° in a 6° range with the exposure time of about 10 seconds per frame.

Table 2.1. Crystal data and structure refinement for complexes **2a** and **2c**.

	2a	2c
Empirical formula	C ₃₄ H ₃₉ Cl ₂ CoNP ₂	C ₃₁ H ₃₅ Cl ₂ CoNP ₂
Formula weight	653.43	613.37
Temperature K	173(2)	173(2)
Wavelength Å	0.71073	0.71073
Crystal system	Monoclinic	Monoclinic
Space group	P2 ₁ /c	P2 ₁ /c
a (Å)	9.7475(16)	9.1436(3)
b (Å)	11.1289(18)	16.8343(5)
c (Å)	30.195(5)	19.0478(6)
α (°)	90	90
β (°)	104.044(9)	95.1650(10)
γ (°)	90	90
Volume (Å ³)	3177.6(9)	2920.05(16)
Z	4	4
Density _{calc} Mg/m ³	1.366	1.395
Absorption coefficient mm ⁻¹	0.833	0.902
F(000)	1364	1276
Crystal size (mm ³)	0.19 x 0.11 x 0.11	0.19 x 0.11 x 0.11
Theta range (°)	1.96 to 25.00	2.15 to 25.00
Index ranges	-11 ≤ h ≤ 11 -13 ≤ k ≤ 13 -30 ≤ l ≤ 35	-10 ≤ h ≤ 10, -20 ≤ k ≤ 20, -22 ≤ l ≤ 22
Reflections collected	28020	59698
Independent reflections	5547 [R(int) = 0.1299]	5132 [R(int) = 0.0314]
Completeness to theta	25.00°; 99.1%	100.0
Absorption correction	Semi-empirical from equivalents	Semi-empirical from equivalents
Max. and min. trans	0.9139 and 0.8577	0.9073 and 0.8473
Refinement method	Full-matrix least-squares on F ²	Full-matrix least-squares on F ²
Data / restraints / parameters	5547 / 0 / 361	5132 / 0 / 336
Goodness-of-fit on F ²	1.170	1.025
Final R indices [I>2σ(I)]	R1 = 0.1014, wR2 = 0.2331	R1 = 0.0229, wR2 = 0.0496
R indices (all data)	R1 = 0.1375, wR2 = 0.2449	R1 = 0.0301, wR2 = 0.0534
Extinction coefficient	N/A	N/A
Largest diff. peak and hole (e.Å ⁻³)	1.035 and -0.804	0.364 and -0.268

The reflections were successfully indexed by an automated indexing routine built in the *APEXII* program suite.⁵⁸ Data collection method involved ω scans of width 0.5°. Data reduction was carried using the program *SAINT+*.⁵⁸ The structure was solved by direct methods using *SHELXS*⁵⁹ and refined by *SHELXL*⁵⁸. All structures were checked for solvent-accessible cavities using *PLATON*⁶⁰ and the graphics were performed with ORTEP3 .

Non-H atoms were first refined isotropically and then by anisotropic refinement with full-matrix least-squares calculations based on F^2 using *SHELXS*.⁶⁰ All H atoms were positioned geometrically and allowed to ride on their respective parent atoms. All H atoms were refined isotropically. Crystal data and structure refinement information for all the complexes are summarized in Table 2.1 (Appendix A). (These data can be obtained free of charge from the Cambridge Crystallographic Data Centre via www.ccdc.cam.ac.uk/data_request/cif. The data of the crystal structure are available quoting CCDC 10282560 and 1028261).

2.3.3 Oxidation of *n*-octane

All catalytic reactions were performed under inert conditions in moisture free glassware with anhydrous solvents. MeCN was degassed for 10-15 minutes before use. All reagents were weighed and handled in air. All products were analyzed using a PerkinElmer Auto System gas chromatograph fitted with a Flame Ionisation Detector (FID) set at 260 °C. A Pona column (50 m x 0.20 mm x 0.5μm) was utilized with the injector temperature set at 240 °C. Catalytic testing was carried out in acetonitrile at 80 °C, using *tert*-butyl hydroperoxide (TBHP) as the respective oxidant. The catalyst to substrate ratio was kept constant at 1:100. A two-necked pear shaped flask was charged with 10 mg of the respective catalyst, pentanoic acid (as an internal standard), *n*-octane, TBHP and 10 ml of the solvent. The flask was equipped with a reflux condenser. The mixture was stirred, heated to the respective temperature and maintained for 48 hours in an oil bath. After a time period, an aliquot was removed using a Pasteur pipette and filtered through cotton wool and a silica gel plug, after which PPh₃ was added (for reduction of the remaining TBHP and alkylperoxides which are formed as primary products in alkane oxidation)³³. An aliquot (0.5 μl) was injected into the GC and quantified.

2.4 Results and Discussion

2.4.1 Synthesis and characterization of the compounds

Complexes **1** and **2** were synthesized by adaptation of a procedure by Romerosa et al.⁵⁷ The respective ligands were added to a solution of CoCl₂.6H₂O in ethanol and after refluxing for 24 hours, diethyl ether was added to allow precipitation of the respective complex. The precipitates of complexes **1** were green, whilst those of **2** were blue. The complexes were fully characterized by elemental analyses, infrared spectroscopy and single crystal X-ray diffraction. The complexes are paramagnetic, hence elucidation by NMR was unsuccessful.^[57] The elemental

analyses of the complexes matched the calculated values and this is indicative of complexation, as are the sharp melting points and crystal structures of **2a** and **2c**. A shift in the ν_{P-N} band in the IR spectra of complexes **1** and their respective ligands also are noted and shown in Table 2.2.

Table 2.2. Comparison of the ν_{P-N} band shifts of complexes **1** and their respective ligands.

Substituent	ν_{P-N} (Ligand)/ cm^{-1}	ν_{P-N} (Complex 1)/ cm^{-1}
a	982	997
b	977	998
c	986	998

2.4.2 Description of the X-ray crystal structures

Blue crystals of complexes **2a** and **2c** were obtained by vapour diffusion of diethyl ether into a dichloromethane solutions of complexes **2a** and **2c**. *ORTEP* diagrams of **2a** and **2c** are given in Fig. 2.2, while bond distances and angles are provided in Table 2.3. Both compounds crystallize with one molecule of the respective complexes in the asymmetric units. In both complexes the cobalt metal is bound to one ligand through the phosphorous atoms of the ligand and two chlorine atoms, resulting in a distorted tetrahedral geometry around the metal center. The P—Co—P bond angles are 116.42(9) and 116.32(2) $^{\circ}$ in **2a** and **2c** respectively, while the two Cl—Co—P angles lie between 100.53(7) and 108.35(1) $^{\circ}$. The Cl—Co—Cl bond angles are 120.4(1) and 118.50(2) $^{\circ}$ in **2a** and **2c** respectively. The P—Co bond lengths for both complexes are comparable to related complexes found in literature.⁶¹

Table 2.3. Selected bond lengths (\AA) and angles ($^{\circ}$) for complexes **2a** and **2c**.

	2a		2c
Bond lengths			
Co(1)—P(1)	2.348(3)	Co(1)—P(1)	2.3618(5)
Co(1)—P(2)	2.368(3)	Co(1)—P(2)	2.3684(5)
Co(1)—Cl(1)	2.225(3)	Co(1)—Cl(1)	2.2363(5)
Co(1)—Cl(2)	2.245(3)	Co(1)—Cl(2)	2.2169(5)
Bond angles			
P(1)—Co(1)—P(2)	116.42(9)	P(1)—Co(1)—P(2)	116.32(2)
Cl(1)—Co(1)—Cl(1)	120.39(10)	Cl(1)—Co(1)—Cl(1)	118.50(2)
Cl(1)—Co(1)—P(1)	106.15(7)	Cl(2)—Co(1)—P(2)	103.357(18)
Cl(2)—Co(1)—P(2)	102.53(9)	Cl(1)—Co(1)—P(1)	108.346(18)
Cl(2)—Co(1)—P(1)	100.53(7)	Cl(2)—Co(1)—P(1)	102.530(18)
Cl(1)—Co(1)—P(2)	110.99(10)	Cl(1)—Co(1)—P(2)	108.116(18)

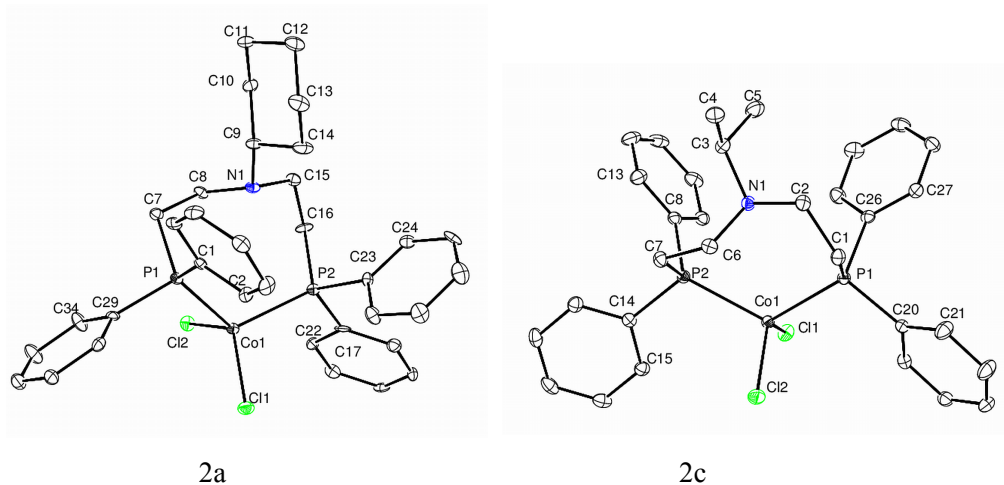


Figure 2.2. The molecular structures of complexes **2a** and **2c** showing part of the atom-numbering scheme. Displacement ellipsoids are drawn at 50% probability level and H atoms have been omitted for clarity.

2.4.3 Oxidation of *n*-octane

The catalytic activity of complexes **1** and **2** were explored in the oxidation of *n*-octane. All catalytic runs were carried out (in duplicate or triplicate in some cases) at 80 °C in acetonitrile with TBHP (*t*-BuOOH) as the oxidant under argon atmosphere. Preliminary work showed low conversions with no significant change in product selectivity at lower temperatures. At lower reaction times poor selectivity to the alcohols and low conversion was observed. TBHP as an oxidant has been used in a number of oxidation reactions and has the advantage over other oxidants in that it has higher solubility in organic solvents, which contain dissolved hydrophobic hydrocarbons.⁶² Optimization of the substrate to oxidant ratio was carried out, by investigating *n*-octane to TBHP ratios of 1:2.5; 1:5; 1:7.5 and 1:10, where the ratio of 1:5 gave the highest conversion with good selectivity. Control experiments were carried out in the absence of the catalyst and oxidant respectively. In the former, a 2% conversion was observed with the highest selectivity to 2-octanone (Fig. 2.3). However, the latter reaction showed a 0% conversion. Blank studies with oxidant and catalysts showed an observable color change from green to blue for catalysts **1** and no change in color for catalysts **2**. Testing was also carried out with cobalt chloride (CoCl₂.6H₂O) under the same catalytic conditions. A 2% conversion was observed, with selectivity to the over oxidized products, namely the ketones and octanoic acid. This is the same conversion as for the blank reaction with TBHP, only but with a greater selectivity to the over oxidized products. It is known that with the simple salts of iron, low activities have been exhibited in oxidation reactions.³³

Comparing the activity of catalysts **1** and **2** (Fig. 2.4), the latter show a higher conversion with the highest being for **2a** with 14% conversion. This can be related to the bite angle (P-

Co-P), where catalysts **2** have a much larger bite angle of 116.32° (**2c**) in comparison to catalysts **1**, $\sim 71.19^\circ$. The more sterically hindered catalysts limit the activity in comparison to the more flexible catalysts **2**. The bite angle is known to have an impact on the activity and selectivity of catalytic reactions.⁶³ It has been reported that the effect of bite angle on C-X bond activation originates from an electronic factor, where the donor-acceptor orbital interactions (metal d orbitals to the substrate σ^*_{c-x}) stabilize the transition state.^[64] As the metal-ligand d-hybrid orbital is driven to smaller bite angles, the transition state becomes more stabilized.⁶⁴ Interestingly, a decrease in the activity for both catalysts **1** and **2** is observed, as one moves from the cyclohexyl (**a**) to the *iso*-propyl (**c**) substituent. Noteworthy, for these ligands used in ethylene tetramerisation, a similar trend is observed in terms of their activity with chromium as the active metal.²⁰ This can be attributed to the basicity of the substituent on the nitrogen atom.²⁰

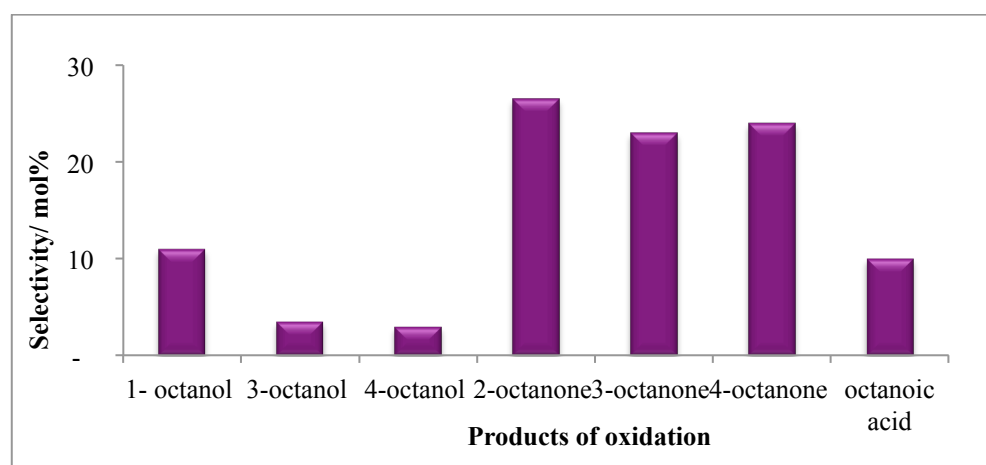


Figure 2.3. Selectivity of the blank reaction (no catalyst) to products of oxidation at a ratio of 1:5 of substrate to oxidant at $80\text{ }^\circ\text{C}$ in acetonitrile.

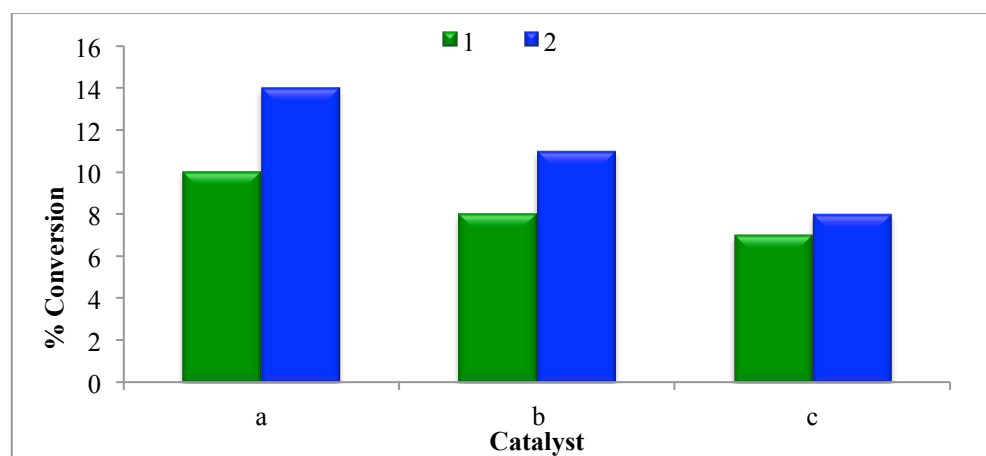


Figure 2.4. Conversion of *n*-octane by catalysts **1** and **2** at a ratio of 1:5 of substrate to oxidant at $80\text{ }^\circ\text{C}$ in acetonitrile.

Both sets of catalysts (**1** and **2**) are highly selective to the ketones, with 2-octanone being the dominant product (Fig. 2.5 and 2.6). This indicates that the catalyst causes oxidation of the internal carbons more readily than the terminal carbon. Such cases, with 2-octanone being the dominant product, have been observed in the biological hydroxylation of alkanes catalyzed by methane monooxygenase.¹³ The C(2) position is three times as active as the C(1), and is most reactive in linear alkane chains as reflected by the regioselectivity in reactions for *n*-heptane, as well as *n*-octane.⁵ Over-oxidation is highly prevalent at the C(1) position of the *n*-octane chain for both catalysts, with higher selectivity to octanoic acid and very low selectivity to 1-octanol and no selectivity to octanal. Ketone formation is also observed with ruthenium phosphine compounds, in which cases only 2 and 4-octanone are observed with a 4% conversion.^{47,48} Chen and White have reported yields to 2 and 3 octanone with no selectivity to primary products using a bulky iron electrophilic catalyst.³

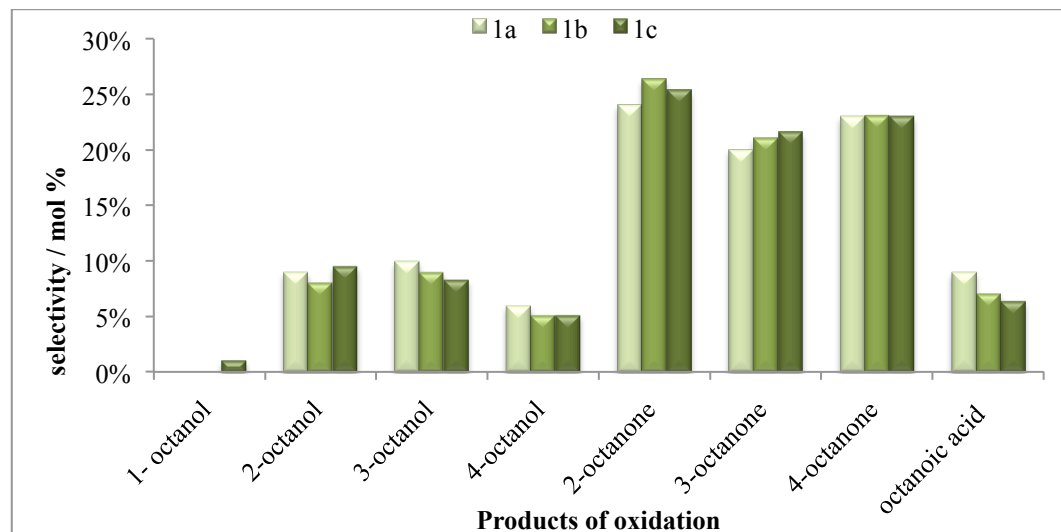


Figure 2.5. Selectivity of catalyst **1** to the products of oxidation at a ratio of 1:5 of substrate to oxidant at 80 °C in acetonitrile.

Following the method of Shul’pin and coworkers, addition of triphenylphosphine to a filtered (through a plug of silica to remove the catalyst) aliquot of the reaction mixture 10 mins prior to GC analysis was performed, since an increase in the alcohol peak and a decrease in the ketone peak can result.³³ This was the true concentration of the alcohols and ketones, since the alkyl hydroperoxides that are present are completely reduced to the corresponding alcohols. For catalysts **1**, a change in the selectivity to the alcohol and ketone before and after addition of the PPh₃ was observed, however, for catalysts **2** no observable change was noted.

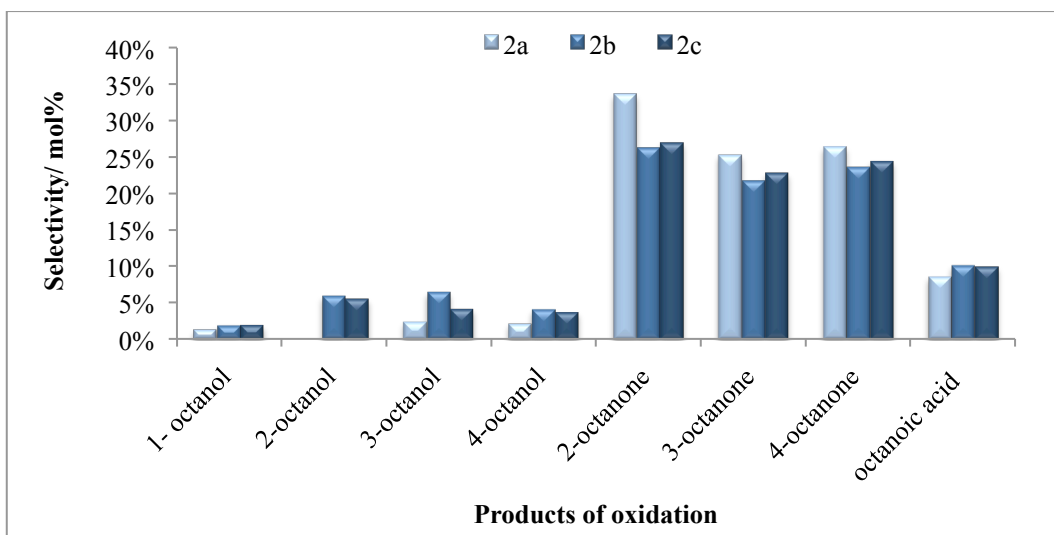


Figure 2.6. Selectivity of catalyst **2** the products of oxidation at a ratio of 1:5 of substrate to oxidant at 80 °C in acetonitrile.

The regioselectivity parameters (Table 2.4) further indicate that the C(2) position is the most activated carbon of the *n*-octane chain, with the C(1) being the least activated. The catalysts with the pentyl and *iso*-propyl (**b** and **c**) substituents are most selective to the alcohols, with catalysts **2** being more selective to the alcohols than **1**.

Table 2.4 Selectivity parameters in the oxidation of *n*-octane by catalysts **1** and **2**.

Catalyst	Alcohol ^a	Ketone ^b	Total ^c
	C(1):C(2):C(3):C(4)	C(2):C(3):C(4)	C(1):C(2):C(3):C(4)
1a	0:1.5:1.7:1	1.2:1:1.2	1:5.5:5:4.8
1b	0:1.6:1.8:1	1.2:1:1.1	1:7.4:6.5:6.1
1c	0:2:1.6:1	1.1:1:1.0	1:7.6:6.5:6.1
2a	1:0:3.3:3.3	1.4:1:1	1:5.2:4.1:4.2
2b	1:4.2:4.2:2.9	1.1:1:1	1:4:3.5:3.4
2c	1:4.2:2.9:2.9	1.2:1:1	1:4.1:3.4:3.5

^a Parameters C(1):C(2):C(3):C(4) are the relative reactivities of hydrogen atoms at carbon 1, 2, 3 and 4 of the *n*-octane chain.

^b The calculated reactivities from the % selectivity are normalized, i.e. calculated taking into account the number of hydrogen atoms at each carbon.

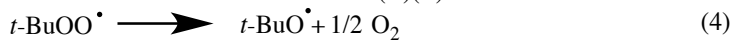
^c Includes the % selectivity of octanoic acid, alcohols and ketones and the values are normalized.

When using TBHP as an oxidant, the ketone product forms from the oxidation of the alcohol (over oxidation).³⁵ Since the selectivity to the ketones is much greater, it is likely that the oxidation reaction proceeds via the formation of hydroxyl radicals where the metal complex activates the oxidant, *t*-BuOOH, forming a reactive species, the hydroxyl radical, which

attacks *n*-octane.^{31,65} Taking into consideration the metal and the substrate being activated we propose a mechanism which is consistent to that present in literature for the oxidation of alkanes using TBHP as an oxidant.^{5,66-70} We assume that the reaction takes place in the coordination sphere of the metal complex which would explain the influence of the ligand system on the reaction. The *t*-BuO[•] is formed by the reduction of *t*-BuOOH by the Co(II)L which generates a hydroxo-Co(III) species (eqn 1).^{66,67}



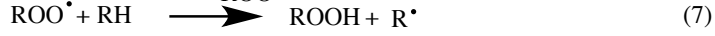
The hydroxo species reacts further with *t*-BuOOH (eqn 2) which then decomposes to form the *t*-BuOO[•] radical (eqn 3) which gives a further *t*-BuO[•] radical after dismutation (eqn 4).^{66,67}



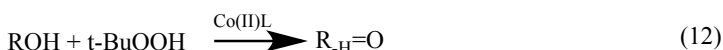
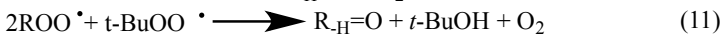
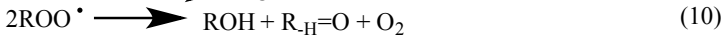
The oxygen centered radicals generated in eqn 1 and 4 attack the *n*-octane with the formation of octyl radicals (eqn 5).^{5,66,67}



The octyl peroxy radical is formed (eqn 6) upon reaction of R[•] with oxygen which reacts with *n*-octane to form ROOH (an organo-hydroperoxide, eqn 7) and thereafter undergoes homolytic decomposition via the cobalt(II)L complex to form the RO[•] (an organooxyl radical, eqn 8).^{5,66,67}



By H-abstraction from the octane, the RO[•] radical forms the octanol (ROH, eqn 9) and the ROO[•] decomposes to octanol and octanone (eqn 10) or is regenerated via eqn 7. Increase in the ketone selectivity occurs when the ROO[•] attacks the *t*-BuOO[•] through mixed molecular Russel termination (eqn 11).⁷¹ Deeper oxidation of octanol forming octanones is generated by the Co(II)L complex (eqn 12).^{5,66,67}



2.5 Conclusion

In this chapter, it is reported that new cobalt aminodiphosphine complexes have been synthesized and fully characterized and were used as catalysts in the oxidation of *n*-octane. Higher conversion is seen with the more flexible complexes **2** as compared to the sterically hindered complexes **1** and this may be attributed to their bite angle. The substituent on the nitrogen atom has an effect of the activity, where the catalysts with the cyclohexyl ring substituents are much more active than those with branched or straight chain substituents. The ketones were the dominant product, with the C(2) position being the most activated in the octane chain contributing to the high selectivity of 2-octanone (34%). 1-Octanol was prominent with catalysts **2**, however, over oxidation was also more evident with these catalysts contributing to the high selectivity of the ketones.

2.6 References

- [1] Crabtree, R. H. *J. Organomet. Chem.* **2004**, *689*, 4083-4091.
- [2] White, M. C. *Science* **2012**, *335*, 807-809.
- [3] Chen, M. S.; White, M. C. *Science* **2010**, *327*, 566-571.
- [4] He, Y.; Gorden, J. D.; Goldsmith, C. R. *Inorg. Chem.* **2011**, *50*, 12651-12660.
- [5] Kirillov, A. M.; Kirillova, M. V.; Shul'pina, L. S.; Figiel, P. J.; Gruenwald, K.R.; Guedes da Silva, M. F.C.; Haukka, M.; Pombeiro, A. J. L.; Shul'pin, G.B. *J. Mol. Catal A: Chem.* **2011**, *350*, 26-34.
- [6] Kirillova, M. V.; Kirillov, A. M.; Mandelli, D.; Carvalho, W. A.; Pombeiro, A. J. L.; Shul'pin, G. B. *J. Catal.* **2010**, *272*, 9-17.
- [7] Conley, B. L.; Tenn III, W. J.; Young, K. J. H.; Ganesh, S. K.; Meier, S. K.; Ziatdinov, V.R.; Mironov, O.; Oxgaard, J.; Gonzales, J.; Goddard III, W. A.; Periana, R. A. *J. Mol. Catal. A: Chem.* **2006**, *251*, 8-23.
- [8] Kopylovich, M. N.; Kirillov, A. M.; Baev, A. K.; Pombeiro, A. J. L. *J. Mol. Catal. A: Chem.* **2003**, *206*, 163-178.
- [9] Sivaramakrishna, A.; Suman, P.; Veerashekhar G, E.; Janardan, S.; Sravani, C.; Sandeep, T.; Vijayakrishna, K.; Clayton, H. S. *J. Coord. Chem.* **2013**, *66*, 2091-2109.
- [10] Young, R. D. *Chem. Euro. J.* **2014**, *20*, 12704-12718.
- [11] Labinger, J. A.; Bercaw, J. E. *Nature* **2002**, *417*, 507-514.
- [12] Klei, S. R.; Tan, K. L.; Golden, J. T.; Yung, C. M.; Thalji, R. K.; Ahrendt, K.A.; Ellman, J. A.; Tilley, T. D.; Bergman, R. G. *J. Am. Chem. Soc.* **2004**, *885*, 46-55.
- [13] Kirillov, A. M.; Kirillova, M. V.; Pombeiro, A. J. L. *Coord. Chem. Rev.* **2012**, *256*, 2741-2759.
- [14] Kirillov, A. M.; Shul'pin, G. B. *Coord. Chem Rev.* **2013**, *257*, 732-754.
- [15] Chen, M. S.; White, M. C. *J. Am. Chem. Soc.* **2004**, *126*, 1346-1347.
- [16] Fraunhoffer, K. J.; Bachovchin, D. A.; White, M. C. *Org. Lett.* **2004**, *7*, 223-226.
- [17] Vermeulen, N. A.; Chen, M. S.; White, M.C. *Tetrahedron* **2009**, *65*, 3078-3084.
- [18] Brodsky, B. H.; Du Bois, J. *J. Am. Chem. Soc.* **2005**, *127*, 15391-15393.
- [19] Teo, S.; Weng, Z.; Hor, T. S. A. *Organometallics* **2008**, *27*, 4188-4192.
- [20] Blann, K.; Bollmann, A.; de Bod, H.; Dixon, J. T.; Killian, E.; Nongodlwana,P. Maumela, M. C.; Maumela, H.; McConnel, A. E.; Morgan, D. H.; Overette, M. J.; Pfetorius, M.; Kuhlmann, S.; Wasserscheid, P. *J. Catal.* **2007**, *249*, 244-249.

- [21] Blann, K.; Bollmann, A.; Dixon, J. T.; Hess, F. M.; Killian, E.; Maumela, H.; Morgan, D. H.; Neveling, A.; Otto, S.; Overett, M. *J. Chem. Commun.* **2005**, 620-621.
- [22] Bollmann, A.; Blann, K.; Dixon, J. T.; Hess, F. M.; Killian, E.; Maumela, H.; McGuiness, D. S.; Morgan, D. H.; Neveling, A.; Otton, S.; Overette, M.; Slawin, A. M. Z.; Wassercheid, P.; Kihlmann, S. *J. Am. Chem. Soc.* **2004**, 126, 14712-14713.
- [23] Overett, M. J.; Blann, K.; Bollmann, A.; Dixon, J. T.; Hess, F.; Killian, E.; Maumela, H.; Morgan, D. H.; Neveling, A.; Otto, S. *Chem. Commun.* **2005**, 622-624.
- [24] Bowen, L. E.; Haddow, M. F.; Orpen, A. G.; Wass, D. F. *Dalton Trans.* **2007**, 1160-1168.
- [25] Bowen, L. E.; Charernsuk, M.; Hey, T. W.; McMullin, C. L.; Orpen, A. G.; Wass, D. F. *Dalton Trans.* **2010**, 39, 560-567.
- [26] Benito-Garagorri, D.; Alves, L. G. a.; Puchberger, M.; Mereiter, K.; Veiros, L. F.; Calhorda, M. J.; Carvalho, M. D.; Ferreira, L. P.; Godinho, M.; Kirchner, K. *Organometallics* **2009**, 28, 6902-6914.
- [27] Benito-Garagorri, D.; Kirchner, K. *Acc. Chem. Res.* **2008**, 41, 201-213.
- [28] van der Boom, M. E.; Milstein, D. *Chem. Rev.* **2003**, 103, 1759-1792.
- [29] Xu, X.; Xi, Z.; Chen, W.; Wang, D. *J. Coord. Chem.* **2007**, 60, 2297-2308.
- [30] Albrecht, M.; van Koten, G. *Angew. Chem. Int. Ed.* **2001**, 40, 3750-3781.
- [31] Shul'pin, G. B. *C.R. Chimie* **2003**, 6, 163-178.
- [32] Gupta, K. C.; Kumar Sutar, A.; Lin, C.C. *Coord. Chem. Rev.* **2009**, 253, 1926-1946.
- [33] Shul'pin, G. B.; Kudinov, A. R.; Shul'pina, L. S.; Petrovskaya, E. A. *J. Organomet. Chem.* **2006**, 691, 837-845.
- [34] Stahl, S. S.; Labinger, J. A.; Bercaw, J. E. *Angew. Chem. Int. Ed.* **1998**, 37, 2180-2192.
- [35] Yiu, S.; Man, W.; Lau, T. *J. Am. Chem. Soc.* **2008**, 130, 10821-10827.
- [36] Nizova, G. V.; Krebs, B.; Süss-Fink, G.; Schindler, S.; Westerheide, L.; Cuervo, G. L.; Shul'pin, G. B. *Tetrahedron* **2002**, 58, 9231-9237.
- [37] Bahramian, B.; Mirkhani, V.; Mogahadam, M.; Tangestaninejad, S. *Catal. Commun.* **2006**, 7, 289-296.
- [38] Doro, F. G.; Smith, J. R. L.; Ferreira, A. G.; Assis, M. D. *J. Mol. Catal. A: Chem.* **2000**, 164, 97-108.
- [39] Kille, S.; Zilly, F. E.; Acevedo, J. P.; Reetz, M. T. *Nat. Chem.* **2011**, 3, 738-743.
- [40] Tordin, E.; List, M.; Monkowius, U.; Schindler, S.; Knör, G. *Inorg. Chimi. Acta* **2013**, 402, 90-96.
- [41] Kanjina, W.; Trakarnpruk, W. *J. Met. Mat. Min.* **2010** 20, 29-34.
- [42] Gormisky, P. E.; White, M. C. *J. Am. Chem. Soc.* **2013**, 135, 14052-14055.
- [43] Bigi, M. A.; Reed, S. A.; White, M. C. *J. Am. Chem. Soc.* **2012**, 134, 9721-9726.
- [44] White, M. C. *Synlett* **2012**, 23, 2746-2748.
- [45] Soobramoney, L.; Bala, M. D.; Friedrich, H. B. *Dalton Trans.* **2014**, 43, 15968-15978.
- [46] Britovsek, G. J. P.; England, J.; Spitzmesser, S. K.; White, A. J. P.; Williams, D. J. *Dalton Trans.* **2005**, 945-955.
- [47] Wong, W. K.; Chen, X. P.; Chik, T. W.; Wong, W. Y.; Guo, J. P.; Lee, F. W. *Euro. J. Inorg. Chem.* **2003**, 2003, 3539-3546.
- [48] Wong, W.K.; Chen, X. P.; Guo, J. P.; Chi, Y. G.; Pan, W. X.; Wong, W. Y. *J. Chem. Soc. Dalton Trans.* **2002**, 1139-1146.
- [49] Mirkhani, V.; Moghadam, M.; Tangestaninejad, S.; Mohammadpoor-Baltork, I.; Rasouli, N. *Catal. Commun.* **2008**, 9, 2411-2416.
- [50] Cagnina, A.; Campestrini, S.; Di Furia, F.; Ghiotti, P. *J. Mol. Catal. A: Chem.* **1998**, 130, 221-231.
- [51] Smith L, J. R.; Iamamoto, Y.; Vinhado, F. S. *J. Mol. Catal. A: Chem* **2006**, 252, 23-30.
- [52] Pereira, R.; Rufo, M.; Schuhardt, U. *J. Braz. Chem. Soc.* **1994**, 5, 83-89.
- [53] Gounden, N.; Friedrich, H.; Mahadevaiah, N.; Fadlalla, M. *Catal. Lett.* **2014**, 144, 2043-2051.
- [54] Dasireddy, V. D. B. C.; Singh, S.; Friedrich, H. B. *J. Mol. Catal. A: Chem* **2014**, 395, 398-408
- [55] Dasireddy, V. D. B. C.; Friedrich, H. B.; Singh, S. *Appl. Catal. A: Gen.* **2013**, 467, 142-153.

- [56] Hii, K. K.; Thornton-Pett, M.; Jutand, A.; Tooze, R. P. *Organometallics* **1999**, *18*, 1887-1896.
- [57] Romerosa, A.; Saraiba-Bello, C.; Serrano-Ruiz, M.; Caneschi, A.; McKee, V.; Peruzzini, M.; Sorace, L.; Zanobini, F. *Dalton Trans.* **2003**, 3233-3239.
- [58] Bruker-AXS Bruker-AXS, Madison, Wisconsin, USA. **2009**.
- [59] Sheldrick, G. M. *Acta Cryst. A*. **2008**, *A64*, 112-122.
- [60] Spek, A. L. *Acta Cryst.D*. **2009**, *D65*, 148-155.
- [61] Dong, Q.; Rose, M. J.; Wong, W.-Y.; Gray, H. B. *Inorg. Chem.* **2011**, *50*, 10213-10224.
- [62] Shul'pin, G. B. *Mini-Rev. Org. Chem.* **2009**, *6*, 95-104.
- [63] van Leeuwen, P. W. N. M.; Kamer, P. C. J.; Reek, J. N. H. *Pure Appl.Chem.* **1999**, *71*, 1443-1452.
- [64] van Zeist, W.-J.; Visser, R.; Bickelhaupt, F. M. *Chem: Euro. J.* **2009**, *15*, 6112-6115.
- [65] Fokin, A. A.; Schreiner, P. R. *Chem. Rev.* **2002**, *102*, 1551-1593.
- [66] Mac Leod, T. C. O.; Kirillova, M. V.; Pombeiro, A. J. L.; Schiavon, M. A.; Assis, M. D. *Appl. Catal. A: Gen.* **2010**, *372*, 191-198.
- [67] Förster, S.; Rieker, A.; Maruyama, K.; Murata, K.; Nishinaga, A. *J. Org. Chem.* **1996**, *61*, 3320-3326.
- [68] Shul'pin, G. B.; Golfeto, C. C.; Süss-Fink, G.; Shul'pina, L. S.; Mandelli, D. *Tetrahedron Lett.* **2005**, *46*, 4563-4567.
- [69] Shul'pin, G. B.; Süss-Fink, G.; Shul'pina L.S. *J. Mol.Catal. A: Chem.* **2001**, *170*, 17-34.
- [70] Shul'pin, G. B.; Kozlov, Y.; Shul'pina, L. S.; Kudinov, A. R.; Mandelli, D. *Inorg. Chem. Commun.* **2009**, *48*, 10480-10482.
- [71] Nowotny, M.; Pedersen, L. N.; Hanefeld, U.; Maschmeyer, T. *Chem. Eur. J.* **2002**, *8*, 3724-3731.

Chapter Three

Oxidation of styrene by TBHP using cobalt “PNP” aminodiphosphine complexes as highly effective catalysts

3.1 Abstract

Two types of new “PNP” aminodiphosphine cobalt complexes, $[\text{Ph}_2\text{PN}(\text{R})\text{PPh}_2]\text{CoCl}_2$ (**1**) and $[\text{Ph}_2\text{P}(\text{CH}_2)_2\text{N}(\text{R})(\text{CH}_2)_2\text{PPh}_2]\text{CoCl}_2$ (**2**) where R= C₆H₁₁ (**a**); C₃H₇ (**b**); C₅H₁₁ (**c**), have been used as catalysts in the oxidation of styrene. Optimization studies were carried out with different oxidants and solvent systems. These complexes showed good activity in the oxidation of styrene with TBHP as the oxidant and DCE ,1,2-dichloroethane, as the solvent. The catalysts bearing the rigid backbone **1** are more active than those with the flexible ligand backbone. The complex with the pentyl substituent (**1c**) gave the highest yield to benzaldehyde and styrene oxide.

Keywords: Cobalt; aminodiphosphine; oxidation; styrene

3.2 Introduction

The oxidation of hydrocarbons provides a cost effective method of converting feedstock obtained from oils into bulk chemicals and is an important transformation in the production of fine chemicals.¹ Oxidation of alkenes to their corresponding carbonyl compounds and epoxides is very important in the fine and pharmaceutical grade chemical industries.²⁻¹⁰ More specifically, the products from styrene oxidation, namely, styrene oxide and benzaldehyde are widely used in perfumery, dyes and agro chemicals.¹¹

Transition metal-based systems are able to catalyze these oxidation reactions, however, the choice of catalyst and the oxidant is significant, as these can modify the course of the reaction.¹² For selective oxidation a suitable ligand system is required which is able to alter the catalytic behavior.¹² One such system could include the aminodiphosphine or “PNP” ligand system which has been used extensively in ethylene oligomerization studies.¹³⁻¹⁶ These bi-dentate or multidentate ligands are part of a system that displays high activity, stability and variability, which makes them ideally suited for catalytic applications.¹⁷⁻¹⁹ The activity of the

metal can be tailored through the modification of the ligand backbone, by using different donor substituents or central anionic atoms. The ligand then places a high demand on the stereochemistry of the complex, allowing the reactions of the metal ions to be rather selective.^{20,21}

First row transition metals have received very little attention in oxidation catalysis due to their tendency to initiate free radical reactions.²² Drago et al. and Zombeck et al. performed early work on cobalt Schiff base complexes on the oxidation of terminal olefins and isoeugenol.^{23,24} Few studies have been reported on homogenous systems using cobalt, since the majority of the work has been done on heterogenizing these complexes using supports such as zeolites.^{8,10,25,26} We herein report the application of two sets of cobalt aminodiphosphine complexes (**1** and **2**) in the catalytic oxidation of styrene (Fig. 3.1). The oxidant, temperature and solvent system were varied so as to find the optimum condition for best selectivity and conversion. The substituent on the nitrogen atom was varied making use of three different types of functional groups, a ringed (cyclohexyl), straight chained (*n*-pentyl) and a branched (*iso*-propyl) substituent, with the intention of observing if these groups have an effect on the catalytic activity and selectivity to the products of oxidation.



Figure 3.1. Complexes of type **1** and **2** used in this study as catalysts in the oxidation of styrene. (R= cyclohexyl (**a**); *iso*-propyl (**b**) and pentyl (**c**)).

3.3 Experimental

3.3.1 Oxidation of styrene

All catalytic reactions were performed under inert conditions in moisture free glassware with anhydrous solvents. All reagents were weighed and handled in air. All products were analyzed using a PerkinElmer Auto System gas chromatograph fitted with a Flame Ionisation Detector (FID) set at 290 °C. A Varian DB-5 capillary column (25 m x 0.15 mm x 2μm) was utilized with the injector temperature set at 250 °C. The catalyst to substrate ratio was kept constant at 1:100. A two-necked pear shaped flask was charged with 5 mg of the respective catalyst, benzophenone (as an internal standard), styrene, the respective oxidant and 10 ml of

the solvent). The flask was equipped with a reflux condenser, stirred and the solution heated to the required temperature. The reaction was monitored by removing aliquots using a Pasteur pipette (which was filtered through a silica and cotton wool plug) and injecting these (0.5 µl) into the GC and quantifying. Catalysts were synthesized according to the procedure described in Chapter 2, Section 2.3. All chemicals used in the catalytic testing were purchased from Sigma-Aldrich.

3.4 Results and discussion

Optimization was carried out using catalyst **1a**. The reaction was monitored at 3 h intervals up to 9 h (Fig. 3.2). The temperature was kept constant at 80 °C in acetonitrile (MeCN) where the molar catalyst:styrene ratio used was 1:100, whilst the styrene:TBHP molar ratio was 1:2.5. The conversion increases with time, however, the yield to benzaldehyde and styrene oxide decreases slightly from 6 to 9 h. After 24 h, a 98% conversion was found, with a lower yield to benzaldehyde (19%) and styrene oxide (4%). These results are consistent with the fact that at high temperatures, vinyl C-H bonds of styrene are highly active.^{8,27,28} All further reactions were stopped after 9 h. Deeper oxidation products, like benzoic acid and carbon dioxide were also observed and obtained in higher yield at longer reaction times (> 9 h). This is also noted with other cobalt systems.²² Unlike other reported studies done on the oxidation of styrene, benzene was formed, which increases over time (7% (3 h) to 12% (9 h)).

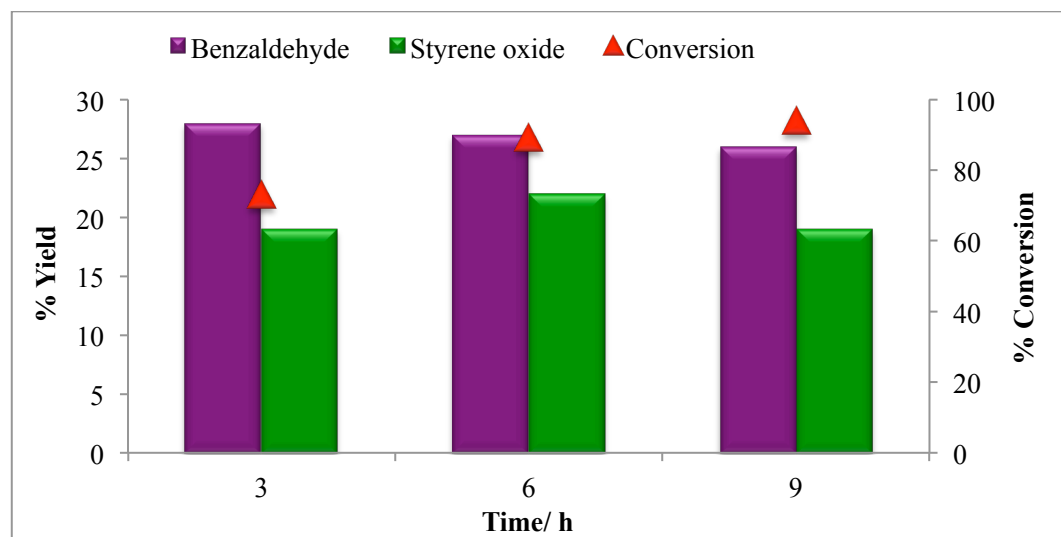


Figure 3.2. Conversion of styrene and yield to benzaldehyde and styrene oxide.

Conditions: Catalyst:Styrene (1:100); Styrene:TBHP (1:2.5); Temperature: 80 °C; Solvent: MeCN;
Catalyst **1a**.

A lower styrene:TBHP molar ratio (1:1.5) under the same conditions mentioned above (catalyst:styrene (1:100); temperature 80 °C; and MeCN as the solvent) was also investigated and after 9 h, the conversion was 82% and the yield to benzaldehyde and styrene oxide was 28% and 15% respectively. However, when the catalyst:styrene ratio was decreased from 1:100 to 1:50 with the styrene:TBHP ratio maintained at 1:2.5 at 80 °C, a 87% conversion was obtained, with lower yields to benzaldehyde (24%) and styrene oxide (10%) due to over oxidation.

The reaction was also carried out at room temperature (RT) and 50 °C where the styrene:TBHP ratio used was 1:2.5 and catalyst:styrene ratio used was 1:100. At 50 °C, using TBHP as the oxidant, a 45% conversion was observed with a 29% yield to benzaldehyde and 2% yield to styrene oxide. At RT no conversion was noted. When the oxidant was changed to hydrogen peroxide, with the same ratios mentioned above at both 50 and 80 °C, the conversion increases, with a higher yield to benzaldehyde at 80 °C (Table 3.1). However, better yields and conversion at these temperatures using TBHP were obtained. The activation energy at these respective temperatures was also calculated. The activation energy for the reaction using TBHP (21 kJ mol⁻¹) as the oxidant was lower than when H₂O₂ (35 kJ mol⁻¹) was used. This explains the higher conversion for the TBHP system. When using H₂O₂, in some reported cases, reactions fail to activate the peroxide or, in others, there is less selectivity to the desired products, such as the epoxides and a greater formation to unwanted and cleaved products.^{7,29,30,33} The oxidant, *N*-methyl morpholine (NMO), was also investigated at 80 °C and no conversion was observed. When *m*-CPBA (meta-chloroperoxybenzoic acid) was used as an oxidant, rapid catalyst decomposition occurred.

Table 3.1. Oxidation of styrene using H₂O₂ at 50 °C and 80 °C.

Temperature/ °C	Conversion	Yield	
		Benzaldehyde	Styrene oxide
50	6	4	1
80	41	33	1

Conditions: Styrene:TBHP ratio (1:2.5) and catalyst:styrene (1:100); Time 9 h; Catalyst **1a**. Other products observed benzene and benzoic acid.

Lastly, the effect of solvent on these reactions was investigated. Using 1,2-dichloroethane (DCE) as the solvent, with TBHP as the oxidant (styrene:TBHP; 1:2.5) at 80 °C, the reaction was monitored up to 9 h (Fig. 3.3). The conversion and yield to benzaldehyde increases up to 3 h and stabilizes thereafter. After 3 h the conversion reached 95% with the yield to benzaldehyde reaching a maximum (25%). The yield to styrene oxide decreased over time

(13% at 3 h to 7% at 9 h), however, the yield to phenylacetaldehyde increase from 3% (3 h) to 7% (9 h). Styrene diol was also observed after 2 and 3 h (2% yield). The increase in conversion could be attributed to the improved solubility of the oxidant in the solvent. When a similar study was carried out using supported vanadium catalysts with DCE as the oxidant, the yield to both benzaldehyde and styrene oxide increased as compared to when MeCN was used.³¹ Also with iridium catalysts an increase in reaction rate was found using a chlorinated solvent (tetrachloroethane (TCE)), due to the solvent radicals generated from the reaction of TBHP and TCE.¹ A blank reaction (with no catalyst) was carried out, and after 3 h, a 20% conversion was observed, with benzoic acid forming as the main product with no yield to styrene oxide and a 1% yield to benzaldehyde.

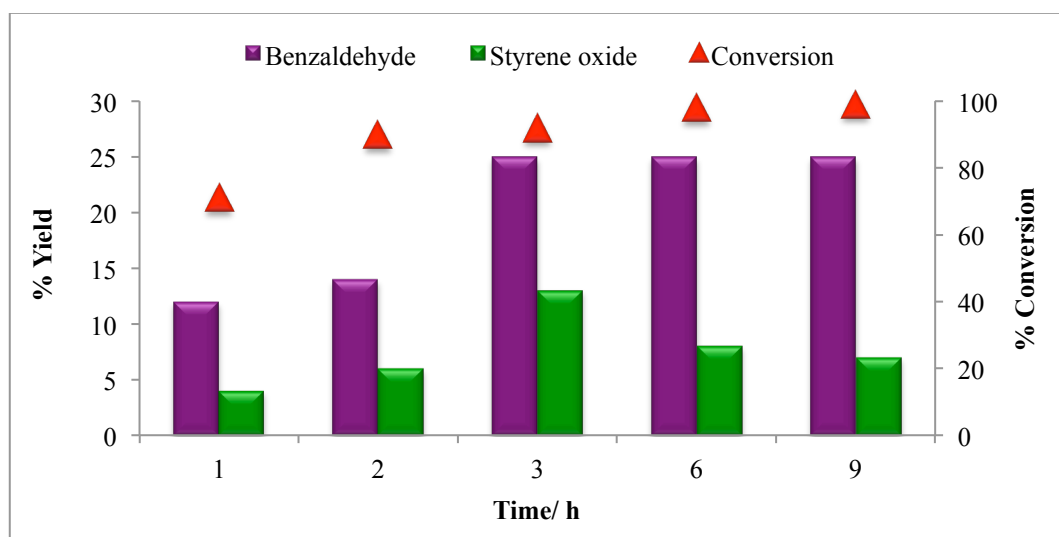


Figure 3.3. Conversion of styrene over time and yield to benzaldehyde and styrene oxide.

Conditions: Catalyst:styrene (1:100); Styrene: TBHP (1:2.5); Temperature: 80 °C; Solvent: DCE; Catalyst **1a**.

To investigate the effect of having an ethylene spacer group between the phosphorous and nitrogen atom (catalyst **2a**), versus no spacer atom (catalyst **1a**), the reactions were compared at 1 h intervals for 3 h (Fig. 3.4). The activities of both catalysts increase over time, where the catalyst with the more rigid ligand backbone (**1a**) is slightly more active than the catalyst with the flexible backbone (**2a**). The yield to benzaldehyde and styrene oxide increases over time, with the yield of both these products greater for the first two hours over catalyst **2a**. The rigidity of complex **1** probably results in the slow formation of the active species. The yield to styrene oxide drops slightly after 2 h for catalyst **2a** due to the formation of phenylacetaldehyde (3% at 3 h). A slightly higher benzene formation after 3 h for catalysts **2a** (7%) in comparison to **1a** (6%) accounts for the slightly lower yield to benzaldehyde over catalyst **2a**.

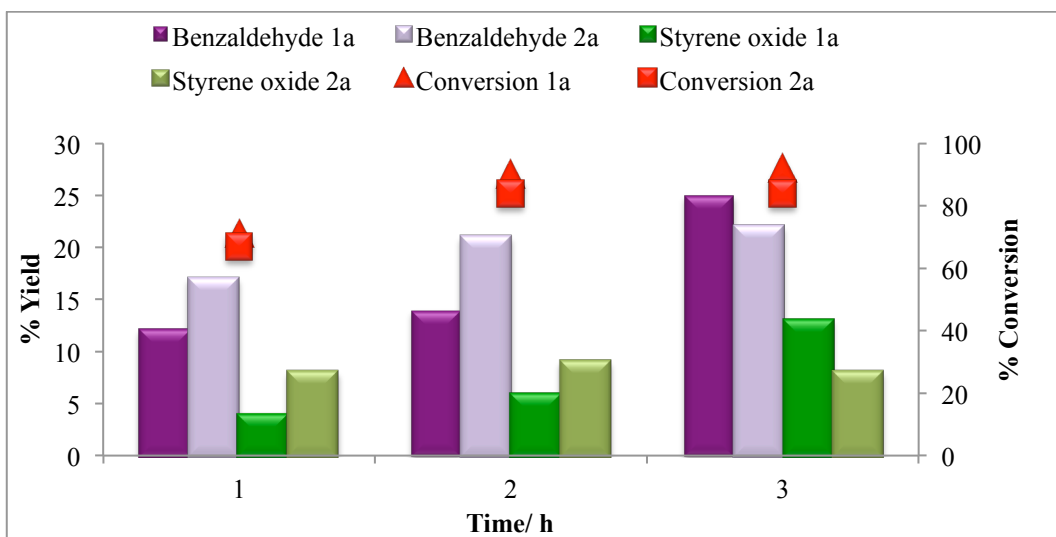


Figure 3.4. Conversion of styrene over time and yield to benzaldehyde and styrene oxide over catalysts **1a** and **2a**.

Conditions: Catalyst:styrene (1:100); Styrene: TBHP (1:2.5); Temperature: 80 °C; Solvent: DCE

The catalysts with the different substituents on the nitrogen atom were then screened under the optimized conditions (Table 3.2). Catalysts **1** are more active than catalysts **2** and a greater yield to benzaldehyde and styrene oxide is found with catalysts **1** than catalysts **2**. This is also seen with the higher turnover number (TON) towards benzaldehyde and styrene oxide of catalysts **1**. The catalysts bearing the cyclohexyl substituent (**1a** and **2a**) on the nitrogen atom are least active. The activity of catalyst **1** bearing the pentyl substituent (**1c**) is highest, with greater TONs towards benzaldehyde and styrene oxide. The TONs towards benzaldehyde of catalysts **2** are comparable.

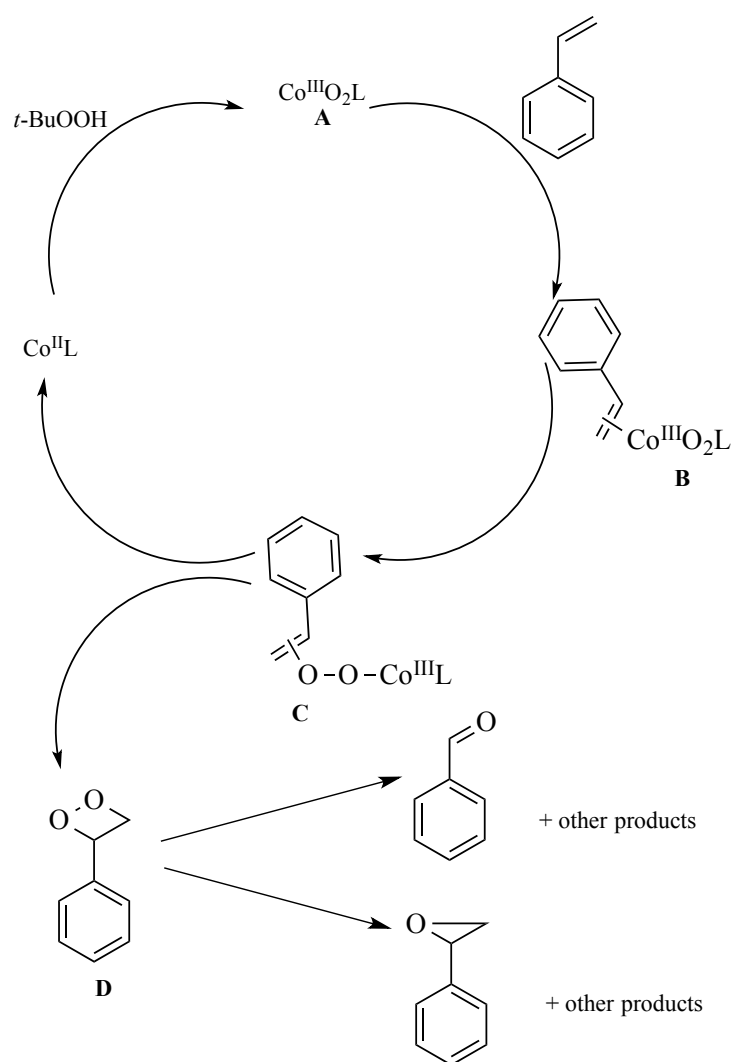
Table 3.2. Screening of catalysts **1** and **2** at optimized conditions.

Catalyst	% Conversion		% Yield ^a		TON	
		Benzaldehyde	Styrene oxide	Benzaldehyde	Styrene oxide	
1a	92	25	13	23	13	
1b	96	22	7	26	9	
1c	96	23	11	28	14	
2a	84	22	8	24	9	
2b	94	19	6	23	7	
2c	95	19	5	24	6	

Conditions: Catalyst:styrene (1:100); Styrene: TBHP (1:2.5); Temperature: 80 °C; Solvent: DCE; Time 3 h.

^aOther products: benzoic acid, benzene, phenylacetaldehyde.

In comparison, other cobalt-based systems are reported to be less efficient. Studies performed using cobalt zeolites gave no yield to benzaldehyde and low conversions and low TONs towards styrene oxide ($0.1 - 15$).³⁰ Li et al. obtained a 63.3% conversion using cobalt-encapsulated zeolite Y with higher selectivity to benzaldehyde than styrene oxide.²⁵ With Schiff based polymer-cobalt complexes, 20% selectivity to benzaldehyde was observed.³² When cobalt oxide was used as a catalyst, a 0.1 % selectivity to benzaldehyde was reported,³³ and when molecular sieves containing cobalt were used as catalysts no yield to benzaldehyde was reported.^{30,34}



Scheme 3.1. Proposed mechanism for the oxidation of styrene by catalysts **1** and **2**, (L=Ligand).

To elucidate the mechanism of this study, benzaldehyde and styrene oxide were used as substrates under optimum catalytic conditions using catalysts **1** and **2**. When the substrate was benzaldehyde, benzene and benzoic acid formed. However, when styrene oxide was used as

the substrate, highest yield to phenylacetaldehyde is obtained. On the basis of this experimental work and information obtained from literature, we propose the mechanism shown in Scheme 3.1. The Co(II) can bind to the oxygen from the TBHP (*t*-BuOOH) to form a Co(III) super oxo species (**A**).^{25,30,35} The oxygen bound cobalt species (Co(III)-(O₂⁻)) reacts with styrene to form an active oxygen intermediate species (**B**) which is responsible for the epoxidation reaction.^{30,35} Rearrangement of intermediate **B** to **C** and generation of the cobalt catalyst then occurs. The formation of the epoxide and benzaldehyde via two different pathways occurs through intermediate **D**.^{16,25,30,35}

3.5 Conclusion

The optimum conditions for the cobalt catalysts in the oxidation of styrene was found to be a 1:100 catalyst:styrene ratio and a 1:2.5 ratio of styrene:TBHP at a temperature of 80 °C using DCE as the solvent. Catalysts **1** bearing a rigid ligand backbone, were more active in the oxidation of styrene compared to the catalysts **2**, bearing the flexible ligand backbone. Greater yield to benzaldehyde and higher TON was obtained for catalysts **1**. The catalyst bearing the pentyl substituent (**1c**) gave the highest TON towards both benzaldehyde and styrene oxide.

3.6 References

- [1] Bruin, de B.; Budzelaar, P. H. M.; Gal, A. W. *Angew. Chem. Int. Ed.* **2004**, *43*, 4142-4157.
- [2] Tada, M.; Muratsugu, S.; Kinoshita, M.; Sasaki, T.; Iwasawa, Y. *J. Am. Chem. Soc.* **2009**, *132*, 713-724.
- [3] Patel, A.; Patel, K. *Inorg. Chimi. Acta* **2014**, *419*, 130-134.
- [4] Karandikar, P.; Agashe, M.; Vijayamohanan, K.; Chandwadkar, A. J. *Appl. Catal. A- Gen.* **2004**, *257*, 133-143.
- [5] Patil, N. S.; Jha, R.; Uphade, B. S.; Bhargava, S. K.; Choudhary, V. R. *Appl. Catal. A- Gen.* **2004**, *275*, 87-93.
- [6] Li, Z.; Wu, S.; Ding, H.; Lu, H.; Liu, J.; Huo, Q.; Guan, J.; Kan, Q. *New J. Chem.* **2013**, *37*, 4220-4229.
- [7] Ding, Y.; Gao, Q.; Li, G.; Zhang, H.; Wang, J.; Yan, L.; Suo, J. *J. Mol. Catal A- Chem.* **2004**, *218*, 161-170.
- [8] Hu, J.; Li, K.; Li, W.; Ma, F.; Guo, Y. *Appl. Catal. A- Gen* **2009**, *364*, 211-220.
- [9] Grigoropoulou, G.; Clark, J. H.; Elings, J. A. *Green Chem.* **2003**, *5*, 1-7.
- [10] Yang, Y.; Ding, H.; Hao, S.; Zhang, Y.; Kan, Q. *Appl. Organomet. Chem.* **2011**, *25*, 262-269.
- [11] Patel, A.; Pathan, S. *Ind. Eng. Chem. Res.* **2011**, *51*, 732-740.
- [12] Kanmani, A. S.; Vancheesan, S. *Stud. Surf. Sci. and Catal.* **1998**, *113*, 285-292.
- [13] Overett, M. J.; Blann, K.; Bollmann, A.; Dixon, J. T.; Hess, F.; Killian, E.; Maumela, H.; Morgan, D. H.; Neveling, A.; Otto, S. *Chem. Commun.* **2005**, 622-624.
- [14] Bollmann, A.; Blann, K.; Dixon, J. T.; Hess, F. M.; Killian, E.; Maumela, H.; McGuiness, D. S.; Morgan, D. H.; Neveling, A.; Otton, S.; Overette, M.; Slawin, A. M.

- Z.; Wassercheid, P.; Kihlmann, S. *J. Am. Chem. Soc.* **2004**, *126*, 14712-14713.
- [15] Blann, K.; Bollmann, A.; Dixon, J. T.; Hess, F. M.; Killian, E.; Maumela, H.; Morgan, D. H.; Neveling, A.; Otto, S.; Overett, M. *J. Chem. Commun.* **2005**, 620-621
- [16] Blann, K.; Bollmann, A.; de Bod, H.; Dixon, J. T.; Killian, E.; Nongodlwana, P.; Maumela, M. C.; Maumela, H.; McConnel, A. E.; Morgan, D. H.; Overette, M. J.; Pfefferius, M.; Kuhlmann, S.; Wasserscheid, P. *J. Catal.* **2007**, *249*, 244-249.
- [17] Benito-Garagorri, D.; Kirchner, K. *Acc. Chem. Res.* **2008**, *41*, 201-213.
- [18] Benito-Garagorri, D.; Alves, L. G. a.; Puchberger, M.; Mereiter, K.; Veiro, L. F.; Calhorda, M. J.; Carvalho, M. D.; Ferreira, L. P.; Godinho, M.; Kirchner, K. *Organometallics* **2009**, *28*, 6902-6914.
- [19] van der Boom, M. E.; Milstein, D. *Chem. Rev.* **2003**, *103*, 175-1792.
- [20] Xu, X.; Xi, Z.; Chen, W.; Wang, D. *J. Coord. Chem.* **2007**, *60*, 2297-2308.
- [21] Albrecht, M.; van Koten, G. *Angew. Chem. Int. Ed.* **2001**, *40*, 3750-3781.
- [22] Lin, Y. H.; Williams, I. D.; Li, P. *Appl. Catal. A-Gen.* **1997**, *150*, 221-229.
- [23] Zombeck, A.; Hamilton, D. E.; Drago, R. S. *J. Am. Chem. Soc.* **1982**, *104*, 6782-6784.
- [24] Drago, R. S.; Corden, B. B.; Barnes, C. W. *J. Am. Chem. Soc.* **1986**, *108*, 2453-2454.
- [25] Li, Z.; Wu, S.; Ma, Y.; Liu, H.; Hu, J.; Liu, L.; Huo, Q.; Guan, J.; Kan, Q. *Trans. Met. Chem.* **2013**, *38*, 243-251.
- [26] Luo, Y.; Lin, J. *Micropor. Mesopor. Mat.* **2005**, *86*, 23-30.
- [27] Maurya, M. R.; Kumar, A.; Costa Pessoa, J. *Coord. Chem. Rev.* **2011**, *255*, 2315-2344.
- [28] Maurya, M. R.; Arya, A.; Adão, P.; Pessoa, J. C. *Appl. Catal. A-Gen.* **2008**, *351*, 239-252.
- [29] Maiti, S. K.; Dinda, S.; Gharah, N.; Bhattacharyya, R. *New J. Chem.* **2006**, *30*, 479-489.
- [30] Tang, Q.; Zhang, Q.; Wu, H.; Wang, Y. *J. Catal.* **2005**, *230*, 384-397.
- [31] Ahmad, A. L.; Kohestani, B.; Bhatia, S.; Ooi, S. B. *Int. J. Appl. Cer. Tech.* **2012**, *9*, 588-598.
- [32] Demetgül, C.; Delikanlı, A.; Sarıbıyık, O. Y.; Karakaplan, M.; Serin, S. *Des. Monomers Polym.* **2012**, *15*, 75-91.
- [33] Choudhary, V. R.; Jha, R.; Jana, P. *Catal. Commun.* **2008**, *10*, 205-207.
- [34] Raja, R.; Sankar, G.; Meurig Thomas, J. *Chem. Commun.* **1999**, 829-830.
- [35] Cui, H.; Zhang, Y.; Zhao, L.; Zhu, Y. *Catal. Commun.* **2011**, *12*, 417-420.

Chapter 4

Iridium and rhodium “PNP” aminodiphosphine complexes used as catalysts in the oxidation of styrene

4.1 Abstract

Six PNP or aminodiphosphine ligands were synthesized and complexed to the transition metals iridium and rhodium to give $[(\eta^5\text{-C}_5\text{Me}_5)\text{MCl}\{\eta^2\text{-}P,P'\text{-}(\text{PPh}_2)_2\text{NR}\}]\text{PF}_6$, where M= Ir (**1**) and Rh (**2**) and R= cyclohexyl (**a**), *iso*-propyl (**b**), pentyl (**c**), phenyl (**d**), chlorophenyl (**e**) and methoxyphenyl (**f**). These complexes were fully characterized by elemental analyses, NMR, IR spectroscopy and HRMS. Crystals of **1f** and **2f** were obtained, which showed a distorted octahedral geometry around the metal centers. These complexes showed good activity in the oxidation of styrene using *tert*-butyl hydroperoxide (TBHP) as the oxidant. The iridium complexes were more active than the rhodium complexes. Higher yields to benzaldehyde were achieved in comparison to styrene oxide for all catalysts.

Keywords: Aminodiphosphine; iridium; rhodium; styrene.

4.2 Introduction

A large amount of feedstock, towards cheap starting materials, can be obtained from oils, which at present are burnt as fuel in the transport industry.¹ The oxidation of hydrocarbons provides a cost-effective method of converting these starting materials into bulk chemicals and is an important transformation in the production of fine chemicals.¹ The oxidation of alkenes to their corresponding epoxides and carbonyl compounds is important in the synthesis of fine and pharmaceutical grade chemicals.²⁻¹² Epoxides are important building blocks and are used as intermediates and precursors for chemical production and in the preparation of resins and drugs.⁹ Benzaldehyde is the second most important aromatic molecule and has a widespread application in the agro chemical industries and synthesis of dyes and perfumes.⁷ The over oxidation of benzaldehyde results in the formation of benzoic acid which is important in the food industry as a preservative inhibiting the growth of mould, yeast and bacteria.¹³ Transition metal-based systems are able to efficiently catalyze epoxidation reactions,¹⁴ and the choice of catalyst and oxidant can modify the course of the reaction.¹⁵ For selective epoxidation, a suitable ligand system is required which is able to control the catalytic

behavior.¹⁵ One such system could include the bi-dentate or multidentate aminodiphosphine or “PNP” ligands, which have been used extensively in ethylene oligomerization studies.¹⁶⁻²² These ligands are part of a system that displays high activity, stability and variability, which makes them ideally suited for catalytic applications.²³⁻²⁵ The activity of the metal can be tailored through the modification of the ligand backbone, by using different donor substituents or central anionic atoms. The ligand then places a high demand on the stereochemistry of the complex allowing the reactions of the metal ions to be selective.^{26,27}

In this study, a new approach has been undertaken in using iridium and rhodium aminodiphosphine complexes in the oxidation of styrene. One of the early studies was carried out by Collman and co workers in 1967 using $\text{IrI}(\text{CO})(\text{PPh}_3)_2$ in the oxidation of cyclohexene.²⁸ In the early 1970’s iridium and rhodium olefin epoxidation was carried out using simple organic salts, which performed poorly when compared to the Wacker palladium oxidation.^{29,30} Since then, less attention has been paid to these transition metals.²⁹⁻³² More recently, Turlington and co workers used a half sandwich Ir complex in the oxidation of styrene obtaining an 11% yield to benzaldehyde and phenylacetaldehyde.³³

We herein report the synthesis and characterization of some new iridium (**1**) and rhodium (**2**) aminodiphosphine complexes and their application in the catalytic oxidation of styrene. Optimization of solvent (acetonitrile (MeCN) and 1,2-dichloroethane (DCE), oxidants (*tert*-butyl hydroperoxide (TBHP), hydrogen peroxide (H_2O_2), *N*-methyl morpholine *N*-oxide (NMO)) and temperature (room temperature (RT), 50 °C and 80 °C) were carried out. The substituents on the nitrogen atom were varied by making use of six different types of functional groups (Fig. 4.1), with the intention of observing if these groups have an effect on the catalytic activity and selectivity to the products of oxidation.

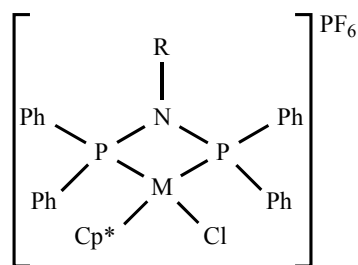


Figure 4.1. General structure of the complexes used as catalysts in the oxidation of styrene.
(M=Ir (**1**) and Rh (**2**); R= cyclohexyl (**a**), *iso*-propyl (**b**), pentyl (**c**), phenyl (**d**), chlorophenyl (**e**) and methoxyphenyl (**f**); Cp^* = η^5 - pentamethylcyclopentadienyl).

4.3 Experimental

4.3.1 Synthesis and characterization of the compounds

All experiments were performed using standard Schlenk techniques under inert conditions in moisture free reaction glassware with anhydrous solvents. All solvents were analytical grade. To render the reaction glassware moisture free, it was heated with a heat gun, followed by cycles of vacuum and nitrogen pressure. The solvents utilized were dry unless otherwise stated. Diethyl ether and hexane were distilled from sodium benzophenoneketyl under nitrogen. Dichloromethane (DCM) was distilled from P₂O₅ and methanol from magnesium turnings. Deuterated solvents were used as received and stored in a desiccator. The NMR spectra were recorded at 400 MHz. (¹H), 100 MHz. (¹³C) and 162 MHz. (³¹P) using a Bruker Ultrashield 400 MHz. spectrometer. ¹H NMR and ¹³C{¹H} NMR chemical shifts are reported in parts per million (ppm) downfield from tetramethylsilane. ¹H NMR and ¹³C{¹H} NMR signals were referenced to the residual hydrogen and carbon signal of DMSO, (2.50 ppm) and (39.52 ppm), respectively. ³¹P NMR chemical shifts are reported in parts per million (ppm) from triphenylphosphine (-17.6 ppm). The 2D ¹⁰³Rh and ³¹P NMR spectrum of compound **2c** was recorded using a Bruker Ultrashield 500 MHz. spectrometer. The FT-IR spectra were recorded using a Perkin Elmer Universal Attenuated Total Reflection (ATR) Sampling Accessory attached to an FT-IR series 100 spectrometer. The HRMS was recorded on a Waters Micromass LCT Premier TOF-MS. All PNP ligands were synthesized with modification of literature procedure.¹⁸ The metal precursors [Ir(Cp*)Cl₂)₂] and [Rh(Cp*)Cl₂)₂] (Cp* = η⁵-pentamethylcyclopentadienyl) were prepared according to literature procedures.³⁴⁻³⁶ (All spectra are shown in Appendix B).

Synthesis of [Ph₂PN(C₆H₁₁)PPh₂]IrCp*(Cl)]⁺PF₆⁻ (1a**).** The synthesis was adapted from a known procedure.³⁷ To a 100 ml two-neck round bottom flask, 6 ml of acetone was added and purged with argon for 10 minutes. Thereafter, [Ph₂PN(C₆H₁₁)PPh₂] (0.250 mmol, 0.12 g) was added. Once completely dissolved, [Ir(Cp*)Cl₂)₂] (0.125 mol, 0.10 g) and NH₄PF₆ (0.250 mmol, 0.04 g) was added to the flask, followed by the addition of 12 ml of methanol. The yellow solution was allowed to stir for 6 h, after which DCM was added. The solution was then filtered through celite and the solvent was reduced to 2 ml. Upon addition of diethyl ether a yellow precipitate formed, which was filtered using a Hirsch funnel. The yellow powder was dried overnight in vacuo. Crystals were grown from diethyl ether and dichloromethane. Yield: 78%, 0.19 g. Melting point: 295-296 °C. IRν_{max} (ATR)/cm⁻¹: 762 (w) (CH_{2n} rocking); 827 (s) (PF₆); 938 (m) (P-N); 1071 (m) (cyclohexyl ring vibrations); 1436 (m) (PPh₂). Anal. % Calcd for C₄₀H₄₆ClF₆IrNP₃: C: 49.3%; H: 4.8%; N: 1.4%. Found: C: 49.6%; H: 4.8%; N: 1.6%. HRMS (ESI) Calcd for: C₄₀H₄₆ClIrNP₂ 830.2423. Found: 830.2417. NMR: (400 MHz.; DMSO): ¹H NMR δ 0.87-1.43 (m, 10H, cyclohexyl ring); δ 1.52 (s, 15H, Cp*); δ 3.59-3.69 (m,

1H, (cyclohexyl ring)); δ 7.44-7.77 (m, 20H, aromatic). ^{13}C NMR δ 8.28 (Cp*); δ 33.82 (cyclohexyl ring); δ 24.30-24.94 (cyclohexyl ring); δ 127.51-133.39 (aromatic); δ 64.57 (cyclohexyl ring). ^{31}P NMR δ -152.99 – -131.04 (PF₆); δ 34.50.

Synthesis of $[\text{Ph}_2\text{PN}(\text{C}_3\text{H}_7)\text{PPh}_2]\text{IrCp}^*(\text{Cl})]^+\text{PF}_6^-$ (1b**)**. Compound **1b** was synthesized according to the procedure described for **1a** except that [Ph₂PN(C₃H₇)PPh₂] (0.250 mmol, 0.11 g) was used. Yield: 88 %, 0.21 g. Melting point: 270-272 °C. IR ν_{max} (ATR)/cm⁻¹: 833 (s) (PF₆); 945 (m) (P-N); 1436 (m) (PPh₂); 1482 (w) (CH₃). Anal. % Calcd for C₃₇H₄₂ClF₆IrNP₃: C: 47.5%; H: 4.5%; N: 1.5%. Found: C: 47.0%; H: 4.3%; N: 2.0%. HRMS (ESI) Calcd for C₃₇H₄₂ClIrNP₂: 790.2110. Found: 790.2092. NMR: (400 MHz.; DMSO): ^1H NMR δ 0.94 (d, 6H, (CH₃)₂; 2J = 6.60 Hz); δ 1.54 (s, 15H, Cp*); δ 3.91-4.12 (m, 1H, CH); δ 7.41-7.78 (m, 20H, aromatic). ^{13}C NMR δ 8.27 (Cp*); δ 23.6 (CH₃)₂; δ 56.1 (CH); δ 128.31-133.07 (aromatic). ^{31}P NMR δ -154.38 – -131.04 (PF₆); δ 34.89.

Synthesis of $[\text{Ph}_2\text{PN}(\text{C}_5\text{H}_{11})\text{PPh}_2]\text{IrCp}^*(\text{Cl})]^+\text{PF}_6^-$ (1c**)**. Compound **1c** was synthesized according to the procedure described for **1a** except that [Ph₂PN(C₅H₁₁)PPh₂] (0.25 mmol, 0.11 g) was used. Yield: 54 %, 0.13 g. Melting point: 262-263 °C. IR ν_{max} (ATR)/cm⁻¹: 751 (m) (CH₂); 833 (s) (PF₆); 999 (m) (P-N); 1437 (m) (PPh₂); 2930 (w) (CH₃). Anal. % Calcd for C₃₉H₄₆ClF₆IrNP₃: C: 48.6%; H: 4.8%; N: 1.5%. Found: C: 49.0%; H: 4.3%; N: 1.6%. HRMS (ESI) Calcd for C₃₉H₄₆ClIrNP₂: 818.4185. Found: 818.2413. NMR: (400 MHz.; DMSO): ^1H NMR δ 0.60 (t, 3H, CH₃; 3J = 6.78 Hz); δ 0.92-0.97 (m, 4H, (CH₂)₂); δ 1.07-1.24 (m, 2H, CH₂); δ 1.58 (s, 15H, Cp*); δ 3.36-3.39 (m, 2H, CH₂); δ 7.35-7.79 (m, 20H, aromatic). ^{13}C NMR δ 8.39 (Cp*); δ 13.38 (CH₃); δ 21.26 (CH₂); δ 28.02 (CH₂); δ 29.15 (CH₂); δ 51.59 (CH₂); δ 128.25-133.34 (aromatic). ^{31}P NMR δ -152.99 – -135.43 (PF₆); δ 34.19.

Synthesis of $[\text{Ph}_2\text{PN}(\text{Ph})\text{PPh}_2]\text{IrCp}^*(\text{Cl})]^+\text{PF}_6^-$ (1d**)**. Compound **1d** was synthesized according to the procedure described for **1a** except that [Ph₂PN(Ph)PPh₂] (0.25 mmol, 0.12 g) was used. Yield: 77 %, 0.19 g. Melting point: 249-251 °C. IR ν_{max} (ATR)/cm⁻¹: 827 (s) (PF₆); 946 (m) (P-N); 1439 (m) (PPh₂); 1494 (w) (Ph). Anal. % Calcd for C₄₀H₄₀ClF₆IrNP₃: C: 49.6%; H: 4.2%; N: 1.4%. Found: C: 49.1%; H: 4.0%; N: 2.9%. HRMS (ESI) Calcd for C₄₀H₄₀ClIrNP₂: 824.1954. Found: 824.1945. NMR: (400 MHz.; DMSO): ^1H NMR δ 1.56 (s, 15H, Cp*); δ 6.64 (d, 2H, CH; 2J = 7.53 Hz); δ 7.14-7.21 (m, 3H, CH); δ 7.41-7.77 (m, 20H, aromatic). ^{13}C NMR δ 8.25 (Cp*); δ 124.08-133.54 (aromatic). ^{31}P NMR δ -152.99 – -135.43 (PF₆); δ 35.84

Synthesis of $[\text{Ph}_2\text{PN}(\text{C}_6\text{H}_4\text{Cl})\text{PPh}_2]\text{IrCp}^*(\text{Cl})]^+\text{PF}_6^-$ (1e**)**. Compound **1e** was synthesized according to the procedure described for **1a** except that [Ph₂PN(C₆H₄Cl)PPh₂] (0.25 mmol, 0.12 g) was used. Yield: 83%, 0.21 g. Melting point: 237-239 °C. IR ν_{max} (ATR)/cm⁻¹: 827 (s) (PF₆); 900 (m) (P-N); 1439 (m) (PPh₂); 1494 (w) (Ph₂). Anal. % Calcd for C₄₀H₃₉ClF₆IrNP₃: C: 47.9%; H: 3.9%; N: 1.4%.

Found: C: 48.2%; H: 4.1%; N: 1.6%. HRMS (ESI) Calcd for $C_{40}H_{39}Cl_2IrNP_2$: 858.1564. Found: 858.1555. NMR: (400 MHz.; DMSO): 1H NMR δ 1.55 (s, 15H, Cp*); δ 6.63 (d, 2H, CH; $^2J = 8.84$ Hz); δ 7.28 (m, 2H, CH; $^2J = 8.88$ Hz); δ 7.42-7.79 (m, 20H, aromatic). ^{13}C NMR δ 8.83 (Cp*); δ 125.46 -133.67 (aromatic). ^{31}P NMR δ -152.99 - -135.43 (PF_6^-); δ 37.05

Synthesis of $[Ph_2PN(C_7H_7O)PPh_2]IrCp^*(Cl)]^+PF_6^-$ (1f). Compound **1f** was synthesized according to the procedure described for **1a** in that $[Ph_2PN(C_7H_7O)PPh_2]$ (0.25 mmol, 0.12 g) was used. Yield: 87%, 0.22 g. Melting point: 239-242 °C. IR ν_{max} (ATR)/cm⁻¹: 832 (s) (PF_6^-); 951 (m) (P-N); 1234 (m) (aromatic ether); 1437 (m) (PPh₂); 1506 (w) (Ph₂). Anal. % Calcd for $C_{41}H_{42}ClF_6IrNOP_3$: C: 49.3%; H: 4.2%; N: 1.4%. Found: C: 49.0%; H 3.8%; N 1.7%. HRMS (ESI) Calcd for $C_{40}H_{42}ClIrNOP_2$: 854.2059. Found: 854.2033. NMR: (400 MHz.; DMSO): 1H NMR δ 1.59 (s, 15H, Cp*); δ 3.66 (s, 3H, CH₃); δ 6.60 (d, 2H, CH; $^2J = 8.84$ Hz); δ 6.78 (d, 2H, CH; $^2J = 9.00$ Hz); δ 7.31-7.78 (m, 20H, aromatic). ^{13}C NMR δ 8.34 (Cp*); δ 55.34 (CH₃); δ 128.21 -133.42 (aromatic). ^{31}P NMR δ -152.99 - -135.43 (PF_6^-); δ 37.05.

Synthesis of $[Ph_2PN(Cy)PPh_2]RhCp^*(Cl)]^+PF_6^-$ (2a). Compound **2a** was synthesized according to the procedure described for **1a** in that $[Ph_2PN(Cy)PPh_2]$ (0.25 mmol, 0.12 g) and $[Rh(Cp^*)Cl_2]_2$ (0.125 mol, 0.08 g) was used. Yield: 90%, 0.20 g of orange powder. Melting point: 256-258 °C. IR ν_{max} (ATR)/cm⁻¹: 762 (w) (CH_{2n} rocking); 829 (s) (PF_6^-); 905 (m) (P-N); 1063 (m) (cyclohexyl ring vibrations); 1435 (m) (PPh₂). Anal. % Calcd for $C_{40}H_{46}ClF_6RhNP_3$: C: 54.2%; H: 5.2%; N: 1.6%. Found: C: 54.0%; H 5.2%; N 1.8%. HRMS (ESI) Calcd for $C_{40}H_{46}ClRhNP_2$: 740.1849. Found: 740.1851 NMR: (400 MHz.; DMSO): 1H NMR δ 1.04-1.42 (m, 10H, cyclohexyl ring); δ 1.48 (s, 15H, Cp*); δ 3.63-3.72 (m, 1H, (cyclohexyl ring)); δ 7.43-7.80 (m, 20H, aromatic). ^{13}C NMR δ 8.78 (Cp*); δ 24.27-33.87 (cyclohexyl ring); δ 128.13-133.44 (aromatic); δ 64.57 (cyclohexyl ring). ^{31}P NMR δ -152.99 - -131.04 (PF_6^-); δ 67.62 (d).

Synthesis of $[Ph_2PN(C_3H_7)PPh_2]RhCp^*(Cl)]^+PF_6^-$ (2b). Compound **2b** was synthesized according to the procedure described for **2a** in that $[Ph_2PN(C_3H_7)PPh_2]$ (0.13 mmol, 0.05 g) was used. Yield: 94%, 0.09 g. Melting point: 242-244 °C. IR ν_{max} (ATR)/cm⁻¹: 834 (s) (PF_6^-); 949 (m) (P-N); 1436 (m) (PPh₂); 1482 (w) (CH₃). Anal. % Calcd for $C_{37}H_{42}ClF_6RhNP_3$: C: 52.5%; H: 5.0%; N: 1.7%. Found: C: 53.0%; H: 5.0%; N: 2.2%. HRMS (ESI) Calcd for $C_{37}H_{42}ClRhNP_2$: 700.1536. Found: 700.1530. NMR: (400 MHz.; DMSO): 1H NMR δ 0.94 (d, 6H, (CH₃)₂; $^2J = 6.64$ Hz); δ 1.48 (s, 15H, Cp*); δ 4.05-4.19 (m, 1H, CH); δ 7.40-7.98 (m, 20H, aromatic). ^{13}C NMR δ 8.80 (Cp*); δ 23.77 (CH₃)₂; δ 55.6 (CH); δ 128.14-133.37 (aromatic). ^{31}P NMR δ -154.38 - -131.04 (PF_6^-); δ 67.79 (d).

Synthesis of $[[\text{Ph}_2\text{PN}(\text{C}_5\text{H}_{11})\text{PPh}_2]\text{RhCp}^*(\text{Cl})]^+\text{PF}_6^-$ (2c). Compound **2c** was synthesized according to the procedure described for **2a** in that $[\text{Ph}_2\text{PN}(\text{C}_5\text{H}_{11})\text{PPh}_2]$ (0.25 mmol, 0.13 g) was used. Yield: 95 %, 0.21 g. Melting point: 240-242 °C. IR ν_{max} (ATR)/cm⁻¹: 750 (m) (CH₂); 834 (s) (PF₆); 999 (m) (P-N); 1436 (m) (PPh₂); 2960 (w) (CH₃). Anal. % Calcd for C₃₉H₄₆ClF₆RhNP₃: C: 53.6%; H: 5.3%; N: 1.6%. Found: C: 53.8%; H: 4.9%; N: 2.0%. HRMS (ESI) Calcd for C₃₉H₄₆ClRhNP₂: 728.1849. Found: 728.1849. NMR: (400 MHz.; DMSO): ¹H NMR δ 0.59 (t, 3H, CH₃; ³J= 6.74 Hz); δ 0.89-0.97 (m, 4H, (CH₂)₂); δ 1.07-1.20 (m, 2H, CH₂); δ 1.52 (s, 15H, Cp^{*}); δ 3.36-3.39 (m, 2H, CH₂); δ 7.34-7.79 (m, 20H, aromatic). ¹³C NMR δ 8.94 (Cp^{*}); δ 13.38 (CH₃); δ 21.26 (CH₂); δ 27.98 (CH₂); δ 29.24 (CH₂); δ 50.68 (CH₂); δ 128.27-132.94 (aromatic). ³¹P NMR δ -152.99 -- 135.43 (PF₆); δ 67.07 (d).

Synthesis of $[[\text{Ph}_2\text{PN}(\text{Ph})\text{PPh}_2]\text{RhCp}^*(\text{Cl})]^+\text{PF}_6^-$ (2d). Compound **2d** was synthesized according to the procedure described for **2a** except that $[\text{Ph}_2\text{PN}(\text{Ph})\text{PPh}_2]$ (0.25 mmol, 0.12 g) was used. Yield: 77 %, 0.19 g. Melting point: 249-251 °C. IR ν_{max} (ATR)/cm⁻¹: 827 (s) (PF₆); 941 (m) (P-N); 1439 (m) (PPh₂); 1494 (w) (Ph₂). Anal. % Calcd for C₄₀H₄₀ClF₆RhNP₃: C: 54.6%; H: 4.6%; N: 1.6%. Found: C: 54.9%; H: 4.5%; N 1.2%. HRMS (ESI) Calcd for C₄₀H₄₀ClRhNP₂: 734.1380. Found: 734.1368 . NMR: (400 MHz.; DMSO): ¹H NMR δ 1.54 (s, 15H, Cp^{*}); δ 6.65-6.67 (d, 2H, CH); δ 7.18-7.19 (m, 3H, CH); δ 7.41-7.78 (m, 20H, aromatic). ¹³C NMR δ 8.83 (Cp^{*}); δ 124.99-133.40 (aromatic). ³¹P NMR δ -152.99 -- 135.43 (PF₆); δ 68.42 (d).

Synthesis of $[[\text{Ph}_2\text{PN}(\text{C}_6\text{H}_4\text{Cl})\text{PPh}_2]\text{RhCp}^*(\text{Cl})]^+\text{PF}_6^-$ (2e). Compound **2e** was synthesized according to the procedure described for **2a** except that $[\text{Ph}_2\text{PN}(\text{C}_6\text{H}_4\text{Cl})\text{PPh}_2]$ (0.25 mmol, 0.12 g) was used. Yield: 87%, 0.20 g. Melting point: 223-225 °C. IR ν_{max} (ATR)/cm⁻¹: 827 (s) (PF₆); 901 (m) (P-N); 1439 (m) (PPh₂); 1494 (w) (Ph₂). Anal. % Calcd for C₄₀H₃₉ClF₆RhNP₃: C: 52.5%; H: 4.3%; N: 1.5%. Found: C: 52.3%; H: 4.6%; N: 2.0%. HRMS (ESI) Calcd for C₄₀H₃₉Cl₂RhNP₂: 768.0990. Found: 768.0995. NMR: (400 MHz.; DMSO): ¹H NMR δ 1.51 (s, 15H, Cp^{*}); δ 6.65 (d, 2H, CH; ²J= 8.92 Hz); δ 7.28 (d, 2H, CH; ²J= 6.88 Hz); δ 7.42-7.76 (m, 20H, aromatic). ¹³C NMR δ 8.83 (Cp^{*}); δ 128.38-133.54 (aromatic). ³¹P NMR δ -152.99 -- 135.43 (PF₆); δ 69.69 (d).

Synthesis of $[[\text{Ph}_2\text{PN}(\text{C}_7\text{H}_7\text{O})\text{PPh}_2]\text{RhCp}^*(\text{Cl})]^+\text{PF}_6^-$ (2f). Compound **2f** was synthesized according to the procedure described for **2a** in that $[\text{Ph}_2\text{PN}(\text{C}_7\text{H}_7\text{O})\text{PPh}_2]$ (0.25 mmol, 0.12 g) was used. Yield: 84%, 0.19 g. Melting point: 224-225 °C. IR ν_{max} (ATR)/cm⁻¹: 833 (s) (PF₆); 949 (m) (P-N); 1231 (m) (aromatic ether); 1436 (m) (PPh₂); 1507 (w) (Ph₂).). Anal. % Calcd for C₄₁H₄₂ClF₆RhNOP₃: C: 54.1%; H: 4.7%; N: 1.5%. Found: C: 54.5%; H 4.3%; N 1.4%. HRMS (ESI) Calcd for C₄₀H₃₉ClRhNOP₂: 764.1485. Found: 764.1478. NMR: (400 MHz.; DMSO): ¹H NMR δ 1.56 (s, 15H, Cp^{*}); δ 3.66 (s, 3H, CH₃); δ 6.60 (d, 2H, CH; ²J= 8.84 Hz); δ 6.77 (d, 2H, CH; ²J= 9.00 Hz); δ 7.32-

7.59 (m, 20H, aromatic). ^{13}C NMR δ 8.91 (Cp^*); δ 55.34 (CH_3); δ 128.21 -133.42 (aromatic). ^{31}P NMR δ -152.99 - -135.43 (PF_6); δ 69.86 (d).

4.3.2 Crystal structure analysis

Single-crystal X-ray diffraction data of complex **1f** were collected on a Bruker KAPPA APEX II DUO diffractometer using graphite-monochromated Mo-K α radiation ($\lambda = 0.71073 \text{ \AA}$). Data collection was carried out at 173(2) K (Table 4.1). Temperature was controlled by an Oxford Cryostream cooling system (Oxford Cryostat). Cell refinement and data reduction were performed using the program SAINT.³⁸ The data were scaled and absorption correction performed using SADABS.³⁸ The structure was solved by direct methods using SHELXS-97 and refined by full-matrix least-squares methods based on F^2 using SHELXL-97.³⁹ X-ray single crystal intensity data of complex **2f** were collected on a Nonius Kappa-CCD diffractometer using graphite monochromated MoK α radiation ($\lambda = 0.71073 \text{ \AA}$). Temperature was controlled by an Oxford Cryostream cooling system (Oxford Cryostat). The strategy for the data collections was evaluated using the Bruker Nonius "Collect" program. Data were scaled and reduced using DENZO-SMN software.⁴⁰ Absorption correction was performed using SADABS.³⁸ The program Olex2 was used to prepare molecular graphic images.⁴¹ All non-hydrogen atoms were refined anisotropically. The ADP restraints and the rigid bond restraints were used on all six fluorine atoms. All hydrogen atoms were placed in idealized positions and refined in riding models with U_{iso} assigned the values to be 1.2 or 1.5 times those of their parent atoms and the distances of C-H were constrained to 0.95 \AA for aromatic hydrogen atoms and 0.98 \AA for CH_3 . (More information is available in Appendix B).

4.3.3 Oxidation of styrene

All reagents were weighed and handled in air. All products were analyzed using a PerkinElmer Auto System gas chromatograph fitted with a Flame Ionisation Detector (FID) set at 290 °C. A Varian DB-5 capillary column (25 m x 0.15 mm x 2 μm) was utilized with the injector temperature set at 250 °C. The catalyst to substrate ratio was kept constant at 1:100. A two-necked pear shaped flask was charged with 5 mg of the respective catalyst, benzophenone (as an internal standard), styrene, the respective oxidant and 10 ml of the solvent). The flask was equipped with a reflux condenser, stirred, and heated to the respective temperature. After specific time intervals, an aliquot was removed using a Pasteur pipette (filtered through a plug of cotton wool and silica) and (0.5 μl) was injected into the GC and quantified.

Table 4.1. Single crystal structural information of complexes **1f** and **2f**.

Compound	1f	2f
Mol. Formula	C ₄₁ H ₄₂ ClIrNOP ₂ F ₆ P	C ₄₁ H ₄₂ Cl NOP ₂ Rh,F ₆ P
Mol. Weight	999.34	910.03
Temperature (k)	173	173
Wavelength (Å)	Mo Kα (0.71073)	Mo Kα (0.71073)
Crystal symmetry	Monoclinic	Monoclinic
Space Group	P21/c	P21/c
a (Å)	14.0391(9)	14.0480(4)
b (Å)	13.7146(8)	13.7160(6)
c (Å)	21.6343(14)	21.6798(9)
α, β, γ (°)	90, 105.8, 90	90, 105.8, 90
Volume (Å ³)	4007.4(4)	4017.5(3)
Z	4	4
Density (g/m ³)	1.656	1.505
Absorption coefficient (mm ⁻¹)	3.580	0.673
F(000)	1984	1856
Crystal size (mm)	0.13 x 0.19 x 0.22	0.12 x 0.15 x 0.18
Θ range for data collection	1.5, 28.4	4.0, 27.5
Reflection (collected, independent, R _{int})	118247, 10018, 0.080	77581, 9164, 0.103
Observed Data [I > 2.0 sigma(I)]	8191	5603
Nref, Npar	10018, 493	9164, 493
R, wR2, S	0.0274, 0.0612, 1.01	0.0464, 0.1213, 1.03
Largest diff. peak, hole (e.Å ⁻³)	0.87, -0.93	0.96, -0.86
No of C—H···X interactions	3	3
No of C-H...π (Cg-Ring) interactions	2	2
No of π...π (Cg- Cg) interactions	24	24

4.4 Results and Discussion

4.4.1 Synthesis and characterization of the compounds

The new complexes (**1** and **2**) were synthesized by adaptation of a reported general method.³⁷ The respective PNP ligands were added to (2:1; v/v) methanol:acetone mixtures after which the metal precursor and NH₄PF₆ salt were added. For the iridium complexes (**1**) a yellow precipitate formed after 1 h of stirring at room temperature, whilst an orange precipitate formed for the rhodium complexes (**2**). The complexes were characterized by elemental analyses, NMR, IR, HRMS and single crystal X-ray diffraction for compounds **1f** and **2f**. A downfield shift is noted in the ³¹P NMR spectra of the rhodium complexes compared to the iridium complexes. Furthermore, the ³¹P NMR spectra for the rhodium complexes show a doublet resonance at ~67 ppm and a singlet resonance for the iridium complexes at ~34 ppm. This is consistent with literature for rhodium complexes of similar nature.^{42,43} The substituents on the nitrogen atom (**a-f**) have very little effect in the shift of the phosphorus peak, as the peak shift is mainly influenced by the phenyl groups on the nitrogen atom, and this is also noted when compared to the ν_{PPH_2} of the free ligand and the complex in the IR spectra. To show the correlation between the phosphorous and Rh metal, a 2D ¹⁰³Rh and ³¹P NMR HMQC experiment of compound **2c** was carried out (Fig. 4.2). Transition metal NMR has the advantage over normal proton NMR, in that the transition metal nuclei offer very large shielding ranges, therefore there is higher sensitivity to subtle structural perturbations.⁴⁴ As in this case, the phosphorous nuclei, are used as a source of polarization transfer as it is a 100% $I = \frac{1}{2}$ nucleus with a high receptibility.⁴⁵ The $^2J(^{31}\text{P}, ^{103}\text{Rh})$ value was calculated from the routine ³¹P NMR spectrum and is consistent with that shown in literature of similar compounds.^{45,46} The *J* coupling constant ($^2J = 119.4$ Hz) is due to the fact that two equivalent ³¹P nuclei are present which is consistent with the spectrum shown in Fig. 4.2.⁴⁷ This constant is an indicator of the Rh-P bond strength.^{45,48} Bulky ligands, such as the one present in this study, weaken the metal-phosphorous bond, which results in a slightly lower *J* values and is also noted in a series of Rh-P complexes that bear such ligands.⁴⁸

The HRMS and elemental analyses match those of the calculated values and the sharp melting points indicate that these complexes are pure.

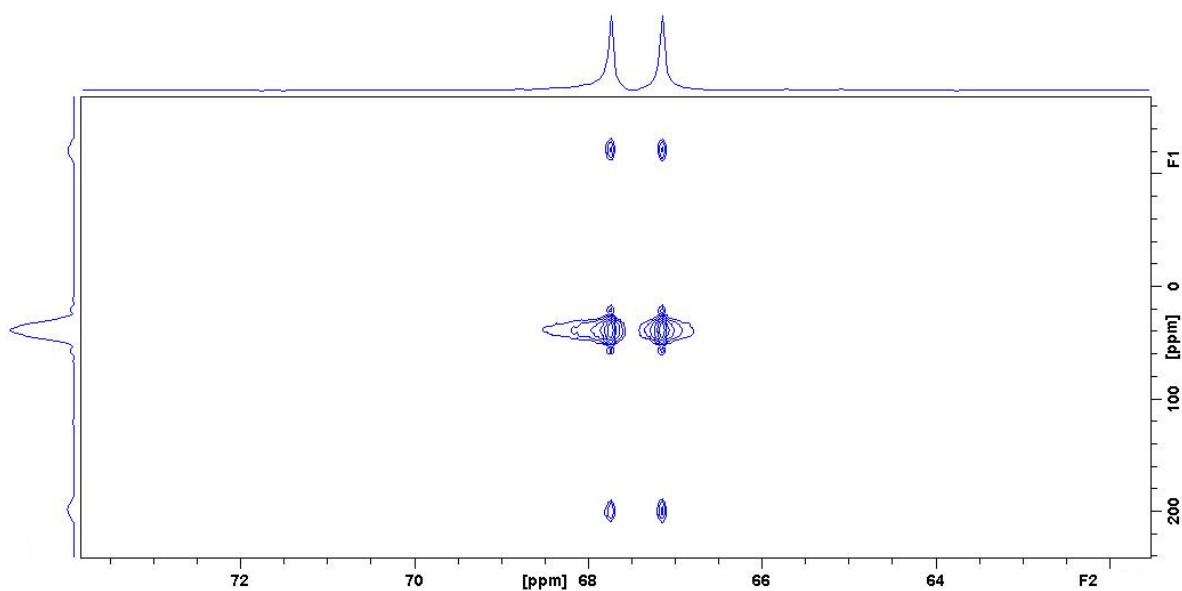


Figure 4.2. 2D ^{103}Rh and ^{31}P NMR spectrum of compound **2c**.

4.4.2 Description of crystal structures

Yellow and orange crystals of **1f** and **2f**, respectively, were obtained by vapor diffusion of diethyl ether into a dichloromethane solution. Structural views of complexes **1f** and **2f** are shown in Fig. 4.3. The selected interatomic distances and angles for **1f** and **2f** are listed in Table 4.2. For both the complexes the iridium/rhodium centers are distorted octahedrally and the chloride anion is coordinated perpendicular to the strained four membered chelate ring, whilst the Cp* ligand is trans to the PNP nitrogen donor. Ir–Cl(1) and Rh–Cl(1) bond lengths are 2.3855(9) Å and 2.3785(9) Å for **1f** and **2f**, respectively, and are comparable to the corresponding values observed for similar Ir and rh complexes.^{42,43} The interatomic distances of Ir···N and Rh···N bonds are 2.942 Å and 2.938 and the P–N–P angles are 101.02(14) $^{\circ}$ and 101.82(16) $^{\circ}$ for **1f** and **2f** respectively. These findings indicate that the phosphinoamine nitrogen atoms do not bind to the metal ions. In addition, the average P(1)···P(2) distances are 2.633 Å (**1f**) and 2.646 Å (**2f**). The P–N bond lengths (~1.70 Å) obtained for compounds **1f** and **2f** lie in a typical P–N single bond range.^{42,43,49,50} The Rh–P bond lengths of **2f** are 2.2998(9) Å for Rh–P(1), 2.3079(9) Å for Rh–P(2), whilst for **1f** the bond length, Ir–P(1) is 2.2916(8) Å and 2.2958(8) Å for Ir–P(2). These are similar to related rhodium and iridium complexes.^{42,43} The Rh–C(ring) and Ir–C(ring) distances are 2.188(4)-2.231(3) and 2.197(3)-2.245(4) Å, respectively, and again are comparable with those found in other pentamethylcyclopentadienyl of compounds rhodium and iridium(III).^{42,43} Although the nitrogen atom of the diphosphinoamine ligand is a tertiary amine, the nitrogen atoms are located within the plane defined by two phosphorus and an ipso carbon atom. The nitrogen

atom is sp^2 -hybridized. Such hybridization is occasionally found in compounds with a P–N bond.^{51,52} Additionally, the aromatic ring attached to the nitrogen atom is largely twisted against the P–N–P plane (ca. 60–90°) as shown also in X-ray crystal structures.^{42,43} The diphosphinoamine ligands show a twist which may be due to steric interactions with the nitrogen atom, and in cases where there is no metal it has shown to be due to intramolecular charge-transfer as noted in compounds such as *p*-dimethylaminobenzonitrile.^{53–55} The crystal structures reveal that in compounds **1f** and **2f**, C-bound H atoms are involved in intermolecular C—H...halogen and π – π interactions (Tables 4.3–4.5). This links the fluorine of the counter ion to the compound via the phenyl ring attached to the phosphorous atom. The crystal packing for compounds **1f** and **2f** form sheets in a zig-zag manner (010) (Fig. 4.4). For complex **1f** and **2f**, the zig-zag plane passes through the Cp^* ring and makes an angle of 9.85° and 10.29° respectively. Through the *c*-axis, compounds **1f** ($\text{C}(34)\text{---H}(34)\cdots\text{F}(2)$ and $\text{C}(39)\cdots\text{H}(39)\cdots\text{F}(4)$) and **2f** ($\text{C}(34)\text{---H}(34)\cdots\text{F}(2)$ and $\text{C}(39)\cdots\text{H}(39)\cdots\text{F}(3)$) a helical structure is observed.

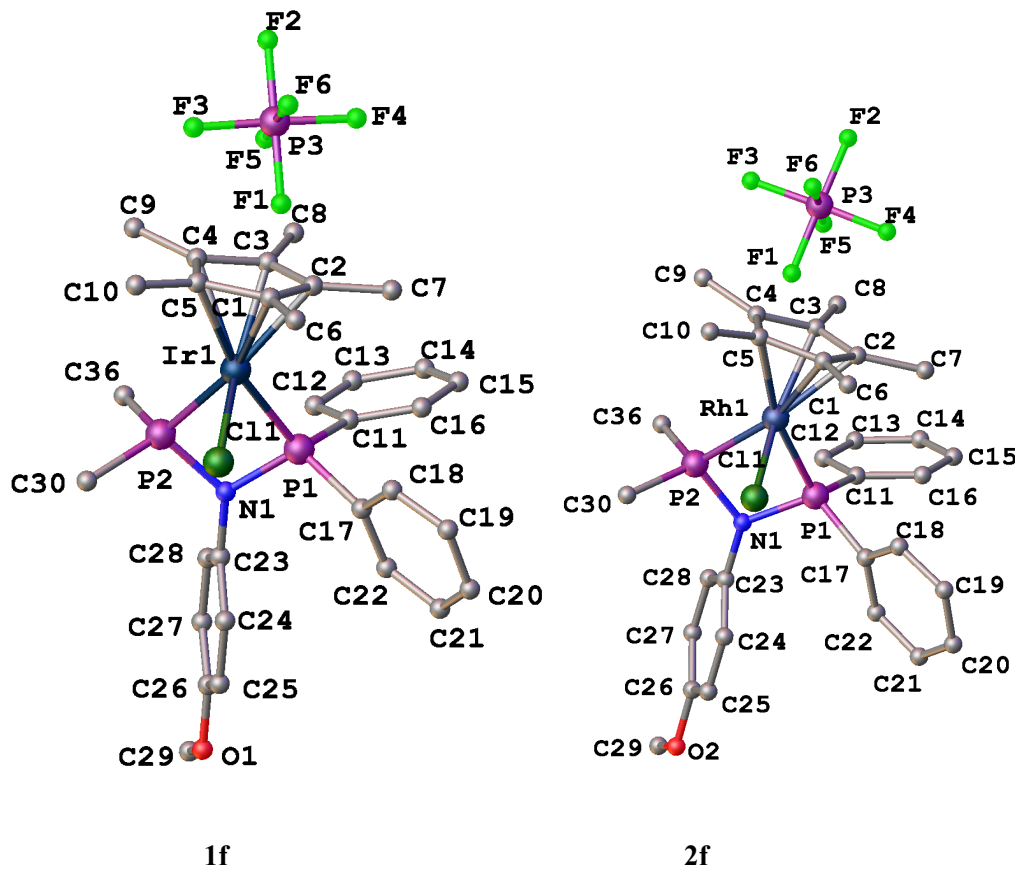


Figure 4.3. Structure of complexes **1f** and **2f** with labeling scheme. The phenyl groups of P(2) are removed/omitted for clarity.

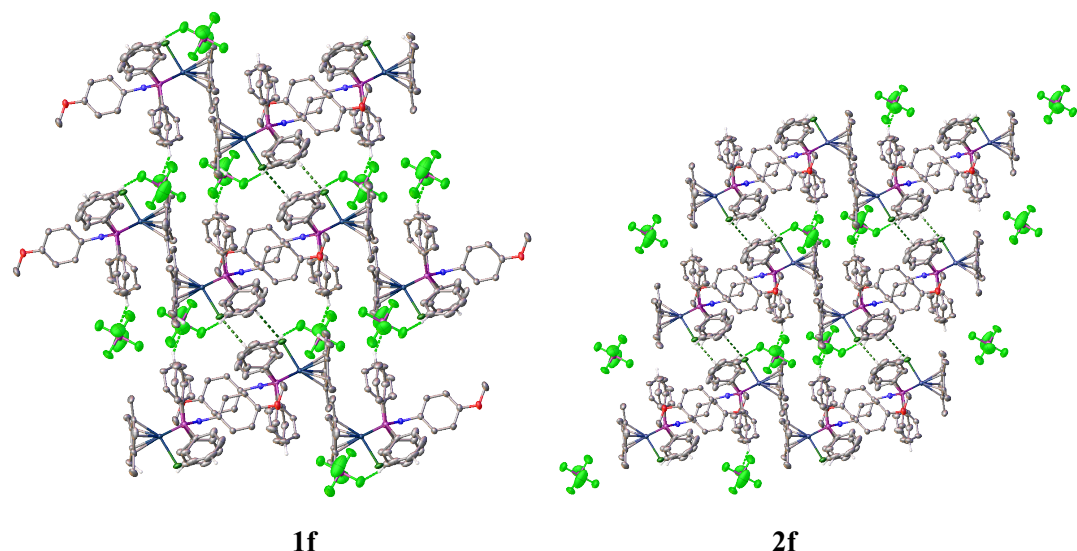


Figure 4.4. Crystal packing of complexes **1f** and **2f** (010) along the *c*-axis.

Table 4.2. Selected bond lengths (\AA) and bond angles ($^\circ$) of complexes **1f** and **2f**.

Bond distances (\AA)	1f	2f
M-P(1)	2.2916(8)	2.2998(9)
M-P(2)	2.2958(8)	2.3079(9)
M-Cl(1)	2.3855(9)	2.3785(9)
M-Cp*(1-5)	2.245(4), 2.227(3), 2.197(3), 2.237(3), 2.233(3)	2.227(4), 2.214(4), 2.188(4), 2.231(3), 2.220(4)
P(1)-N(1)	1.702(2)	1.703(3)
P(2)-N(1)	1.709(2)	1.706(3)
P(1)-C(11)	1.821(3)	1.821(4)
P(1)-C(17)	1.808(3)	1.819(3)
P(2)-C(30)	1.815(3)	1.813(3)
P(2)-C(36)	1.817(3)	1.819(3)
N(1)-C(23)	1.436(4)	1.449(4)

Table 4.2. Selected bond lengths (\AA) and bond angles ($^\circ$) of complexes **1f** and **2f** continued...

Bond angles ($^\circ$)	1f	2f
P(1)-M-P(2)	70.04(3)	70.10(3)
P(1)-N(1)-P(2)	101.02(14)	101.82(16)
P(1)-M-Cl(1)	87.21(3)	87.58(3)
P(2)-M-Cl(1)	84.85(3)	84.96(3)

Table 4.3. Non-classical hydrogen C—H...O bonding and C—H...F interactions of complexes **1f** and **2f**.

Donor --- H...Acceptor	D — H	H...A	D...A	D - H...A	ARU
1f					
C(15)---H(15)...O(1)	0.95	2.59	3.289(4)	131	1-x,1-y,-z
C(34)---H(34)...F(2)	0.95	2.52	3.405(4)	155	-x,-y,-z
C(39)---H(39)...F(4)	0.95	2.46	3.329(4)	152	-x,-1/2+y,-1/2-z
2f					
C(15)---H(15)...O(2)	0.95	2.58	3.275(5)	130	-x,2-y,1-z
C(34)---H(34)...F(2)	0.95	2.52	3.416(5)	157	1-x,-1/2+y,1/2-z
C(39)---H(39)...F(3)	0.95	2.45	3.320(5)	152	1-x,1-y,1-z

Table 4.4. C-H...Cg interactions of complexes **1f** and **2f**.

C---H... π	H...Cg	C...Cg	C - H...Cg	ARU
1f				
C(29)---H(29A)...Cg(5)	0.90	2.95	3.849(4)	1-X,-Y,-Z
C(31)---H(31)...Cg(4)	0.89	2.98	3.868(4)	X,Y,Z
2f				
C(29)---H(29A)...Cg(5)	0.90	2.96	3.868(4)	-X,1-Y,1-Z
C(31)---H(31)...Cg(4)	0.89	2.98	3.867(4)	X,Y,Z

Table 4.5. $\pi \dots \pi$ interactions of complexes **1f** and **2f**.

$\pi \dots \pi$ (Cg...Cg)	Distance (Å)	ARU
1f		
Cg(1)...Cg(2)	5.553(2)	X,Y,Z
Cg(1)...Cg(2)	5.428(2)	-X,1-Y,-Z
Cg(1) ... Cg(6)	5.660(2)	X,Y,Z
Cg(1)...Cg(6)	5.8587(19)	-X,-Y,-Z
Cg(2)...Cg(1)	5.553(2)	X,Y,Z
Cg(2)...Cg(1)	5.428(2)	-X,1-Y,-Z
Cg(2)...Cg(3)	5.599(2)	1-X,1-Y,-Z
Cg(2)...Cg(4)	5.438(2)	X,Y,Z
Cg(2)...Cg(4)	5.1434(19)	1-X,1-Y,-Z
Cg(3)...Cg(2)	4.877(2)	X,Y,Z
Cg(3)...Cg(4)	4.981(2)	1-X,1-Y,-Z
Cg(3)...Cg(5)	4.172(2)	1-X,1/2+Y,1/2-Z
Cg(4)...Cg(2)	5.438(2)	X,Y,Z
Cg(4)...Cg(2)	5.1434(19)	1-X,1-Y,-Z
Cg(4)...Cg(3)	5.218(2)	X,Y,Z
Cg(4)...Cg(3)	4.981(2)	1-X,1-Y,-Z
Cg(4)...Cg(5)	5.2068(19)	X,Y,Z
Cg(4)...Cg(6)	5.1578(18)	1-X,-Y,-Z
Cg(5)...Cg(3)	4.172(2)	1-X,-1/2+Y,1/2-Z
Cg(5)...Cg(4)	5.2786(19)	1-X,-Y,-Z
Cg(5)...Cg(6)	5.073(2)	X,Y,Z
Cg(6)...Cg(1)	5.8588(19)	-X,-Y,-Z
Cg(6)...Cg(2)	5.4511(18)	X,Y,Z
Cg(6)...Cg(4)	5.360(2)	X,Y,Z
2f		
Cg(1)...Cg(2)	5.563(2)	X,Y,Z
Cg(1)...Cg(6)	5.673(2)	X,Y,Z
Cg(1)...Cg(6)	5.858(2)	1-X,1-Y,1-Z
Cg(2)...Cg(1)	5.563(2)	X,Y,Z
Cg(2)...Cg(1)	5.434(3)	1-X,2-Y,1-Z
Cg(2)...Cg(3)	5.601(3)	-X,2-Y,1-Z
Cg(2)...Cg(4)	5.437(2)	X,Y,Z

Table 4.5. $\pi \dots \pi$ interactions of complexes **1f** and **2f** continued...

$\pi \dots \pi$ (Cg...Cg)	Distance (Å)	ARU
Cg(2)...Cg(4)	5.154(2)	-X,2-Y,1-Z
Cg(3)...Cg(2)	4.898(3)	X,Y,Z
Cg(3)...Cg(4)	4.979(2)	-X,2-Y,1-Z
Cg(3)...Cg(5)	4.194(3)	-X,1/2+Y,1/2-Z
Cg(4)...Cg(2)	5.436(2)	X,Y,Z
Cg(4)...Cg(2)	5.154(2)	-X,2-Y,1-Z
Cg(4)...Cg(3)	5.203(2)	X,Y,Z
Cg(4)...Cg(3)	4.979(2)	-X,2-Y,1-Z
Cg(4)...Cg(5)	5.207(2)	X,Y,Z
Cg(4)...Cg(6)	5.164(2)	-X,1-Y,1-Z
Cg(5)...Cg(3)	4.195(3)	= -X,-1/2+Y,1/2-Z
Cg(5)...Cg(4)	5.274(2)	-X,1-Y,1-Z
Cg(5)...Cg(6)	5.078(2)	X,Y,Z
Cg(6)...Cg(1)	5.858(2)	1-X,1-Y,1-Z
Cg(6)...Cg(2)	5.457(2)	X,Y,Z
Cg(6)...Cg(4)	5.363(2)	X,Y,Z

4.4.3 Oxidation of styrene

Both the iridium (**1**) and rhodium catalysts (**2**) were studied under optimum conditions where a catalyst:substrate molar ratio of 1:100 and substrate:oxidant molar ratio of 1:2.5 were used (Fig. 4.5). Under these conditions, good selectivity to the desired products was observed as well as good conversion. When 1,2-dichloroethane (DCE) was used as a solvent, after 3 h, using catalyst **1a**, a 62% conversion was observed, with a 15% yield to benzaldehyde and a 1% yield to styrene oxide. When the reaction was run for a further 6 h, the conversion increased to 96% and the yield to benzaldehyde increased to 18% and styrene oxide to 2%. When the solvent was changed to acetonitrile (MeCN), after 9 h, 83% conversion was observed, with a 30% yield to benzaldehyde and 24% yield to styrene oxide. Higher catalytic activity in acetonitrile is attributed to its polarity, where the different phases are uniform, promoting mass transfer.¹⁰

The Ir (**1**) catalysts are slightly more active than the Rh (**2**) catalysts as shown by the reaction rates. This is suggested to be due to the active super oxo Rh(III) complex having a lower affinity for the olefin.³¹ Such cases also have been observed with Rh(C₂H₄)₂(C₂H₅)

complexes.³¹ The highest activities were exhibited by catalysts **1e** (88%) and **2e** (83%), with the chlorine substituted phenyl group on the nitrogen atom. Catalysts **1c** and **2d** were least active. Comparable activity between catalysts **1** and **2** of the cyclohexyl (**a**) substituted and functionalized phenyl groups are noted (**e** and **f**). The difference in the activity of the catalysts bearing the different substituents could be attributed to their basicity.¹⁸ The basic nature of the ligand is attributed to the substituent on the nitrogen atom, which lowers the activity with an increase in basicity. This basic substituent is likely to increase the electron density at the metal center, which makes it easier for the oxidation process to occur, where the oxidation state of the metal goes from a M(I) to M(III) species. However, the formation of the super oxo species becomes more difficult since the high basic nature of the complex stabilizes the M^{III} oxidation state. Thus, less basic and electron withdrawing substituents such as **1e** and **2e** are more active in comparison to **1c** and **2c**, where the alkyl substituent increases the basic nature of the complex.

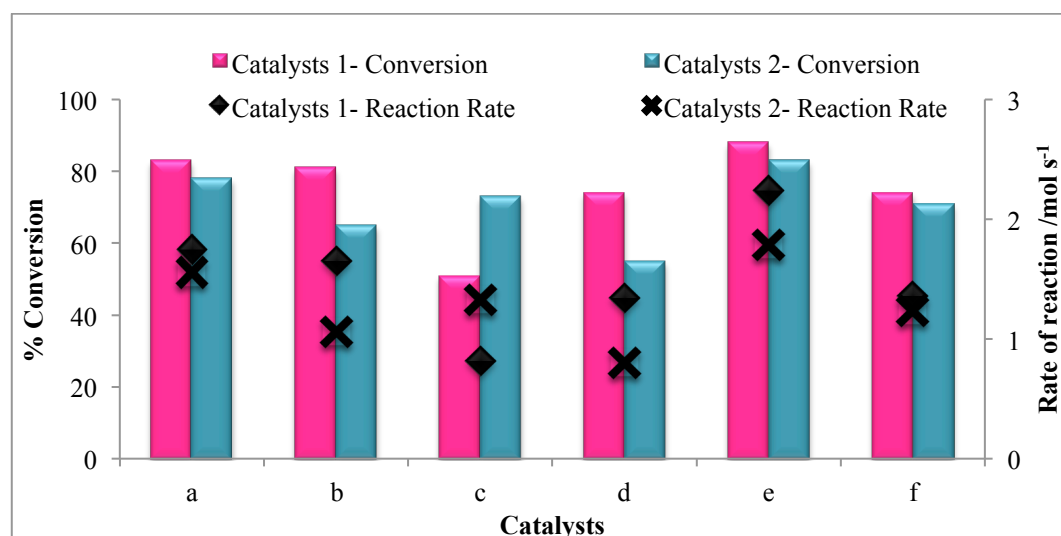


Figure 4.5. Conversion of styrene over catalysts **1** and **2** in MeCN.

Conditions: Catalyst:styrene (1:100); Styrene: TBHP (1:2.5); Temperature: 80 °C.

The yields to benzaldehyde for both catalysts are comparable, however, catalysts **1** are more selective to styrene oxide than catalysts **2** (Fig. 4.6). The TONs towards benzaldehyde for catalysts **2** are slightly greater than catalysts **1**, however, the TONs towards styrene oxide are higher for catalysts **1** (Table 4.6). This is an indication that deeper oxidation is more prevalent when using catalysts **1**, which also reflects their high activity. The catalyst with the chlorine substituted phenyl group (**1e**) is most selective to styrene oxide, also giving the highest yield (28%) and TON (23). The catalysts with the methoxy substituent (**f**) and the unsubstituted phenyl group (**d**) exhibit similar activity and selectivity. Catalysts with the cyclohexyl (**a**) and isopropyl (**b**) substituted nitrogen atoms are comparable in terms of activity and yield to

benzaldehyde and styrene oxide and this is also noted in chromium catalysts bearing the same functional groups in ethylene oligomerisation.¹⁸

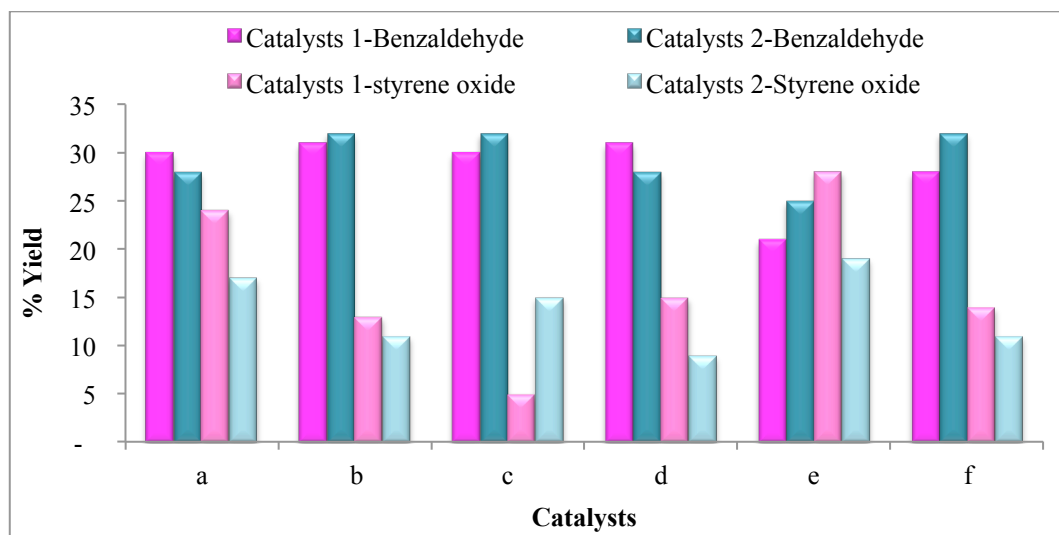


Figure 4.6. Yield to benzaldehyde and styrene oxide over catalysts **1** and **2** in MeCN.

Conditions: Catalyst:styrene (1:100); Styrene: TBHP (1:2.5); Temperature: 80 °C.

This is due to these ligands having similar basic properties. It has been reported that increasing the chain length by at least four carbons improves the selectivity, which accounts for the good selectivity to benzaldehyde and poor selectivity to styrene oxide by catalyst **1c**.¹⁸ This could be due to the basic nature of catalyst **1c**, where the increase in carbon chain length increases the basic nature of the catalyst. This controls the reaction whereby the metal goes from a M(I) to M(III) species, thus controlling the selectivity to one product (benzaldehyde).

Table 4.6. Turnover numbers for catalysts **1** and **2** towards benzaldehyde and styrene oxide.

Catalysts	Turnover number (TON)			
	1		2	
	Benzaldehyde	Styrene Oxide	Benzaldehyde	Styrene oxide
a	23	19	25	15
b	24	15	27	10
c	25	5	27	12
d	26	12	23	7
e	18	23	22	17
f	24	12	27	9

Unlike other studies reported, such as styrene oxidation carried out by iridium cyclopentadienyl half sandwich complexes using PhIO as an oxidant where low yields to

benzaldehyde (6-11%) and no selectivity to styrene oxide was found,³³ these systems achieve a relatively good yield to both benzaldehyde and styrene oxide. In comparison, bis(pyridylimino)isoindolato-iridium complexes gave a 55% conversion over a 48 h period with 50% yield to the epoxide.⁵⁶ Furthermore, triphenylphosphine complexes of Ir and Rh used in the oxidation of styrene gave low yields to styrene oxide.^{29,30} Using a PNNP system, Stoop et al. also reported low conversions in the epoxidation of styrene.⁵⁷

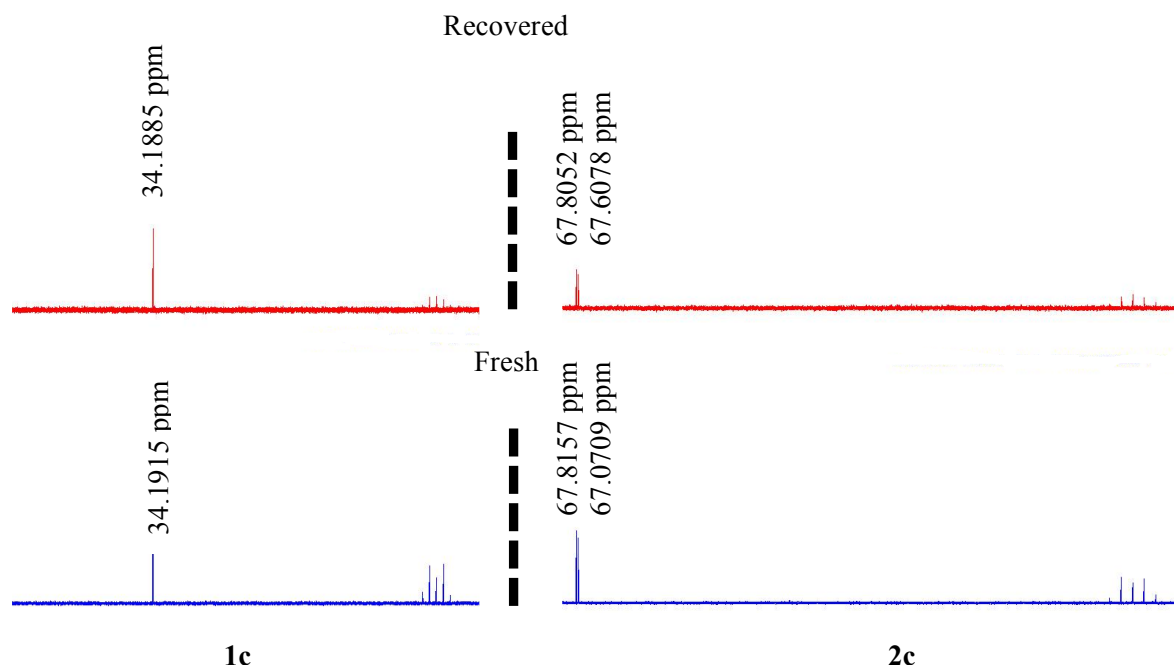


Figure 4.7. ^{31}P NMR of the recovered and fresh catalysts **1c** and **2c**.

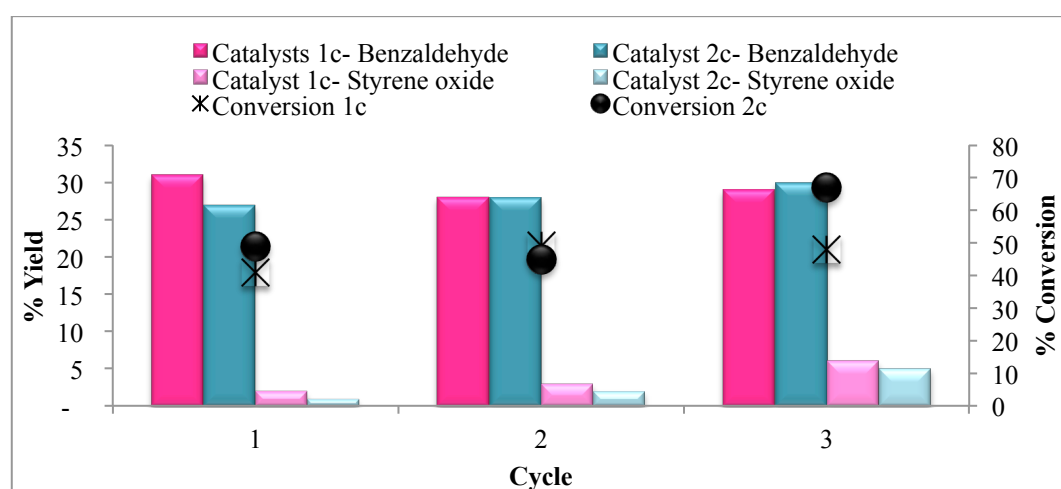
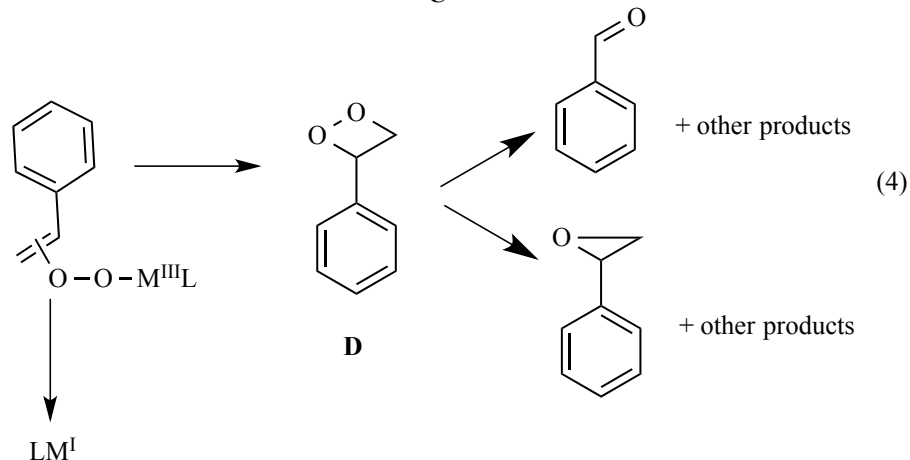
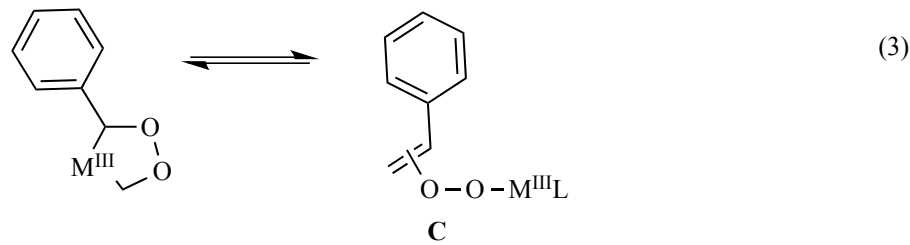
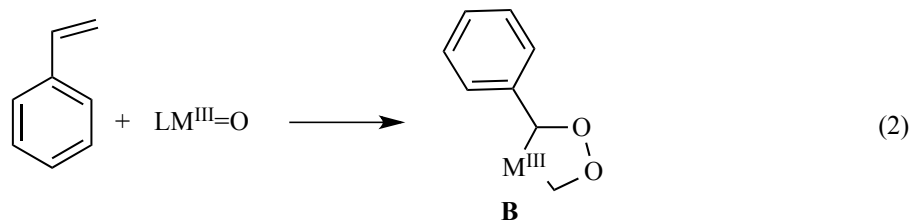


Figure 4.8. Conversion of styrene by recovered catalysts over **1c** and **2c** over three cycles in MeCN.

Conditions: Catalyst:styrene (1:100); Styrene: TBHP (1:2.5); Temperature: 80 °C.

The recovery of the catalyst was investigated. The used catalytic mixtures were evaporated to dryness to which diethyl ether was added. This caused the precipitation of the used catalysts. The recovered catalysts were washed several times with diethyl ether and reused. It has been reported that when using phosphine based ligands the catalysts are destroyed due to progressive oxidation of the ligands.⁵⁸ The used catalysts were recovered and characterized and the melting points (catalyst **1c** recovered melting point: 263-264 °C) and NMR (Fig. 4.7) are comparable to those of the fresh catalysts. Furthermore, the recovered catalysts **1c** and **2c** were re-used over 3 cycles (Fig 4.8). However, the amount of catalyst recovered decreased over time, due to mechanical loss of the small quantities involved. The conversion over catalyst **1c** after cycle 1 decreased slightly from the original run (53% to 41%) and thereafter increased to be essentially constant at 49% in cycle 2 and 48 % in cycle 3, results of which are probably within experimental error. Also, the repeat reactions were slightly more dilute. The yield to benzaldehyde is comparable to the first run, however, the yield to styrene oxide increases from cycle 1 (2%) to cycle 3 (6%). The recycled catalyst **2c** showed a decrease in conversion compared to the first run, but significantly increased in cycle 3 (from 45 % to 65 %). This could be due to concentration effects. The yield to benzaldehyde is comparable to the first run, however, the yield to styrene oxide decreased (from 15% to 5 %).

To elucidate the mechanism by which these two products form, styrene oxide was used as a substrate with catalyst **1** under conditions. The reaction was monitored over 9 h, during which time no conversion took place. When benzaldehyde was used as a substrate, under the same conditions, the deeper oxidized product, benzoic acid and the cleaved product benzene formed. On the basis of this experimental work and the mechanism proposed by Li et al. on a cobalt system, a probable mechanism is proposed in Scheme 4.1.⁸ The metal complex (LM(I)) can activate and bind to oxygen from the oxidant (*t*-BuOOH) forming a peroxy LM(III) species (**A**) (eqn 1) which then reacts with styrene to form the intermediate (**B**) eqn (2).^{1,59-61} Rearrangement of intermediate **B** to form **C** (eqn 3). The formation of benzaldehyde and styrene oxide via two different pathways occurs through **D** and generation of the catalyst (eqn 4).^{1,18,59-61}



Scheme 4.1. Proposed mechanism for the oxidation of styrene by complexes **1** and **2**.

4.5 Conclusion

In this paper, new iridium and rhodium complexes have been synthesized and fully characterized and were used as catalysts in the oxidation of styrene. The iridium catalysts are more active than the rhodium catalysts. This could be due to the active super oxo Rh(III) complex having a lower affinity for the olefin. The yield to benzaldehyde by both catalysts is comparable and is much higher than that of styrene oxide. However, the iridium catalysts gave a higher yield to styrene oxide. The catalysts bearing the chlorine substituted phenyl group on the nitrogen atom is most active and gave the highest yield to styrene oxide. The difference in the activity of the catalysts bearing the different substituents on the nitrogen atom, of the ligand backbone, could be attributed to the basicity of the ligand backbone. The catalysts were recovered, characterized and recycled over 3 cycles. The activity and yield to styrene oxide dropped, however, the yield to benzaldehyde remains constant. The results

show that PNP complexes of Ir and Rh may indeed have considerable potential in the selective oxidation of styrene.

4.6 References

- [1] Bruin, de B.; Budzelaar, P. H. M.; Gal, A. W. *Angew. Chem. Int. Ed.* **2004**, *43*, 4142-4157.
- [2] Tada, M.; Muratsugu, S.; Kinoshita, M.; Sasaki, T.; Iwasawa, Y. *J. Am. Chem. Soc.* **2009**, *132*, 713-724.
- [3] Ahmad, A. L.; Kohestani, B.; Bhatia, S.; Ooi, S. B. *Int. J Appl. Cer. Tech.* **2012**, *9*, 588-598.
- [4] Patel, A.; Patel, K. *Inorg. Chimi. Acta* **2014**, *419*, 130-134.
- [5] Karandikar, P.; Agashe, M.; Vijayamohanan, K.; Chandwadkar, A. *J. Appl. Catal. A- Gen.* **2004**, *257*, 133-143.
- [6] Patil, N. S.; Jha, R.; Uphade, B. S.; Bhargava, S. K.; Choudhary, V. R. *Appl. Catal. A-Gen.* **2004**, *275*, 87-93.
- [7] Patel, A.; Pathan, S. *Ind. Eng. Chem. Res.* **2011**, *51*, 732-740.
- [8] Li, Z.; Wu, S.; Ding, H.; Lu, H.; Liu, J.; Huo, Q.; Guan, J.; Kan, Q. *New J. Chem.* **2013**, *37*, 4220-4229.
- [9] Ding, Y.; Gao, Q.; Li, G.; Zhang, H.; Wang, J.; Yan, L.; Suo, J. *J. Mol. Catal A- Chem.* **2004**, *218*, 161-170.
- [10] Hu, J.; Li, K.; Li, W.; Ma, F.; Guo, Y. *Appl. Catal. A- Gen* **2009**, *364*, 211-220.
- [11] Grigoropoulou, G.; Clark, J. H.; Elings, J. A. *Green Chem.* **2003**, *5*, 1-7.
- [12] Yang, Y.; Ding, H.; Hao, S.; Zhang, Y.; Kan, Q. *Appl. Organomet. Chem.* **2011**, *25*, 262-
- [13] Warth A, D. *Appl. Environ. Microbiol.* **1991**, *57*, 3410-3414.
- [14] Chiappe, C.; Sanzone, A.; Dyson, P. J. *Green Chem.* **2011**, *13*, 1437-1441.
- [15] Kanmani, A. S.; Vancheesan, S. *Stud. Surf. Sci. and Catal.* **1998**, *113*, 285-292.
- [16] Teo, S.; Weng, Z.; Hor, T. S. A. *Organometallics* **2008**, *27*, 4188-4192.
- [17] Blann, K.; Bollmann, A.; Dixon, J. T.; Hess, F. M.; Killian, E.; Maumela, H.; Morgan, D. H.; Neveling, A.; Otto, S.; Overett, M. J. *Chem. Commun.* **2005**, 620-621
- [18] Blann, K.; Bollmann, A.; de Bod, H.; Dixon, J. T.; Killian, E.; Nongodlwana, P.; Maumela, M. C.; Maumela, H.; McConnel, A. E.; Morgan, D. H.; Overette, M. J.; Pfeotorius, M.; Kuhlmann, S.; Wasserscheid, P. *J. Catal.* **2007**, *249*, 244-249.
- [19] Overett, M. J.; Blann, K.; Bollmann, A.; Dixon, J. T.; Hess, F.; Killian, E.; Maumela, H.; Morgan, D. H.; Neveling, A.; Otto, S. *Chem. Commun.* **2005**, 622-624.
- [20] Bollmann, A.; Blann, K.; Dixon, J. T.; Hess, F. M.; Killian, E.; Maumela, H.; McGuiness, D. S.; Morgan, D. H.; Neveling, A.; Otton, S.; Overette, M.; Slawin, A. M. Z.; Wassercheid, P.; Kihlmann, S. *J. Am. Chem. Soc.* **2004**, *126*, 14712-14713.
- [21] Bowen, L. E.; Haddow, M. F.; Orpen, A. G.; Wass, D. F. *Dalton Trans.* **2007**, 1160-1168.
- [22] Bowen, L. E.; Charernsuk, M.; Hey, T. W.; McMullin, C. L.; Orpen, A. G.; Wass, D. F. *Dalton Trans.* **2010**, *39*, 560-567.
- [23] Benito-Garagorri, D.; Alves, L. G. a.; Puchberger, M.; Mereiter, K.; Veiros, L. F.; Calhorda, M. J.; Carvalho, M. D.; Ferreira, L. P.; Godinho, M.; Kirchner, K. *Organometallics* **2009**, *28*, 6902-6914.
- [24] Benito-Garagorri, D.; Kirchner, K. *Acc. Chem. Res.* **2008**, *41*, 201-213.
- [25] van der Boom, M. E.; Milstein, D. *Chem. Rev.* **2003**, *103*, 1759-1792.
- [26] Xu, X.; Xi, Z.; Chen, W.; Wang, D. *J. Coord. Chem.* **2007**, *60*, 2297-2308.
- [27] Albrecht, M.; van Koten, G. *Angew. Chem. Int. Ed.* **2001**, *40*, 3750-3781.
- [28] Collman, J. P.; Kubota, M.; Hosking, J. W. *J. Am. Chem. Soc.* **1967**, *89*, 4809-4811.
- [29] Takao, K.; Wayaku, M.; Fujiwara, Y.; Imanaka, T.; Teranishi, S. B. *Chem. Soc. Jpn.*

- 1970**, **43**, 3898-3900.
- [30] Takao, K.; Fujiwara, Y.; Imanaka, T.; Teranishi, S. *B. Chem. Soc. Jpn.* **1970**, **43**, 1153-1157.
- [31] Farrar, J.; Holland, D.; Milner, D. *J. Dalton Trans.* **1975**, 815-821.
- [32] Suzuki, T. *Chem. Rev.* **2011**, **111**, 1825-1845.
- [33] Burlington, C. R.; Harrison, D. P.; White, P. S.; Brookhart, M.; Templeton, J. L. *Inorg. Chem.* **2013**, **52**, 11351-11360.
- [34] Kang, J. W.; Moseley, K.; Maitlis, P. M. *J. Am. Chem. Soc.* **1969**, **91**, 5970-5977.
- [35] Ball, R. G.; Garaham, W. A. G.; Heinekey, D. M.; Hoyano, J. K.; McMaster, A. D.; Mattson, B. M.; Michel, S. T. *Inorg. Chem.* **1990**, **29**, 2023-2025.
- [36] White, C.; Yates, A.; Maitlis, P. M. *Inorg. Syn.* **1992**, **29**, 228-234.
- [37] Govindaswamy, P.; Mozhariovskyj, Y. A.; Kollipara, M. R. *Polyhedron* **2005**, **24**, 1710-1716.
- [38] Sheldrick, G. M.; 2.05 ed.; SHELXS-97, SHELXL-97 and SADABS version 2.05, University of Göttingen, Germany: **1997**.
- [39] Sheldrick, G. *Acta Crystallogr., Sect. A*: **2008**, **64**, 112-122.
- [40] Otwinski, Z and Minor, Z. *Processing of X-ray Diffraction Data Collected in Oscillation Mode, Methods in Enzymology, Macro. Cryst. A*, **1997**, **276**, 307-326. C.W. Carter, Jr. and R. M. Sweet, Eds., Academic Press (New York).
- [41] Dolomanov, O. V.; Bourhis, L. J.; Gildea, R. J.; Howard, J. A. K.; Puschmann, H. J. *Appl. Crystallogr.* **2009**, **42**, 339-341.
- [42] Valderrama, M.; Contreras, R.; Boys, D. *J. Organomet. Chem.* **2003**, **665**, 7-12.
- [43] Simón-Manso, E.; Valderrama, M. *J. Organomet. Chem.* **2006**, **691**, 380-386.
- [44] von Philipsborn, W. *Chem. Soc. Rev.* **1999**, **28**, 95-105.
- [45] Elsevier, C. J.; Ernsting, J. M.; de Lange, W. G. J. *J. Chem. Soci. Chem. Commun.* **1989**, 585-586.
- [46] Carlton, L. *Magn. Reson. Chem.* **1997**, **35**, 153-158.
- [47] Ernsting, J. M.; Gaemers, S.; Elsevier, C. J. *Magnetic Resonance in Chemistry* **2004**, **42**, 721-736.
- [48] Elsevier, C. J.; Kowall, B.; Kragten, H. *Inorg. Chem.* **1995**, **34**, 4836-4839.
- [49] Appleby, T.; Derek Woollins, J. *Coord. Chem. Rev.* **2002**, **235**, 121-140.
- [50] Fei, Z.; Dyson, P. J. *Coord. Chem. Rev.* **2005**, **249**, 2056-2074.
- [51] Albright, T. A.; Burdett, J. K. *Problems in Molecular Orbital Theory*. **1992**, 103-104, Oxford University Press: New York.
- [52] Browning, C. S.; Farrat, D. H.; Frankel, D. C. *Acta Cryst. Sec. C* **1992**, **C48**, 806-811.
- [53] Grabowski, Z. R.; Rotkiewicz, K.; Rettig, W. *Chem. Rev.* **2003**, **103**, 3899-4032.
- [54] Druzhinin, S. I.; Dubbaka, S. R.; Knochel, P.; Kovalenko, S. A.; Mayer, P.; Senyushkina, T.; Zachariasse, K. A. *J. Phys. Chem. A* **2008**, **112**, 2749-2761.
- [55] Ganeshamoorthy, C.; Balakrishna Ms Fau - Mague, J. T.; Mague Jt Fau - Tuononen, H. M.; Tuononen, H. M. *Inorg. Chem.* **2008**, **47**, 7035-7047.
- [56] Camerano, J. A.; Sämann, C.; Wadeohl, H.; Gade, L. H. *Organometallics* **2011**, **30**, 379-382.
- [57] Stoop, R. M.; Bachmann, S.; Valentini, M.; Mezzetti, A. *Organometallics* **2000**, **19**, 4117-4126.
- [58] Bressan, M.; Morville, A. *Inorg. Chem.* **1989**, **28**, 950-953.
- [59] Tang, Q.; Zhang, Q.; Wu, H.; Wang, Y. *J. Catal.* **2005**, **230**, 384-397.
- [60] Cui, H.; Zhang, Y.; Zhao, L.; Zhu, Y. *Catal. Commun.* **2011**, **12**, 417-420
- [61] Li, Z.; Wu, S.; Ma, Y.; Liu, H.; Hu, J.; Liu, L.; Huo, Q.; Guan, J.; Kan, Q. *Trans. Met Chem* **2013**, **38**, 243-251.

Chapter Five

Iridium and rhodium “PNP” aminodiphosphine complexes used as catalysts in the oxidation of *n*-octane

5.1 Abstract

Six PNP or aminodiphosphine ligands were synthesized and complexed to the transition metals iridium and rhodium to give $[(\eta^5\text{-C}_5\text{Me}_5)\text{MCl}\{\eta^2\text{-}P,P'\text{-}(\text{PPh}_2)_2\text{NR}\}]\text{PF}_6$, where M= Ir (**1**) and Rh (**2**) and R= cyclohexyl (**a**), *iso*-propyl (**b**), pentyl (**c**), phenyl (**d**), chlorophenyl (**e**) and methoxyphenyl (**f**). Crystals of **1c**, **2c** and **2d** were obtained, which showed a distorted octahedral geometry around the metal centers. These complexes showed good activity in the oxidation of *n*-octane using *tert*-butyl hydroperoxide (TBHP) as the oxidant. The rhodium complexes were more active than the iridium complexes. Octanones were the dominant products, however, good selectivities to the alcohols were also observed for both types of catalysts. Catalyst **2c** was the most active catalyst in the series. The catalysts were recovered, characterized and reused.

Keywords: Aminodiphosphine; iridium; rhodium; oxidation; *n*-octane.

5.2 Introduction

The conversion of saturated hydrocarbons to oxygen containing compounds such as alcohols, ketones, aldehydes and acids has been a topic of interest over the past 20 years.¹⁻¹² There is a current need and economic urgency to replace current petrochemical feedstocks (olefins) by easily accessible alkanes, which can result in more proficient use of energy and efficient strategies for fine chemical synthesis.¹³⁻¹⁶ Terminally oxidized hydrocarbons are valuable starting materials in the pharmaceutical and chemical industry.¹⁷ However, one of the main challenges in activation of alkane C–H bonds is the low selectivity in forming the desired products, i.e. the preferential activation of sp^2 over sp^3 hybridized C–H bonds.¹⁸⁻²⁰ Furthermore, the chemical inertness of alkanes, together with their high ionization energy, pKa values and low electron affinity makes activation of the C–H bonds difficult.^{11,17,19,21,22} To overcome such problems there has been a rapid development of catalytic systems inspired by biological systems of cytochrome P450 and methane monooxygenase.²³⁻³² These enzymes have the ability to efficiently catalyze a number of exogenous and endogenous organic compounds such as medium chain alkanes to large molecules including triterpenes, as well as steroidial, polyaromatic compounds and more importantly oxygenates. Metalloporphyrins and Schiff

based systems have been developed to mimic such biological systems.³³⁻⁴² Site selective C–H activation by iron complexes has been reported by White and co workers in trying to mimic enzymes.^{3,43-46} These catalytic processes are carried out by a variety of oxidants namely, PhIO, NaOCl, H₂O₂, alkyl hydroperoxides, percarboxylic acids and molecular oxygen.^{34,40,47-55}

The design of a suitable ligand system is one way of achieving selective activation of paraffins. These could include the aminodiphosphine or PNP ligand system.⁵⁶⁻⁶² These hybrid ligands which consist of both soft (N) and hard (P) donors are of particular interest in that they are part of a system that displays high activity, stability and variability.⁶³⁻⁶⁶ By modifying the ligand backbone through substitution of the donor atoms, the activity of the metal can be tailored.^{67,68} These ligands may bind to the metal centers as either monodentate, bidentate or as bridged ligands, which allow the reactions of the metal ions to be selective, due to the high demand the ligands place on the stereochemistry of the complex.⁶⁹

In general, phosphine based ligands are limited in their application in oxidation reactions due to ligand loss and degradation.⁷⁰ Ruthenium based phosphine complexes have been studied in the oxidation of *n*-octane, however, low conversions and over-oxidation is prevalent.^{71,72} The activation of alkane C–H bonds by rhodium and iridium complexes has not been thoroughly explored. However, Nomura and Uemura⁷³ have used rhodium compounds such as Rh₃O, [Rh(acac)₃], [RhCl(CO)₂]₂, [RhCl(PPh₃)₃] and [Rh₂(OAc)₄] in the oxidation of cyclohexane using peracetic acid, H₂O₂, TBHP (*t*-butyl hydroperoxide) and *m*-CPBA (meta chloroperoxybenzoic acid).⁷³

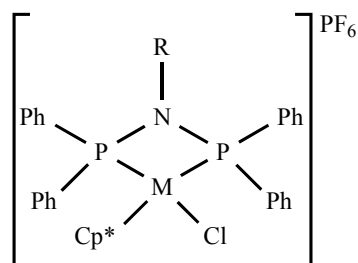


Figure 5.1. General structure of the complexes used as catalysts in the oxidation of *n*-octane.

(M = Ir (**1**) and Rh (**2**); R = cyclohexyl (**a**), *iso*-propyl (**b**), pentyl (**c**), phenyl (**d**), chlorophenyl (**e**) and methoxyphenyl (**f**); Cp* = η^5 -pentamethylcyclopentadienyl).

With the worldwide increase in gas to liquid plants, there is an increase in the production of medium to long chain paraffins, which increases the need to functionalize these hydrocarbons.⁷⁴⁻⁷⁶ Hence, in this study we report the application of iridium (**1**) and rhodium (**2**) aminodiphosphine “PNP” complexes in the oxidation of *n*-octane. Optimization of solvent, temperature and oxidant was carried out. The substituents on the nitrogen atom were varied by making use of six functional groups (Fig.

5.1), having different basic properties, with the intention of observing if these groups have an effect on the catalytic activity and selectivity to the products of oxidation.

5.3 Experimental

5.3.1 Crystal structure analysis

The single-crystal X-ray diffraction data of complex **1c** were collected on a Bruker KAPPA APEX II DUO diffractometer using graphite-monochromated Mo-K α radiation ($\lambda = 0.71073 \text{ \AA}$). The crystal structure data of complexes **1c**, **2c** and **2d** are presented in Table 5.1. Data collection was carried out at 173(2) K. Temperature was controlled by an Oxford Cryostream cooling system (Oxford Cryostat). Cell refinement and data reduction were performed using the program SAINT.⁷⁷ The data were scaled and absorption correction performed using SADABS.⁷⁷ The structure was solved by direct methods using SHELXS-97 and refined by full-matrix least-squares methods based on F² using SHELXL-97.⁷⁸

X-ray single crystal intensity data of complexes **2c** and **2d** were collected on a Nonius Kappa-CCD diffractometer using graphite monochromated MoK α radiation ($\lambda = 0.71073 \text{ \AA}$). Temperature was controlled by an Oxford Cryostream cooling system (Oxford Cryostat). The strategy for the data collections was evaluated using the Bruker Nonius "Collect" program. Data were scaled and reduced using DENZO-SMN software.⁷⁹ The data were scaled and absorption correction performed using SADABS.⁷⁷ The structure was solved by direct methods using SHELXS-97 and refined by full-matrix least-squares methods based on F² using SHELXL-97.⁷⁸

The program Olex2 was used to prepare molecular graphic images.⁸⁰ All non-hydrogen atoms were refined anisotropically. Anisotropic displacement parameters restraints were applied to all six fluorine atoms, which display relatively high thermal motions. All hydrogen atoms were placed in idealized positions and refined in riding models with U_{iso} assigned the values to be 1.2 or 1.5 times those of their parent atoms and the distances of C-H were constrained from 0.95 \AA to 0.99 \AA . (More information is available in Appendix C).

Table 5.1. Single crystal structural information of complexes **1c** and **2c** and **2d**.

Compound	1c	2c	2d
Mol. Formula	C _{39.05} H ₃₅ ClIrNP ₂ , F ₆ P, CH ₃ O	C ₃₉ H ₄₆ CINP ₂ Rh, F ₆ P	C ₄₀ H ₄₀ CINP ₂ Rh, F ₆ P, CH ₂ Cl ₂
Mol. Weight	983.27	874.04	964.93
Temperature (k)	173	173	173
Wavelength (Å)	Mo Kα (0.71073)	Mo Kα (0.71073)	Mo Kα (0.71073)
Crystal symmetry	orthohombic	monoclinic	monoclinic
Space Group	Pnma	P21/n	P21/c
a (Å)	17.537(3)	9.6887(3)	15.4861(10)
b (Å)	12.704(3)	29.0830(6)	16.5387(11)
c (Å)	18.730(4)	14.5669(4)	17.5188(11)
α, β, γ (°)	90, 90, 90	90, 106.65(1), 90	90, 108.946(2), 90
Volume (Å ³)	4172.9(15)	3932.33(18)	4243.8(5)
Z	4	4	4
Density (g/m ³)	1.566	1.476	1.510
Absorption coefficient (mm ⁻¹)	3.437	0.682	0762
F(000)	1945	1792	1960
Crystal size (mm)	0.48 x 0.81 x 1.05	0.15 x 0.22 x 0.24	0.12 x 0.14 x 0.15
Θ range for data collection	1.6, 28.2	4.1, 28.3	1.4, 28.4
Reflection (collected, independent, R _{int})	75016, 5332, 0.028	179500, 9670, 0.074	88058, 10572, 0.055
Observed Data [I > 2.0 sigma(I)]	4733	7456	8540
Nref, Npar	5332, 269	9670, 466	10572, 501
R, wR2, S	0.0248, 0.0639, 1.15	0.0349, 0.0801, 1.10	0.0316, 0.0758, 1.03
Largest diff. peak, hole (e.Å ⁻³)	1.79, -1.12	0.84, -0.65	0.81,-0.64
No of C—H···X interactions	2	4	7
No of X-Y...π (Cg-Ring) interactions	2	2	5
No of π...π (Cg- Cg) interactions	-	13	20

5.3.2 Oxidation of *n*-octane

All reagents were weighed and handled in air. The compounds **1** and **2** were synthesized and characterized according to the procedure described in Chapter 4, Section 4.3 and 4.4. All products in the *n*-octane oxidation were analyzed using a PerkinElmer Auto System gas chromatograph fitted with a Flame Ionisation Detector (FID) set at 260 °C. A Pona column (50 m x 0.20 mm x 0.5 µm) was utilized with the injector temperature set at 240 °C. Catalytic testing was carried out in a two-necked pear shaped flask charged with 10 mg of the respective catalyst, pentanoic acid (as an internal standard), *n*-octane, the respective oxidant and 10 ml of the solvent. The flask was equipped with a reflux condenser, stirred, heated to the required temperature and maintained at this temperature for 48 hours in an oil bath. After the time period, an aliquot was removed using a Pasteur pipette and filtered through cotton wool and a silica gel plug after which PPh₃ was added (for reduction of the remaining TBHP and alkylperoxides which are formed as primary products in alkane oxidation)⁴⁸. An aliquot (0.5 µl) was injected into the GC and quantified.

5.4 Results and discussion

5.4.1 Description of crystal structures

Olex views of **1c**, **2c** and **2d** are shown in Fig. 5.2. The selected interatomic distances and angles for **1c**, **2c** and **2d** are listed in Table 5.2. For both **1c**, **2c** and **2d**, the rhodium/iridium centers are distorted octahedrally coordinated, and the chloride is coordinated perpendicular to the strained four membered chelate ring, whilst the Cp* ligand is trans to the PNP nitrogen donor. In the structure of compound **2d** co crystallization of DCM occurred via C–H...F interaction (3.492 Å). Ir–Cl(1) Rh–Cl(1) and Ir–Cl(1) bond lengths are 2.4036(11, 2.3849(6) and 2.3849(6) Å for **1c**, **2c** and **2d**, respectively and comparable to the corresponding values observed for similar Ir and Rh compounds.^{69,81} The interatomic distances of the Ir···N and Rh···N bonds are 2.942, 2.961 and 2.949 Å and the P–N–P angles are 101.54(19), 100.53(10) and 101.70(9)° for **1c**, **2c** and **2d** respectively. These findings indicate that the phosphinoamine nitrogen atoms do not bind to the metal ions. In addition, the average P(1)···P(2) distances are 2.636, 2.646 and 2.651 Å, for compounds **1c**, **2c** and **2d** respectively. The P–N bond lengths (~1.70 Å) lie in a typical P–N single bond range.^{69,81-83} The Rh–P bond lengths of **2c** and **2d** are 2.2907(7) Å for Rh–P(1), 2.2946(7) Å for Rh–P(2), whilst for **1c** the Ir–P(1) is 2.2916(8) Å and 2.2958(8) Å for Ir–P(2). These are similar in related rhodium and iridium complexes.^{69,81} The Rh–C(ring) and Ir–C(ring) distances distance are in the ranges 2.188(3)-2.243(2) and 2.177(2)-2.229(3) Å for **2c** and **2d**, respectively, and 2.232(4)-2.254(3) Å for compound **1c**, and compare well with the those found in other pentamethylcyclopentadienylrhodium(III) or

iridium(III) complexes.^{69,81} Although the nitrogen atom of the diphosphinoamine ligand is a tertiary amine, the nitrogen atoms are located within the plane defined by the two phosphorus and the ipso carbon atoms. The nitrogen atom is sp^2 -hybridized. Such hybridization is occasionally found in compounds with a P–N bond bond.^{84,85} Additionally, the aromatic ring attached to the nitrogen atom is largely twisted against the P–N–P plane (ca. 60–90°) as shown in the x-ray crystal structures. The diphosphinoamine ligands show a twist motion, which may be due to steric interactions with nitrogen atom and this observed in intramolecular charge-transfer compounds such as *p*-dimethylaminobenzonitrile.^{86–88}

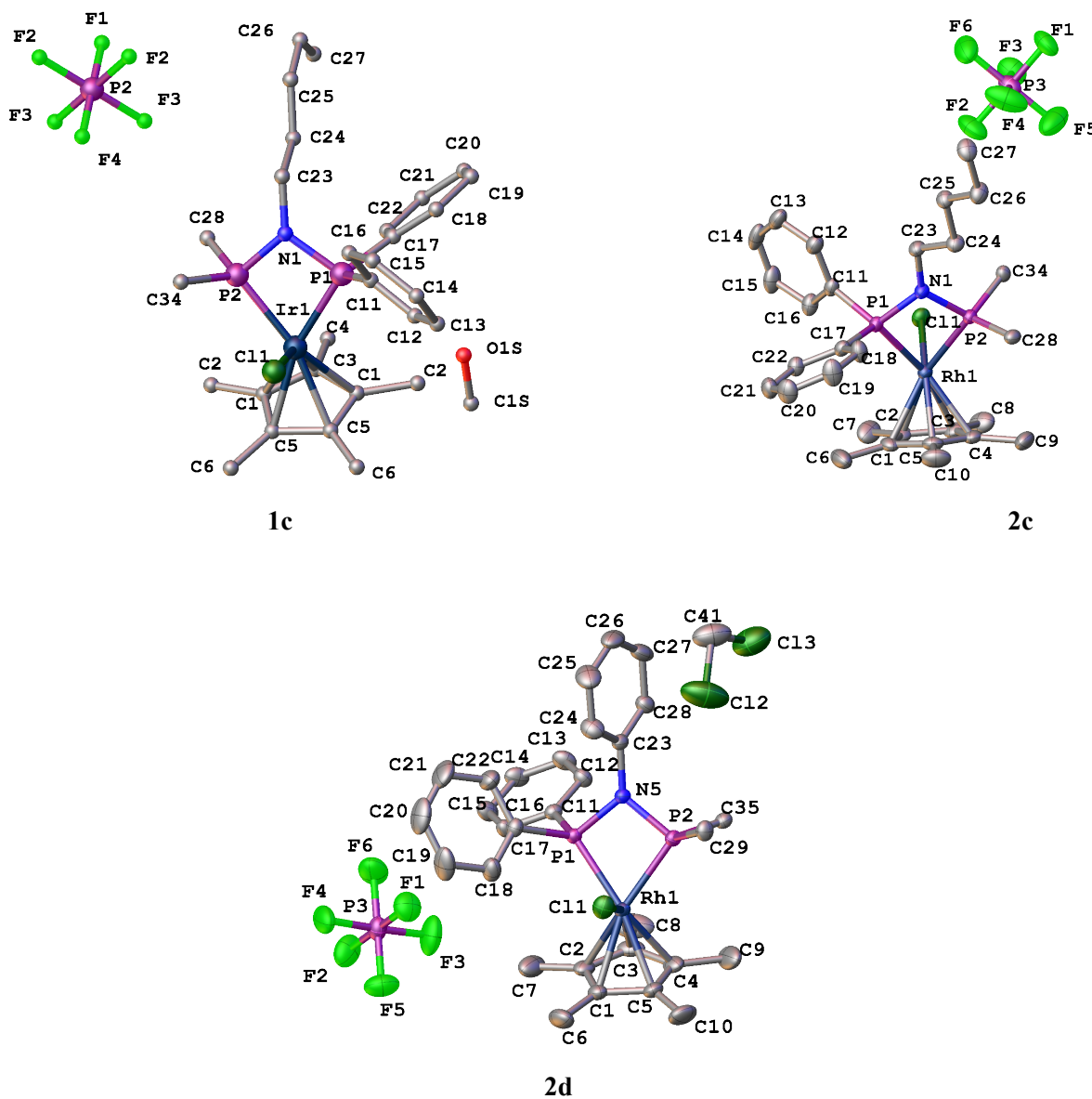


Figure 5.2. Structures of compounds **1c**, **2c** and **2d** with labeling scheme. The phenyl groups of P(2) are removed/omitted for clarity.

Table 5.2. Selected bond lengths (\AA) and bond angles ($^\circ$) of complexes **1c**, **2c** and **2d**.

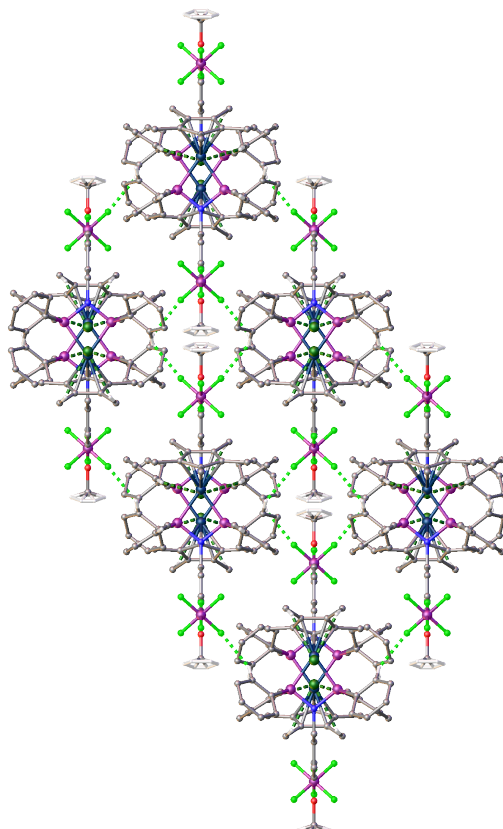
Bond distances (\AA)	1c	2c	2d
M-P(1)	2.3011(10)	2.2907(7)	2.2977(6)
M-P(2)	2.3011(10)	2.2946(7)	2.2995(6)
M-Cl(1)	2.4036(11)	2.3849(6)	2.3849(6)
M-Cp*(1-5)	2.254(3), 2.232(4), 2.243(3), 2.254(3), 2.243(3)	2.243(2), 2.226(2), 2.229(3), 2.235(2), 2.188(3)	2.228(2), 2.229(3), 2.177(2), 2.221(2), 2.218(2)
P(1)-N	1.701(2)	1.7026(19)	1.7106(18)
P(2)-N	1.701(2)	1.7046(19)	1.7076(18)
P(1)-C(11)	1.822(3)	1.818(2)	1.816(2)
P(1)-C(17)	1.818(3)	1.815(2)	1.814(2)
P(2)-C	1.822(3)	1.813(2)	1.807(2)
P(2)-C(36)	1.818(3)	1.810(2)	1.814(2)
N(1)-C(23)	1.43(2)	1.489(3)	1.444(3)
Bond angles ($^\circ$)	1c	2c	2d
P(1)-M-P(2)	69.88(3)	69.70(2)	70.42(2)
P(1)-N(1)-P(2)	101.54(19)	100.53(10)	101.70(9)
P(1)-M-Cl(1)	86.63(3)	91.05(3)	89.30(2)
P(2)-M-Cl(1)	86.63(3)	88.70(2)	85.94(2)

The crystal structures reveal that in all compounds, C-bound H atoms are involved in intermolecular C—H...halogen, C—H...C_g and π - π interactions (Tables 5.3-5.5). This links the fluorine of the counter ion to the compounds via the phenyl ring attached to the phosphorous atom.

The crystal structure of compound **1c** reveals the crystallization of methanol. The crystal packing of compound **1c** form sheets in a layered manner through the *a* axis (100) (Fig. 5.3). In every alternate layer the hydroxyl group of the methanol faces the same direction. Five PF₆ molecules interact with one molecule of the complex **1c** via C—H...F interaction. Along the *a* axis, a chain-like structural formation is observed between the PF₆ counterion and complex **1c**. Whilst along the *a* and *c* axis, a layered like structure is noted. Along the *b* axis, C—H...Cl interaction makes a helical like structure.

The crystal packing for compound **2c** form sheets in a zig-zag manner (110 and 001) (Fig. 5.3). For complex **2c** the zig-zag plane passes through the Cp* ring, makes an angle of 38.30°. The pentyl chain of compound **2c** is kept rigid by C(7)—H(7A)...F(4) and C(35)—H(35)...F(2) (3.441 and 3.227 Å) and C₂₇—H_{27C}...C_{g2} (3.878 Å) interaction.

The crystal packing for compounds **2d** form sheets in a parallel and zig-zag manner through *b* and *c* axis respectively (010 and 001) (Fig. 5.3). Along the *b* axis, the Cp* ring is aligned facing the same direction to each other, whilst along the *c* axis, they face in opposite directions. The crystal packing is dominated by π-π interactions because of the substituted phenyl ring on the nitrogen atom (Table 5.5).



1c

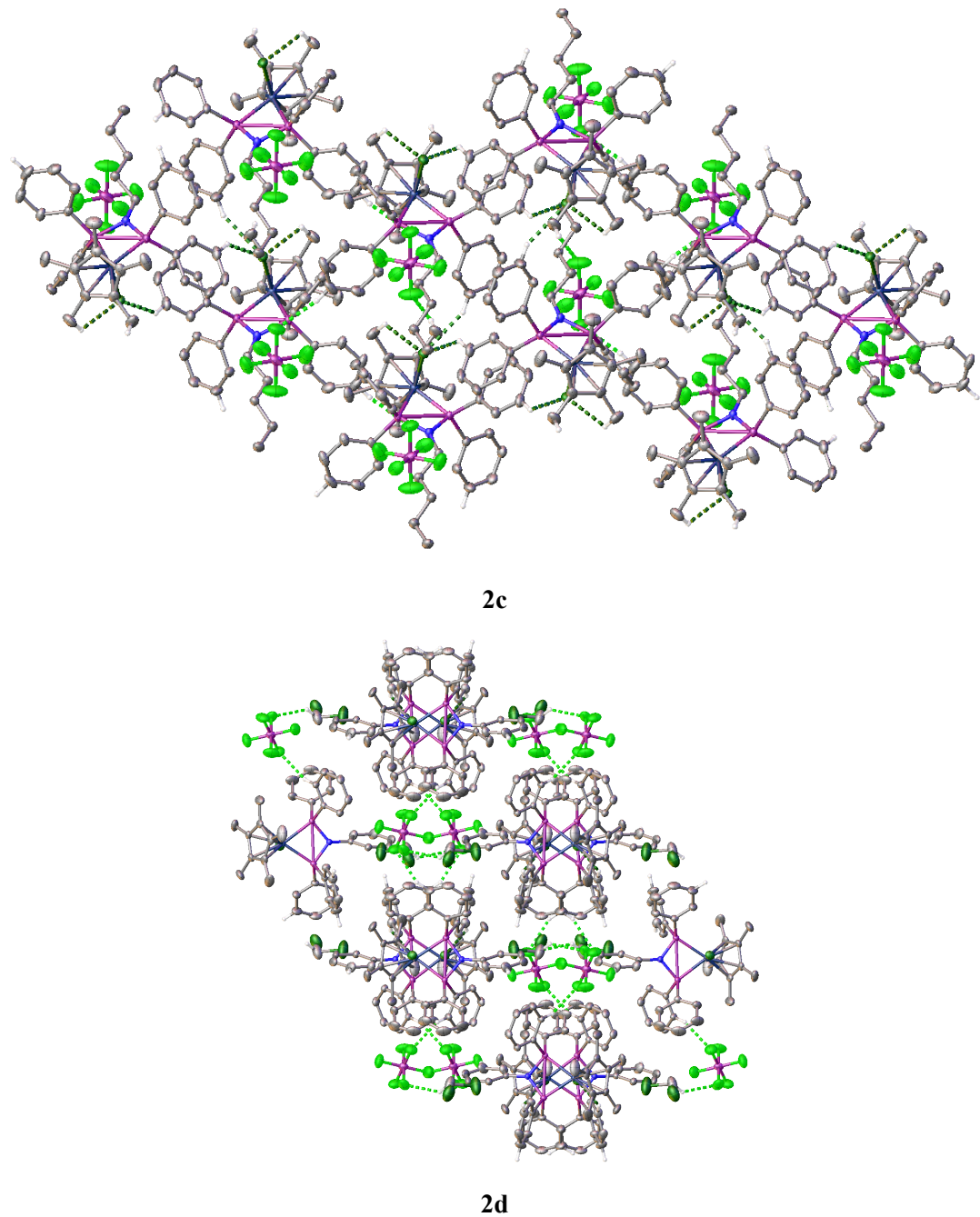


Figure 5.3. Crystal packing of compounds **1c**, **2c** and **2d** along the *c*-axis.

Table 5.3. Non-classical hydrogen C—H...X interactions of complexes **1c**, **2c** and **2d**.

Donor --- H...Acceptor	D — H	H...A	D...A	D - H...A	ARU
1c					
C21---H11...Cl1	0.95	2.81	3.650(4)	148	-1/2+x,1/2-y,1/2-z
C12---H14...F3	0.95	2.51	3.246(4)	135	1-x,1/2+y,1-z
2c					
C(7)---H(7A)...F(4)	0.98	2.47	3.441(4)	170	-1+x,y,-1+z
C(19)---H(19)...Cl(1)	0.95	2.74	3.622(3)	155	1+x,y,z
C(31)---H(31)...F(3)	0.95	2.41	3.345(4)	170	1/2+x,1/2-y,-1/2+z
C(35)---H(35)...F(2)	0.95	2.52	3.227(3)	131	-
2d					
C(15)---H(15)...F(6)	0.95	2.55	3.352(3)	143	-
C(16)---H(16)...F(1)	0.95	2.51	3.391(3)	155	-
C(18)---H(18)...Cl(1)	0.95	2.69	3.225(3)	116	-
C(25)---H(25)...F(5)	0.95	2.49	3.419(3)	165	2-x,-1/2+y,3/2-z
C(33)---H(33)...F(2)	0.95	2.47	3.349(4)	153	-1+x,y,z
C(37) ---H(37)...F(4)	0.95	2.44	3.028(3)	120	-1+x,1/2-y,-1/2+z
C(41)---H(41B)...F(4)	0.99	2.50	3.286(4)	136	2-x,-y,1-z

Table 5.4. X-Y...Cg interactions of complexes **1c**, **2c** and **2d**.

X---Y...π	X...Y	Y...Cg	X - Y...Cg	ARU
1c				
C36---C24A...Cg22	-	2.766(14)	-	X,Y,Z
C26---C24A...Cg22	-	2.766(14)	-	X,1/2-Y,Z
2c				
C(9) ---H(9B) ...Cg(4)	0.923	2.92	3.843(3)	X,Y,Z
C(32) ---H(32) ...Cg(1)	0.618	2.92	3.538(3)	1/2+X,1/2-Y,1/2+Z
2d				
C(14)---H(14)...Cg(4)	0.834	2.94	3.774(3)	2-X,-Y,1-Z
C(30)---H(30)...Cg(4)	0.859	2.95	3.809(3)	X,Y,Z
C(31)---H(31)...Cg(6)	0.918	2.99	3.908(3)	1-X,-Y,1-Z
P(3)---F(1)...Cg(3)	1.5572	3.831(2)	5.3882(14)	X,Y,Z
P(3)---F(5)...Cg(1)	1.2078	3.332(2)	4.5398(13)	2-X,1-Y,1-Z

Table 5.5. $\pi \dots \pi$ interactions of complexes **2c** and **2d**.

$\pi \dots \pi$ (Cg...Cg)	Distance (Å)	ARU
2c		
Cg(1)...Cg(3)	5.4628(16)	X,Y,Z
Cg(1)...Cg(4)	4.6439(15)	-1/2+X,1/2-Y,-1/2+Z
Cg(2)...Cg(2)	3.7223(16)	1-X,-Y,1-Z
Cg(2)...Cg(3)	5.9144(16)	-1+X,Y,Z
Cg(2)...Cg(3)	4.8958(16)	X,Y,Z
Cg(3)...Cg(1)	5.4627(16)	X,Y,Z
Cg(4)...Cg(1)	5.3746(16)	X,Y,Z
Cg(4)...Cg(1)	4.6441(15)	1/2+X,1/2-Y,1/2+Z
Cg(4)...Cg(5)	5.8041(16)	1+X,Y,Z
Cg(4)...Cg(5)	5.6938(15)	1/2+X,1/2-Y,-1/2+Z
Cg(5)...Cg(1)	5.9940(16)	1/2+X,1/2-Y,1/2+Z
Cg(5)...Cg(2)	5.6025(14)	1-X,-Y,1-Z
Cg(5)...Cg(4)	5.0696(16)	X,Y,Z
2d		
Cg(1)...Cg(2)	5.6558(15)	X,Y,Z
Cg(1)...Cg(6)	5.4906(15)	X,Y,Z
Cg(2)...Cg(1)	5.6559(15)	X,Y,Z
Cg(2)...Cg(2)	4.0571(13)	2-X,-Y,1-Z
Cg(2)...Cg(3)	5.2473(15)	X,1/2-Y,-1/2+Z
Cg(2)...Cg(4)	5.3704(15)	X,Y,Z
Cg(4)...Cg(2)	5.3703(15)	X,Y,Z
Cg(4)...Cg(2)	5.0602(15)	2-X,-Y,1-Z
Cg(4)...Cg(3)	5.1454(16)	X,Y,Z
Cg(4)...Cg(5)	5.1313(16)	X,Y,Z
Cg(4)...Cg(5)	4.9937(16)	2-X,-Y,1-Z
Cg(4)...Cg(6)	5.4052(16)	2-X,-Y,1-Z
Cg(5)...Cg(4)	4.9937(16)	2-X,-Y,1-Z
Cg(5)...Cg(6)	4.9819(15)	X,Y,Z
Cg(5)...Cg(6)	5.2364(15)	X,1/2-Y,-1/2+Z
Cg(6)...Cg(1)	5.4906(15)	X,Y,Z
Cg(6)...Cg(4)	5.6007(15)	X,Y,Z
Cg(6)...Cg(5)	5.2596(16)	2-X,-Y,1-Z
Cg(6)...Cg(5)	5.2364(15)	X,1/2-Y,-1/2+Z

5.4.2 Oxidation of *n*-octane

The complexes were used as catalysts in the oxidation of *n*-octane. The solubility of the catalysts is rather limited in that these are only soluble in 1,2-dichloroethane (DCE) and acetonitrile (MeCN). The reaction was initially carried out at 80 °C with *tert*-butyl hydroperoxide (TBHP) as the oxidant in acetonitrile using catalyst **1a**. The catalyst:substrate molar ratio was kept constant at 1:100 and the substrate:oxidant molar ratio was varied (1:2.5; 1:5; 1:7.5; 1:10) (Fig. 5.4). The substrate:oxidant molar ratio of 1:5 was found to be the optimum ratio with the best balance of conversion and lowest selectivity to the ketones.

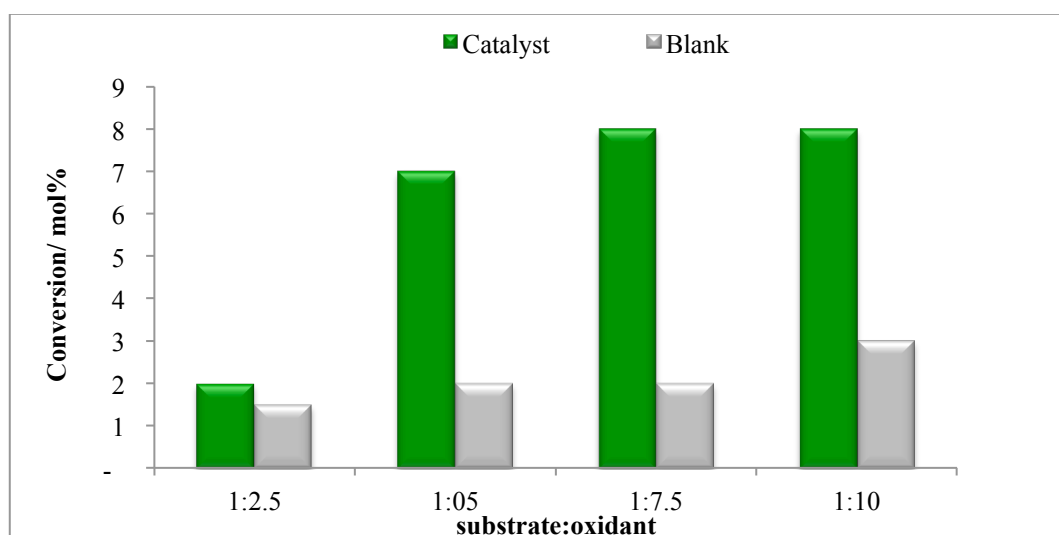


Figure 5.4. Optimization of the substrate:oxidant ratio in the oxidation of *n*-octane.

Conditions: Catalyst:substrate (1:100); Temperature : 80 °C; Solvent: MeCN; Catalyst: **1a**

A lower catalyst:substrate molar ratio of 1:50 under the optimum conditions mentioned above gave a 7% conversion with selectivity to only the ketones (2-octanone (35%); 3-octanone (31%) and 4-octanone (34%)). The reaction was also carried out using DCE at 25 °C, 50 °C and 80 °C (Fig. 5.5) with a catalyst:substrate molar ratio of 1:100 and a substrate:oxidant molar ratio of 1:5. At 25 °C, octanoic acid was the only product that formed at a 1% conversion of *n*-octane. At 50 °C, a 4% conversion of *n*-octane was noted. However, the blank (no catalyst) conversion was 2% and selectivity to the products of oxidation with and without the catalyst was comparable. The highest conversion (9%) was obtained at 80 °C with good selectivity to the primary products. This could be attributed to the solubility of the oxidant in the solvent. Similar studies carried out in alkene oxidation showed better conversion in chlorinated solvents.^{89,90} It has been shown that some catalytic reactions proceed more efficiently in a mixture of solvents⁹¹, however, when a 1:1 ratio of DCE:MeCN was used, the reaction with and without the catalyst was comparable.

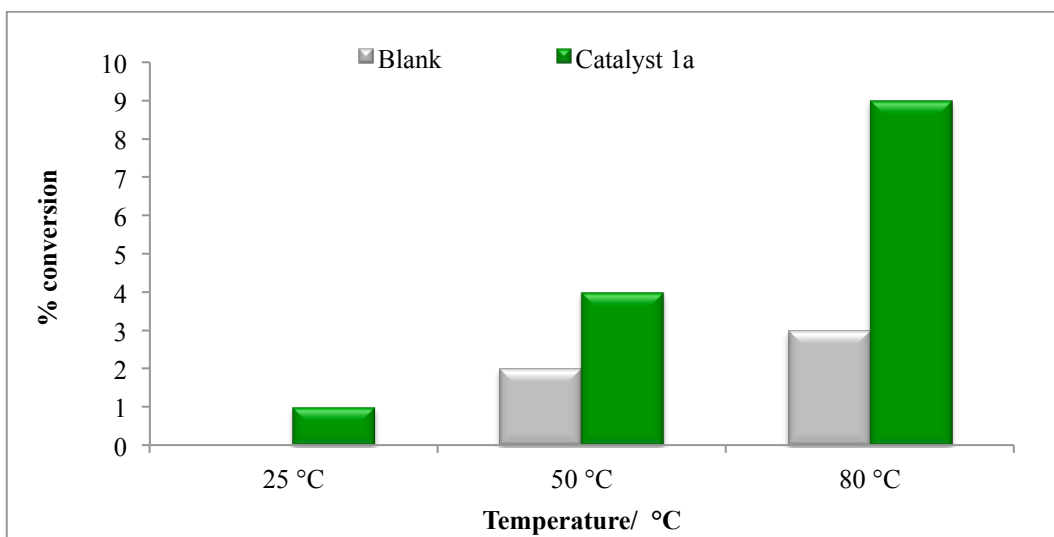


Figure 5.5. Optimization of temperature in the oxidation of *n*-octane.

Conditions: Catalyst:substrate (1:100); Substrate:oxidant (1:5); Solvent: DCE; Catalyst: **1a**

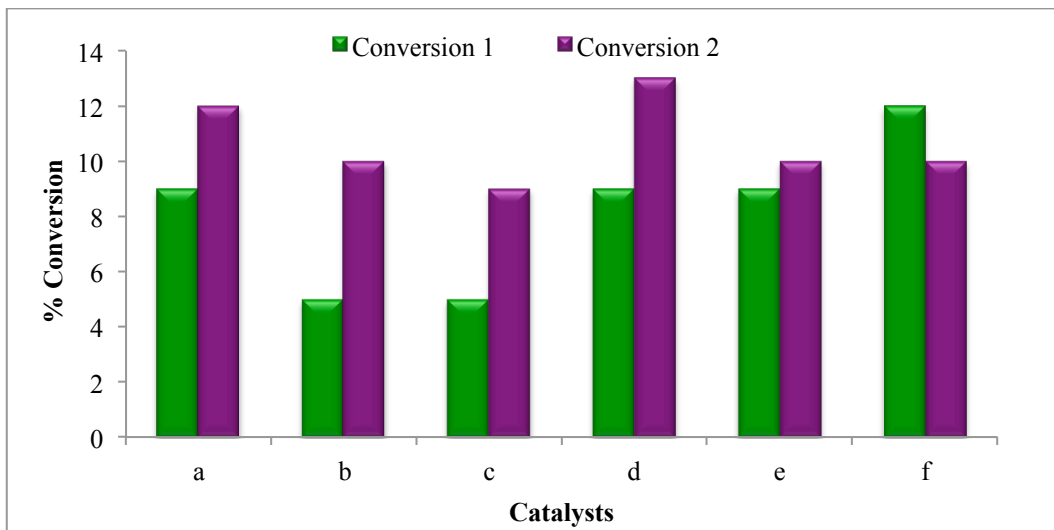


Figure 5.6. Screening of the iridium (**1**) and rhodium (**2**) catalysts with the different substituents on the nitrogen atom (**a-f**).

Conditions: Catalyst:substrate (1:100); Substrate:oxidant (1:5); Solvent: DCE; Temperature: 80 °C.

Oxidants such as hydrogen peroxide and *m*CPBA (*meta* chloropeoxybenzoic acid) were also investigated in the oxidation study. However, with these oxidants, catalyst decomposition occurred. Furthermore, no conversion was observed with hydrogen peroxide. It has been noted that some reactions fail to activate the peroxide or there is less selectivity to the desired products.⁹²⁻⁹⁴ Therefore, using the optimum conditions (catalyst:substrate molar ratio of 1:00, substrate:oxidant molar ratio of 1:5 at 80 °C in MeCN) screening of the iridium (**1**) and

rhodium (**2**) catalysts bearing the different substituents on the nitrogen atom of the ligand backbone was undertaken. In general, the Rh catalysts were found to be more active than the corresponding Ir catalysts with the same substituents (Fig. 5.6). This maybe due to the rhodium complexes having a greater ability to coordinate to larger hydrocarbons than the iridium catalysts, which results in the higher conversion.⁹⁵ Periana and Bergman have shown that the relative rate constants for rhodium catalysts are almost double those of the iridium catalysts in reactions involving *n*-hexane and *n*-pentane.⁹⁶

Comparing the catalysts with the alkyl substituents on the nitrogen atom (**a-c**), the longer alkyl chains render the complexes more basic, as in catalysts **1c** and **2c**. The more basic the nature of the catalyst, the stronger is its electron donating ability resulting in a greater electron density located at the metal center. This renders it easier to go from a M^I to M^{III} state upon activation by the oxidant. However, the formation of the active *tert*-butoxy radical becomes more difficult, since the high basic nature of the complex stabilizes the M^{III} oxidation state. It is noted that electron-donating substituents decrease the reactivity of the oxo species.²⁸ Catalysts **2a** and **2b** are comparable in terms of their activity, which is also observed with Cr complexes bearing the same ligand backbone in ethylene oligomerisation.⁵⁷ The Rh catalyst with the phenyl substituent **2d** gives the highest conversion (13%). Comparing the catalysts with the substituted phenyl rings, it is observed that the chloro (**e**) or the methoxy (**f**) group has very little effect in changing the catalytic activity.

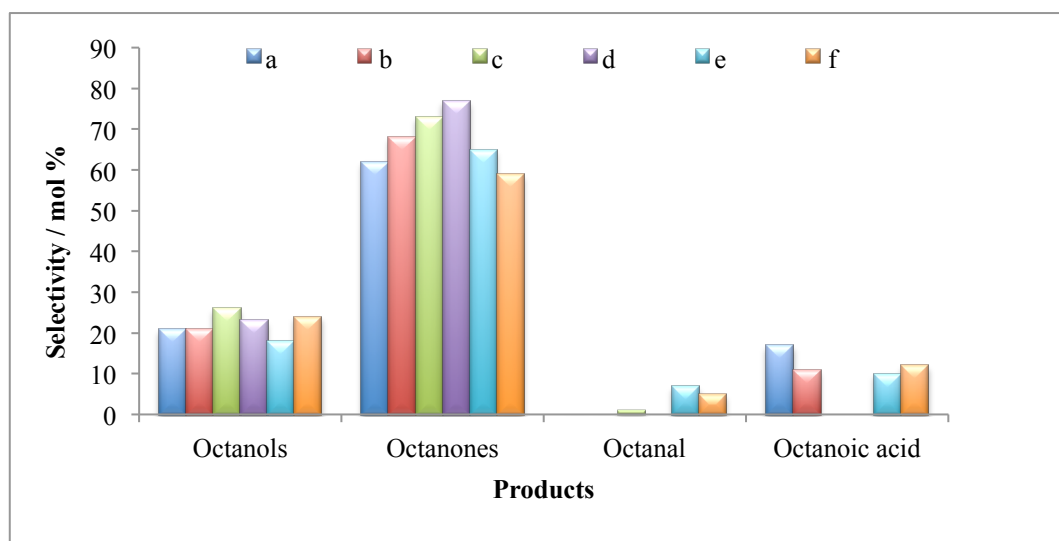


Figure 5.7. Selectivity to the products of oxidation of *n*-octane by the Ir (**1**) catalysts.

Conditions: Catalyst:substrate (1:100); Substrate:oxidant (1:5); Solvent: DCE; 80 °C.

The selectivity to the products of oxidation by the Ir catalysts is shown in Fig. 5.7, with the regioselectivity parameters shown in Table 5.6. Deeper oxidation to the ketonic product is

prevalent, as seen by the high selectivity to the octanones (59% - 77%). However, the octanols are also produced in good yield (18% - 26%). The C(1) position of the *n*-octane chain is the least activated, with the C(2) and (C3) positions being the most activated carbons. For the catalysts with the ligand backbone containing the substituted phenyl groups (**1e** and **1f**), the over oxidation of 1-octanol to octanal and thereafter octanoic acid is much slower in comparison to the catalysts with the alkyl substituent. For both catalysts **1e** and **1f**, a 3% selectivity to 1-octanol is observed with a 7% and 5% selectivity to octanal respectively. However, for the catalysts with the alkyl substituents, **1a** and **1b**, a respective 17% and 11% selectivity to octanoic acid is observed, with no selectivity to octanal. The selectivity to 2-, 3-, 4- octanols is between 5% to 10%. The selectivity and regioselectivity to the ketones over the rhodium catalysts is similar to those over the iridium catalysts (41% - 77% collectively).

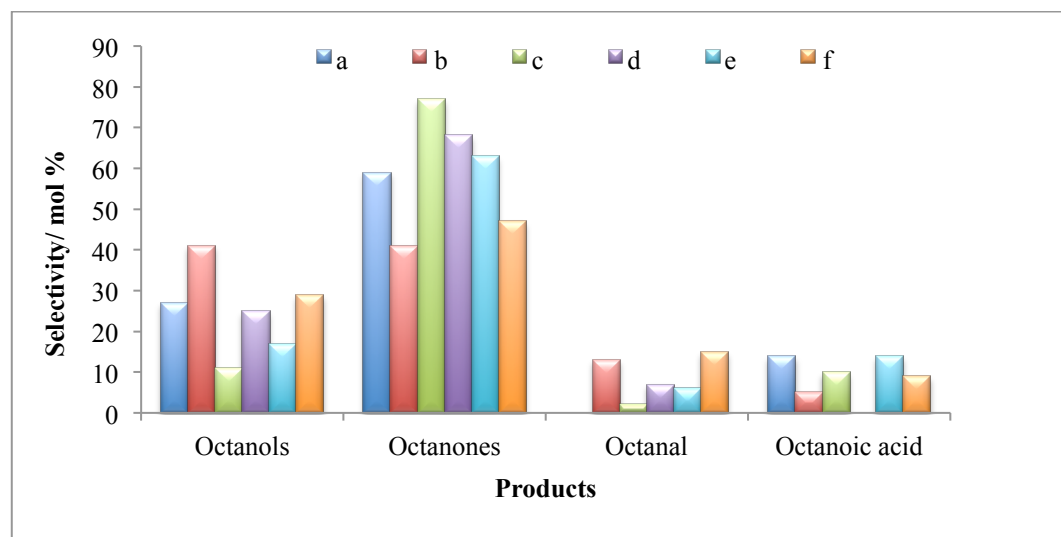


Figure 5.8. Selectivity to the products of oxidation of *n*-octane by the Rh (2) catalysts.

Conditions: Catalyst:substrate (1:100); Substrate:oxidant (1:5); Solvent: DCE; Temperature: 80 °C.

The deeper oxidation process is much slower with the rhodium catalysts, which is noted by the higher selectivity to the octanols (11% - 41%), with catalyst **2b** being most selective (41%) and **2c** being the least selective towards these octanols. An increase in the octanal selectivity when compared to the iridium catalysts is also observed (Fig. 5.8). As noted also with the iridium catalysts, the C(1) position is least active with the C(2) and C(3) position being the most active carbons. The higher activity of the internal carbons is observed in other oxidation systems.^{21,48,97} Research has been quite limited using Ir and Rh catalysts in the oxidation of alkanes. Nomura and Uemura report TONS of 93 for the oxidation of *n*-octane using Rh catalysts.⁷³ In other reported studies the regioselectivity parameters at the C(2), C(3) and C(4) positions of the alkane chain are much higher, due to the primary selectivity being

substantially lower, whereas in this system, the primary selectivity at C(1) position is high, accounting for the lower internal regioselectivity parameters.^{5,21,48,50,54,97}. Unlike the system reported in this study, some studies report no selectivity to the primary products, with only the ketones being obtained.^{3,40,71,72}

Table 5.6. Selectivity parameters by Ir and Rh catalysts in the oxidation of *n*-octane.^a

	Alcohol^{b,c}	Ketone^{b,c}	Total^d
			C(1):C(2):C(3):C(4)
Ir	a	1:9:12:9	1:2:2:2
	b	1:5:6:4	1:3:3:3
	c	1:4:5:3	1:17:16:16
	d	0:1:2:1	0:1:2:2
	e	1:4:0:4	1:2:1:2
	f	1:3:3:4	1:2:2:2
Rh	a	1:4:5:4	1:2:2:3
	b	0:1:1:1	1:2:2:3
	c	1:2:1:2	1:2:3:3
	d	1:1:6:4	1:3:5:5
	e	1:2:4:2	1:1:2:2
	f	1:3:6:5	1:1:1:2

^a Conditions: Catalyst:substrate (1:100); Substrate:oxidant (1:5); Solvent: DCE; Temperature: 80 °C.

^b Parameters C(1):C(2):C(3):C(4) are the relative reactivities of hydrogen atoms at carbon 1, 2, 3 and 4 of the *n*-octane chain.

^c The calculated reactivities from the % selectivity are normalized, i.e. calculated taking into account the number of hydrogen atoms at each carbon.

^d Includes the % selectivity of octanoic acid, octanal, alcohols and ketones and the values are normalized.

Catalysts **1c** and **2c** were recovered and re-used over two cycles (Fig. 5.9). The amounts of catalyst recovered were low due to mechanical loss during sampling and the small amounts of catalyst used. The selectivity profiles towards the alcohols, ketones, aldehyde and acid for both catalysts are shown in Figs. 5.10 and 5.11. For catalysts **1c**, the fresh and cycle 2 results are comparable, however, only the octanones were detected during re-cycle 1. The ³¹P NMR spectra imply slight differences in the catalyst structure with the formation of a new peak (for catalysts **2c**) (Fig. 5.12). It can be postulated that the ligand backbone remains unchanged, since the characteristic phosphorous peak for both the fresh and recovered catalysts are observed. However, the formation of the new phosphorous peak (20.4 ppm) in the ³¹P NMR

spectrum of the recovered catalyst **2c**, may indicate the formation of a new intermediate species during the catalytic cycle. The melting points of the recovered catalyst **1c** (166-168 °C) and used catalyst (262-263 °C) are also different, which can explain the difference in the selectivity. For catalyst **2c**, the fresh run and recovered cycles are comparable, with only cycle 1 being slightly different in the octanone selectivity.

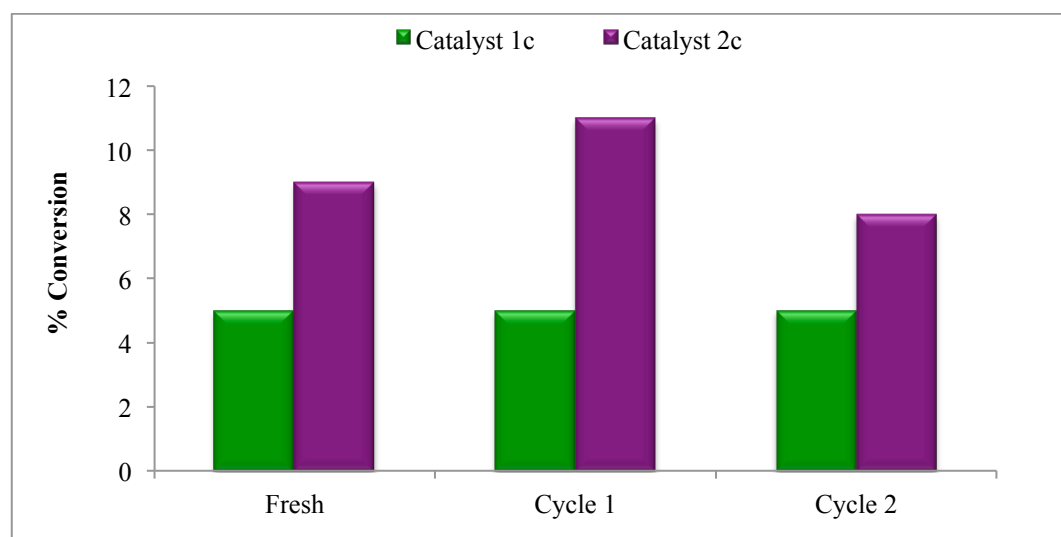


Figure 5.9. Recyclability testing of catalysts **1c** and **2c** in the oxidation of *n*-octane.

Conditions: Catalyst:substrate (1:100); Substrate:oxidant (1:5); Solvent: DCE; 80 °C.

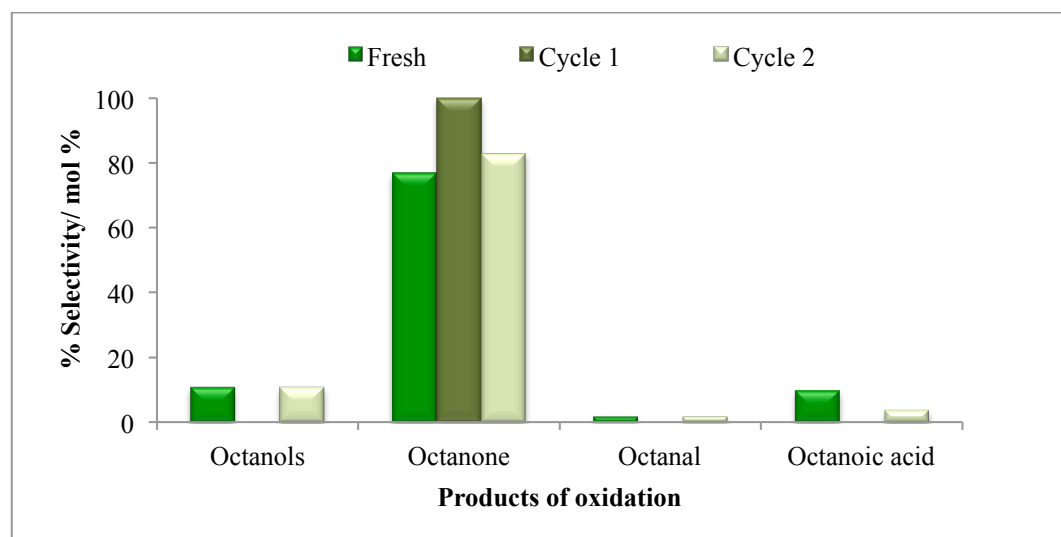


Figure 5.10. Recyclability testing of catalysts **1c** - selectivity to the products of oxidation.

Conditions: Catalyst:substrate (1:100); Substrate:oxidant (1:5); Solvent: DCE; 80 °C.

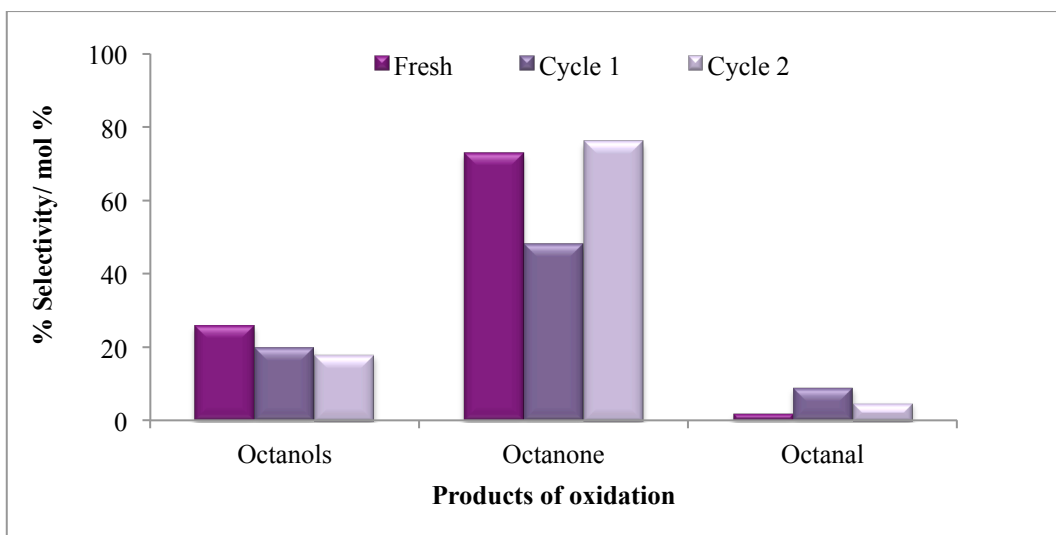


Figure 5.11. Recyclability testing of catalysts **2c** - selectivity to the products of oxidation.

Conditions: Catalyst:substrate (1:100); Substrate:oxidant (1:5); Solvent: DCE; 80 °C.

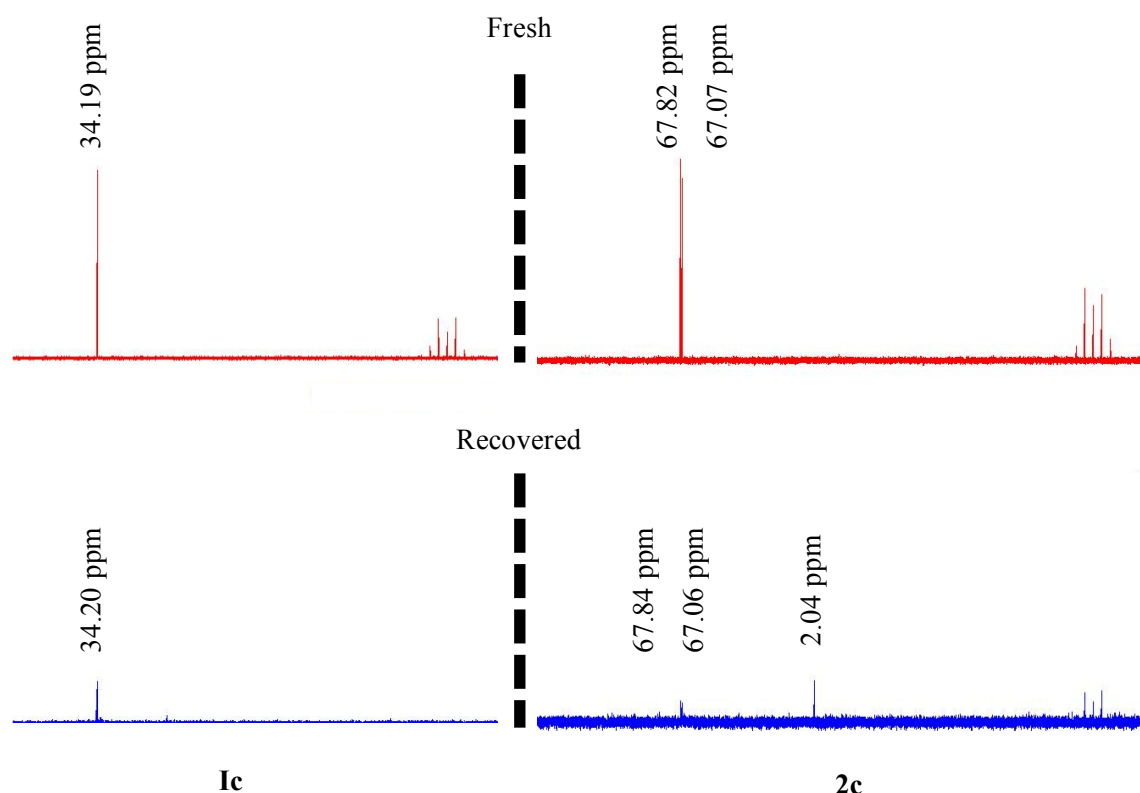


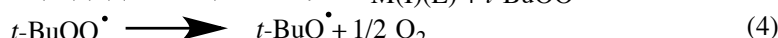
Figure 5.12. ^{31}P NMR of the fresh and recovered catalysts **1c** and **2c**.

Ketone formation, due to deeper oxidation, is common when TBHP (*t*-BuOOH) is used as an oxidant.²⁵ It can be postulated that the reaction proceeds through the formation of hydroxyl radicals which attack the alkane chain via the activation of the oxidant by the metal complex.^{5,98} Taking these factors into consideration, as well as the metal and substrate being

activated, we propose a mechanism, which is consistent with that presented in literature, for the activation of *n*-alkanes using TBHP as an oxidant.^{20,21,23,99-101} The reaction proceeds with the formation of the *t*-BuO[•] radical via the reduction of the oxidant by the metal complex, M(I)L, which generates a hydroxo-M(III) species (eqn 1) (M= Ir/ Rh; L= ligand).^{20,99}



The hydroxo species [M(III)(L)OH] reacts further with *t*-BuOOH (eqn 2) which decomposes to form the *t*-BuOO[•] radical. This radical is dismutated to form the *t*-BuO[•] radical (eqn 4).^{20,99}



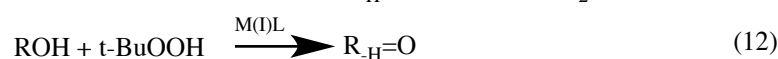
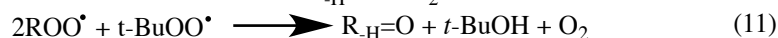
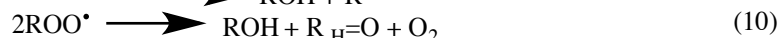
The oxygen centered radicals generated in eqns 1 and 4 attack the hydrocarbon with the formation of alkyl radicals (eqn 5).^{20,21,99}



The alkyl peroxy radical is formed (eqn 6) upon reaction of R[•] with oxygen which reacts with the alkane to form ROOH (organo-hydroperoxide, eqn 7) and thereafter undergoes homolytic decomposition via the M(III)L complex to form RO[•] (organooxyl radical, eqn 8).^{20,21,99}



By H-abstraction from the alkane, the RO[•] radical forms the alcohol (ROH, eqn 9) and the ROO[•] decomposes to the alcohol and then the ketone (eqn 10) or is regenerated via eqn 7. Increase in the ketone selectivity occurs when the ROO[•] attacks the *t*-BuOO[•] through mixed molecular Russel termination (eqn 11).¹⁰² Deeper oxidation of the alcohols forming the ketones is caused by the M(I)L complex (eqn 12).^{20,21,99}



5.5 Conclusion

New iridium and rhodium aminodiphosphine complexes have been used as catalysts in the oxidation of *n*-alkanes. To our knowledge this is one of the very few Ir and Rh systems reported that are used in this type of application. The rhodium catalysts are more active than the iridium catalysts. The deeper oxidation products, the octanones, are the dominant products, however, good selectivities to the alcohols are also observed for both types of

catalysts. The rhodium catalyst bearing the ligand with the phenyl substituent on the nitrogen atom is the most active catalyst in the series. One of the remarkable achievements of this homogenous system was the catalyst recovery and reusability.

5.6 References

- [1] Stahl, S. S.; Labinger, J. A.; Bercaw, J. E. *Angew. Chem. Int. Ed.* **1998**, *37*, 2180- 2192.
- [2] White, M. C. *Science* **2012**, *335*, 807-809.
- [3] Chen, M. S.; White, M. C. *Science* **2010**, *327*, 566-571.
- [4] Shul'pin, G. B. *J. Mol. Catal. A: Chem.* **2002**, *189*, 39-66.
- [5] Shul'pin, G. B. *C.R. Chimie* **2003**, *6*, 163-178.
- [6] Crabtree, R. H. *J. Organomet. Chem.* **2004**, *689*, 4083-4091.
- [7] Amini, M.; Haghdoost, M. M.; Bagherzadeh, M. *Coord. Chem. Rev.* **2013**, *257*, 1093-1121.
- [8] Shilov, A. E.; Shul'pin, G. B. *Chem. Rev.* **1997**, *97*, 2879-2932.
- [9] Sivaramakrishna, A.; Suman, P.; Veerashekhar Goud, E.; Janardan, S.; Sravani, C.; Sandeep, T.; Vijayakrishna, K.; Clayton, H. S. *J. Coord. Chem.* **2013**, *66*, 2091-2109.
- [10] Kirillov, A. M.; Kirillova, M. V.; Pombeiro, A. J. L. *Coord. Chem. Rev.* **2012**, *256*, 2741-2759.
- [11] Kirillov, A. M.; Shul'pin, G. B. *Coord. Chem. Rev.* **2013**, *257*, 732-754.
- [12] Conley, B. L.; Tenn I, W. J.; Young, K. J. H.; Ganesh, S. K.; Meier, S. K.; Ziatdinov, V. R.; Mironov, O.; Oxgaard, J.; Gonzales, J.; Goddard III, W. A.; Periana, R. A. *J. Mol. Catal. A: Chem.* **2006**, *251*, 8-23.
- [13] Labinger, J. A.; Bercaw, J. E. *Nature* **2002**, *417*, 507-514.
- [14] Klei, S. R.; Tan, K. L.; Golden, J. T.; Yung, C. M.; Thalji, R. K.; Ahrendt, K. A.; Ellman, J. A.; Tilley, T. D.; Bergman, R. G. *In Activation and Functionalization of C-H Bonds: Am. Chem. Soc.* **2004**, *885*, 46-55
- [15] Maurya, M. R.; Kumar, A.; Costa Pessoa, J. *Coord. Chem. Rev.* **2011**, *255*, 2315-2344.
- [16] Mizuno, N.; Kamata, K. *Coord. Chem. Rev.* **2011**, *255*, 2358-2370.
- [17] Anisia, K. S.; Kumar, A. *J. Mol. Catal. A: Chem.* **2004**, *219*, 319-326.
- [18] Bonon, A. J.; Mandelli, D.; Kholdeeva, O. A.; Barmatova, M. V.; Kozlov, Y. N.; Shul'pin, G. B. *Appl. Catal. A: Gen.* **2009**, *365*, 96-104.
- [19] Arndtsen, B. A.; Bergman, R. G.; Mobley, T. A.; Peterson, T. H. *Acc. Chem. Res.* **1995**, *28*, 154-162.
- [20] Mac Leod, T. C. O.; Kirillova, M., V.; Pombeiro, A. J. L.; Schiavon, M. A.; Assis, M. D. *Appl. Catal. A: Gen.* **2010**, *372*, 191-198.
- [21] Kirillov, A. M.; Kirillova, M. V.; Shul'pina, L. S.; Figiel, P. Ç. J.; Gruenwald, K. R.; Guedes da Silva, M. F. T. C.; Haukka, M.; Pombeiro, A. J. L.; Shul'pin, G. B. *J. Mol. Catal. A: Chem.* **2011**, *350*, 26-34.
- [22] Silva, A. C.; Fernández, T. L.; Carvalho, N. M. F.; Herbst, M. H.; Bordinhão, J.; Jr, A. H.; Wardell, J. L.; Oestreicher, E. G.; Antunes, O. A. C. *Appl. Catal. A: Gen.* **2007**, *317*, 154-160.
- [23] Shul'pin, G. B.; Süss-Fink, G.; Shul'pina *J. Mol. Catal. A: Chem.* **2001**, *170*, 17-34.
- [24] Curci, R.; D'Accolti, L.; Fusco, C. *Acc. Chem. Res.* **2005**, *39*, 1-9.
- [25] Yiu, S.; Man, W.; Lau, T. *J. Am. Chem. Soc.* **2008**, *130*, 10821-10827.
- [26] Nizova, G. V.; Krebs, B.; Süss-Fink, G.; Schindler, S.; Westerheide, L.; Cuervo, G. L.; Shul'pin, G. B. *Tetrahedron* **2002**, *58*, 9231-9237.
- [27] Shul'pin, G. B.; Stoeckli-Evans, H.; Mandelli, D.; Kozlov, Y. N.; Vallina, A. T.; Woitiski, C. B.; Jimenez, R. S.; Carvalho, W. A. *J. Mol. Catal. A: Chem.* **2004**, *219*, 255-264.
- [28] Katsuki, T. *Coord. Chem. Rev.* **1995**, *140*, 189-214.

- [29] Balamurugan, M.; Mayilmurugan, R.; Suresh, E.; Palaniandavar, M. *Dalton Trans.* **2011**, *40*, 9413-9424.
- [30] Barton, D. H. R.; Doller, D. *Acc. Chem. Res.* **1992**, *25*, 504-512.
- [31] Nam, W.; Ryu, J. Y.; Kim, I.; Kim, C. *Tetrahedron Lett.* **2002**, *43*, 5487-5490.
- [32] Kille, S.; Zilly, F. E.; Acevedo, J. P.; Reetz, M. T. *Nat. Chem.* **2011**, *3*, 738-743.
- [33] Doro, F. G.; Smith, J. R. L.; Ferreira, A. G.; Assis, M. D. *J. Mol. Catal. A: Chem.* **2000**, *164*, 97-108.
- [34] Cagnina, A.; Campestrini, S.; Di Furia, F.; Ghiotti, P. *J. Mol. Catal. A: Chem.* **1998**, *130*, 221-231.
- [35] Cagnina, A.; Campestrini, S.; Di Furia, F.; Ghiotti, P. *J. Mol. Catal. A: Chem.* **1998**, *130*, 221-231.
- [36] Islam, S. M.; Roy, A. S.; Mondal, P.; Mubarak, M.; Mondal, S.; Hossain, D.; Banerjee, S.; Santra, S. C. *J. Mol. Catal. A: Chem.* **2011**, *336*, 106-114.
- [37] Bahramian, B.; Mirkhani, V.; Moghadam, M.; Tangestaninejad, S. *Catal. Commun.* **2006**, *7*, 289-296.
- [38] Gupta, K. C.; Kumar Sutar, A.; Lin, C-C. *Coord. Chem. Rev.* **2009**, *253*, 1926-1946.
- [39] Cook, B. R.; Reinert, T. J.; Suslick, K. S. *J. Am. Chem. Soc.* **1986**, *108*, 7281-7286.
- [40] Lindsay Smith, J. R.; Iamamoto, Y.; Vinhado, F. S. *J. Mol. Catal. A: Chem.* **2006**, *252*, 23-30
- [41] Vinhado, F. S.; Gandini, M. E. F.; Iamamoto, Y.; Silva, A. M. G.; Simões, M. M. Q.; Neves, M. G. P. M. S.; Tomé, A. C.; Rebelo, S. L. H.; Pereira, A. M. V. M.; Cavaleiro, J. A. S. *J. Mol. Catal. A: Chem.* **2005**, *239*, 138-143.
- [42] Lu, H.; Zhang, X. P. *Chem. Soc. Rev.* **2011**, *40*, 1899-1909.
- [43] Gormisky, P. E.; White, M. C. *J. Am. Chem. Soc.* **2013**, *135*, 14052-14055.
- [44] Bigi, M. A.; Reed, S. A.; White, M. C. *J. Am. Chem. Soc.* **2012**, *134*, 9721.
- [45] White, M. C. *Synlett* **2012**, *23*, 2746-2748.
- [46] Vermeulen, N. A.; Chen, M. S.; White, M.C. *Tetrahedron* **2009**, *65*, 3078-3084.
- [47]] Mirkhani, V.; Moghadam, M.; Tangestaninejad, S.; Mohammadpoor-Baltork, I.; Rasouli, N. *Catal. Commun.* **2008**, *9*, 2411-2416.
- [48] Shul'pin, G. B.; Kudinov, A. R.; Shul'pina, L. S.; Petrovskaya, E. A. *J. Organomet. Chem.* **2006**, *691*, 837-845.
- [49] Pereira, R.; Rufo, M.; Schuhardt, U. *J. Braz. Chem. Soc.* **1994**, *5*, 83-89.
- [50] Shul'pina, L. S.; Kirillova, M. V.; Pombeiro, A., J.L.; Shul'pin, G. B. *Tetrahedron* **2009**, *65*, 2424-2429.
- [51] Dunford, H. B. *Coord. Chem. Rev.* **2002**, *233–234*, 311-318.
- [52] Nagataki, T.; Ishii, K.; Tachi, Y.; Itoh, S. *Dalton Trans.* **2007**, 1120-1128.
- [53] Nagataki, T.; Tachi, Y.; Itoh, S. *Chem. Commun.* **2006**, 4016-4018.
- [54] Kirillova, M. V.; Kirillov, A. M.; Mandelli, D.; Carvalho, W. A.; Pombeiro, A. J. L.; Shul'pin, G. B. *J. Catal.* **2010**, *272*, 9-17.
- [55] Remias, J. E.; Sen, A. *J. Mol. Catal. A: Chem.* **2002**, *189*, 33-38.
- [56] Teo, S.; Weng, Z.; Hor, T. S. A. *Organometallics* **2008**, *27*, 4188-4192.
- [57] Blann, K.; Bollmann, A.; de Bod, H.; Dixon, J. T.; Killian, E.; Nongodlwana, P.; Maumela, M. C.; Maumela, H.; McConnel, A. E.; Morgan, D. H.; Overette, M. J.; Přetorius, M.; Kuhlmann, S.; Wasserscheid, P. *J. Catal.* **2007**, *249*, 244-249.
- [58] Blann, K.; Bollmann, A.; Dixon, J. T.; Hess, F. M.; Killian, E.; Maumela, H.; Morgan, D. H.; Neveling, A.; Otto, S.; Overett, M. J. *Chem. Commun.* **2005**, 620-621
- [59] Bollmann, A.; Blann, K.; Dixon, J. T.; Hess, F. M.; Killian, E.; Maumela, H.; McGuiness, D. S.; Morgan, D. H.; Neveling, A.; Otton, S.; Overette, M.; Slawin, A. M. Z.; Wassercheid, P.; Kihlmann, S. *J. Am. Chem. Soc.* **2004**, *126*, 14712-14713.
- [60] Overett, M. J.; Blann, K.; Bollmann, A.; Dixon, J. T.; Hess, F.; Killian, E.; Maumela, H.; Morgan, D. H.; Neveling, A.; Otto, S. *Chem. Commun.* **2005**, 622-624.
- [61] Bowen, L. E.; Haddow, M. F.; Orpen, A. G.; Wass, D. F. *Dalton Trans.* **2007**, 1160-1168.
- [62] Bowen, L. E.; Charernsuk, M.; Hey, T. W.; McMullin, C. L.; Orpen, A. G.; Wass, D. F. *Dalton Trans.* **2010**, *39*, 560-567.

- [63] Grüger, N.; Wadeohl, H.; Gade, L. H. *Euro. J. Inorg. Chem.* **2013**, *2013*, 5358-5365.
- [64] Benito-Garagorri, D.; Alves, L. G. a.; Puchberger, M.; Mereiter, K.; Veiros, L. F.; Calhorda, M. J.; Carvalho, M. D.; Ferreira, L. P.; Godinho, M.; Kirchner, K. *Organometallics* **2009**, *28*, 6902-6914.
- [65] Benito-Garagorri, D.; Kirchner, K. *Acc. Chem. Res.* **2008**, *41*, 201-213.
- [66] van der Boom, M. E.; Milstein, D. *Chem. Rev.* **2003**, *103*, 1759-1792.
- [67] Xu, X.; Xi, Z.; Chen, W.; Wang, D. *J. Coord. Chem.* **2007**, *60*, 2297-2308.
- [68] Albrecht, M.; van Koten, G. *Angew. Chem. Int. Ed.* **2001**, *40*, 3750-3781.
- [69] Valderrama, M.; Contreras, R.; Boys, D. *J. Organomet. Chem.* **2003**, *665*, 7-12.
- [70] Britovsek, G. J. P.; England, J.; Spitzmesser, S. K.; White, A. J. P.; Williams, D. J. *Dalton Trans.* **2005**, 945-955.
- [71] Wong, W.-K.; Chen, X.-P.; Guo, J.-P.; Chi, Y.-G.; Pan, W.-X.; Wong, W.-Y. *J. Chem. Soc. Dalton Trans.* **2002**, 1139-1146.
- [72] Wong, W.-K.; Chen, X.-P.; Chik, T.-W.; Wong, W.-Y.; Guo, J.-P.; Lee, F.-W. *Euro. J. Inorg. Chem.* **2003**, *2003*, 3539-3546.
- [73] Nomura, K.; Uemura, S. *J. Chem. Soc. Chem. Commun.* **1994**, 129-130.
- [74] Friedrich, H. B.; Mahomed, A. S. *Appl. Catal. A: Gen.* **2008**, *347*, 11-22.
- [75] Friedrich, H. B.; Govender, N.; Mathebula, M. R. *Appl. Catal. A: Gen.* **2006**, *297*, 81-89.
- [76] El Khalifa, E. A.; Friedrich, H. B. *Appl. Catal. A: Gen.* **2010**, *373*, 122-131.
- [77] Sheldrick, G. M.; 2.05 ed.; SHELXS-97, SHELXL-97 and SADABS version 2.05, University of Göttingen, Germany: **1997**.
- [78] Sheldrick, G. *Acta Crystallogr., Sect. A:* **2008**, *64*, 112-122.
- [79] Otwinowski, Z and Minor, Z. *Processing of X-ray Diffraction Data Collected in Oscillation Mode, Methods in Enzymology, Macro. Cryst. A*, **1997**, *276*, 307-326. C.W. Carter, Jr. and R. M. Sweet, Eds., Academic Press (New York).
- [80] Dolomanov, O. V.; Bourhis, L. J.; Gildea, R. J.; Howard, J. A. K.; Puschmann, H. J. *Appl. Crystallogr.* **2009**, *42*, 339-341.
- [81] Simón-Manso, E.; Valderrama, M. *Journal of Organometallic Chemistry* **2006**, *691*, 380-386.
- [82] Appleby, T.; Derek Woollins, J. *Coord. Chem. Rev.* **2002**, *235*, 121-140.
- [83] Fei, Z.; Dyson, P. J. *Coord. Chem. Rev.* **2005**, *249*, 2056-2074.
- [84] Albright, T. A.; Burdett, J. K. *Problems in Molecular Orbital Theory*. **1992**, 103-104, Oxford University Press: New York.
- [85] Browning, C. S.; Farrat, D. H.; Frankel, D. C. *Acta Cryst. Sec. C* **1992**, *C48*, 806-811.
- [86] Grabowski, Z. R.; Rotkiewicz, K.; Rettig, W. *Chem. Rev.* **2003**, *103*, 3899-4032.
- [87] Druzhinin, S. I.; Dubbaka, S. R.; Knochel, P.; Kovalenko, S. A.; Mayer, P.; Senyushkina, T.; Zachariasse, K. A. *J. Phys. Chem. A* **2008**, *112*, 2749-2761.
- [88] Ganeshamoorthy, C.; Balakrishna Ms Fau - Mague, J. T.; Mague Jt Fau - Tuononen, H. M.; Tuononen, H. M. *Inorg. Chem.* **2008**, *47*, 7035-7047.
- [89] Ahmad, A. L.; Kohestani, B.; Bhatia, S.; Ooi, S. B. *Int. J Appl. Cer. Tech.* **2012**, *9*, 588-598.
- [90] Bruin, de B.; Budzelaar, P. H. M.; Gal, A. W. *Angew. Chem. Int. Ed.* **2004**, *43*, 4142-4157.
- [91] Tordin, E.; List, M.; Monkowius, U.; Schindler, S.; Knör, G. *Inorg. Chim. Acta* **2013**, *402*, 90-96.
- [92] Ding, Y.; Gao, Q.; Li, G.; Zhang, H.; Wang, J.; Yan, L.; Suo, J. *J. Mol. Catal. A: Chem.* **2004**, *218*, 161-170.
- [93] Maiti, S. K.; Dinda, S.; Gharah, N.; Bhattacharyya, R. *New J. Chem.* **2006**, *30*, 479-489.
- [94] Tang, Q.; Zhang, Q.; Wu, H.; Wang, Y. *J. Catal.* **2005**, *230*, 384-397.
- [95] Bengali, A. A.; Arndsten, B. A.; Burger, P. M.; Schultz, R. H.; Weiller, B. H.; Kyle, K. R.; Moore, C. B.; Bergman, R. G. *Pure Appl. Chem* **1995**, *67*, 218-288.
- [96] Periana, R. A.; Bergman, R. G. *Organometallics* **1984**, *3*, 508-510.
- [97] Kirillova, M. V.; Kozlov, Y. N.; Shul'pina, L. C.; Lyakin, O. Y.; Kirillov, A. M.; Talsi, E. P.; Pompeiro, A. J. L.; Shul'pin, G., B. *J. Catal.* **2009**, *268*, 26-38.
- [98] Fokin, A. A.; Schreiner, P. R. *Chem. Rev.* **2002**, *102*, 1551-1593.

- [99] Förster, S.; Rieker, A.; Maruyama, K.; Murata, K.; Nishinaga, A. *J. Org. Chem.* **1996**, *61*, 3320-3326.
- [100] Shul'pin, G. B.; Golfeto, C. C.; Süss-Fink, G.; Shul'pina, L. S.; Mandelli, D. *Tetrahedron Lett.* **2005**, *46*, 4563-4567.
- [101] Shul'pin, G. B.; Kozlov, Y.; Shul'pina, L. S.; Kudinov, A. R.; Mandelli, D. *Inorg. Chem. Commun.* **2009**, *48*, 10480-10482.
- [102] Nowotny, M.; Pedersen, L. N.; Hanefeld, U.; Maschmeyer, T. *Chem.-Euro. J.* **2002**, *8*, 3724-3731.

Chapter Six

Ruthenium “spider” complexes used as catalysts in the oxidation of *n*-octane and styrene

6.1 Abstract

The ruthenium complexes, $[\text{Ph}_2\text{PN}(\text{R})\text{PPh}_2]_2\text{RuCl}_2$, where $\text{R} = \text{C}_6\text{H}_{11}$ (**a**); C_3H_7 (**b**); C_5H_{11} (**c**), have been synthesized and characterized by NMR and IR spectroscopy, elemental analyses and HRMS. The functional groups on the nitrogen atom (R) were varied from a cyclohexyl ring, to a branched *iso*-propyl group and to a *n*-pentyl alkyl chain substituent. Complex **a** was analyzed using single crystal X-ray diffraction. An octahedral geometry around the metal center was observed. All complexes showed good activity as catalysts in the oxidation of *n*-octane and styrene using *tert*-butyl hydroperoxide (TBHP) as the oxidant. From *n*-octane, good selectivities to the octanols were obtained, with the highest selectivities being towards 2-and 3 octanol by catalyst **a**. In styrene oxidation, the highest selectivity to benzaldehyde was at room temperature.

Keywords: Aminodiphosphine, ruthenium, oxidation, *n*-octane, styrene

6.2 Introduction

The synthesis of transition metal complexes, which are key intermediates in significant catalytic oxidation reactions, has become an area of immense interest.¹ Electron deficient metal complexes are of great importance in catalytic epoxidation and C-H bond activation and functionalization due to their ability to mimic biological enzymes such as cytochrome P450 and for the development of novel industrial applications.¹⁻⁷ The catalytic selectivity and efficiency is dependent on the metal ion and the ligand architecture.³ Ruthenium based complexes have gained much interest over the years, in various fields such as photomolecular devices, probes for biological macromolecules and artificial photosynthesis, due to their wider range of chemically accessible oxidation states (Ru^{+2} to Ru^{+8}), making them versatile as energy transfer and electron transfer compounds.^{8,9}

One of the key steps in ruthenium catalyzed oxidation reactions is the formation of an intermediate ruthenium-oxo species through the mediation of a suitable oxidant,^{4,10-14} and ruthenium catalysts have been widely explored in epoxidation reactions using different oxidants and ligand systems.^{1-6,8-25} The products from these reactions, such as carbonyls and epoxides, are used extensively in perfumes, dyes, and pharmaceutical grade and fine chemical synthesis.²⁶⁻³⁶

The oxidation of saturated hydrocarbons by ruthenium complexes to more valuable products has also gained the interest of scientists.^{23,37-48} A selective, efficient and catalytic system needs to be put in place to functionalize the unactivated paraffin C-H bonds.^{37,49-55} Many challenges, such as the chemical inertness of the alkanes, the preferential activation of substrates containing sp^2 hybridized C–H bonds over sp^3 hybridized C–H bonds, and cases where the intermediate products are more reactive than the alkane and may thus react more effortlessly with the metal center, are prevalent in the activation of alkanes.^{56,57-59} One of the ways to overcome such problems is with the use of an appropriate ligand system, which can enhance the catalytic activity and selectivity through ligand modifications and concomitant changes of the electronic backbone.^{3,44,60} One such ligand system could include the aminodiphosphine or PNP ligand system. These bi-dentate or multidentate ligands have been used extensively in ethylene oligomerization with chromium as the active metal,⁶¹⁻⁶⁷ where they are part of a system that displays high activity, stability and variability.⁶⁸⁻⁷⁰

Modification of the ligand backbone, by using different donor substituents or central anionic atoms, tailors the activity of the metals, allowing the reactions of the metal ions to be selective, due to the high demand ligands place on the stereochemistry of the complex.^{71,72} Phosphine ligands complexed to ruthenium have not been widely explored in oxidation studies due to ligand degradation or loss of the ligand from the original complex.⁴⁰ Early work done by Bressan and Morillo on the epoxidation of alkenes using diphenylphosphino ruthenium complexes reported that the catalysts were destroyed due to progressive oxidation of the ligands.² Stoop et al. synthesized five coordinate PNNP ruthenium complexes and obtained low conversions in the epoxidation of styrene.²⁵ In the oxidation of *n*-octane and styrene, Wong and co workers reported low conversions and yield to only 2 and 4-octanone and higher yield to benzaldehyde than styrene oxide in the oxidation and epoxidation studies respectively.^{73,74}

In this study we report the synthesis and characterization of some new ruthenium “PNP” aminodiphosphine compounds and their application in the oxidation of *n*-octane and styrene using *tert*-butyl hydroperoxide (TBHP) as the oxidant (Fig. 6.1). The substituent on the

nitrogen atom was varied making use of three different types of functional groups, a cyclic (cyclohexyl), straight chained (*n*-pentyl) and a branched (*iso*-propyl) substituent, with the intention of observing if these groups have an effect on the catalytic activity and selectivity to the products of oxidation.

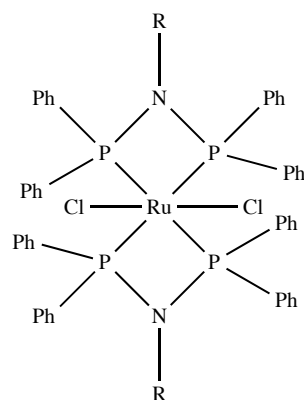


Figure 6.1. Ruthenium complexes bearing the PNP ligand backbone used in this study
(R = cyclohexyl (**a**); *iso*-propyl (**b**) and pentyl (**c**)).

6.3 Experimental

6.3.1 Synthesis and characterization of the compounds

All experiments were performed using standard Schlenk techniques under inert conditions in moisture free reaction glassware with anhydrous solvents. All solvents were analytical grade. To render the reaction glassware moisture free, it was heated with a heat gun followed by cycles of vacuum and nitrogen pressure. Deuterated solvents were used as received and stored in a vacuum desiccator. The NMR spectra were recorded at 400 MHz. (¹H), 100 MHz. (¹³C) and 162 MHz. (³¹P) using a Bruker ultrashield 400 MHz. spectrometer. ¹H NMR and ¹³C NMR chemical shifts are reported in parts per million (ppm) downfield from tetramethylsilane. ¹H NMR and ¹³C{¹H} NMR signals were referenced to the residual signal of CDCl₃ (7.26 ppm) and (53.84 ppm) respectively. ³¹P NMR chemical shifts were reported in parts per million (ppm) from triphenylphosphine (-17.6 ppm). The FT-IR spectra were recorded using a Perkin Elmer Universal Attenuated Total Reflection (ATR) Sampling Accessory attached to the FT-IR series 100 spectrometer. Elemental analyses were carried out on a ThermoScientific Flash2000 Organic Elemental Analyser. All PNP ligands were

synthesized with modification of literature procedure.⁶² The precursor, RuCl₂(PPh₃)₃, was purchased from Sigma Aldrich. (NMR spectra are shown in Appendix D).

Synthesis of [(Ph₂PN(C₆H₁₁)PPh₂)₂Ru(Cl)₂] (a). The synthesis was adapted from a known procedure.⁷⁵ To a 100 ml round bottom flask, 20 ml of acetone was added and purged with argon for 10 minutes. Thereafter, [Ph₂PN(C₆H₁₁)PPh₂] (0.210 mmol, 0.098 g) was added. Once completely dissolved, the complex RuCl₂(PPh₃)₃ (0.105 mol, 0.998 g) was added and was refluxed for 4 h during which a yellow precipitate formed. The solution was filtered using a Hirsch funnel, washed several times with cold acetone and left to dry *in vacuo* overnight. Crystals were grown from diethyl ether and dichloromethane. Yield: 42 %, 0.048 g. Melting point: 327-329 °C. IR_{max} (ATR)/cm⁻¹: 739 (*m*) (CH₂)_n rocking); 856 (*m*) (P-N); 1080 (*m*) (cyclohexyl ring vibrations); 1432 (*m*) (PPh₂). Anal. (%) Calcd for C₆₀H₆₂Cl₂N₂P₄Ru: C: 65.10 %; H: 5.65 %; N: 2.53 %. Found: C: 64.98 %; H: 5.19 %; N: 2.50 %. NMR: (400 MHz.; CDCl₃): ¹H NMR δ 0.61-0.90 (m, 6H, cyclohexyl ring, CH₂); δ 1.17-1.43 (m, 10H, cyclohexyl ring, CH₂); δ 1.77-1.80 (d, 4H, cyclohexyl ring, CH₂); δ 3.3 (m, 2H, (cyclohexyl ring, CH)); δ 7.09 (t, 16H, aromatic, CH, ³J= 6.72 Hz); δ 7.29 (t, 8H, aromatic, CH, ³J=7.28 Hz); δ 7.65 (d, 16H, aromatic, CH, ²J=5.96 Hz). ¹³C NMR δ 25.19 (cyclohexyl ring); δ 26.43 (cyclohexyl ring); δ 34.41 (cyclohexyl ring); δ 126.61-134.90 (aromatic). ³¹P NMR δ 75.70.

Synthesis of [(Ph₂PN(C₃H₇)PPh₂)₂Ru(Cl)₂] (b). Compound **b** was synthesized according to the procedure described for **a** except that [Ph₂PN(C₃H₇)PPh₂] (0.21 mmol, 0.0898 g) was used. Yield: 71 %, 0.077 g. Melting point: 300-302 °C. IR_{max} (ATR)/cm⁻¹: 847 (*m*) (P-N); 1432 (*m*) (PPh₂); 1482 (*w*) (CH₃). Anal. (%) Calcd for C₅₄H₅₄Cl₂N₂P₄Ru: C: 63.16 %; H: 5.30 %; N: 2.73 %. Found: C: 63.31 %; H: 4.97 %; N: 2.66 %. NMR: (400 MHz.; CDCl₃): ¹H NMR δ 1.02 (d, 12H, (CH₃)₂, ²J= 6.64 Hz); δ 3.85 (m, 2H, CH); δ 7.10 (t, 16H, aromatic, CH, ³J= 7.04 Hz); δ 7.29 (t, 8H, aromatic, CH, ³J= 7.28); δ 7.63 (d, 16H, aromatic, CH, ²J= 6.88 Hz). ¹³C NMR δ 24.44 (CH₃)₂; δ 126.70-134.91 (aromatic). ³¹P NMR δ 75.83.

Synthesis of [(Ph₂PN(C₅H₁₁)PPh₂)₂Ru(Cl)₂] (c). Compound **c** was synthesized according to the procedure described for **a** except that [Ph₂PN(C₅H₁₁)PPh₂] (0.21 mmol, 0.0957 g) was used. Yield: 57 %, 0.06 g. Melting point: 281-282 °C. IR_{max} (ATR)/cm⁻¹: 744 (*m*) (CH₂)_n rocking); 874 (*m*) (P-N); 1432 (*m*) (PPh₂); 1481 (*w*) (CH₃). Anal. (%) Calcd for C₅₈H₆₂Cl₂N₂P₄Ru: C: 64.32 %; H: 5.77 %; N: 2.59 %. Found: C: 64.21 %; H: 45.35 %; N: 2.56 %. NMR: (400 MHz.; CDCl₃): ¹H NMR δ 0.71 (t, 6H, (CH₃), ³J= 7.18 Hz); δ 0.96-1.03 (m, 4H, CH₂); δ 1.07-1.16 (m, 4H, CH₂); δ 1.57 (m, 4H, CH₂); δ 3.05-3.42 (m, 4H, CH₂); δ

7.12 (t, 16H, aromatic); δ 7.30-7.36 (m, 24H, aromatic). ^{13}C NMR δ 21.99; δ 30.49; δ 76.70; δ 77.02; δ 126.81-134.62 (aromatic). ^{31}P NMR δ 76.87.

6.3.2 Crystal structure analysis

Single-crystal X-ray diffraction data of compound **a** were collected on a Bruker KAPPA APEX II DUO diffractometer using graphite-monochromated Mo-K α radiation ($\lambda = 0.71073 \text{ \AA}$). Data collection was carried out at 173(2) K. The temperature was controlled by an Oxford Cryostream cooling system (Oxford Cryostat). Cell refinement and data reduction were performed using the program SAINT.⁷⁶ The data were scaled and absorption correction performed using SADABS.⁷⁶ The structure was solved by direct methods using SHELXS-97 and refined by full-matrix least-squares methods based on F^2 using SHELXL-97.⁷⁷ The crystallographic data are shown in Table 6.1.

X-ray single crystal intensity data of **a** were collected on a Nonius Kappa-CCD diffractometer using graphite monochromated MoK α radiation ($\lambda = 0.71073 \text{ \AA}$). Temperature was controlled by an Oxford Cryostream cooling system (Oxford Cryostat). The strategy for the data collections was evaluated using the Bruker Nonius "Collect" program. Data were scaled and reduced using DENZO-SMN software.⁷⁸ Absorption correction was performed using SADABS.⁷⁶

The program Olex2 was used to prepare molecular graphic images.⁷⁹ All non-hydrogen atoms were refined anisotropically. The similar-ADP restraints and the rigid-bond restraints were used on all six fluorine atoms. All hydrogen atoms were placed in idealised positions and refined in riding models with U_{iso} assigned the values to be 1.2 or 1.5 times those of their parent atoms and the distances of C-H were constrained to 0.95 \AA for aromatic hydrogen atoms and 0.98 \AA for CH₃. (More information is available in Appendix D).

Table 6.1. Single crystal structural information of complex **a**.

Compound	a
Empirical formula	C ₃₀ H ₃₁ CINP ₂ Ru _{0.5}
Formula weight	553.52
Temperature/K	99.96
Crystal system	Triclinic
Space group	P-1
a/Å	10.329(4)
b/Å	11.704(5)
c/Å	13.405(6)
α/°	95.57(2)
β/°	110.60(2)
γ/°	116.13(2)
Volume/Å ³	1299.2(10)
Z	2
Density _{calc} g/cm ³	1.4148
μ/mm ⁻¹	0.570
F(000)	573.6
Crystal size/mm ³	0.22 × 0.19 × 0.12
Radiation	Mo Kα ($\lambda = 0.71073$)
2Θ range for data collection/°	3.4 to 57.7
Index ranges	-13 ≤ h ≤ 13, -14 ≤ k ≤ 15, -16 ≤ l ≤ 16
Reflections collected	16436
Independent reflections	5340 [R _{int} = 0.0537, R _{sigma} = 0.0578]
Data/restraints/parameters	5340/0/437
Goodness-of-fit on F ²	1.099
Final R indexes [I>=2σ (I)]	R ₁ = 0.0738, wR ₂ = 0.1700
Final R indexes [all data]	R ₁ = 0.1112, wR ₂ = 0.2063
Largest diff. peak/hole / e Å ⁻³	1.54/-2.06

6.3.3 Oxidation studies

All reagents were weighed and handled in air. All products from the *n*-octane oxidation were analyzed and quantified using a PerkinElmer Auto System gas chromatograph fitted with a Flame Ionisation Detector (FID) set at 260 °C. A Pona column (50 m x 0.20 mm x 0.5 μ m) was utilized with the injector temperature set at 240 °C. Catalytic testing was carried out in acetonitrile at 80 °C, using *tert*-butyl hydroperoxide (TBHP) as the oxidant. The catalyst:substrate molar ratio was kept constant at 1:100. A two-necked pear shaped flask was charged with 10 mg of the respective catalyst, pentanoic acid (0.1 mmol) (as an internal standard), *n*-octane (0.9 mmol), the oxidant (6.7 mmol) and 10 ml of the solvent. The flask was equipped with a reflux condenser, stirred, heated to the required temperature and maintained at that temperature for 48 h in an oil bath. After certain time periods, aliquots were removed using a Pasteur pipette and filtered through cotton wool and a silica gel plug. To these aliquots, triphenylphosphine (PPh_3) (for reduction of the remaining TBHP and alkylperoxides which are formed as primary products in alkane oxidation)⁸⁰ was added. An aliquot (0.5 μ l) was injected into the GC and quantified.

For the analysis of the products of the oxidation of styrene a PerkinElmer Auto System gas chromatograph fitted with a Flame Ionisation Detector (FID) set at 290 °C was used. A Varian capillary DB-5 column (25 m x 0.15 mm x 2 μ m) was utilized with the injector temperature set at 250 °C. The catalyst:substrate molar ratio was kept constant at 1:100. A two-necked pear shaped flask was charged with 5 mg of the respective catalyst, benzophenone (as an internal standard), styrene, the respective oxidant and 10 ml of the solvent). The flask was equipped with a reflux condenser, stirred and the solution heated to the required temperature. The reaction was monitored by removing aliquots using a Pasteur pipette, filtered through cotton wool and a silica gel plug and injecting these (0.5 μ l) into the GC and quantifying.

6.4 Results and discussion

6.4.1 Synthesis and characterization of complexes

The complexes were synthesized by adaptation of a reported general method.⁷⁵ The complexes **a** and **c** are new, however, complex **b** and structures of similar type have been reported.⁸¹⁻⁸³ Once the ruthenium precursor was added to the solution of the respective ligand in acetone, the solution turns red and after 1 h of stirring at 40 °C a yellow precipitate formed.

The complexes were characterized by NMR and IR spectroscopy and elemental analyses and for complex **a** the single crystal structure was obtained (Appendix D). A downfield shift is noted in the ^{31}P NMR spectra of the complexes relative to the free ligand. Complexes **a** and **b** exhibited similar peak shifts in the ^{31}P NMR spectra, whilst the shift of compound **c** is further downfield by ~ 1 ppm. This indicates that the substituents on the nitrogen atom have very little effect on the phosphorous peak shift, as the phenyl groups and the ruthenium metal mainly influence this. Furthermore, the PPh_3 ligands of the ruthenium precursor are lost from the metal upon complexation to the PNP ligand. The sharp melting points and elemental analyses that match those expected indicate that these complexes are pure.

6.4.2 Description of crystal structures

Yellow crystals of complex **a** were obtained by slow diffusion of diethyl ether into a dichloromethane solution. Good quality crystals of **a** were not obtained despite many attempts. An OLEX diagram of **a** is shown in Fig. 6.2. It is clearly observed that the two Cl atoms, as well as two phosphorous atoms of the ligand in **a**, are connected to the Ru metal. The selected interatomic distances and angles for **a** are given in Table 6.2.

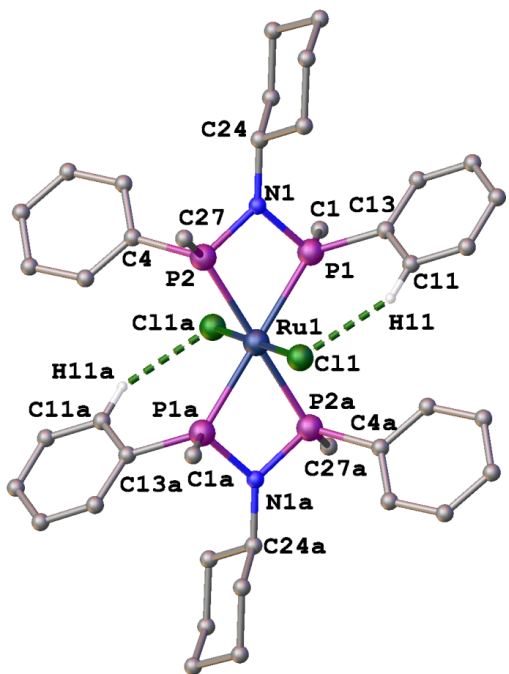


Figure 6.2. Structure of compound **a** with selected atom labeling scheme. The phenyl groups of P1, P2, P1a and P2a are removed/omitted for clarity.

Table 6.2. Selected bond lengths (\AA) and bond angles ($^\circ$) of complex **a**.

Bond distances (\AA)	a
Ru-P(1)	2.373(2)
Ru-P(2)	2.338(2)
Ru-Cl(1)	2.420(2)
Ru-Cl(2)	2.420(2)
P(1)-N(1)	1.725(7)
P(2)-N(1)a	1.726(7)
P(1)-C(1)	1.825(8)
P(1)-C(13)	1.843(10)
P(2)-C(4)	1.815(10)
P(2)-C(27)	1.832(8)
N(1)-C(24)	1.520(10)
Bond angles ($^\circ$)	
P(1)-Ru-P(2)	68.87(7)
P(1)-N(1)-P(2)	101.1(3)
P(1)-Ru-Cl(1)	84.58(7)
P(2)-Ru-Cl(1)	88.27(7)

The crystal structure of **a** (Fig. 6.2) shows the ruthenium(II) center to be essentially octahedral with two chloride and two PNP ligands arranged in trans configurations. Within the four membered RuP₂N ring there is considerable ring strain which is reflected by an acute P(1)-Ru(1)-P(2) angle of 68.87°(7) and is slightly higher than that of similar reported structures.⁸²⁻⁸⁴ The Ru-P(1) 2.373(2), Ru-P(2) 2.338(2) and Ru-Cl 2.420(2) \AA in **a** are slightly shorter than those of a similar complex [Ru(η^5 -C₅H₅)Cl{Ph₂P)₂NH}]] (2.2813(10), 2.4607(10) and 1.692(3) \AA , respectively), whilst the P-N (1.725(7) \AA) distance of complex **a** is slightly higher (1.694(3) \AA).^{84,85} Within the RuP metallacycles, the P-N-P bond angles of 101.1(3) and 101.2(4) $^\circ$ are smaller with respect to those of similar reported structures.^{83,84}

The interatomic distances of the Ru \cdots N bonds is 3.033 \AA and is less than that of a similar reported structure, 3.138 \AA .⁸³ These findings indicate that the nitrogen atoms do not bind to

the metal ion. In addition, the average P(1)…P(2) and P(1)…P(2) distances are 2.664 Å and 3.886 Å for **a**, and show rectangular arrangement. This is due to the distances not being the same and are slightly shorter than those of similar reported structures.^{83,84}

The crystal structures reveal that in compound **a**, C-bound H atoms are involved in intermolecular C—H…halogen and π-π interactions (Tables 6.3 and 6.4). The crystal packing of the molecule is presented in Fig. 6.3. The molecule extends via a C---H…Cl interaction making infinite chains along the *c* axis. The molecules are organized in a layered structure parallel to each other through the *a*-axis via π…π interactions (Table 6.4). The molecules are organized in a spiral ladder like structure by extension of the C---H…π interaction through the cyclohexyl C-H and PNP-phenyl ring.

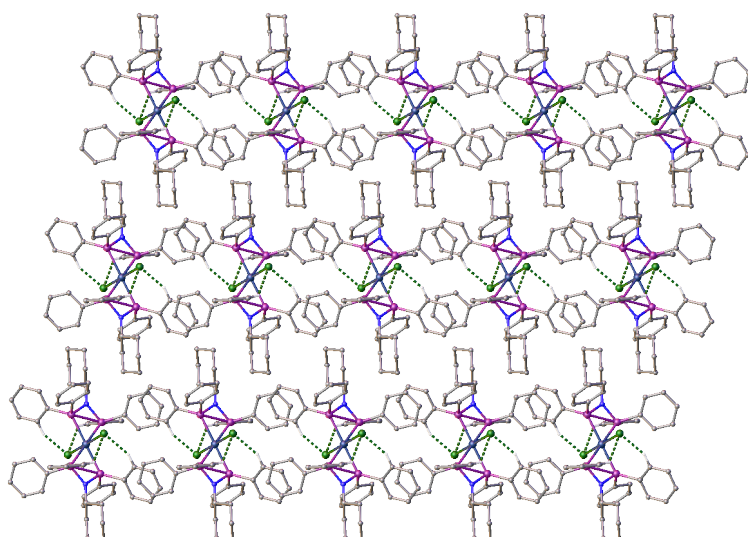


Figure 6.3. Crystal packing of compound **a** along the *c*-axis.

Table 6.3. Non-classical hydrogen C—H…O, C—H…Cl and C—H…Cg interactions of the complex **a** (110).

Donor---H…Acceptor	D - H	H...A	D...A	D - H...A	ARU
C(9)---H(9)...Cl(1)	1.00(13)	2.76(15)	3.579(13)	139(9)	-1+x,y,z
C(11)---H(11)...Cl(1)	1.03(9)	2.39(9)	3.348(10)	156(7)	2-x,-y,1-z
C(19)---H(19)...Cl(1)	0.82(9)	2.72(7)	3.328(9)	133(7)	-
C(25)---H(25B)...Cg(5)	0.91	2.86(8)	3.770(11)	164(5)	X,Y,Z

Table 6.4. $\pi\ldots\pi$ interactions of the complex a.

$\pi\ldots\pi$ (Cg...Cg)	Distance (Å)	ARU
Cg(1)...Cg(3)	4.169(5)	X,Y,Z
Cg(1)...Cg(4)	4.160(6)	2-X,-Y,1-Z
Cg(1)...Cg(5)	4.281(6)	X,Y,Z
Cg(1)...Cg(6)	4.226(5)	2-X,-Y,1-Z
Cg(2)...Cg(3)	4.169(5)	2-X,-Y,1-Z
Cg(2)...Cg(4)	4.160(6)	X,Y,Z
Cg(2)...Cg(5)	4.281(6)	2-X,-Y,1-Z
Cg(2)...Cg(6)	4.226(5)	X,Y,Z
Cg(3)...Cg(1)	5.898(6)	2-X,-Y,1-Z
Cg(3)...Cg(2)	5.898(6)	X,Y,Z
Cg(3)...Cg(5)	5.865(7)	1-X,-Y,-Z
Cg(3)...Cg(6)	5.450(6)	X,Y,Z
Cg(3)...Cg(6)	5.179(7)	3-X,1-Y,1-Z
Cg(4)...Cg(3)	5.712(7)	2-X,1-Y,1-Z
Cg(4)...Cg(5)	4.416(7)	1-X,-Y,1-Z
Cg(4)...Cg(6)	4.975(7)	X,Y,Z
Cg(5)...Cg(4)	5.443(6)	X,Y,Z
Cg(5)...Cg(4)	4.417(7)	1-X,-Y,1-Z
Cg(5)...Cg(6)	5.304(6)	2-X,1-Y,1-Z
Cg(6)...Cg(3)	5.450(6)	X,Y,Z
Cg(6)...Cg(4)	5.890(6)	2-X,1-Y,1-Z
Cg(6)...Cg(6)	4.911(7)	3-X,1-Y,1-Z

6.4.3 Oxidation of *n*-octane

The catalytic activity of the ruthenium complexes was explored in the oxidation of *n*-octane. The reactions were run under optimized conditions i.e. catalyst:substrate molar ratio of 1:100; substrate:oxidant molar ratio of 1:5 in 1,2-dichloroethane (DCE) as solvent system at 80 °C. The oxidant used was *tert*-butyl hydroperoxide (TBHP). Control experiments were carried out in the absence of the catalyst and oxidant respectively. In the former case, a 3% conversion was observed with highest selectivity to octanoic acid (Fig. 6.4). In the absence of the oxidant, no conversion was observed. The reaction was also carried out using the ruthenium precursor ($\text{RuCl}_2(\text{PPh}_3)_3$) as a catalyst. A 10% conversion was observed, with

selectivity to the deeper oxidized products, namely the ketones and acid. It is known that with simple salts of iron, low activity is exhibited in oxidation reactions.⁸⁰

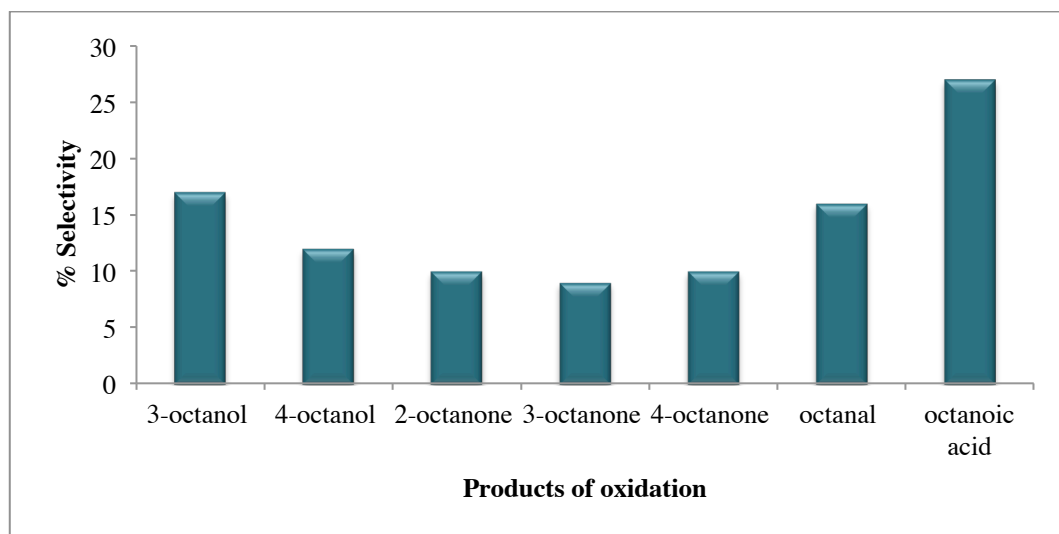


Figure 6.4. Selectivity to the products of oxidation of the blank reaction (no catalyst) at a substrate:oxidant molar ratio of 1:5.

Conditions: Catalyst:*n*-octane (1:100); Temperature: 80 °C; Solvent: DCE

The activity of catalysts **a** is lower than those of **b** and **c** (Fig. 6.5). In contrast, chromium complexes bearing the same ligand backbones as **a** and **b** showed comparable activity in ethylene oligomerisation.⁶² Compared to the blank reaction, the catalysts are more selective to the alcohols than the deeper oxidized products such as the ketones and octanoic acid (Fig. 6.6). Following the method of Shul’pin and coworkers, addition of triphenylphosphine 10 mins prior to GC analysis resulted in an increase in the alcohol peak and a decrease in the ketone peak.⁸⁰ This is the true concentration of the alcohols and ketones since the alkyl hydroperoxides that are present are completely reduced to the corresponding alcohols.

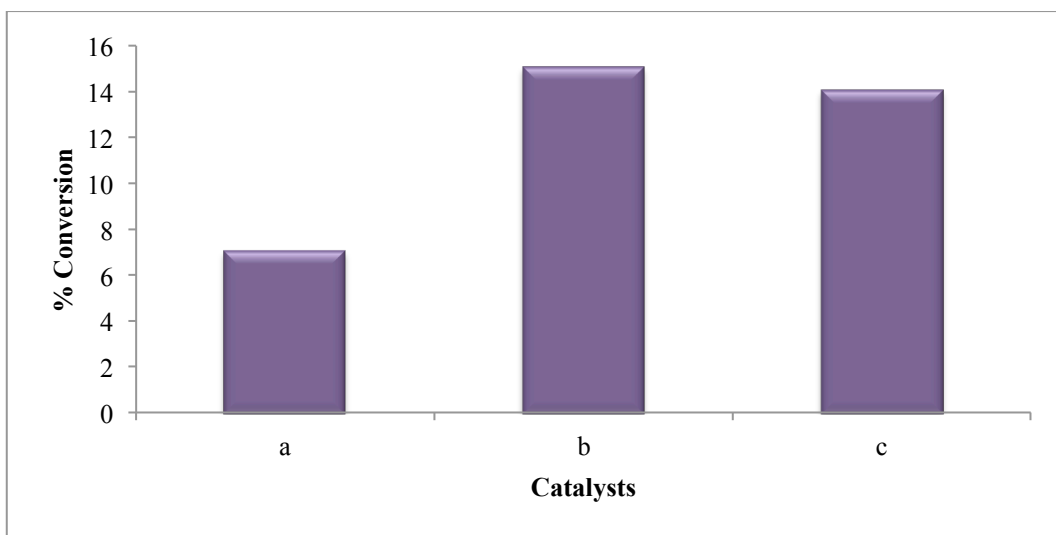


Figure 6.5. Conversion of *n*-octane by catalysts **a-c**.

Conditions: Catalyst:*n*-Octane (1:100); *n*-Octane: TBHP (1:5); Temperature: 80 °C; Solvent: DCE.

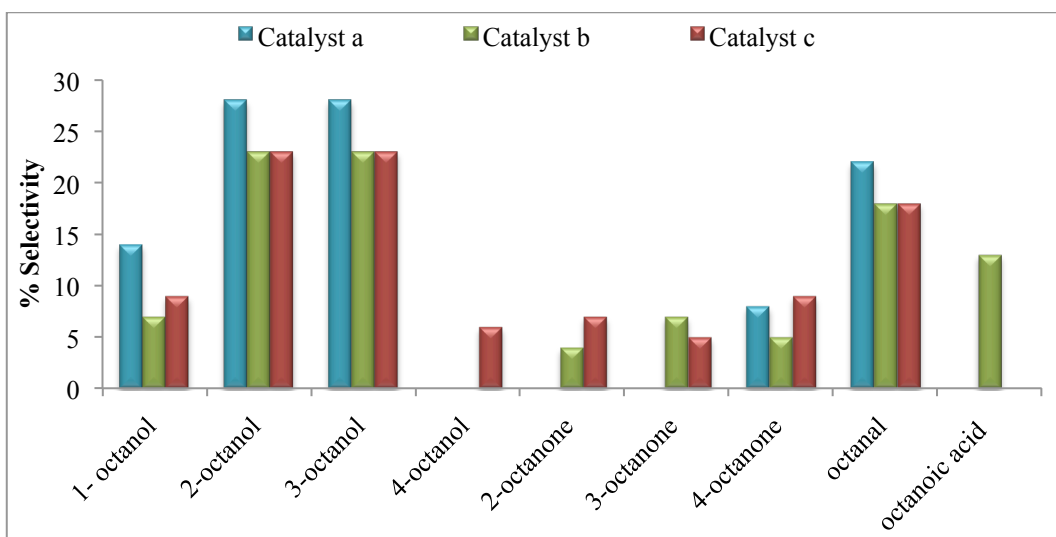


Figure 6.6. Selectivity to products of oxidation of *n*-octane by catalysts **a-c**.

Conditions: Catalyst:*n*-Octane (1:100); *n*-Octane: TBHP (1:5); Temperature: 80 °C; Solvent: DCE.

Bailey et al. reported 15 % and 14% yields to 2- and 3-octanone under similar conditions with ruthenium amine complexes.³⁸ Using diaminophosphine ligands complexed to ruthenium, Wong and co-workers reported selectivity to only 4-octanone.^{73,74} With lower *n*-alkane chains (heptane and propane) using ruthenium complexes ($[\text{BaRuO}_3]\text{OH}_2$) and Ru/C-CH₃CO₃H) as catalysts, higher yields to the ketonic products and very low yields to the alcohols were observed.^{42,45} There is a much higher selectivity to the primary oxidation products using catalyst **a** compared to the deeper oxidized products (ketones and acid), which indicated that the reaction proceeds more slowly using this catalyst, accounting for the lower activity. The

selectivities of catalysts **b** and **c** are comparable, however, the acid is only observed for catalyst **b**.

The regioselectivity parameters (Table 6.5) indicate that the C(2) and C(3) position of the *n*-octane chain are the most activated. However, the activation at the C(1) position in the total selectivity is relatively high compared to other oxidation studies using liner alkanes.

Table 6.5. Selectivity parameters in the oxidation of *n*-octane by catalysts **a-c**.

Catalyst	Alcohol^a	Total^{b,c}
	C(1):C(2):C(3)	C(1):C(2):C(3):C(4)
a	1:3:3	3:3.5:3.5:1
b	1:5:5	1.7:1.8:2:1
c	1:3.8:3.8	3.6:6:5.6:1

^a Parameters C(1):C(2):C(3):C(4) are the relative reactivities of hydrogen atoms at carbons 1, 2, 3 and 4 of the *n*-octane chain.

^b The calculated reactivities from the % selectivity are normalized, i.e. calculated taking into account the number of hydrogen atoms at each carbon.

^c Includes the % selectivity of octanal, octanoic acid, alcohols and ketones and the values are normalized.

6.4.4 Oxidation of styrene

The catalysts were also explored in the oxidation of styrene under optimized conditions of styrene:oxidant molar ratio of 1:2.5 and catalyst:styrene molar ratio of 1:100. The reaction was monitored at room temperature, 50 °C and 80 °C to determine the optimum temperature for the highest selectivity to benzaldehyde (Figs. 6.7 and 6.8). The conversion increases with an increase in temperature and reaction time. After 6 h, the reaction rate is slightly faster at 50 °C than at 80 °C, which could be due to the stability of the Ru-oxo species at these temperatures.

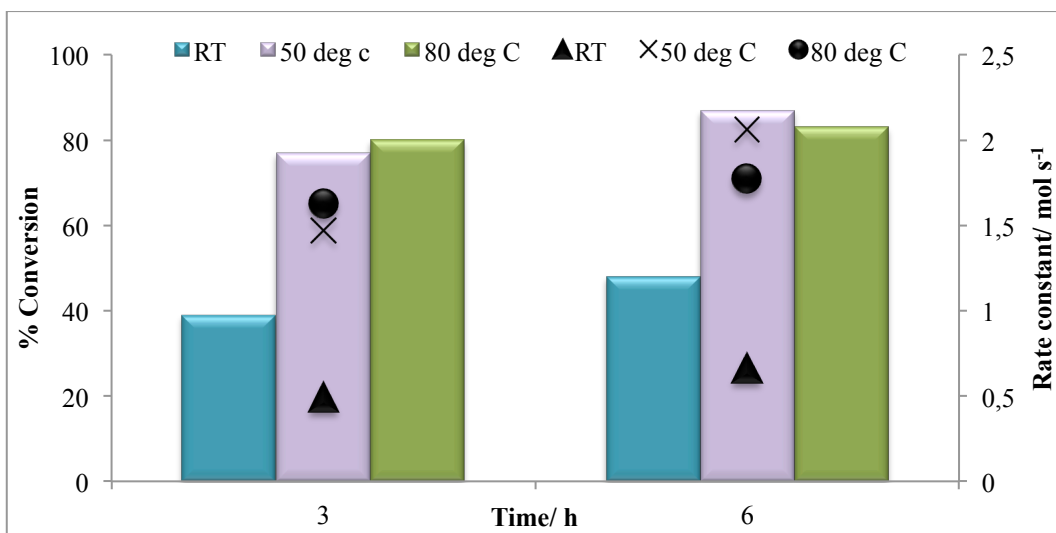


Figure 6.7. Conversion of styrene and reaction rate using catalyst **a** at room temperature, 50 °C and 80 °C.

Conditions: Catalyst:styrene (1:100); Styrene: TBHP (1:2.5); Solvent: DCE; Catalyst **a**.

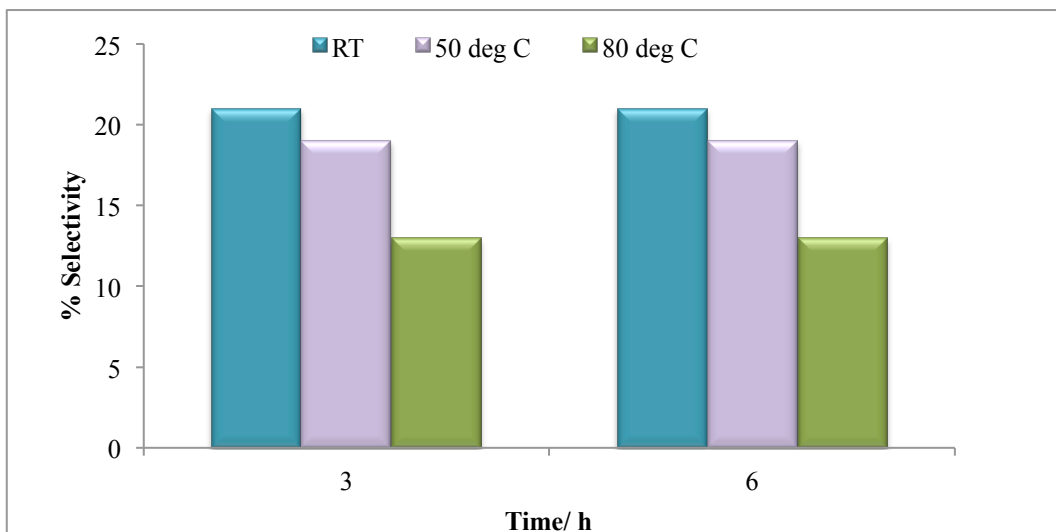


Figure 6.8. Selectivity to benzaldehyde at room temperature, 50 °C and 80 °C.

Conditions: Catalyst:styrene (1:100); Styrene: TBHP (1:2.5); Solvent: DCE; Catalyst **a**.

The selectivity to benzaldehyde decreases with an increase in temperature, which is due to over oxidation to benzoic acid at high temperatures. Cleavage of benzaldehyde (to form benzene) is more prominent at 50 °C (7%) and 80 °C (5%). Only at room temperature and 50 °C does styrene oxide form (1%), with phenyl acetaldehyde forming at 50 °C and 80 °C (2%). Screening of catalysts **b** and **c** was carried out at room temperature up to 6 h, since no further change in selectivity was observed if the reaction was carried out for a longer time (Table 6.6). This could be due to decomposition of TBHP to form *tert*-butanol, which competes for the same coordination site on the metal.⁹ The blank reaction, with no catalyst, at room

temperature shows no conversion. The benzaldehyde selectivity over catalysts **a** and **b** are comparable which is expected since these catalysts have similar basic properties. The conversion and benzaldehyde selectivity after 3 h for catalyst **c** is much lower than those of catalysts **a** and **b**. This could be attributed to the formation of the active oxo species, which takes longer to form for catalyst **c** in comparison to the other two catalysts. This is also noted by the lower reaction rate observed for catalyst **c** after 3 h. This is once again attributed to the basicity of the substituent on the nitrogen.⁶² The longer alkyl chains on the nitrogen atom, increases the basicity, which increases the electron density on the metal resulting in a slower formation of the active oxo species. However, once the active species is formed, the highest selectivity to benzaldehyde is noted after 6 h. Early research by Aneetha et al. using Ru(III) triphenylphosphine complexes reported yields only to styrene oxide.¹⁶ Indeed most studies involving ruthenium report higher yields to styrene oxide, but very little or no yield to benzaldehyde under ambient conditions.^{4,8,9,17,18} In one reported case no conversion was observed using TBHP as an oxidant.¹⁹ Supported Ru based catalysts have been shown to be selective only to the epoxide (16%) at a 9% conversion at 25 °C.¹¹ Using PNPN ligands complexed to ruthenium, Stoop et al. report low selectivity to benzaldehyde (9%).²⁵

Table 6.6. Catalytic results of catalysts **a-c** under optimum conditions^a.

Catalyst (Time/ h)	% Conversion	Bza selectivity/ mol %	TON (Bza)	Rate constant/ mol s ⁻¹
a (3)	39	21	9	0.49
a (6)	48	21	11	0.66
b (3)	36	22	11	0.45
b (6)	42	24	11	0.54
c (3)	20	8	2	0.22
c (6)	53	19	13	0.76

^aConditions: Catalyst:styrene (1:100); Styrene: TBHP (1:2.5); Solvent: DCE; Bza= benzaldehyde

Both reactions (styrene and *n*-octane oxidation) proceed with the formation of a Ru^{IV}-oxo (~300 nm) species as observed in the IR/UV spectra shown for catalyst **b** in Fig 6.9.⁸⁶ This is also noted in the color change of the reaction, which goes from initially yellow to dark brown and yellow again (reaction is complete). This indicates that the active oxo species is formed and thereafter the catalyst is regenerated, which is further observed in the phosphorous peak position in the ³¹P NMR spectra (styrene oxidation) (Fig 6.10). An 8 ppm difference is noted between the fresh and recovered catalyst. The single peak indicates that no ligand degradation occurred and the slight shift may be due to a difference in the catalyst structure brought about during the catalytic reaction. It is known that the epoxidation of alkenes by metal complexes proceeds via the formation of a metal-oxo intermediate via the addition of the oxidant.¹⁵

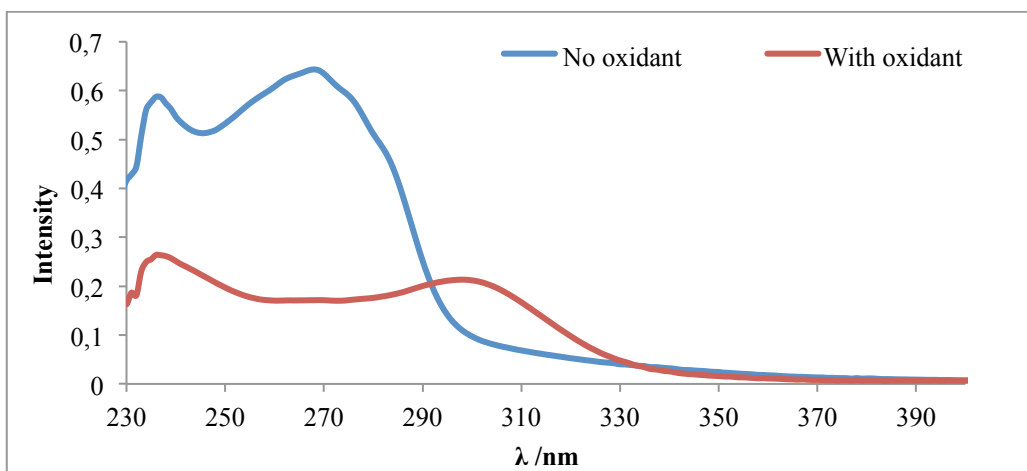


Figure 6.9. UV spectrum of catalyst **b** with oxidant and without oxidant.

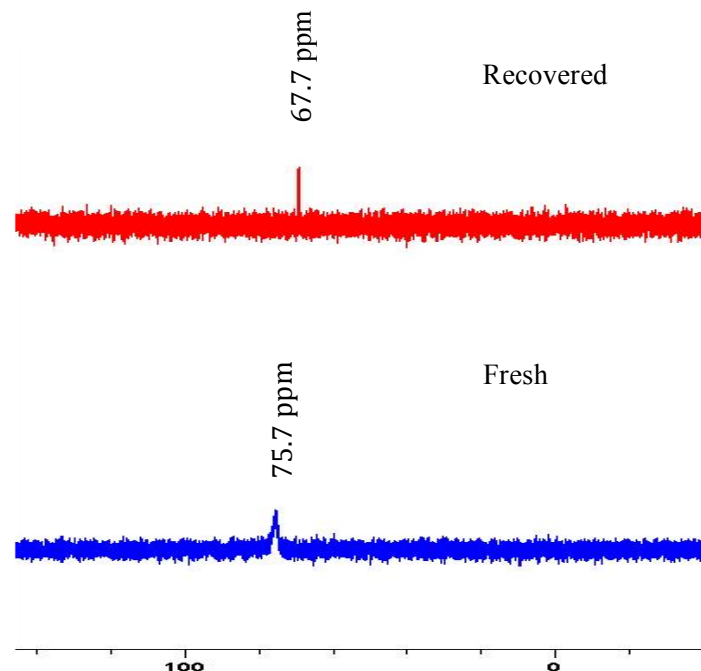


Figure 6.10. ^{31}P NMR spectra of the fresh and recovered catalyst **a** after styrene oxidation.

6.5 Conclusion

Aminodiphosphine ruthenium complexes have been successfully synthesized and characterized and were used as catalysts in the oxidation of *n*-octane and styrene. In the alkane oxidation, good selectivities to the alcohols were observed, with the highest selectivities being towards 2-and 3-octanol by catalyst **a**. Overoxidation is less prevalent in this system as compared to other reported systems in literature. In the oxidation of styrene the

highest selectivity to benzaldehyde was at room temperature. The difference in activity of the complexes is attributed to the basicity of the substituents on the nitrogen atom.

6.6 References

- [1] Jahromi, B. T.; Kharat, A. N.; Zamanian, S. *Chinese Chem. Lett.* **2014**, In press.
- [2] Bressan, M.; Morville, A. *Inorg. Chem.* **1989**, *28*, 950-953.
- [3] Benet-Buchholz, J.; Comba, P.; Llobet, A.; Roeser, S.; Vadivelu, P.; Wadeppohl, H.; Wiesner, S. *Dalton Trans.* **2009**, 5910-5923.
- [4] Cheng, W.-C.; Fung, W.-H.; Che, C.-M. *J. Mol. Catal. A: Chem.* **1996**, *113*, 311-319.
- [5] Gallo, E.; Caselli, A.; Ragagni, F.; Fantauzzi, S.; Masciocchi, N.; Sironi, A.; Cenini, S. *Inorg. Chem.* **2005**, *44*, 2039-2049.
- [6] Chatterjee, D.; Basak, S.; Mitra, A.; Sengupta, A.; Le Bras, J.; Muzart, J. *Catal. Commun.* **2005**, *6*, 459.
- [7] Kille, S.; Zilly, F. E.; Acevedo, J. P.; Reetz, M. T. *Nat. Chem.* **2011**, *3*, 738-743.
- [8] Moghadam, M.; Mirkhani, V.; Tangestaninejad, S.; Mohammadpoor-Baltork, I.; Kargar, H.; Sheikholeslami, I.; Hatifi, M. *J. Iran. Chem. Soc.* **2011**, *8*, 1019-1029.
- [9] Chatterjee, D.; Basak, S.; Riahi, A.; Muzart, J. *J. Mol. Catal. A: Chem.* **2006**, *255*, 283-289.
- [10] Dakkach, M.; López, M. I.; Romero, I.; Rodríguez, M.; Atlamsani, A.; Parella, T.; Fontrodona, X.; Llobet, A. *Inorg. Chem.* **2010**, *49*, 7072-7079.
- [11] Dakkach, M.; Fontrodona, X.; Parella, T.; Atlamsani, A.; Romero, I.; Rodriguez, M. *Dalton Trans.* **2014**, *43*, 9916-9923.
- [12] Dakkach, M.; Atlamsani, A.; Parella, T.; Fontrodona, X.; Romero, I.; Rodriguez, M. *Inorg. Chem.* **2013**, *52*, 5077-5087.
- [13] Mahalingam, V.; Karvembu, R.; Chinnusamy, V.; Natarajan, K. *Spectrochim. Acta A* **2006**, *64*, 886-890.
- [14] Nishiyama, H.; Motoyama, Y. *Chem. Commun.* **1997**, 1863-1864.
- [15] Agarwala, H.; Ehret, F.; Chowdhury, A. D.; Maji, S.; Mobin, S. M.; Kaim, W.; Lahiri, G. K. *Dalton Trans.* **2013**, *42*, 3721-3734.
- [16] Aneetha, H.; Padmaja, J.; Zacharias, P. S. *Polyhedron* **1996**, *15*, 2445-2451.
- [17] Antony, R.; Tembe, G. L.; Ravindranathan, M.; Ram, R. N. *Euro. Polym. J.* **2000**, *36*, 1579-1589.
- [18] Barf, G. A.; van den Hoek, D.; Sheldon, R. A. *Tetrahedron* **1996**, *52*, 12971-12978.
- [19] Chowdhury, A. D.; Das, A.; K, I.; Mobin, S. M.; Lahiri, G. K. *Inorg. Chem.* **2011**, *50*, 1775-1785.
- [20] Klawonn, M.; Tse, M. K.; Bhor, S.; Döbler, C.; Beller, M. *J. Mol. Catal. A: Chem.* **2004**, *218*, 13-19.
- [21] Spannring, P.; Bruijnincx, P. C. A.; Weckhuysen, B. M.; Klein Gebbink, R. J. M. *Catal. Sci. Tech.* **2014**, *4*, 2182-2209.
- [22] Kogan, V.; Quintal, M. M.; Neumann, R. *Org. Lett.* **2005**, *7*, 5039-5042.
- [23] Robbins, M. H.; Drago, R. S. *J. Chem. Soc. Dalton Trans.* **1996**, 105-110.
- [24] Sala, X.; Rodríguez, A. M.; Rodríguez, M.; Romero, I.; Parella, T.; von Zelewsky, A.; Llobet, A.; Benet-Buchholz, J. *J. Org. Chem.* **2006**, *71*, 9283-9290.
- [25] Stoop, R. M.; Bachmann, S.; Valentini, M.; Mezzetti, A. *Organometallics* **2000**, *19*, 4117-4126.
- [26] Tada, M.; Muratsugu, S.; Kinoshita, M.; Sasaki, T.; Iwasawa, Y. *J. Am. Chem. Soc.* **2009**, *132*, 713-724.
- [27] Ahmad, A. L.; Kohestani, B.; Bhatia, S.; Ooi, S. B. *Int. J. Appl. Cer. Tech.* **2012**, *9*, 588-598.
- [28] Patel, A.; Patel, K. *Inorg. Chim. Acta* **2014**, *419*, 130-134.

- [29] Karandikar, P.; Agashe, M.; Vijayamohanan, K.; Chandwadkar, A. *J. Appl. Catal. A: Gen.* **2004**, *257*, 133-143.
- [30] P Patil, N. S.; Jha, R.; Uphade, B. S.; Bhargava, S. K.; Choudhary, V. R. *Appl. Catal. A: Gen.* **2004**, *275*, 87-93.
- [31] Patel, A.; Pathan, S. *Ind. Eng. Chem. Res.* **2011**, *51*, 732-740.
- [32] Li, Z.; Wu, S.; Ding, H.; Lu, H.; Liu, J.; Huo, Q.; Guan, J.; Kan, Q. *New J. Chem.* **2013**, *37*, 4220-4229.
- [33] Ding, Y.; Gao, Q.; Li, G.; Zhang, H.; Wang, J.; Yan, L.; Suo, J. *J. Mol. Catal. A: Chem.* **2004**, *218*, 161-170.
- [34] Hu, J.; Li, K.; Li, W.; Ma, F.; Guo, Y. *Appl. Catal. A: Gen.* **2009**, *364*, 211-220.
- [35] Grigoropoulou, G.; Clark, J. H.; Elings, J. A. *Green Chem.* **2003**, *5*, 1-7.
- [36] Yang, Y.; Ding, H.; Hao, S.; Zhang, Y.; Kan, Q. *Appl. Organomet. Chem.* **2011**, *25*, 262-269.
- [37] Crabtree, R. H. *J. Organomet. Chem.* **2004**, *689*, 4083-4091.
- [38] Bailey, A. J.; Griffith, W. P.; Savage, P. D. *J. Chem. Soc. Dalton Trans.* **1995**, 3537-3542.
- [39] Drees, M.; Strassner, T. *J. Org. Chem.* **2005**, *71*, 1755-1760.
- [40] Britovsek, G. J. P.; England, J.; Spitzmesser, S. K.; White, A. J. P.; Williams, D. J. *Dalton Trans.* **2005**, 945-955.
- [41] Che, C.-M.; Zhang, J.-L.; Zhang, R.; Huang, J.-S.; Lai, T.-S.; Tsui, W.-M.; Zhou, X.-G.; Zhou, Z.-Y.; Zhu, N.; Chang, C. K. *Chem. – Eur. J.* **2005**, *11*, 7040-7053.
- [42] Lau, T.-C.; Mak, C.-K. *J. Chem. Soc. Chem. Commun.* **1995**, 943-944.
- [43] Man, W.-L.; Lam, W. W. Y.; Kwong, H.-K.; Yiu, S.-M.; Lau, T.C. *Angew. Chem. Int. Ed.* **2012**, *51*, 9101-9104.
- [44] Murali, M.; Mayilmurugan, R.; Palaniandavar, M. *Eur. J. Inorg. Chem.* **2009**, 2009, 3238-3249.
- [45] Murahashi, S.; Saito, T.; Hanaoka, H.; Murakami, Y.; Naota, T.; Kumobayashi, H.; Akutagawa, S. *J. Org. Chem.* **1993**, *58*, 2929-2930.
- [46] Valodkar, V. B.; Tembe, G. L.; Ravindranathan, M.; Rama, H. S. *J. Mol. Catal. A: Chem.* **2004**, *223*, 31-38.
- [47] Yamaguchi, M.; Kousaka, H.; Izawa, S.; Ichii, Y.; Kumano, T.; Masui, D.; Yamagishi, T. *Inorg. Chem.* **2006**, *45*, 8342-8354.
- [48] Yi, C. S.; Kwon, K.-H.; Lee, D. W. *Org. Lett.* **2009**, *11*, 1567-1569.
- [49] He, Y.; Gorden, J. D.; Goldsmith, C. R. *Inorg. Chem.* **2012**, *51*, 12651-12660.
- [50] Kirillov, A. M.; Kirillova, M. V.; Shul'pina, L. S.; Figiel, P. C. J.; Gruenwald, K. R.; Guedes da Silva, M. F. T. C.; Haukka, M.; Pombeiro, A. J. L.; Shul'pin, G. B. *J. Mol. Catal. A: Chem.* **2011**, *350*, 26-34.
- [51] Kirillova, M. V.; Kirillov, A. M.; Mandelli, D.; Carvalho, W. A.; Pombeiro, A. J. L.; Shul'pin, G. B. *J. Catal.* **2010**, *272*, 9-17.
- [52] Mac Leod, T. C. O.; Kirillova, M., V.; Pombeiro, A. J. L.; Schiavon, M. A.; Assis, M. D. *Appl. Catal. A: Gen.* **2010**, *372*, 191-198.
- [53] Conley, B. L.; Tenn I, W. J.; Young, K. J. H.; Ganesh, S. K.; Meier, S. K.; Ziatdinov, V. R.; Mironov, O.; Oxgaard, J.; Gonzales, J.; Goddard III, W. A.; Periana, R. A. *J. Mol. Catal. A: Chem.* **2006**, *251*, 8-23.
- [54] Kopylovich, M. N.; Kirillov, A. M.; Baev, A. K.; Pombeiro, A. J. L. *J. Mol. Catal. A: Chem.* **2003**, *206*, 163-178.
- [55] Sivaramakrishna, A.; Suman, P.; Veerashekhar Goud, E.; Janardan, S.; Sravani, C.; Sandeep, T.; Vijayakrishna, K.; Clayton, H. S. *J. Coord. Chem.* **2013**, *66*, 2091-2109.
- [56] Zhu, Y. J.; Fan, L.; Chen, C. H.; Finnell, S. R.; Foxman, B. M.; Ozerov, O. V. *Organometallics* **2007**, *26*, 6701-6703.
- [57] Kirillov, A. M.; Shul'pin, G. B. *Coord. Chem. Rev.* **2013**, *257*, 732-754.
- [58] White, M. C. *Synlett* **2012**, *23*, 2746-2748.
- [59] White, M. C. *Science* **2012**, *335*, 807-809
- [60] Chen, M. S.; White, M. C. *Science* **2010**, *327*, 566-571.
- [61] Teo, S.; Weng, Z.; Hor, T. S. A. *Organometallics* **2008**, *27*, 4188-4192.

- [62] Blann, K.; Bollmann, A.; de Bod, H.; Dixon, J. T.; Killian, E.; Nongodlwana, P.; Maumela, M. C.; Maumela, H.; McConnel, A. E.; Morgan, D. H.; Overette, M. J.; Pretorius, M.; Kuhlmann, S.; Wasserscheid, P. *J. Catal.* **2007**, *249*, 244-249.
- [63] Blann, K.; Bollmann, A.; Dixon, J. T.; Hess, F. M.; Killian, E.; Maumela, H.; Morgan, D. H.; Neveling, A.; Otto, S.; Overett, M. J. *Chem. Commun.* **2005**, 620-621
- [64] Bollmann, A.; Blann, K.; Dixon, J. T.; Hess, F. M.; Killian, E.; Maumela, H.; McGuiness, D. S.; Morgan, D. H.; Neveling, A.; Otton, S.; Overette, M.; Slawin, A. M. Z.; Wasserscheid, P.; Kihlmann, S. *J. Am. Chem. Soc.* **2004**, *126*, 14712-14713.
- [65] Overett, M. J.; Blann, K.; Bollmann, A.; Dixon, J. T.; Hess, F.; Killian, E.; Maumela, H.; Morgan, D. H.; Neveling, A.; Otto, S. *Chem. Commun.* **2005**, 622-624.
- [66] Bowen, L. E.; Haddow, M. F.; Orpen, A. G.; Wass, D. F. *Dalton Trans.* **2007**, 1160-1168.
- [67] Bowen, L. E.; Charernsuk, M.; Hey, T. W.; McMullin, C. L.; Orpen, A. G.; Wass, D. F. *Dalton Trans.* **2010**, *39*, 560-567.
- [68] Benito-Garagorri, D.; Alves, L. G. a.; Puchberger, M.; Mereiter, K.; Veiros, L. F.; Calhorda, M. J.; Carvalho, M. D.; Ferreira, L. P.; Godinho, M.; Kirchner, K. *Organometallics* **2009**, *28*, 6902-6914.
- [69] Benito-Garagorri, D.; Kirchner, K. *Acc. Chem. Res.* **2008**, *41*, 201-213.
- [70] van der Boom, M. E.; Milstein, D. *Chem. Rev.* **2003**, *103*, 1759-1792.
- [71] Xu, X.; Xi, Z.; Chen, W.; Wang, D. *J. Coord. Chem.* **2007**, *60*, 2297-2308.
- [72] Albrecht, M.; van Koten, G. *Angew. Chem. Int. Ed.* **2001**, *40*, 3750-3781.
- [73] Wong, W.-K.; Chen, X.-P.; Guo, J.-P.; Chi, Y.-G.; Pan, W.-X.; Wong, W.-Y. *J. Chem. Soc. Dalton Trans.* **2002**, 1139-1146.
- [74] Wong, W.-K.; Chen, X.-P.; Chik, T.-W.; Wong, W.-Y.; Guo, J.-P.; Lee, F.-W. *Eur. J. Inorg. Chem.* **2003**, *2003*, 3539-3546.
- [75] Khan, M. M. T.; Reddy, V. V. S. *Inorg. Chem.* **1986**, *25*, 208-214.
- [76] Shul'pin, G. B.; Kudinov, A. R.; Shul'pina, L. S.; Petrovskaya, E. A. *J. Organomet. Chem.* **2006**, *691*, 837-845.
- [77] Sheldrick, G. M.; 2.05 ed.; SHELXS-97, SHELXL-97 and SADABS version 2.05, University of Göttingen, Germany: **1997**.
- [78] Sheldrick, G. *Acta Crystallogr., Sect. A:* **2008**, *64*, 112-122.
- [79] Otwinowski, Z and Minor, Z. *Processing of X-ray Diffraction Data Collected in Oscillation Mode, Methods in Enzymology, Macro. Cryst. A*, **1997**, *276*, 307-326. C.W. Carter, Jr. and R. M. Sweet, Eds., Academic Press (New York).
- [80] Dolomanov, O. V.; Bourhis, L. J.; Gildea, R. J.; Howard, J. A. K.; Puschmann, H. *J. Appl. Crystallogr.* **2009**, *42*, 339-341.
- [81] Aydemir, M.; Baysal, A.; Özkar, S.; Yıldırım, L. T. *Inorg. Chim. Acta* **2011**, *367*, 166.
- [82] Balakrishna, M. S.; Panda, R.; Mague, J. T. *Polyhedron* **2003**, *22*, 587-593.
- [83] Ogawa, T.; Kajita, Y.; Wasada-Tsutsui, Y.; Wasada, H.; Masuda, H. *Inorg. Chem.* **2012**, *52*, 182-195.
- [84] Gaw, K. G.; Smith, M. B.; Slawin, A. M. Z. *New J. Chem.* **2000**, *24*, 429-435.
- [85] Geicke, J.; Lorenz, I. P.; Engel, M.; Polborn, K. *Inorg. Chim. Acta* **1998**, *269*, 157-161.
- [86] Che, C.-M.; Ho, C.; Lau, T.-C. *J. Chem. Soc. Dalton Trans.* **1991**, 1901-1907.

Chapter Seven

Summary

The oxidation of C-H bonds of both alkanes and alkenes in trying to achieve good selectivity to valuable products still remains a challenge. This study has presented new work in using the aminodiphosphine or “PNP” ligand system in the oxidation of *n*-octane and styrene. These ligands have been prepared according to known procedures in literature. The substituent on the nitrogen atom of the PNP ligand was varied by making use of alkyl functional groups (cyclohexyl, iso-propyl and pentyl) as well as phenyl and substituted phenyl (methoxy phenyl and chloro-phenyl) functional groups. To add flexibility to the ligand backbone, ligands containing ethylene spacer groups between the phosphorous and nitrogen atoms were also synthesized.

The ligands were successfully complexed to the transition metals cobalt, iridium, rhodium and ruthenium. These complexes were characterized by NMR spectroscopy, elemental analyses, HRMS, IR spectroscopy and in some cases single crystal XRD studies.

The ligands (both rigid and flexible) bearing the alkyl substituent on the nitrogen atom were complexed to cobalt and used as catalysts in the oxidation of *n*-octane and styrene. In the oxidation of *n*-octane with *tert*-butyl hydroperoxide (TBHP), this new study shows that all complexes showed good activity. A mechanism was proposed and it is assumed that the reaction takes place in the coordination sphere of the metal complex, which would explain the influence of the ligand system on the reaction. The complexes bearing the flexible ligand backbone with the cyclohexyl substituent on the nitrogen atom were most active with the highest selectivity to 2-octanone. In this study, the effect of bite angle comes into play, where the catalysts with the larger bite angle (flexible ligand backbone) are more active than those with a smaller bite angle. These catalysts, in comparison to other studies, showed good selectivity to the octanols.

In the oxidation of styrene using the cobalt catalysts, optimization of solvent, temperature, and oxidant was undertaken. Unlike the previous study (oxidation of *n*-octane), the catalysts bearing the rigid backbone were more active than those with the flexible ligand backbone. These catalysts showed good activity when DCE was used as a solvent and TBHP as an oxidant at 80 °C. The aim of this study was to achieve good yield to styrene oxide and

benzaldehyde. The ligand bearing the pentyl substituent on the nitrogen atom gave the highest yield of these two products. The activities of the different catalysts, bearing the different substituents on the ligand backbone, are comparable. It was postulated that the reaction proceeds with Co(II) binding to the oxygen from the TBHP (*t*-BuOOH) to form a Co(III) super oxo species.

The oxidation of both *n*-octane and styrene using iridium and rhodium complexes has not been thoroughly explored by other workers. Very few cases have been reported and most work was undertaken in the 1980's. To gain scientific insight and to develop the chemistry of these metal complexes, bearing the "PNP" ligand backbone, it was therefore decided that these complexes be investigated for the oxidation of styrene and *n*-octane. Optimization studies were carried out in the oxidation of *n*-octane and the rhodium catalysts where found to be more active than the iridium catalysts. This could be attributed to the rhodium complexes having a greater ability to coordinate to larger hydrocarbons than the iridium catalysts. Highest selectivity was to the octanones, however, good selectivity to the octanols for both sets of catalysts was also observed. One of the remarkable achievements of this study was that the catalysts would be recovered (showing no ligand degradation) and re-used over 2 cycles. It can be postulated that the reaction proceeds with the formation of the *t*-BuO[•] radical via the reduction of the oxidant by the metal complex, M(I)L, which generates a hydroxo-M(III) species.

Both iridium and rhodium complexes showed good activity in the oxidation of styrene using TBHP as the oxidant. It can be proposed that the reaction takes places via the formation of a super oxo M(III) species. The iridium complexes were more active than the rhodium complexes. This could be due to the active super oxo Rh(III) complex having a lower affinity for the olefin. Higher yields to benzaldehyde were achieved in comparison to styrene oxide for all catalysts. In this study, the catalysts were recovered and reused over three cycles.

The difference in the activity of the catalysts bearing the different substituents on the nitrogen atom of the ligand backbone could be attributed to the basicity of the ligand backbone. The more basic nature of the catalyst, the stronger is its electron donating ability, resulting in a greater electron density located at the metal center. This renders it easier to go from a M^I to M^{III} state upon activation by the oxidant. However, the formation of the active *tert*-butoxy radical becomes more difficult since the high basic nature of the complex stabilizes the M^{III} oxidation state.

For the oxidation of styrene, ruthenium based catalysts have been widely explored, however, when using phosphines as the respective ligand, noticeable ligand degradation is observed. In this study, some new PNP “spider” complexes were prepared and used as catalysts in the oxidation of styrene and *n*-octane. Both reactions proceeded via the formation of a Ru-oxo species as observed in the UV spectrum. In the oxidation of *n*-octane, good selectivities to the alcohols were observed with the catalyst bearing the *iso*-propyl functional group on the nitrogen atom being the most active. In the oxidation of styrene, the catalysts were only selective to benzaldehyde, with the highest selectivity being observed at room temperature. The used catalyst was isolated and characterized and no ligand degradation had occurred.

Appendix A

Data for crystal structure **2a**

Table A1. Atomic coordinates ($\times 10^4$) and equivalent isotropic displacement parameters ($\text{\AA}^2 \times 10^3$) for **2a**. U(eq) is defined as one third of the trace of the orthogonalized U^{ij} tensor.

	x	y	z	U(eq)
C(1)	-2587(9)	6242(8)	-794(3)	12(2)
C(2)	-3560(10)	6057(8)	-1212(3)	16(2)
C(3)	-3951(11)	4903(9)	-1363(3)	23(2)
C(4)	-3386(10)	3914(9)	-1105(3)	21(2)
C(5)	-2428(10)	4099(9)	-692(3)	21(2)
C(6)	-2047(9)	5234(8)	-532(3)	16(2)
C(7)	-262(9)	7792(9)	-307(3)	16(2)
C(8)	655(9)	8253(8)	-623(3)	15(2)
C(9)	912(10)	6352(8)	-999(3)	16(2)
C(10)	2552(10)	6197(9)	-860(3)	19(2)
C(11)	2959(11)	4902(9)	-763(3)	24(2)
C(12)	2316(11)	4086(9)	-1167(4)	26(2)
C(13)	715(10)	4264(9)	-1303(4)	27(2)
C(14)	279(10)	5561(9)	-1408(4)	26(2)
C(15)	1043(10)	8275(8)	-1380(3)	17(2)
C(16)	262(9)	9440(8)	-1562(3)	18(2)
C(17)	-2120(9)	10701(9)	-2087(3)	20(2)
C(18)	-2644(10)	10700(9)	-2565(3)	20(2)
C(19)	-2994(10)	11758(9)	-2801(3)	20(2)
C(20)	-2856(9)	12852(9)	-2574(3)	18(2)
C(21)	-2330(10)	12861(9)	-2100(3)	21(2)
C(22)	-1997(10)	11802(9)	-1860(3)	18(2)
C(23)	-2032(10)	8153(8)	-2181(3)	14(2)
C(24)	-1087(10)	7874(8)	-2449(3)	18(2)
C(25)	-1469(10)	7041(8)	-2800(3)	22(2)
C(26)	-2782(12)	6509(10)	-2895(4)	30(3)
C(27)	-3735(11)	6787(10)	-2634(4)	28(2)
C(28)	-3356(11)	7601(9)	-2275(3)	24(2)

C(29)	-3072(9)	8007(8)	-152(3)	14(2)
C(30)	-4226(10)	7308(9)	-118(3)	17(2)
C(31)	-4967(10)	7584(9)	199(3)	22(2)
C(32)	-4598(11)	8559(9)	493(3)	23(2)
C(33)	-3477(11)	9260(10)	462(4)	29(2)
C(34)	-2708(11)	9003(9)	143(3)	23(2)
Cl(1)	-5129(2)	9206(2)	-1398(1)	22(1)
Cl(2)	-1799(2)	10904(2)	-724(1)	19(1)
Co(1)	-2792(1)	9319(1)	-1140(1)	13(1)
N(1)	404(8)	7605(7)	-1055(3)	15(2)
P(1)	-2151(2)	7770(2)	-602(1)	13(1)
P(2)	-1662(2)	9322(2)	-1752(1)	14(1)

Table A2. Bond lengths [\AA] and angles [$^\circ$] for **2a**.

C(1)-C(2)	1.397(13)
C(1)-C(6)	1.400(13)
C(1)-P(1)	1.814(9)
C(2)-C(3)	1.385(13)
C(2)-H(2)	0.9500
C(3)-C(4)	1.383(14)
C(3)-H(3)	0.9500
C(4)-C(5)	1.379(14)
C(4)-H(4)	0.9500
C(5)-C(6)	1.372(14)
C(5)-H(5)	0.9500
C(6)-H(6)	0.9500
C(7)-C(8)	1.545(12)
C(7)-P(1)	1.841(9)
C(7)-H(7A)	0.9900
C(7)-H(7B)	0.9900
C(8)-N(1)	1.460(12)
C(8)-H(8A)	0.9900
C(8)-H(8B)	0.9900
C(9)-N(1)	1.476(11)
C(9)-C(14)	1.520(13)
C(9)-C(10)	1.560(12)
C(9)-H(9)	1.0000
C(10)-C(11)	1.505(14)
C(10)-H(10A)	0.9900
C(10)-H(10B)	0.9900
C(11)-C(12)	1.528(14)
C(11)-H(11A)	0.9900
C(11)-H(11B)	0.9900
C(12)-C(13)	1.527(14)
C(12)-H(12A)	0.9900
C(12)-H(12B)	0.9900
C(13)-C(14)	1.516(15)
C(13)-H(13A)	0.9900
C(13)-H(13B)	0.9900
C(14)-H(14A)	0.9900

C(14)-H(14B)	0.9900
C(15)-N(1)	1.483(11)
C(15)-C(16)	1.537(13)
C(15)-H(15A)	0.9900
C(15)-H(15B)	0.9900
C(16)-P(2)	1.828(9)
C(16)-H(16A)	0.9900
C(16)-H(16B)	0.9900
C(17)-C(22)	1.396(14)
C(17)-C(18)	1.408(13)
C(17)-P(2)	1.833(10)
C(18)-C(19)	1.376(14)
C(18)-H(18)	0.9500
C(19)-C(20)	1.388(14)
C(19)-H(19)	0.9500
C(20)-C(21)	1.400(14)
C(20)-H(20)	0.9500
C(21)-C(22)	1.380(14)
C(21)-H(21)	0.9500
C(22)-H(22)	0.9500
C(23)-C(28)	1.394(13)
C(23)-C(24)	1.401(13)
C(23)-P(2)	1.811(9)
C(24)-C(25)	1.389(14)
C(24)-H(24)	0.9500
C(25)-C(26)	1.376(15)
C(25)-H(25)	0.9500
C(26)-C(27)	1.391(15)
C(26)-H(26)	0.9500
C(27)-C(28)	1.393(14)
C(27)-H(27)	0.9500
C(28)-H(28)	0.9500
C(29)-C(30)	1.391(13)
C(29)-C(34)	1.413(13)
C(29)-P(1)	1.820(9)
C(30)-C(31)	1.367(13)
C(30)-H(30)	0.9500
C(31)-C(32)	1.393(14)

C(31)-H(31)	0.9500
C(32)-C(33)	1.364(15)
C(32)-H(32)	0.9500
C(33)-C(34)	1.385(13)
C(33)-H(33)	0.9500
C(34)-H(34)	0.9500
Cl(1)-Co(1)	2.225(3)
Cl(2)-Co(1)	2.245(3)
Co(1)-P(1)	2.348(3)
Co(1)-P(2)	2.368(3)
C(2)-C(1)-C(6)	118.2(8)
C(2)-C(1)-P(1)	118.8(7)
C(6)-C(1)-P(1)	122.9(7)
C(3)-C(2)-C(1)	120.4(9)
C(3)-C(2)-H(2)	119.8
C(1)-C(2)-H(2)	119.8
C(4)-C(3)-C(2)	120.8(9)
C(4)-C(3)-H(3)	119.6
C(2)-C(3)-H(3)	119.6
C(5)-C(4)-C(3)	118.7(9)
C(5)-C(4)-H(4)	120.6
C(3)-C(4)-H(4)	120.6
C(6)-C(5)-C(4)	121.5(9)
C(6)-C(5)-H(5)	119.2
C(4)-C(5)-H(5)	119.2
C(5)-C(6)-C(1)	120.3(9)
C(5)-C(6)-H(6)	119.8
C(1)-C(6)-H(6)	119.8
C(8)-C(7)-P(1)	111.5(6)
C(8)-C(7)-H(7A)	109.3
P(1)-C(7)-H(7A)	109.3
C(8)-C(7)-H(7B)	109.3
P(1)-C(7)-H(7B)	109.3
H(7A)-C(7)-H(7B)	108.0
N(1)-C(8)-C(7)	113.1(7)
N(1)-C(8)-H(8A)	109.0
C(7)-C(8)-H(8A)	109.0

N(1)-C(8)-H(8B)	109.0
C(7)-C(8)-H(8B)	109.0
H(8A)-C(8)-H(8B)	107.8
N(1)-C(9)-C(14)	113.2(8)
N(1)-C(9)-C(10)	115.4(7)
C(14)-C(9)-C(10)	110.0(8)
N(1)-C(9)-H(9)	105.8
C(14)-C(9)-H(9)	105.8
C(10)-C(9)-H(9)	105.8
C(11)-C(10)-C(9)	111.3(8)
C(11)-C(10)-H(10A)	109.4
C(9)-C(10)-H(10A)	109.4
C(11)-C(10)-H(10B)	109.4
C(9)-C(10)-H(10B)	109.4
H(10A)-C(10)-H(10B)	108.0
C(10)-C(11)-C(12)	112.1(8)
C(10)-C(11)-H(11A)	109.2
C(12)-C(11)-H(11A)	109.2
C(10)-C(11)-H(11B)	109.2
C(12)-C(11)-H(11B)	109.2
H(11A)-C(11)-H(11B)	107.9
C(13)-C(12)-C(11)	109.5(8)
C(13)-C(12)-H(12A)	109.8
C(11)-C(12)-H(12A)	109.8
C(13)-C(12)-H(12B)	109.8
C(11)-C(12)-H(12B)	109.8
H(12A)-C(12)-H(12B)	108.2
C(14)-C(13)-C(12)	113.3(8)
C(14)-C(13)-H(13A)	108.9
C(12)-C(13)-H(13A)	108.9
C(14)-C(13)-H(13B)	108.9
C(12)-C(13)-H(13B)	108.9
H(13A)-C(13)-H(13B)	107.7
C(13)-C(14)-C(9)	110.2(8)
C(13)-C(14)-H(14A)	109.6
C(9)-C(14)-H(14A)	109.6
C(13)-C(14)-H(14B)	109.6
C(9)-C(14)-H(14B)	109.6

H(14A)-C(14)-H(14B)	108.1
N(1)-C(15)-C(16)	114.2(8)
N(1)-C(15)-H(15A)	108.7
C(16)-C(15)-H(15A)	108.7
N(1)-C(15)-H(15B)	108.7
C(16)-C(15)-H(15B)	108.7
H(15A)-C(15)-H(15B)	107.6
C(15)-C(16)-P(2)	115.7(6)
C(15)-C(16)-H(16A)	108.4
P(2)-C(16)-H(16A)	108.4
C(15)-C(16)-H(16B)	108.4
P(2)-C(16)-H(16B)	108.4
H(16A)-C(16)-H(16B)	107.4
C(22)-C(17)-C(18)	118.1(9)
C(22)-C(17)-P(2)	118.9(7)
C(18)-C(17)-P(2)	123.0(8)
C(19)-C(18)-C(17)	120.9(9)
C(19)-C(18)-H(18)	119.6
C(17)-C(18)-H(18)	119.6
C(18)-C(19)-C(20)	120.8(9)
C(18)-C(19)-H(19)	119.6
C(20)-C(19)-H(19)	119.6
C(19)-C(20)-C(21)	118.6(9)
C(19)-C(20)-H(20)	120.7
C(21)-C(20)-H(20)	120.7
C(22)-C(21)-C(20)	120.8(9)
C(22)-C(21)-H(21)	119.6
C(20)-C(21)-H(21)	119.6
C(21)-C(22)-C(17)	120.8(9)
C(21)-C(22)-H(22)	119.6
C(17)-C(22)-H(22)	119.6
C(28)-C(23)-C(24)	119.4(8)
C(28)-C(23)-P(2)	118.4(7)
C(24)-C(23)-P(2)	121.9(7)
C(25)-C(24)-C(23)	119.8(9)
C(25)-C(24)-H(24)	120.1
C(23)-C(24)-H(24)	120.1
C(26)-C(25)-C(24)	120.7(9)

C(26)-C(25)-H(25)	119.7
C(24)-C(25)-H(25)	119.7
C(25)-C(26)-C(27)	120.1(10)
C(25)-C(26)-H(26)	120.0
C(27)-C(26)-H(26)	120.0
C(26)-C(27)-C(28)	119.9(10)
C(26)-C(27)-H(27)	120.0
C(28)-C(27)-H(27)	120.0
C(27)-C(28)-C(23)	120.1(9)
C(27)-C(28)-H(28)	119.9
C(23)-C(28)-H(28)	119.9
C(30)-C(29)-C(34)	118.4(8)
C(30)-C(29)-P(1)	121.8(7)
C(34)-C(29)-P(1)	119.4(7)
C(31)-C(30)-C(29)	120.0(9)
C(31)-C(30)-H(30)	120.0
C(29)-C(30)-H(30)	120.0
C(30)-C(31)-C(32)	121.6(9)
C(30)-C(31)-H(31)	119.2
C(32)-C(31)-H(31)	119.2
C(33)-C(32)-C(31)	119.2(9)
C(33)-C(32)-H(32)	120.4
C(31)-C(32)-H(32)	120.4
C(32)-C(33)-C(34)	120.5(10)
C(32)-C(33)-H(33)	119.8
C(34)-C(33)-H(33)	119.8
C(33)-C(34)-C(29)	120.3(9)
C(33)-C(34)-H(34)	119.8
C(29)-C(34)-H(34)	119.8
Cl(1)-Co(1)-Cl(2)	120.39(10)
Cl(1)-Co(1)-P(1)	106.15(10)
Cl(2)-Co(1)-P(1)	100.53(9)
Cl(1)-Co(1)-P(2)	110.99(10)
Cl(2)-Co(1)-P(2)	102.53(9)
P(1)-Co(1)-P(2)	116.42(9)
C(8)-N(1)-C(9)	112.6(7)
C(8)-N(1)-C(15)	109.7(7)
C(9)-N(1)-C(15)	111.6(7)

C(1)-P(1)-C(29)	104.8(4)
C(1)-P(1)-C(7)	107.3(4)
C(29)-P(1)-C(7)	104.6(4)
C(1)-P(1)-Co(1)	117.7(3)
C(29)-P(1)-Co(1)	108.3(3)
C(7)-P(1)-Co(1)	113.1(3)
C(23)-P(2)-C(16)	106.7(4)
C(23)-P(2)-C(17)	103.1(4)
C(16)-P(2)-C(17)	101.9(4)
C(23)-P(2)-Co(1)	120.5(3)
C(16)-P(2)-Co(1)	113.1(3)
C(17)-P(2)-Co(1)	109.6(3)

Symmetry transformations used to generate equivalent atoms:

Table A3. Anisotropic displacement parameters ($\text{\AA}^2 \times 10^3$) for **2a**. The anisotropic displacement factor exponent takes the form: $-2\pi^2 [h^2 a^{*2} U^{11} + \dots + 2 h k a^{*} b^{*} U^{12}]$

	U^{11}	U^{22}	U^{33}	U^{23}	U^{13}	U^{12}
C(1)	9(4)	13(5)	16(5)	-3(4)	6(3)	-3(3)
C(2)	22(5)	10(4)	17(5)	6(4)	5(4)	0(4)
C(3)	26(5)	20(5)	20(5)	-10(4)	-2(4)	-5(4)
C(4)	25(5)	12(5)	27(5)	-4(4)	9(4)	-1(4)
C(5)	19(5)	16(5)	31(6)	11(4)	8(4)	4(4)
C(6)	10(4)	18(5)	22(5)	3(4)	7(4)	-1(4)
C(7)	13(5)	16(5)	17(5)	-3(4)	3(4)	0(4)
C(8)	11(4)	15(5)	21(5)	-3(4)	7(4)	-3(4)
C(9)	15(5)	8(4)	24(5)	2(4)	4(4)	3(4)
C(10)	15(5)	21(5)	19(5)	-1(4)	1(4)	-1(4)
C(11)	21(5)	24(5)	25(5)	3(4)	3(4)	12(4)
C(12)	25(5)	17(5)	36(6)	-4(5)	9(4)	6(4)
C(13)	21(5)	21(5)	39(6)	-8(5)	9(5)	-2(4)
C(14)	14(5)	24(5)	38(6)	-10(5)	0(4)	3(4)
C(15)	15(5)	16(5)	22(5)	1(4)	7(4)	-1(4)
C(16)	7(4)	14(5)	29(5)	1(4)	-4(4)	-1(4)
C(17)	8(4)	25(5)	28(5)	7(4)	6(4)	10(4)
C(18)	18(5)	22(5)	21(5)	2(4)	6(4)	1(4)
C(19)	19(5)	30(6)	11(5)	0(4)	5(4)	1(4)
C(20)	11(4)	16(5)	27(5)	12(4)	5(4)	4(4)
C(21)	23(5)	15(5)	28(6)	1(4)	11(4)	0(4)
C(22)	13(5)	22(5)	16(5)	-4(4)	0(4)	-2(4)
C(23)	20(5)	9(4)	12(4)	-3(4)	3(4)	-3(4)
C(24)	19(5)	12(5)	23(5)	3(4)	5(4)	2(4)
C(25)	22(5)	15(5)	34(6)	-5(4)	17(4)	5(4)
C(26)	44(7)	18(5)	31(6)	-7(5)	14(5)	-5(5)
C(27)	23(5)	29(6)	31(6)	-11(5)	7(5)	-15(5)
C(28)	26(5)	23(5)	26(5)	-3(4)	13(4)	-5(4)
C(29)	12(4)	12(5)	17(5)	3(4)	5(4)	6(3)
C(30)	18(5)	17(5)	13(5)	-1(4)	-1(4)	0(4)
C(31)	16(5)	30(6)	19(5)	2(4)	7(4)	-1(4)
C(32)	25(5)	26(6)	22(5)	0(4)	11(4)	4(4)
C(33)	34(6)	26(6)	34(6)	-14(5)	18(5)	-3(5)

C(34)	32(6)	16(5)	29(6)	-6(4)	19(5)	-6(4)
Cl(1)	14(1)	24(1)	24(1)	-4(1)	1(1)	1(1)
Cl(2)	23(1)	12(1)	21(1)	-3(1)	5(1)	-2(1)
Co(1)	13(1)	10(1)	15(1)	-1(1)	3(1)	0(1)
N(1)	10(4)	13(4)	21(4)	-2(3)	3(3)	-1(3)
P(1)	13(1)	11(1)	15(1)	-1(1)	4(1)	0(1)
P(2)	13(1)	12(1)	16(1)	0(1)	3(1)	0(1)

Table A4. Hydrogen coordinates ($\times 10^4$) and isotropic displacement parameters ($\text{\AA}^2 \times 10^3$) for 13zs_hbf_dn4_0ma.

	x	y	z	U(eq)
H(2)	-3956	6727	-1394	19
H(3)	-4615	4789	-1647	28
H(4)	-3653	3123	-1210	25
H(5)	-2022	3424	-515	26
H(6)	-1415	5337	-241	20
H(7A)	-121	8318	-35	19
H(7B)	44	6971	-201	19
H(8A)	454	9117	-686	18
H(8B)	1665	8176	-462	18
H(9)	559	6018	-739	19
H(10A)	2959	6493	-1109	23
H(10B)	2949	6685	-584	23
H(11A)	2637	4632	-492	29
H(11B)	4002	4830	-690	29
H(12A)	2724	4283	-1428	31
H(12B)	2538	3237	-1082	31
H(13A)	314	3768	-1576	32
H(13B)	308	3975	-1053	32
H(14A)	-765	5625	-1483	31
H(14B)	610	5838	-1676	31
H(15A)	1063	7745	-1642	20
H(15B)	2034	8474	-1226	20
H(16A)	628	9729	-1822	22
H(16B)	495	10057	-1319	22
H(18)	-2758	9959	-2726	25
H(19)	-3334	11739	-3124	23
H(20)	-3114	13580	-2738	22
H(21)	-2201	13605	-1941	25
H(22)	-1679	11823	-1537	21
H(24)	-188	8254	-2391	22
H(25)	-818	6837	-2977	26
H(26)	-3038	5950	-3139	36

H(27)	-4643	6422	-2701	33
H(28)	-4000	7781	-2093	28
H(30)	-4498	6639	-315	20
H(31)	-5752	7100	219	26
H(32)	-5120	8733	713	28
H(33)	-3223	9930	660	35
H(34)	-1932	9499	124	28

Table A5. Torsion angles [°] for **2a**.

C(6)-C(1)-C(2)-C(3)	-1.3(13)
P(1)-C(1)-C(2)-C(3)	-178.0(7)
C(1)-C(2)-C(3)-C(4)	-0.2(15)
C(2)-C(3)-C(4)-C(5)	0.3(15)
C(3)-C(4)-C(5)-C(6)	1.1(15)
C(4)-C(5)-C(6)-C(1)	-2.6(14)
C(2)-C(1)-C(6)-C(5)	2.6(13)
P(1)-C(1)-C(6)-C(5)	179.2(7)
P(1)-C(7)-C(8)-N(1)	-53.1(9)
N(1)-C(9)-C(10)-C(11)	174.1(8)
C(14)-C(9)-C(10)-C(11)	-56.4(11)
C(9)-C(10)-C(11)-C(12)	56.2(11)
C(10)-C(11)-C(12)-C(13)	-54.6(12)
C(11)-C(12)-C(13)-C(14)	55.4(12)
C(12)-C(13)-C(14)-C(9)	-57.2(12)
N(1)-C(9)-C(14)-C(13)	-173.5(8)
C(10)-C(9)-C(14)-C(13)	55.8(11)
N(1)-C(15)-C(16)-P(2)	-46.1(10)
C(22)-C(17)-C(18)-C(19)	1.4(13)
P(2)-C(17)-C(18)-C(19)	179.0(7)
C(17)-C(18)-C(19)-C(20)	-0.9(14)
C(18)-C(19)-C(20)-C(21)	1.1(13)
C(19)-C(20)-C(21)-C(22)	-2.0(14)
C(20)-C(21)-C(22)-C(17)	2.7(14)
C(18)-C(17)-C(22)-C(21)	-2.4(13)
P(2)-C(17)-C(22)-C(21)	180.0(7)
C(28)-C(23)-C(24)-C(25)	-0.9(14)
P(2)-C(23)-C(24)-C(25)	-174.6(7)
C(23)-C(24)-C(25)-C(26)	1.7(15)
C(24)-C(25)-C(26)-C(27)	-1.0(16)
C(25)-C(26)-C(27)-C(28)	-0.4(17)
C(26)-C(27)-C(28)-C(23)	1.1(16)
C(24)-C(23)-C(28)-C(27)	-0.4(15)
P(2)-C(23)-C(28)-C(27)	173.4(8)
C(34)-C(29)-C(30)-C(31)	-0.8(14)
P(1)-C(29)-C(30)-C(31)	-174.1(7)

C(29)-C(30)-C(31)-C(32)	0.1(15)
C(30)-C(31)-C(32)-C(33)	0.6(16)
C(31)-C(32)-C(33)-C(34)	-0.5(16)
C(32)-C(33)-C(34)-C(29)	-0.3(17)
C(30)-C(29)-C(34)-C(33)	0.9(15)
P(1)-C(29)-C(34)-C(33)	174.3(8)
C(7)-C(8)-N(1)-C(9)	-68.7(9)
C(7)-C(8)-N(1)-C(15)	166.3(7)
C(14)-C(9)-N(1)-C(8)	162.3(8)
C(10)-C(9)-N(1)-C(8)	-69.8(10)
C(14)-C(9)-N(1)-C(15)	-73.7(10)
C(10)-C(9)-N(1)-C(15)	54.2(10)
C(16)-C(15)-N(1)-C(8)	-71.4(10)
C(16)-C(15)-N(1)-C(9)	163.0(7)
C(2)-C(1)-P(1)-C(29)	105.2(7)
C(6)-C(1)-P(1)-C(29)	-71.3(8)
C(2)-C(1)-P(1)-C(7)	-143.9(7)
C(6)-C(1)-P(1)-C(7)	39.5(8)
C(2)-C(1)-P(1)-Co(1)	-15.1(8)
C(6)-C(1)-P(1)-Co(1)	168.3(6)
C(30)-C(29)-P(1)-C(1)	-21.2(9)
C(34)-C(29)-P(1)-C(1)	165.6(8)
C(30)-C(29)-P(1)-C(7)	-133.9(8)
C(34)-C(29)-P(1)-C(7)	52.9(8)
C(30)-C(29)-P(1)-Co(1)	105.2(7)
C(34)-C(29)-P(1)-Co(1)	-68.0(8)
C(8)-C(7)-P(1)-C(1)	98.5(7)
C(8)-C(7)-P(1)-C(29)	-150.6(6)
C(8)-C(7)-P(1)-Co(1)	-32.9(7)
Cl(1)-Co(1)-P(1)-C(1)	59.3(3)
Cl(2)-Co(1)-P(1)-C(1)	-174.6(3)
P(2)-Co(1)-P(1)-C(1)	-64.8(3)
Cl(1)-Co(1)-P(1)-C(29)	-59.2(3)
Cl(2)-Co(1)-P(1)-C(29)	66.9(3)
P(2)-Co(1)-P(1)-C(29)	176.7(3)
Cl(1)-Co(1)-P(1)-C(7)	-174.7(3)
Cl(2)-Co(1)-P(1)-C(7)	-48.6(3)
P(2)-Co(1)-P(1)-C(7)	61.2(3)

C(28)-C(23)-P(2)-C(16)	159.1(8)
C(24)-C(23)-P(2)-C(16)	-27.2(9)
C(28)-C(23)-P(2)-C(17)	-94.0(8)
C(24)-C(23)-P(2)-C(17)	79.7(8)
C(28)-C(23)-P(2)-Co(1)	28.4(9)
C(24)-C(23)-P(2)-Co(1)	-157.9(6)
C(15)-C(16)-P(2)-C(23)	-56.3(8)
C(15)-C(16)-P(2)-C(17)	-164.0(7)
C(15)-C(16)-P(2)-Co(1)	78.4(7)
C(22)-C(17)-P(2)-C(23)	178.3(7)
C(18)-C(17)-P(2)-C(23)	0.8(8)
C(22)-C(17)-P(2)-C(16)	-71.2(8)
C(18)-C(17)-P(2)-C(16)	111.3(8)
C(22)-C(17)-P(2)-Co(1)	48.8(8)
C(18)-C(17)-P(2)-Co(1)	-128.7(7)
Cl(1)-Co(1)-P(2)-C(23)	-53.2(4)
Cl(2)-Co(1)-P(2)-C(23)	177.0(4)
P(1)-Co(1)-P(2)-C(23)	68.3(4)
Cl(1)-Co(1)-P(2)-C(16)	179.0(3)
Cl(2)-Co(1)-P(2)-C(16)	49.2(3)
P(1)-Co(1)-P(2)-C(16)	-59.5(4)
Cl(1)-Co(1)-P(2)-C(17)	66.0(4)
Cl(2)-Co(1)-P(2)-C(17)	-63.8(4)
P(1)-Co(1)-P(2)-C(17)	-172.4(3)

Symmetry transformations used to generate equivalent atoms:

Data for crystal structure **2c**

Table A6. Atomic coordinates ($\times 10^4$) and equivalent isotropic displacement parameters ($\text{\AA}^2 \times 10^3$) for **2c**. $U(\text{eq})$ is defined as one third of the trace of the orthogonalized U^{ij} tensor.

	x	y	z	$U(\text{eq})$
C(1)	-2520(2)	3349(1)	2545(1)	19(1)
C(2)	-2425(2)	2948(1)	1833(1)	18(1)
C(3)	-875(2)	2443(1)	957(1)	21(1)
C(4)	-2053(2)	1857(1)	657(1)	28(1)
C(5)	-859(2)	3186(1)	503(1)	31(1)
C(6)	-503(2)	2007(1)	2191(1)	19(1)
C(7)	1145(2)	1826(1)	2234(1)	20(1)
C(8)	3001(2)	3057(1)	1627(1)	18(1)
C(9)	3540(2)	3831(1)	1625(1)	21(1)
C(10)	4190(2)	4119(1)	1048(1)	27(1)
C(11)	4325(2)	3634(1)	471(1)	30(1)
C(12)	3778(2)	2873(1)	463(1)	30(1)
C(13)	3120(2)	2582(1)	1036(1)	24(1)
C(14)	3979(2)	2258(1)	2884(1)	17(1)
C(15)	4554(2)	2561(1)	3533(1)	20(1)
C(16)	5818(2)	2233(1)	3877(1)	25(1)
C(17)	6510(2)	1605(1)	3579(1)	28(1)
C(18)	5953(2)	1300(1)	2934(1)	26(1)
C(19)	4695(2)	1628(1)	2587(1)	22(1)
C(20)	-1832(2)	4669(1)	3483(1)	17(1)
C(21)	-3303(2)	4675(1)	3619(1)	29(1)
C(22)	-3753(2)	5103(1)	4185(1)	33(1)
C(23)	-2750(2)	5525(1)	4622(1)	25(1)
C(24)	-1288(2)	5532(1)	4487(1)	22(1)
C(25)	-835(2)	5106(1)	3924(1)	20(1)
C(26)	-1250(2)	4760(1)	2009(1)	16(1)
C(27)	-2572(2)	5123(1)	1779(1)	21(1)
C(28)	-2668(2)	5608(1)	1190(1)	24(1)
C(29)	-1452(2)	5727(1)	819(1)	26(1)
C(30)	-135(2)	5363(1)	1042(1)	27(1)
C(31)	-30(2)	4886(1)	1638(1)	23(1)

N(1)	-952(2)	2660(1)	1710(1)	17(1)
P(1)	-1114(1)	4103(1)	2769(1)	15(1)
P(2)	2309(1)	2697(1)	2438(1)	15(1)
Cl(1)	2763(1)	4672(1)	3317(1)	23(1)
Cl(2)	810(1)	2921(1)	4110(1)	26(1)
Co(1)	1247(1)	3631(1)	3171(1)	15(1)

Table A7. Bond lengths [Å] and angles [°] for **2c**.

C(1)-C(2)	1.524(2)
C(1)-P(1)	1.8287(17)
C(1)-H(1A)	0.9900
C(1)-H(1B)	0.9900
C(2)-N(1)	1.470(2)
C(2)-H(2A)	0.9900
C(2)-H(2B)	0.9900
C(3)-N(1)	1.489(2)
C(3)-C(5)	1.520(3)
C(3)-C(4)	1.533(2)
C(3)-H(3)	1.0000
C(4)-H(4A)	0.9800
C(4)-H(4B)	0.9800
C(4)-H(4C)	0.9800
C(5)-H(5A)	0.9800
C(5)-H(5B)	0.9800
C(5)-H(5C)	0.9800
C(6)-N(1)	1.465(2)
C(6)-C(7)	1.533(2)
C(6)-H(6A)	0.9900
C(6)-H(6B)	0.9900
C(7)-P(2)	1.8317(17)
C(7)-H(7A)	0.9900
C(7)-H(7B)	0.9900
C(8)-C(9)	1.393(2)
C(8)-C(13)	1.393(2)
C(8)-P(2)	1.8256(17)

C(9)-C(10)	1.384(3)
C(9)-H(9)	0.9500
C(10)-C(11)	1.382(3)
C(10)-H(10)	0.9500
C(11)-C(12)	1.376(3)
C(11)-H(11)	0.9500
C(12)-C(13)	1.383(3)
C(12)-H(12)	0.9500
C(13)-H(13)	0.9500
C(14)-C(19)	1.393(2)
C(14)-C(15)	1.395(2)
C(14)-P(2)	1.8337(17)
C(15)-C(16)	1.391(2)
C(15)-H(15)	0.9500
C(16)-C(17)	1.379(3)
C(16)-H(16)	0.9500
C(17)-C(18)	1.385(3)
C(17)-H(17)	0.9500
C(18)-C(19)	1.390(3)
C(18)-H(18)	0.9500
C(19)-H(19)	0.9500
C(20)-C(21)	1.392(2)
C(20)-C(25)	1.393(2)
C(20)-P(1)	1.8307(17)
C(21)-C(22)	1.389(3)
C(21)-H(21)	0.9500
C(22)-C(23)	1.379(3)
C(22)-H(22)	0.9500
C(23)-C(24)	1.383(3)
C(23)-H(23)	0.9500
C(24)-C(25)	1.384(2)
C(24)-H(24)	0.9500
C(25)-H(25)	0.9500
C(26)-C(31)	1.389(2)
C(26)-C(27)	1.390(2)
C(26)-P(1)	1.8180(17)
C(27)-C(28)	1.383(2)
C(27)-H(27)	0.9500

C(28)-C(29)	1.384(3)
C(28)-H(28)	0.9500
C(29)-C(30)	1.384(3)
C(29)-H(29)	0.9500
C(30)-C(31)	1.386(3)
C(30)-H(30)	0.9500
C(31)-H(31)	0.9500
P(1)-Co(1)	2.3618(5)
P(2)-Co(1)	2.3684(5)
Cl(1)-Co(1)	2.2363(5)
Cl(2)-Co(1)	2.2169(5)
C(2)-C(1)-P(1)	114.84(11)
C(2)-C(1)-H(1A)	108.6
P(1)-C(1)-H(1A)	108.6
C(2)-C(1)-H(1B)	108.6
P(1)-C(1)-H(1B)	108.6
H(1A)-C(1)-H(1B)	107.5
N(1)-C(2)-C(1)	114.47(13)
N(1)-C(2)-H(2A)	108.6
C(1)-C(2)-H(2A)	108.6
N(1)-C(2)-H(2B)	108.6
C(1)-C(2)-H(2B)	108.6
H(2A)-C(2)-H(2B)	107.6
N(1)-C(3)-C(5)	110.48(14)
N(1)-C(3)-C(4)	115.12(14)
C(5)-C(3)-C(4)	111.07(15)
N(1)-C(3)-H(3)	106.5
C(5)-C(3)-H(3)	106.5
C(4)-C(3)-H(3)	106.5
C(3)-C(4)-H(4A)	109.5
C(3)-C(4)-H(4B)	109.5
H(4A)-C(4)-H(4B)	109.5
C(3)-C(4)-H(4C)	109.5
H(4A)-C(4)-H(4C)	109.5
H(4B)-C(4)-H(4C)	109.5
C(3)-C(5)-H(5A)	109.5
C(3)-C(5)-H(5B)	109.5

H(5A)-C(5)-H(5B)	109.5
C(3)-C(5)-H(5C)	109.5
H(5A)-C(5)-H(5C)	109.5
H(5B)-C(5)-H(5C)	109.5
N(1)-C(6)-C(7)	113.63(14)
N(1)-C(6)-H(6A)	108.8
C(7)-C(6)-H(6A)	108.8
N(1)-C(6)-H(6B)	108.8
C(7)-C(6)-H(6B)	108.8
H(6A)-C(6)-H(6B)	107.7
C(6)-C(7)-P(2)	113.72(12)
C(6)-C(7)-H(7A)	108.8
P(2)-C(7)-H(7A)	108.8
C(6)-C(7)-H(7B)	108.8
P(2)-C(7)-H(7B)	108.8
H(7A)-C(7)-H(7B)	107.7
C(9)-C(8)-C(13)	118.74(16)
C(9)-C(8)-P(2)	117.61(13)
C(13)-C(8)-P(2)	123.46(14)
C(10)-C(9)-C(8)	120.52(17)
C(10)-C(9)-H(9)	119.7
C(8)-C(9)-H(9)	119.7
C(11)-C(10)-C(9)	119.97(18)
C(11)-C(10)-H(10)	120.0
C(9)-C(10)-H(10)	120.0
C(12)-C(11)-C(10)	120.06(17)
C(12)-C(11)-H(11)	120.0
C(10)-C(11)-H(11)	120.0
C(11)-C(12)-C(13)	120.25(18)
C(11)-C(12)-H(12)	119.9
C(13)-C(12)-H(12)	119.9
C(12)-C(13)-C(8)	120.44(18)
C(12)-C(13)-H(13)	119.8
C(8)-C(13)-H(13)	119.8
C(19)-C(14)-C(15)	119.00(16)
C(19)-C(14)-P(2)	121.33(13)
C(15)-C(14)-P(2)	119.67(13)
C(16)-C(15)-C(14)	120.23(17)

C(16)-C(15)-H(15)	119.9
C(14)-C(15)-H(15)	119.9
C(17)-C(16)-C(15)	120.19(17)
C(17)-C(16)-H(16)	119.9
C(15)-C(16)-H(16)	119.9
C(16)-C(17)-C(18)	120.22(17)
C(16)-C(17)-H(17)	119.9
C(18)-C(17)-H(17)	119.9
C(17)-C(18)-C(19)	119.83(17)
C(17)-C(18)-H(18)	120.1
C(19)-C(18)-H(18)	120.1
C(18)-C(19)-C(14)	120.53(17)
C(18)-C(19)-H(19)	119.7
C(14)-C(19)-H(19)	119.7
C(21)-C(20)-C(25)	118.34(16)
C(21)-C(20)-P(1)	123.98(13)
C(25)-C(20)-P(1)	117.67(13)
C(22)-C(21)-C(20)	120.43(17)
C(22)-C(21)-H(21)	119.8
C(20)-C(21)-H(21)	119.8
C(23)-C(22)-C(21)	120.56(18)
C(23)-C(22)-H(22)	119.7
C(21)-C(22)-H(22)	119.7
C(22)-C(23)-C(24)	119.56(17)
C(22)-C(23)-H(23)	120.2
C(24)-C(23)-H(23)	120.2
C(23)-C(24)-C(25)	120.05(17)
C(23)-C(24)-H(24)	120.0
C(25)-C(24)-H(24)	120.0
C(24)-C(25)-C(20)	121.06(16)
C(24)-C(25)-H(25)	119.5
C(20)-C(25)-H(25)	119.5
C(31)-C(26)-C(27)	119.20(16)
C(31)-C(26)-P(1)	119.79(13)
C(27)-C(26)-P(1)	120.99(13)
C(28)-C(27)-C(26)	120.35(17)
C(28)-C(27)-H(27)	119.8
C(26)-C(27)-H(27)	119.8

C(27)-C(28)-C(29)	120.27(17)
C(27)-C(28)-H(28)	119.9
C(29)-C(28)-H(28)	119.9
C(30)-C(29)-C(28)	119.72(17)
C(30)-C(29)-H(29)	120.1
C(28)-C(29)-H(29)	120.1
C(29)-C(30)-C(31)	120.14(17)
C(29)-C(30)-H(30)	119.9
C(31)-C(30)-H(30)	119.9
C(30)-C(31)-C(26)	120.32(17)
C(30)-C(31)-H(31)	119.8
C(26)-C(31)-H(31)	119.8
C(6)-N(1)-C(2)	110.89(13)
C(6)-N(1)-C(3)	112.59(13)
C(2)-N(1)-C(3)	110.97(13)
C(26)-P(1)-C(1)	103.88(8)
C(26)-P(1)-C(20)	105.71(7)
C(1)-P(1)-C(20)	104.05(8)
C(26)-P(1)-Co(1)	117.28(6)
C(1)-P(1)-Co(1)	116.45(6)
C(20)-P(1)-Co(1)	108.22(6)
C(8)-P(2)-C(7)	108.96(8)
C(8)-P(2)-C(14)	100.86(7)
C(7)-P(2)-C(14)	102.71(8)
C(8)-P(2)-Co(1)	118.02(6)
C(7)-P(2)-Co(1)	113.28(6)
C(14)-P(2)-Co(1)	111.27(6)
Cl(2)-Co(1)-Cl(1)	118.501(19)
Cl(2)-Co(1)-P(1)	102.530(18)
Cl(1)-Co(1)-P(1)	108.346(18)
Cl(2)-Co(1)-P(2)	103.357(18)
Cl(1)-Co(1)-P(2)	108.116(18)
P(1)-Co(1)-P(2)	116.322(17)

Symmetry transformations used to generate equivalent atoms:

Table A8. Anisotropic displacement parameters ($\text{\AA}^2 \times 10^3$) for **2c**. The anisotropic displacement factor exponent takes the form: $-2\pi^2 [h^2 a^{*2} U^{11} + \dots + 2 h k a^{*} b^{*} U^{12}]$

	U^{11}	U^{22}	U^{33}	U^{23}	U^{13}	U^{12}
C(1)	16(1)	18(1)	22(1)	0(1)	4(1)	0(1)
C(2)	15(1)	19(1)	21(1)	-2(1)	1(1)	-1(1)
C(3)	22(1)	23(1)	18(1)	-3(1)	3(1)	3(1)
C(4)	29(1)	30(1)	22(1)	-5(1)	-4(1)	1(1)
C(5)	43(1)	30(1)	20(1)	1(1)	9(1)	3(1)
C(6)	19(1)	18(1)	19(1)	1(1)	1(1)	-3(1)
C(7)	20(1)	16(1)	22(1)	-1(1)	0(1)	0(1)
C(8)	13(1)	24(1)	16(1)	1(1)	1(1)	3(1)
C(9)	18(1)	25(1)	20(1)	1(1)	0(1)	2(1)
C(10)	23(1)	33(1)	26(1)	10(1)	0(1)	-3(1)
C(11)	22(1)	52(1)	17(1)	10(1)	2(1)	-1(1)
C(12)	25(1)	50(1)	17(1)	-7(1)	2(1)	1(1)
C(13)	22(1)	31(1)	21(1)	-4(1)	2(1)	-1(1)
C(14)	14(1)	19(1)	19(1)	3(1)	4(1)	-2(1)
C(15)	18(1)	24(1)	19(1)	2(1)	4(1)	0(1)
C(16)	21(1)	35(1)	20(1)	5(1)	-1(1)	-4(1)
C(17)	17(1)	34(1)	32(1)	14(1)	2(1)	4(1)
C(18)	21(1)	22(1)	35(1)	6(1)	10(1)	5(1)
C(19)	21(1)	22(1)	22(1)	1(1)	6(1)	-1(1)
C(20)	20(1)	17(1)	16(1)	2(1)	2(1)	3(1)
C(21)	21(1)	40(1)	26(1)	-12(1)	2(1)	-2(1)
C(22)	21(1)	49(1)	31(1)	-12(1)	10(1)	0(1)
C(23)	31(1)	27(1)	18(1)	-5(1)	6(1)	4(1)
C(24)	27(1)	18(1)	20(1)	-1(1)	-2(1)	1(1)
C(25)	18(1)	18(1)	23(1)	1(1)	2(1)	2(1)
C(26)	21(1)	14(1)	15(1)	-2(1)	0(1)	-2(1)
C(27)	21(1)	22(1)	19(1)	-2(1)	2(1)	2(1)
C(28)	27(1)	22(1)	23(1)	2(1)	-4(1)	4(1)
C(29)	35(1)	21(1)	20(1)	5(1)	-3(1)	-5(1)
C(30)	25(1)	31(1)	25(1)	5(1)	5(1)	-9(1)
C(31)	18(1)	26(1)	26(1)	3(1)	1(1)	-1(1)
N(1)	16(1)	17(1)	17(1)	-1(1)	2(1)	1(1)
P(1)	14(1)	16(1)	15(1)	0(1)	2(1)	0(1)

P(2)	15(1)	16(1)	15(1)	-1(1)	1(1)	0(1)
Cl(1)	20(1)	24(1)	26(1)	-6(1)	3(1)	-5(1)
Cl(2)	35(1)	25(1)	20(1)	5(1)	8(1)	3(1)
Co(1)	15(1)	16(1)	14(1)	0(1)	1(1)	0(1)

Table A9. Hydrogen coordinates ($\times 10^4$) and isotropic displacement parameters ($\text{\AA}^2 \times 10^3$) for **2c**

	x	y	z	U(eq)
H(1A)	-2445	2936	2916	22
H(1B)	-3498	3601	2548	22
H(2A)	-3114	2493	1796	22
H(2B)	-2752	3330	1456	22
H(3)	93	2175	927	25
H(4A)	-2058	1391	964	41
H(4B)	-1838	1692	184	41
H(4C)	-3018	2115	630	41
H(5A)	-1808	3457	500	46
H(5B)	-683	3037	21	46
H(5C)	-76	3542	697	46
H(6A)	-1053	1523	2034	22
H(6B)	-774	2142	2668	22
H(7A)	1384	1602	1778	23
H(7B)	1377	1418	2601	23
H(9)	3461	4163	2023	25
H(10)	4544	4650	1047	33
H(11)	4795	3827	80	36
H(12)	3853	2545	62	36
H(13)	2746	2055	1027	29
H(15)	4081	2993	3740	24
H(16)	6206	2442	4318	30
H(17)	7371	1382	3817	33
H(18)	6431	867	2731	31
H(19)	4320	1422	2142	26

H(21)	-4003	4385	3322	35
H(22)	-4760	5104	4271	40
H(23)	-3061	5809	5013	30
H(24)	-595	5830	4781	26
H(25)	172	5112	3837	24
H(27)	-3414	5038	2027	25
H(28)	-3572	5860	1039	29
H(29)	-1522	6058	413	31
H(30)	699	5439	787	32
H(31)	880	4644	1794	28

Table A10. Torsion angles [°] for **2c**.

P(1)-C(1)-C(2)-N(1)	48.87(18)
N(1)-C(6)-C(7)-P(2)	53.12(17)
C(13)-C(8)-C(9)-C(10)	-0.4(3)
P(2)-C(8)-C(9)-C(10)	174.70(13)
C(8)-C(9)-C(10)-C(11)	-0.8(3)
C(9)-C(10)-C(11)-C(12)	1.7(3)
C(10)-C(11)-C(12)-C(13)	-1.4(3)
C(11)-C(12)-C(13)-C(8)	0.1(3)
C(9)-C(8)-C(13)-C(12)	0.8(3)
P(2)-C(8)-C(13)-C(12)	-174.02(14)
C(19)-C(14)-C(15)-C(16)	-0.4(2)
P(2)-C(14)-C(15)-C(16)	179.91(13)
C(14)-C(15)-C(16)-C(17)	-0.1(3)
C(15)-C(16)-C(17)-C(18)	0.3(3)
C(16)-C(17)-C(18)-C(19)	0.1(3)
C(17)-C(18)-C(19)-C(14)	-0.6(3)
C(15)-C(14)-C(19)-C(18)	0.8(3)
P(2)-C(14)-C(19)-C(18)	-179.56(13)
C(25)-C(20)-C(21)-C(22)	-0.5(3)
P(1)-C(20)-C(21)-C(22)	178.07(16)
C(20)-C(21)-C(22)-C(23)	-0.2(3)
C(21)-C(22)-C(23)-C(24)	1.0(3)
C(22)-C(23)-C(24)-C(25)	-1.1(3)
C(23)-C(24)-C(25)-C(20)	0.4(3)

C(21)-C(20)-C(25)-C(24)	0.4(3)
P(1)-C(20)-C(25)-C(24)	-178.24(13)
C(31)-C(26)-C(27)-C(28)	-0.4(3)
P(1)-C(26)-C(27)-C(28)	-178.50(13)
C(26)-C(27)-C(28)-C(29)	0.9(3)
C(27)-C(28)-C(29)-C(30)	-0.4(3)
C(28)-C(29)-C(30)-C(31)	-0.6(3)
C(29)-C(30)-C(31)-C(26)	1.0(3)
C(27)-C(26)-C(31)-C(30)	-0.5(3)
P(1)-C(26)-C(31)-C(30)	177.59(14)
C(7)-C(6)-N(1)-C(2)	-164.53(14)
C(7)-C(6)-N(1)-C(3)	70.47(18)
C(1)-C(2)-N(1)-C(6)	66.73(18)
C(1)-C(2)-N(1)-C(3)	-167.35(14)
C(5)-C(3)-N(1)-C(6)	-161.65(14)
C(4)-C(3)-N(1)-C(6)	71.55(18)
C(5)-C(3)-N(1)-C(2)	73.38(18)
C(4)-C(3)-N(1)-C(2)	-53.42(19)
C(31)-C(26)-P(1)-C(1)	-122.09(14)
C(27)-C(26)-P(1)-C(1)	55.98(15)
C(31)-C(26)-P(1)-C(20)	128.68(14)
C(27)-C(26)-P(1)-C(20)	-53.25(15)
C(31)-C(26)-P(1)-Co(1)	7.99(16)
C(27)-C(26)-P(1)-Co(1)	-173.94(12)
C(2)-C(1)-P(1)-C(26)	52.73(14)
C(2)-C(1)-P(1)-C(20)	163.18(12)
C(2)-C(1)-P(1)-Co(1)	-77.84(13)
C(21)-C(20)-P(1)-C(26)	89.56(17)
C(25)-C(20)-P(1)-C(26)	-91.84(14)
C(21)-C(20)-P(1)-C(1)	-19.55(18)
C(25)-C(20)-P(1)-C(1)	159.05(13)
C(21)-C(20)-P(1)-Co(1)	-144.01(15)
C(25)-C(20)-P(1)-Co(1)	34.59(14)
C(9)-C(8)-P(2)-C(7)	161.70(13)
C(13)-C(8)-P(2)-C(7)	-23.42(17)
C(9)-C(8)-P(2)-C(14)	-90.67(14)
C(13)-C(8)-P(2)-C(14)	84.21(15)
C(9)-C(8)-P(2)-Co(1)	30.69(15)

C(13)-C(8)-P(2)-Co(1)	-154.43(13)
C(6)-C(7)-P(2)-C(8)	-101.48(13)
C(6)-C(7)-P(2)-C(14)	152.16(12)
C(6)-C(7)-P(2)-Co(1)	32.04(14)
C(19)-C(14)-P(2)-C(8)	-61.46(15)
C(15)-C(14)-P(2)-C(8)	118.20(14)
C(19)-C(14)-P(2)-C(7)	51.02(15)
C(15)-C(14)-P(2)-C(7)	-129.32(14)
C(19)-C(14)-P(2)-Co(1)	172.52(12)
C(15)-C(14)-P(2)-Co(1)	-7.82(15)
C(26)-P(1)-Co(1)-Cl(2)	177.51(6)
C(1)-P(1)-Co(1)-Cl(2)	-58.56(6)
C(20)-P(1)-Co(1)-Cl(2)	58.14(6)
C(26)-P(1)-Co(1)-Cl(1)	51.45(6)
C(1)-P(1)-Co(1)-Cl(1)	175.38(6)
C(20)-P(1)-Co(1)-Cl(1)	-67.92(6)
C(26)-P(1)-Co(1)-P(2)	-70.53(6)
C(1)-P(1)-Co(1)-P(2)	53.41(6)
C(20)-P(1)-Co(1)-P(2)	170.10(6)
C(8)-P(2)-Co(1)-Cl(2)	-174.54(6)
C(7)-P(2)-Co(1)-Cl(2)	56.44(6)
C(14)-P(2)-Co(1)-Cl(2)	-58.68(6)
C(8)-P(2)-Co(1)-Cl(1)	-48.12(6)
C(7)-P(2)-Co(1)-Cl(1)	-177.14(6)
C(14)-P(2)-Co(1)-Cl(1)	67.74(6)
C(8)-P(2)-Co(1)-P(1)	73.97(6)
C(7)-P(2)-Co(1)-P(1)	-55.04(6)
C(14)-P(2)-Co(1)-P(1)	-170.17(6)

Symmetry transformations used to generate equivalent atoms:

Appendix B

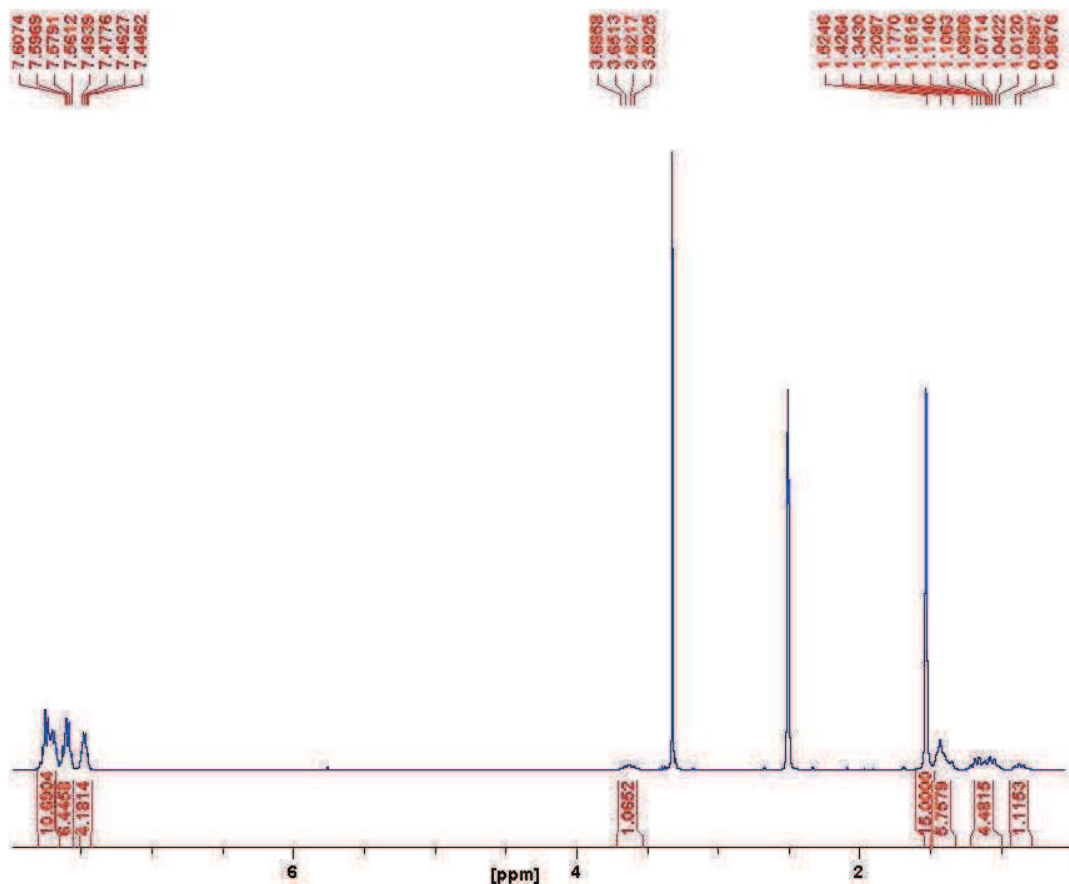


Figure B1. ^1H NMR of $[\text{Ph}_2\text{PN}(\text{C}_6\text{H}_{11})\text{PPh}_2]\text{IrCp}^*(\text{Cl})^+\text{PF}_6^-$ (**1a**).

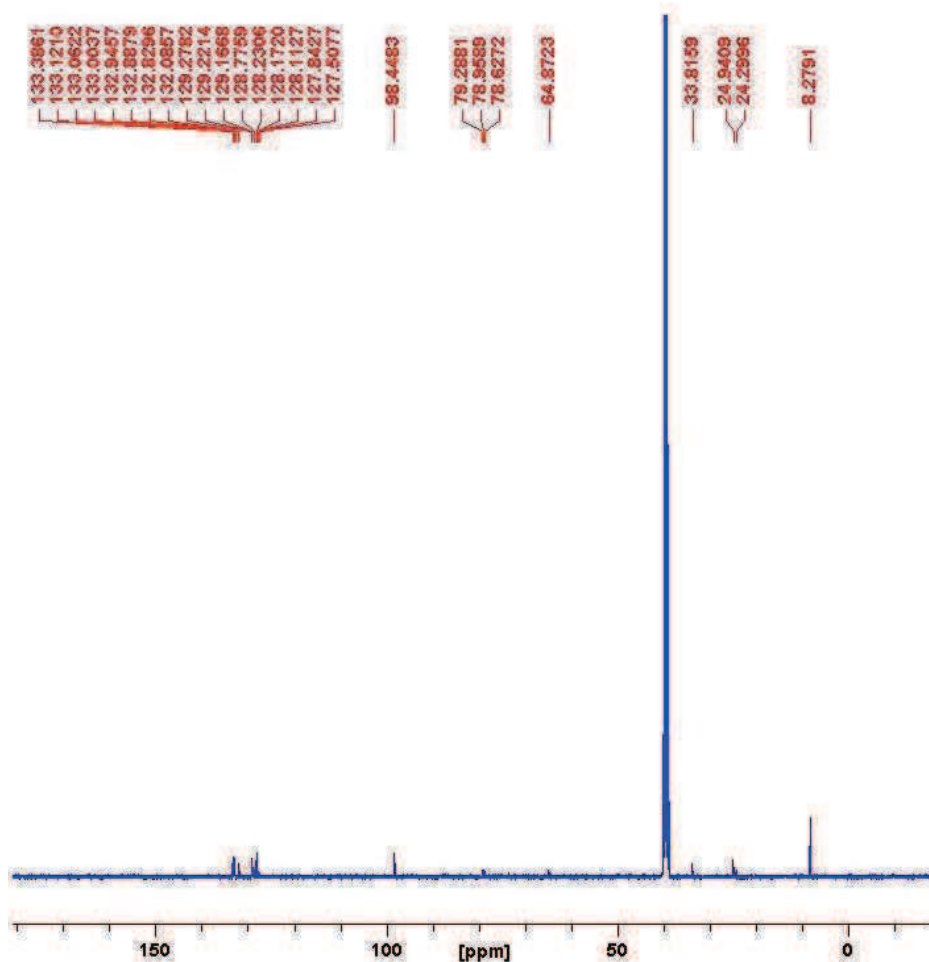


Figure B2. ¹³C NMR of $[\text{Ph}_2\text{PN}(\text{C}_6\text{H}_{11})\text{PPh}_2]\text{IrCp}^*(\text{Cl})^+\text{PF}_6^-$ (**1a**).

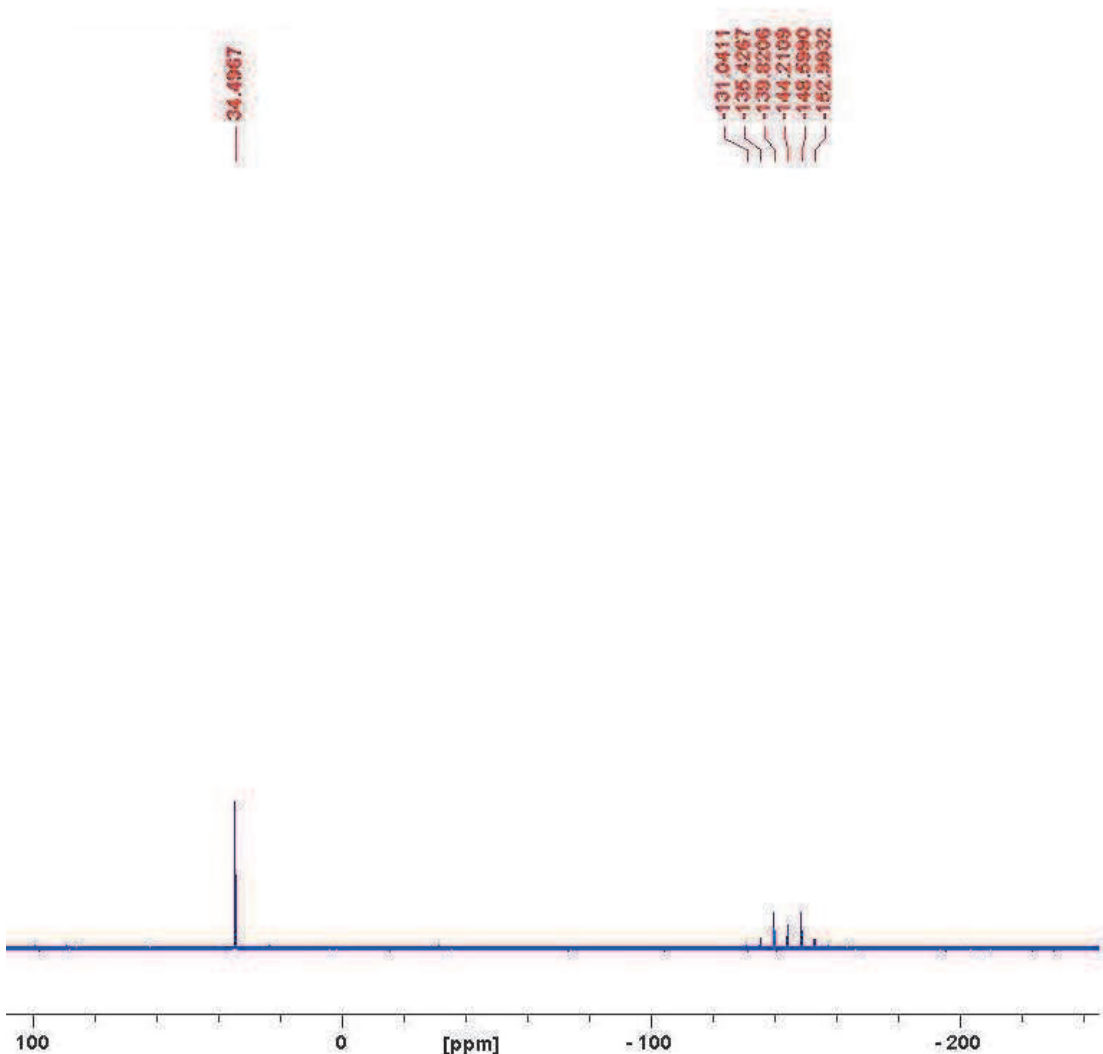


Figure B3. ^{31}P NMR of $[\text{Ph}_2\text{PN}(\text{C}_6\text{H}_{11})\text{PPh}_2]\text{IrCp}^*(\text{Cl})]^+\text{PF}_6^-$ (**1a**).

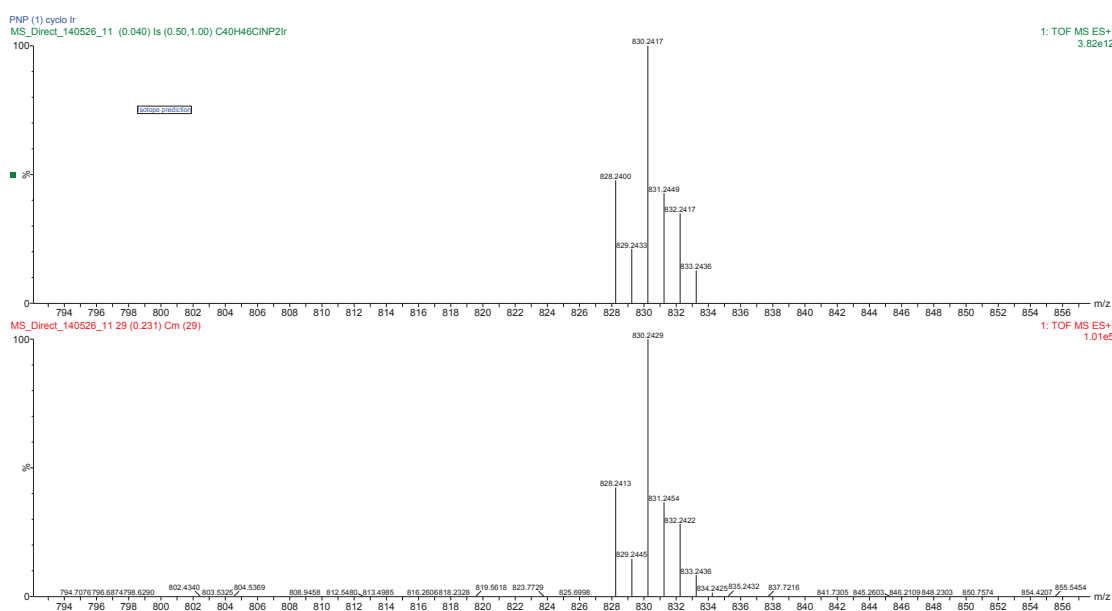


Figure B4. HRMS of $[\text{Ph}_2\text{PN}(\text{C}_6\text{H}_{11})\text{PPh}_2]\text{IrCp}^*(\text{Cl})]^+\text{PF}_6^-$ (**1a**).

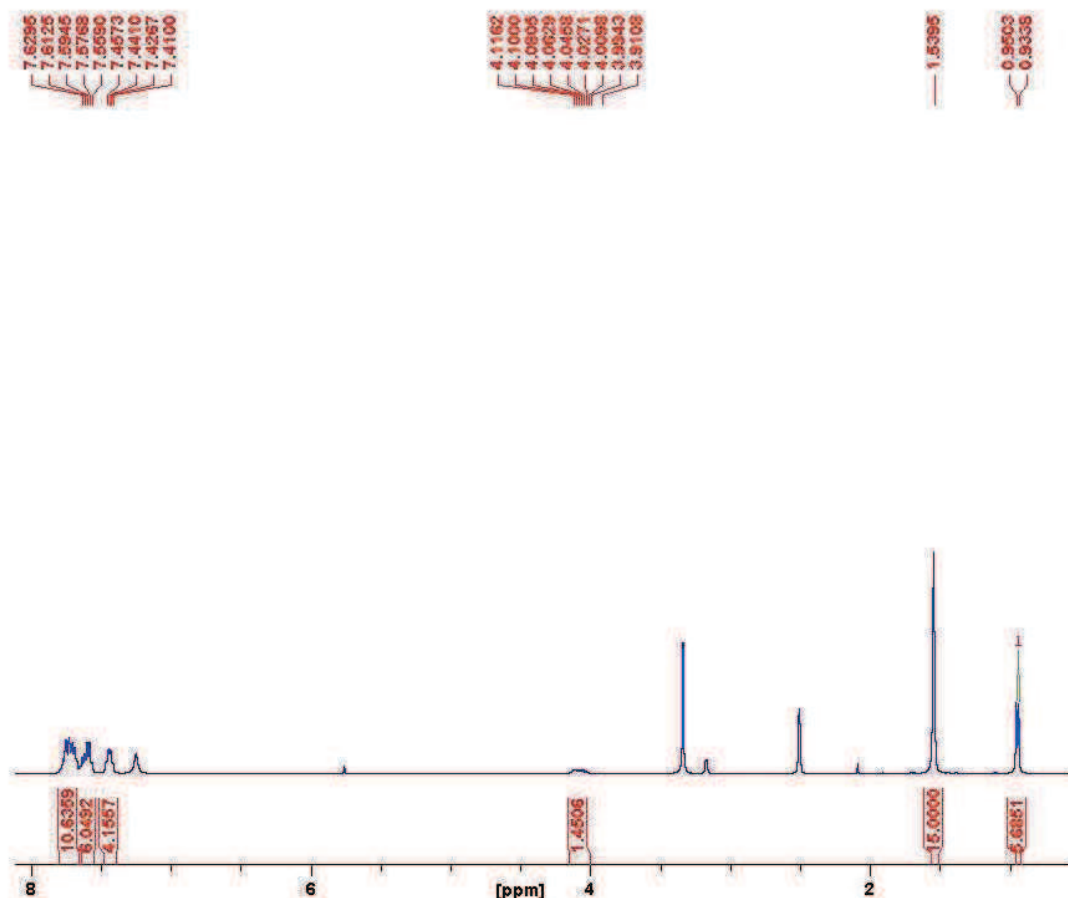


Figure B5. ¹H NMR of $[\text{Ph}_2\text{PN}(\text{C}_3\text{H}_7)\text{PPh}_2]\text{IrCp}^*(\text{Cl})^+\text{PF}_6^-$ (**1b**).

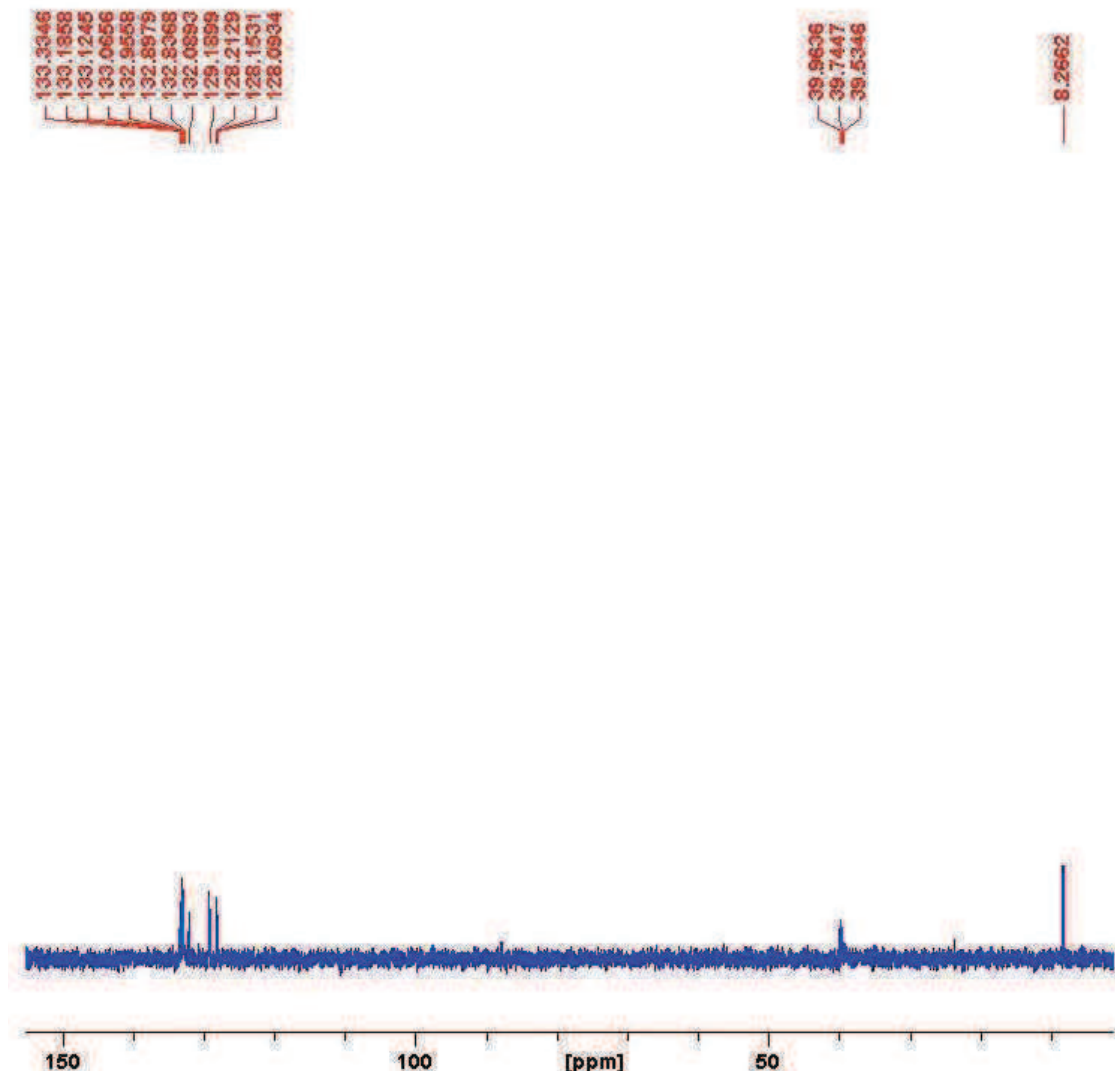


Figure B6. ^{13}C NMR of $[\text{Ph}_2\text{PN}(\text{C}_3\text{H}_7)\text{PPh}_2]\text{IrCp}^*(\text{Cl})^+\text{PF}_6^-$ (**1b**).

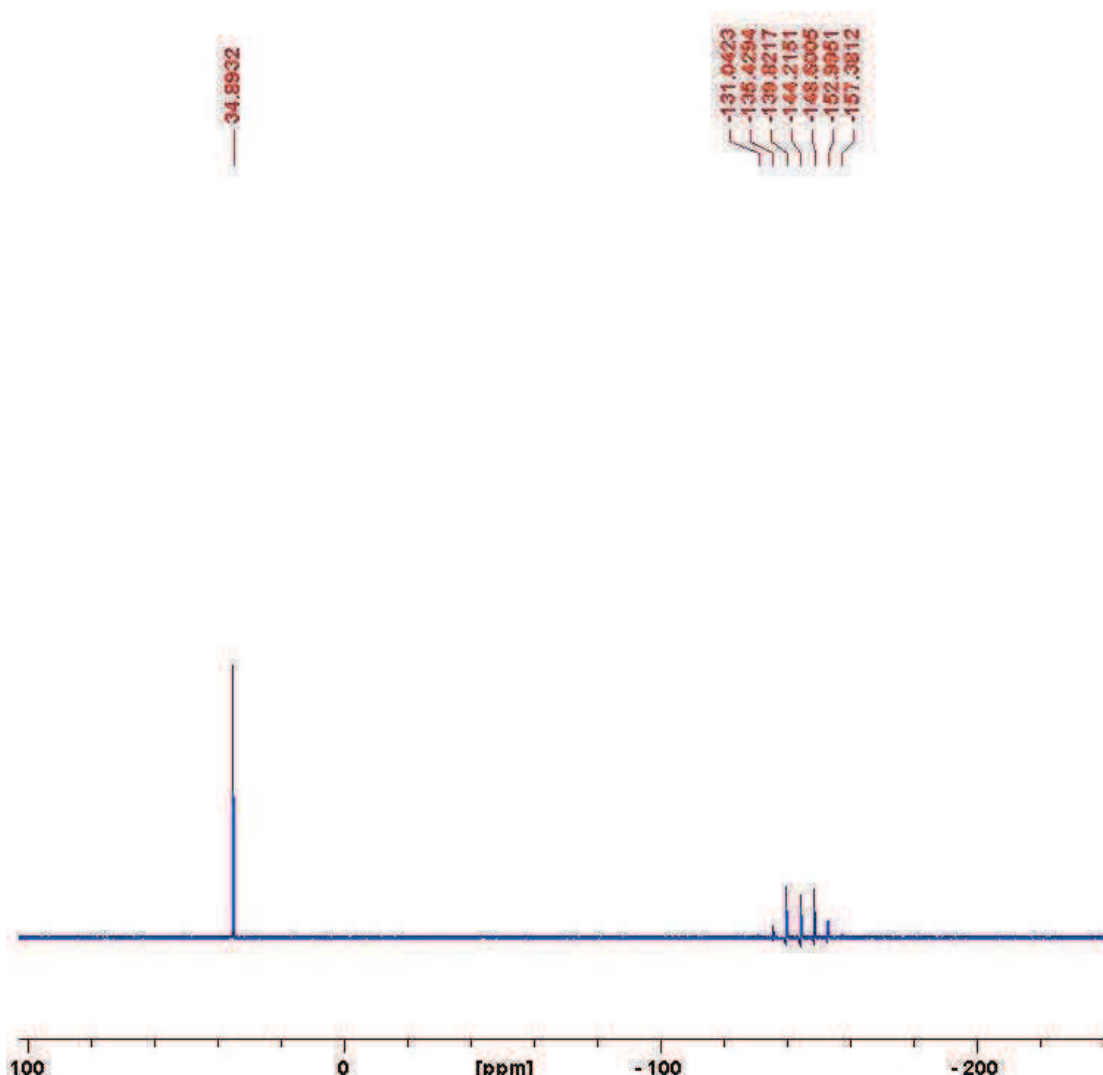


Figure B7. ^{31}P NMR of $[\text{Ph}_2\text{PN}(\text{C}_3\text{H}_7)\text{PPh}_2]\text{IrCp}^*(\text{Cl})^+\text{PF}_6^-$ (**1b**).

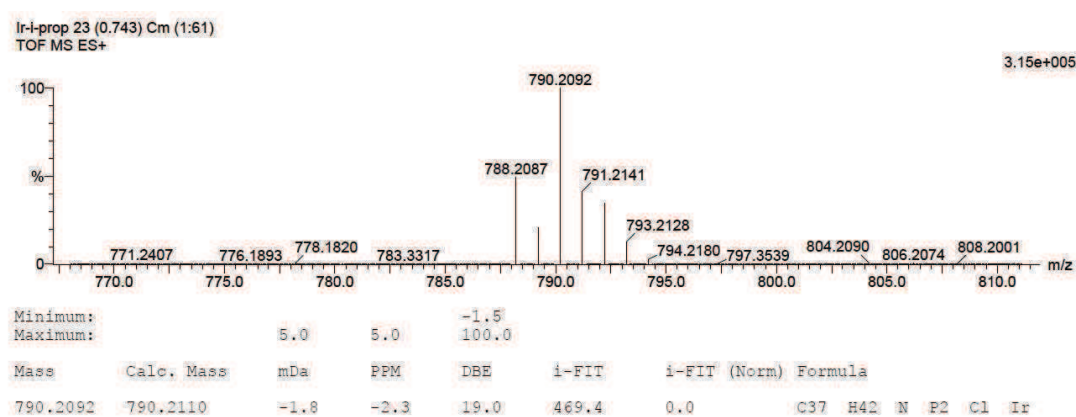


Figure B8. HRMS of $[\text{Ph}_2\text{PN}(\text{C}_3\text{H}_7)\text{PPh}_2]\text{IrCp}^*(\text{Cl})^+\text{PF}_6^-$ (**1b**).

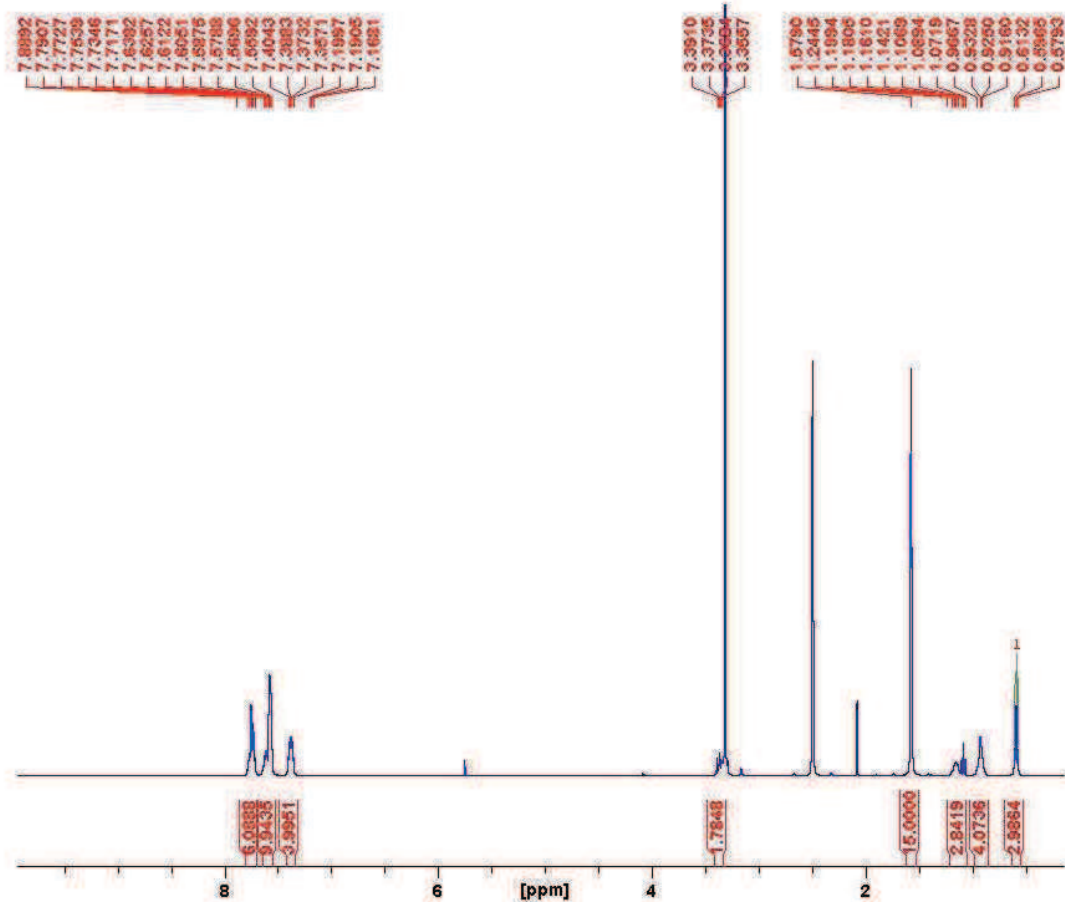


Figure B9. ¹H NMR of [Ph₂PN(C₅H₁₁)PPh₂]IrCp*(Cl)⁺PF₆⁻ (**1c**).

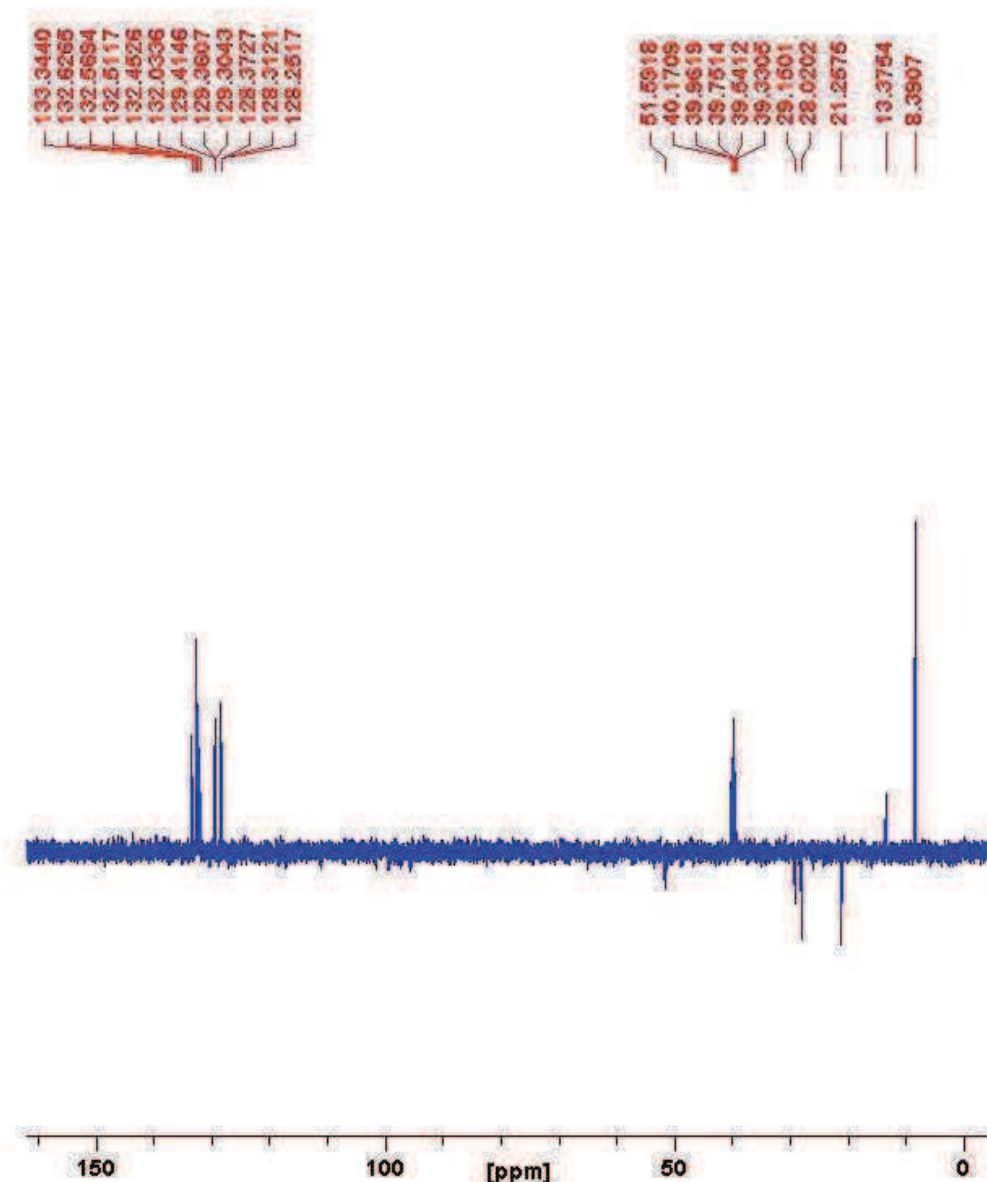


Figure B10. ¹³C NMR of $[\text{Ph}_2\text{PN}(\text{C}_5\text{H}_{11})\text{PPh}_2]\text{IrCp}^*(\text{Cl})^+\text{PF}_6^-$ (**1c**).

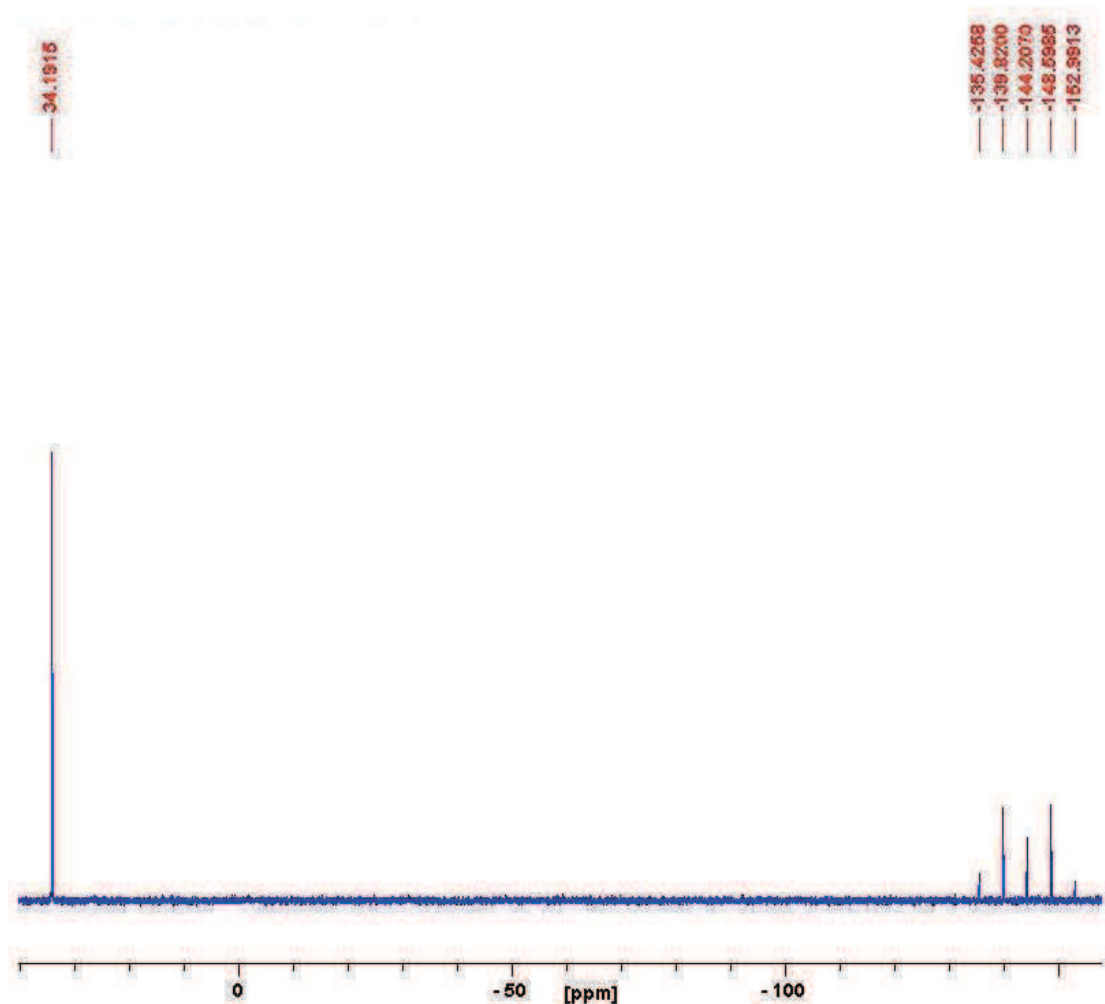


Figure B11. ^{31}P NMR of $[\text{Ph}_2\text{PN}(\text{C}_5\text{H}_{11})\text{PPh}_2]\text{IrCp}^*(\text{Cl})^+\text{PF}_6^-$ (**1c**).

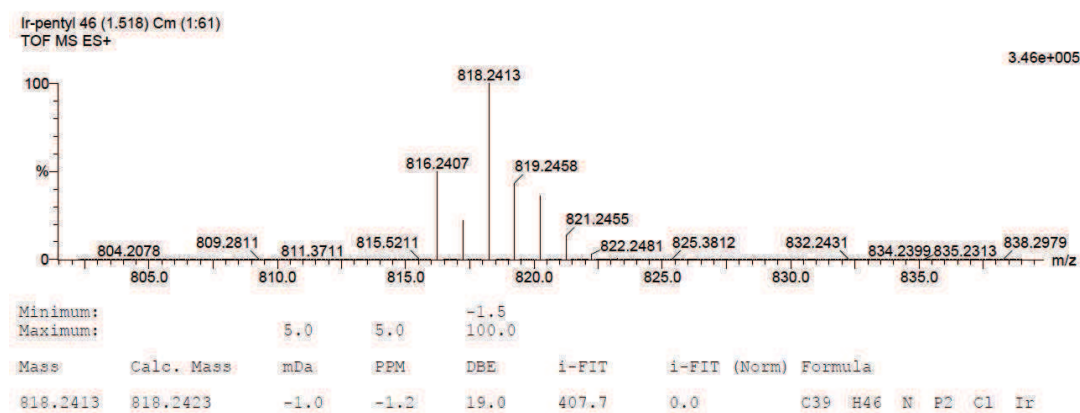


Figure B12. HRMS of $[\text{Ph}_2\text{PN}(\text{C}_5\text{H}_{11})\text{PPh}_2]\text{IrCp}^*(\text{Cl})^+\text{PF}_6^-$ (**1c**).

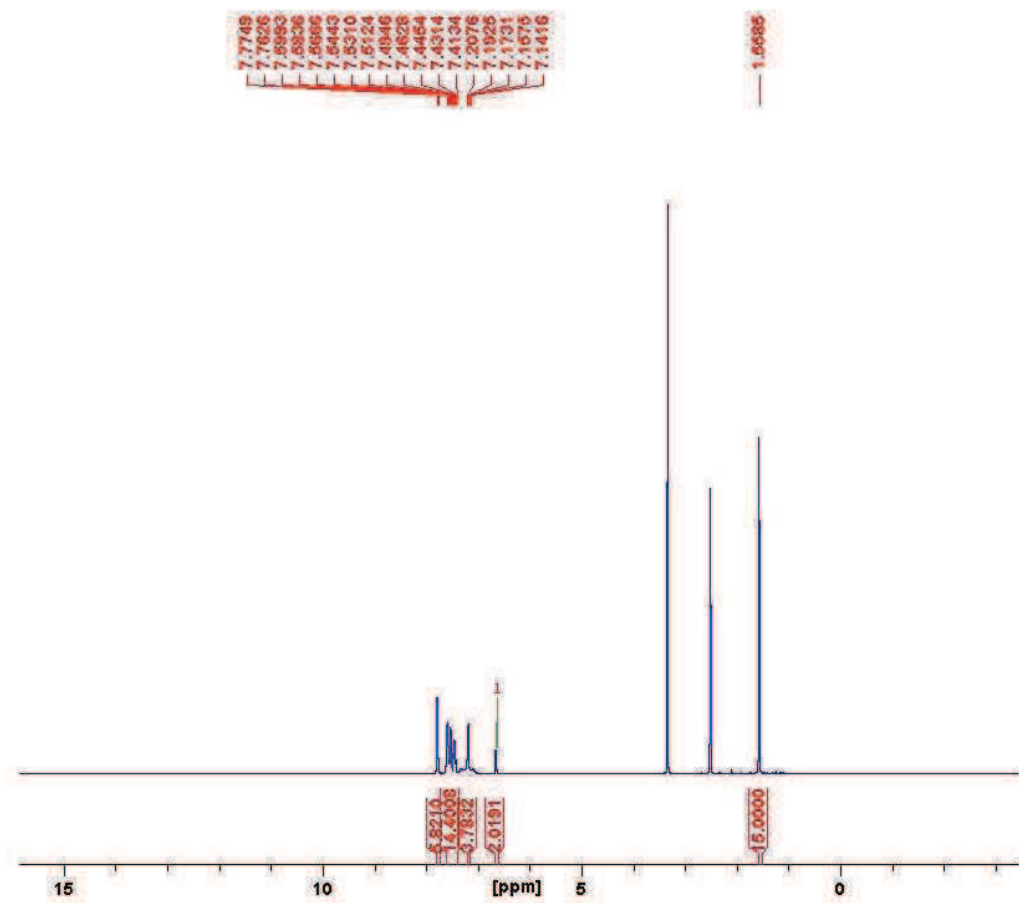


Figure B13. ¹H NMR of $[\text{Ph}_2\text{PN}(\text{Ph})\text{PPh}_2]\text{IrCp}^*(\text{Cl})]^+\text{PF}_6^-$ (**1d**).

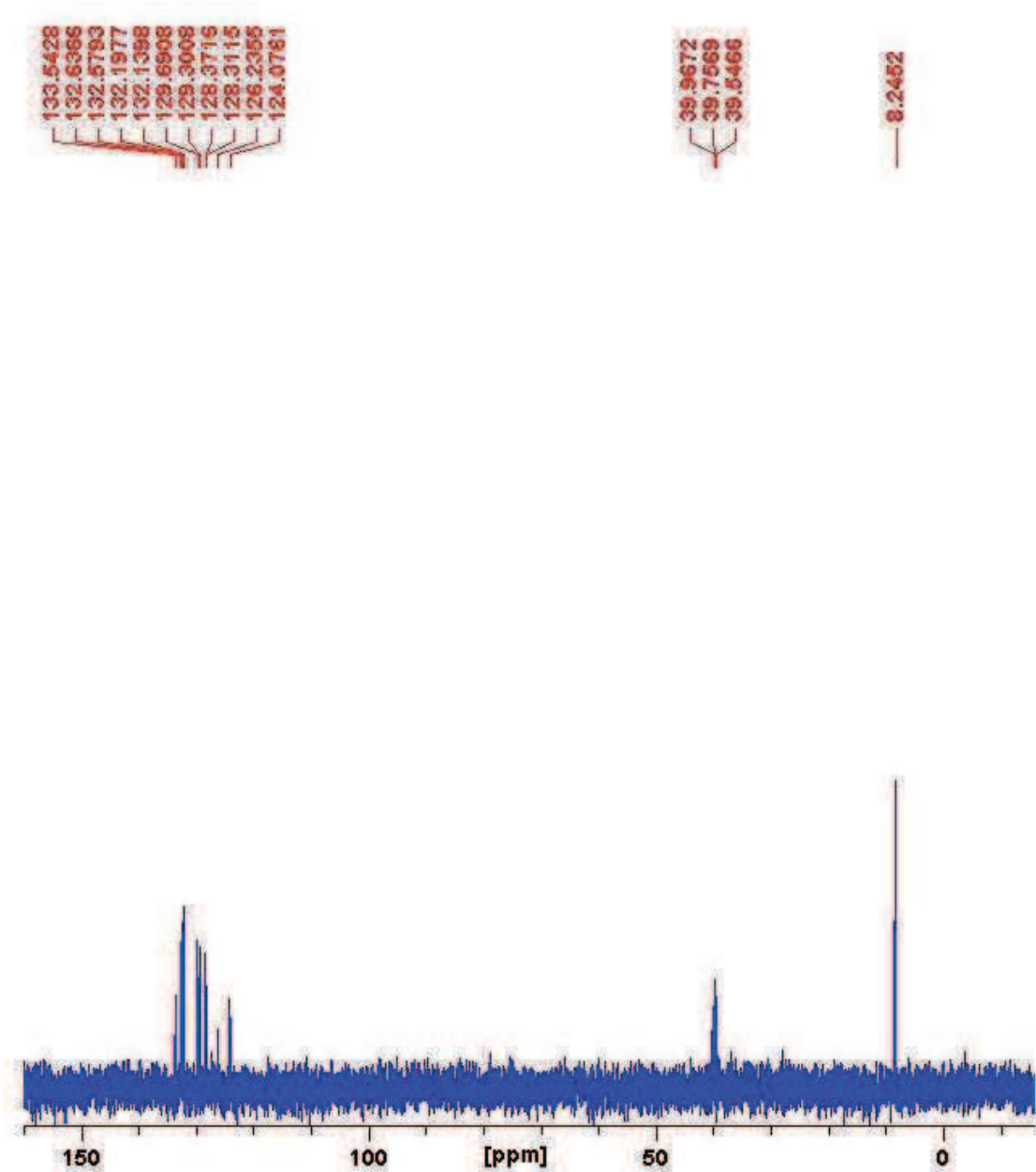


Figure B14. ^{13}C NMR of $[\text{Ph}_2\text{PN}(\text{Ph})\text{PPh}_2]\text{IrCp}^*(\text{Cl})^+\text{PF}_6^-$ (**1d**).

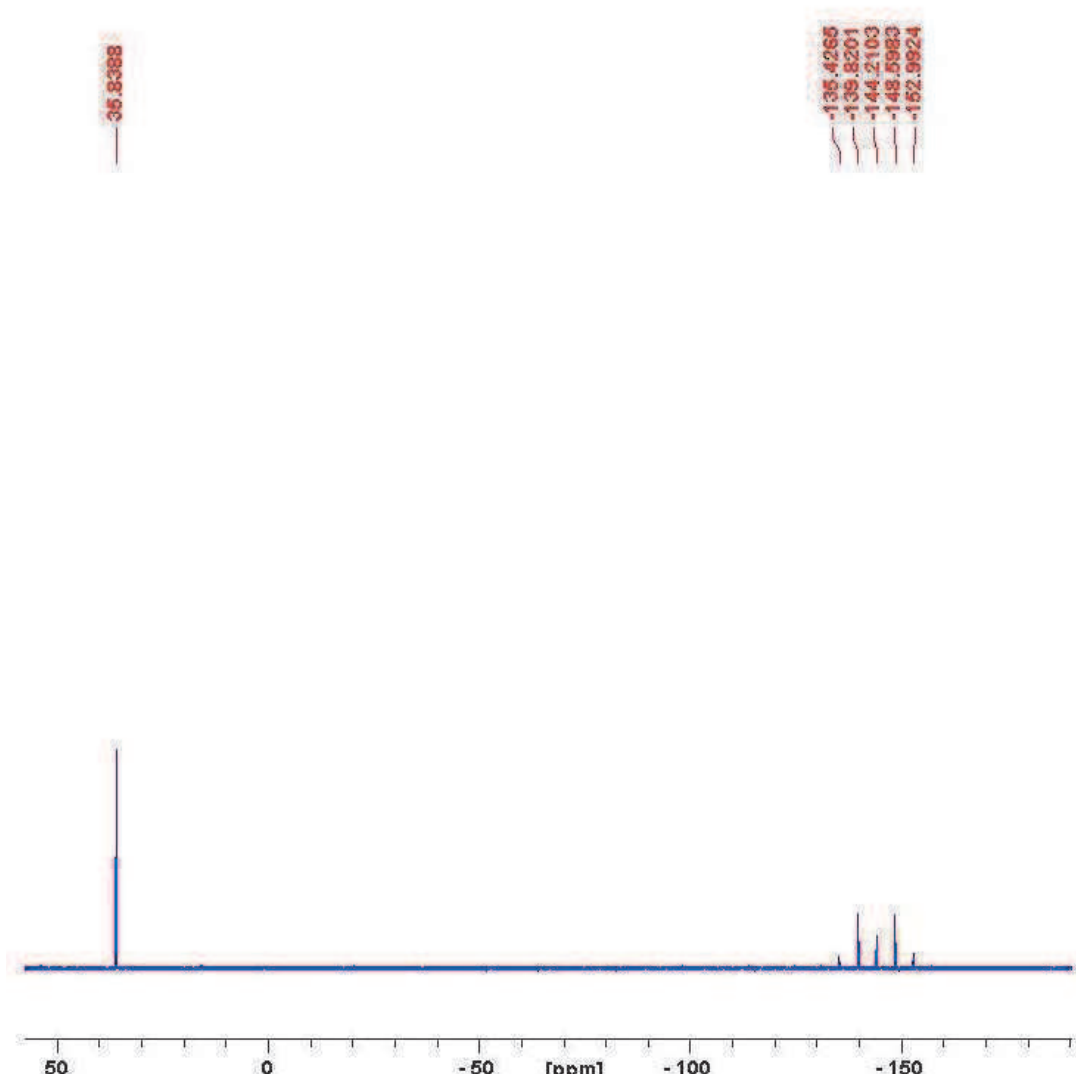


Figure B15. ^{31}P NMR of $[\text{Ph}_2\text{PN}(\text{Ph})\text{PPh}_2]\text{IrCp}^*(\text{Cl})]^+\text{PF}_6^-$ (**1d**).

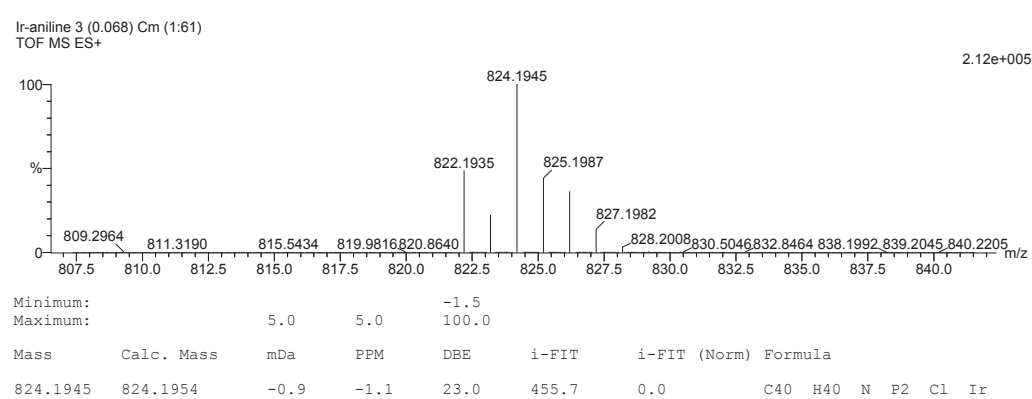


Figure B16. HRMS of $[\text{Ph}_2\text{PN}(\text{Ph})\text{PPh}_2]\text{IrCp}^*(\text{Cl})]^+\text{PF}_6^-$ (**1d**).

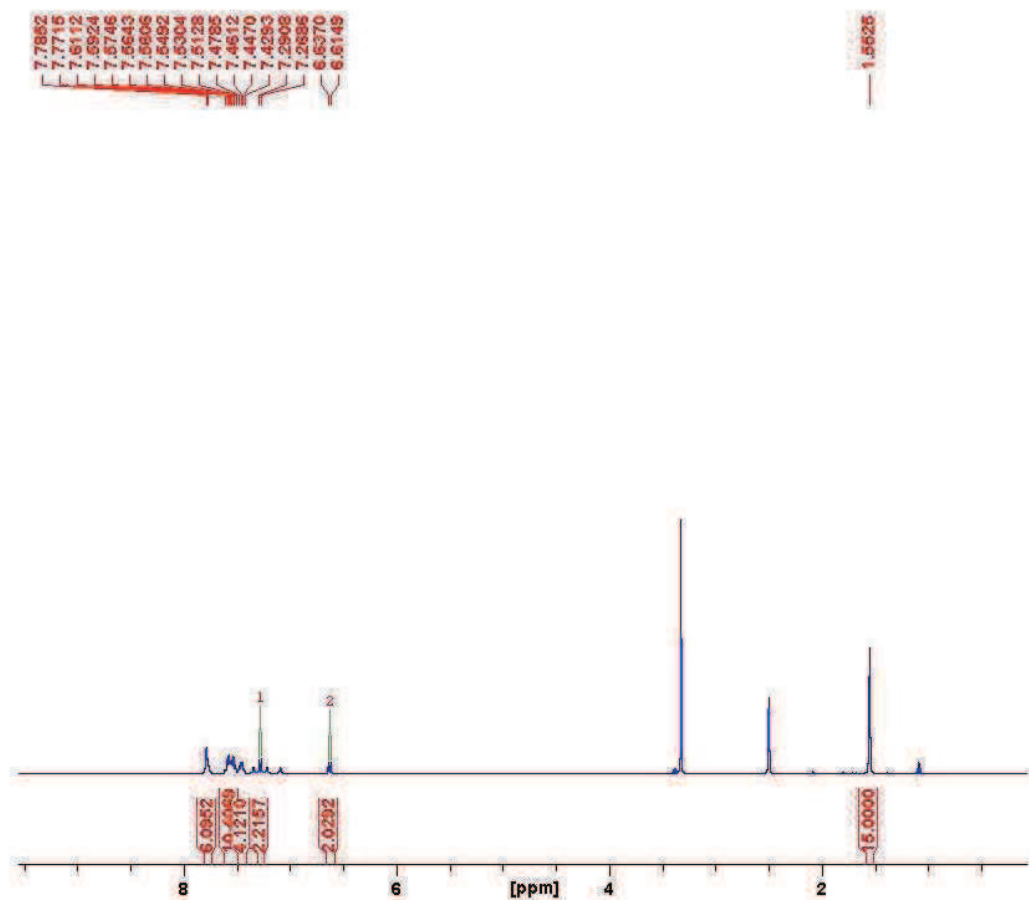


Figure B17. ¹H NMR of $[\text{Ph}_2\text{PN}(\text{C}_6\text{H}_4\text{Cl})\text{PPh}_2]\text{IrCp}^*(\text{Cl})^+\text{PF}_6^-$ (**1e**).

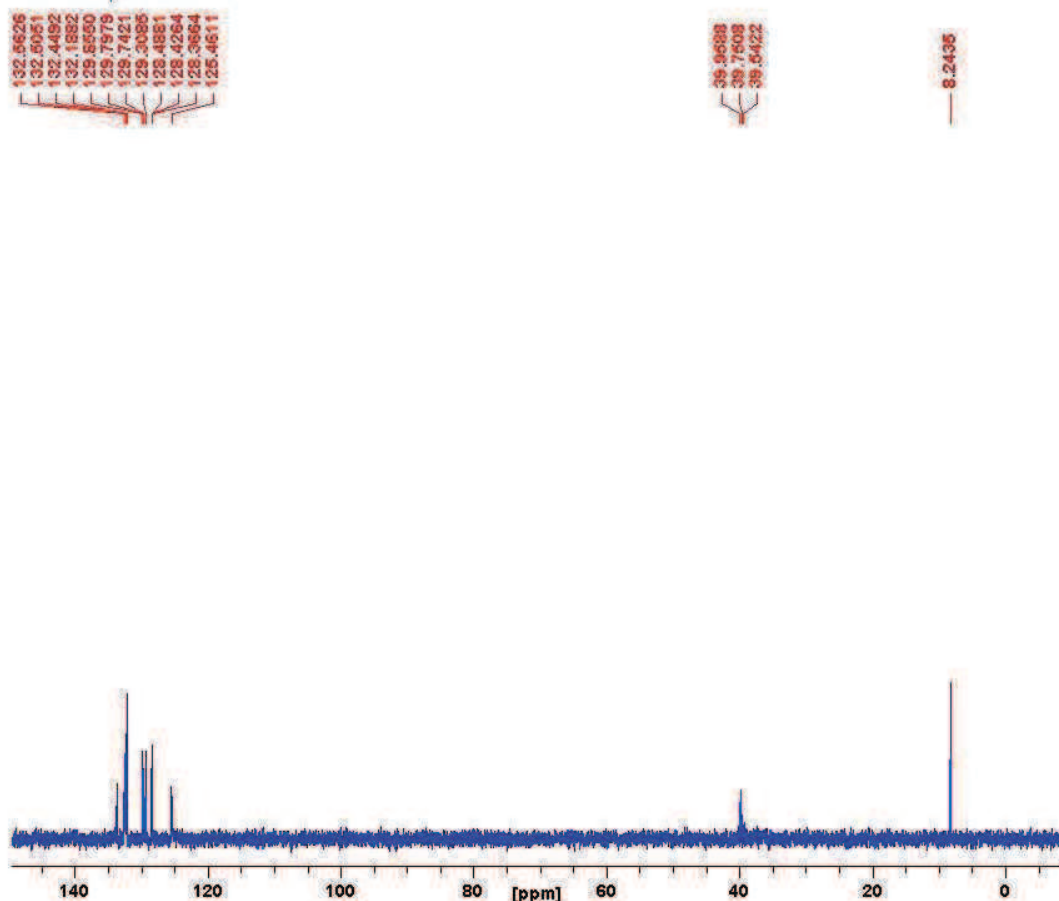


Figure B18. ^{13}C NMR of $[\text{Ph}_2\text{PN}(\text{C}_6\text{H}_4\text{Cl})\text{PPh}_2]\text{IrCp}^*(\text{Cl})^+\text{PF}_6^-$ (**1e**).

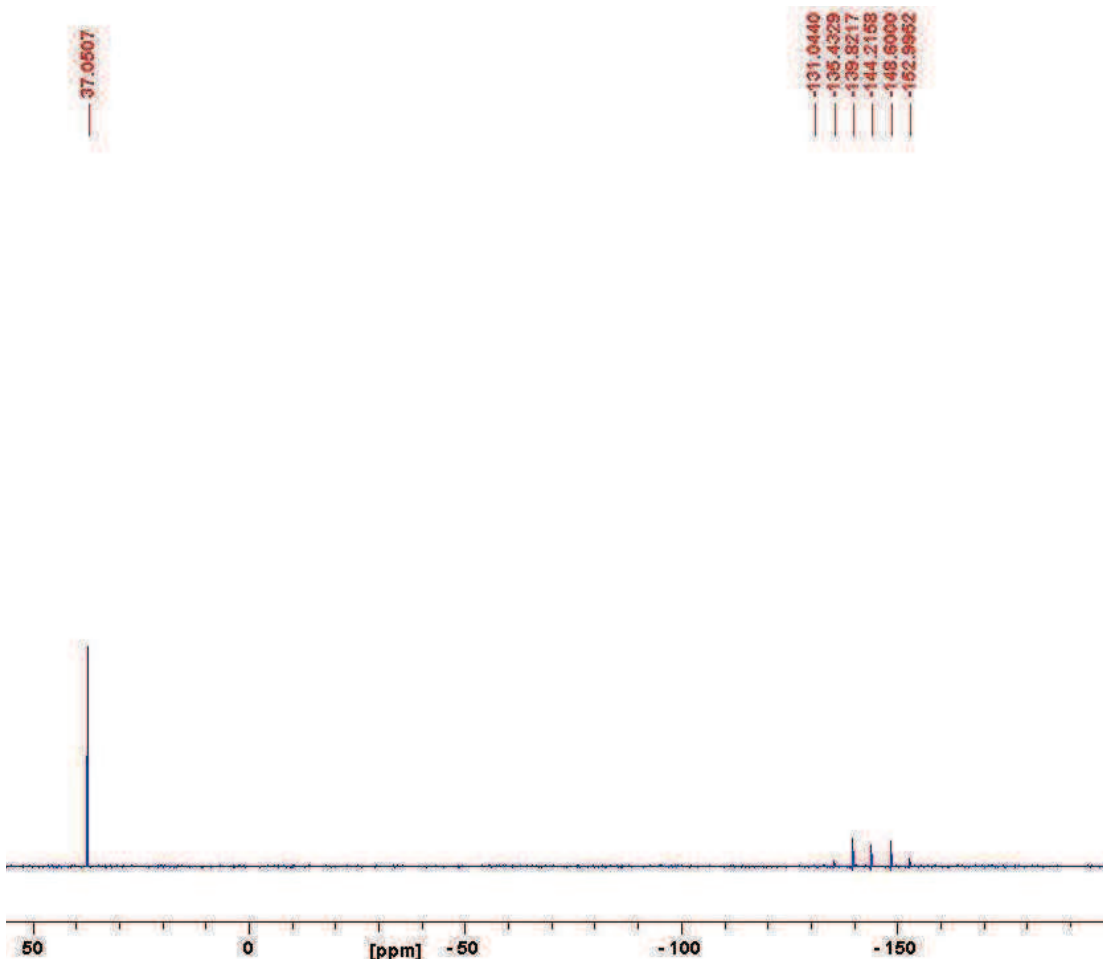


Figure B19. ^{31}P NMR of $[\text{Ph}_2\text{PN}(\text{C}_6\text{H}_4\text{Cl})\text{PPh}_2]\text{IrCp}^*(\text{Cl})^+\text{PF}_6^-$ (**1e**).

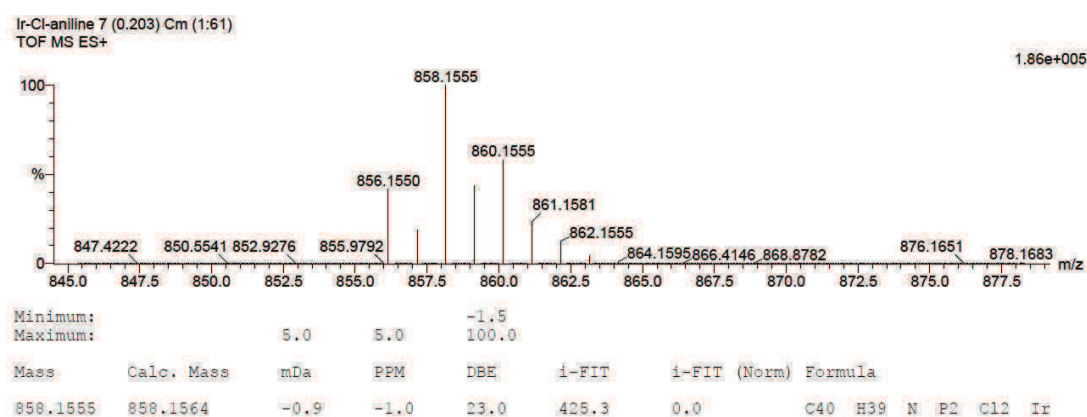


Figure B20. HRMS of $[\text{Ph}_2\text{PN}(\text{C}_6\text{H}_4\text{Cl})\text{PPh}_2]\text{IrCp}^*(\text{Cl})^+\text{PF}_6^-$ (**1e**).

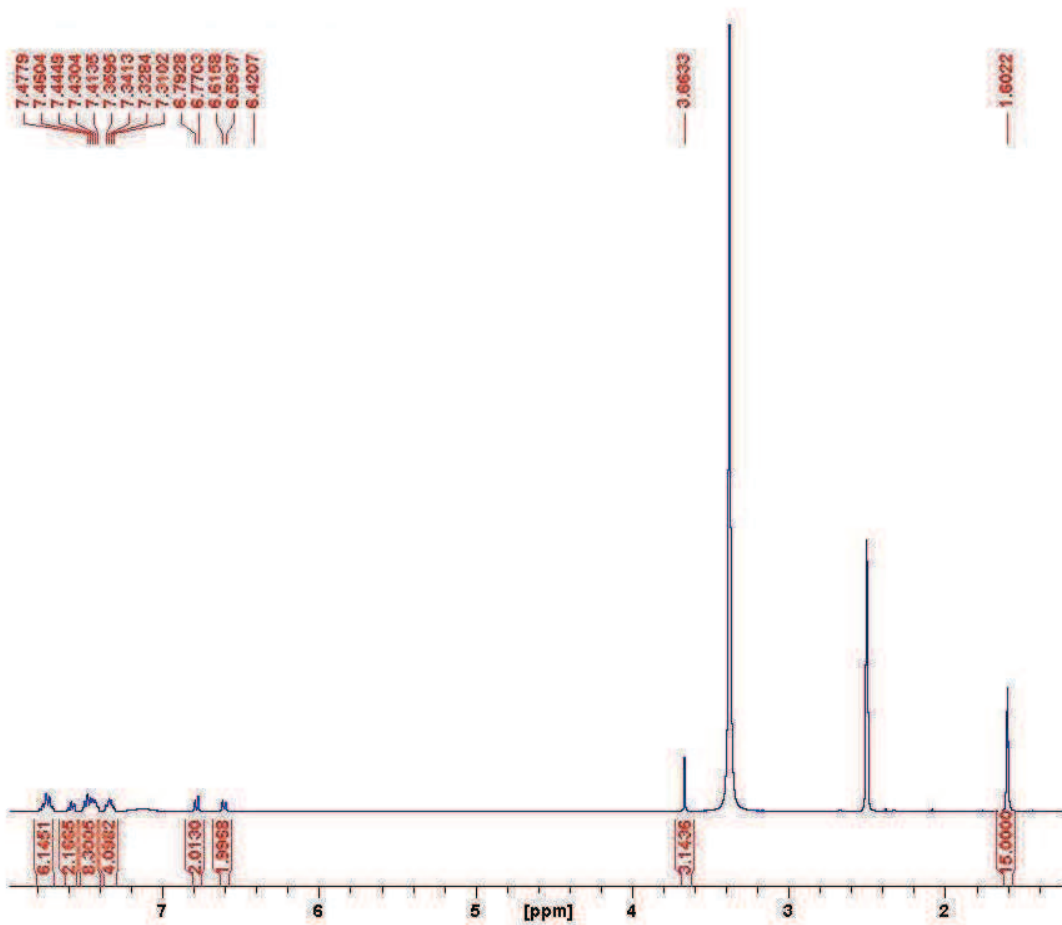


Figure B21. ¹H NMR of [Ph₂PN(C₇H₇O)PPh₂]IrCp*(Cl)⁺PF₆⁻ (**1f**).

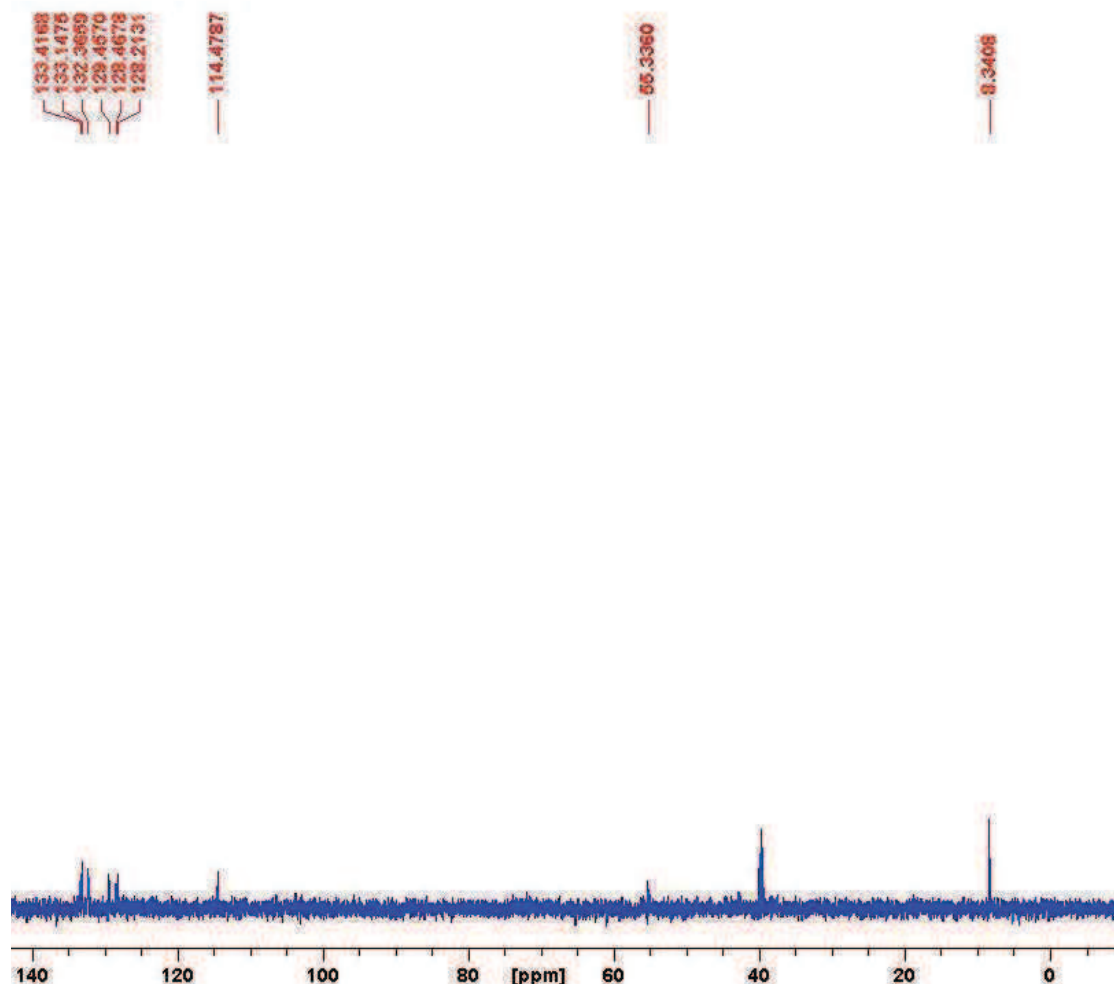


Figure B22. ^{13}C NMR of $[\text{Ph}_2\text{PN}(\text{C}_7\text{H}_7\text{O})\text{PPh}_2]\text{IrCp}^*(\text{Cl})^+\text{PF}_6^-$ (**1f**).

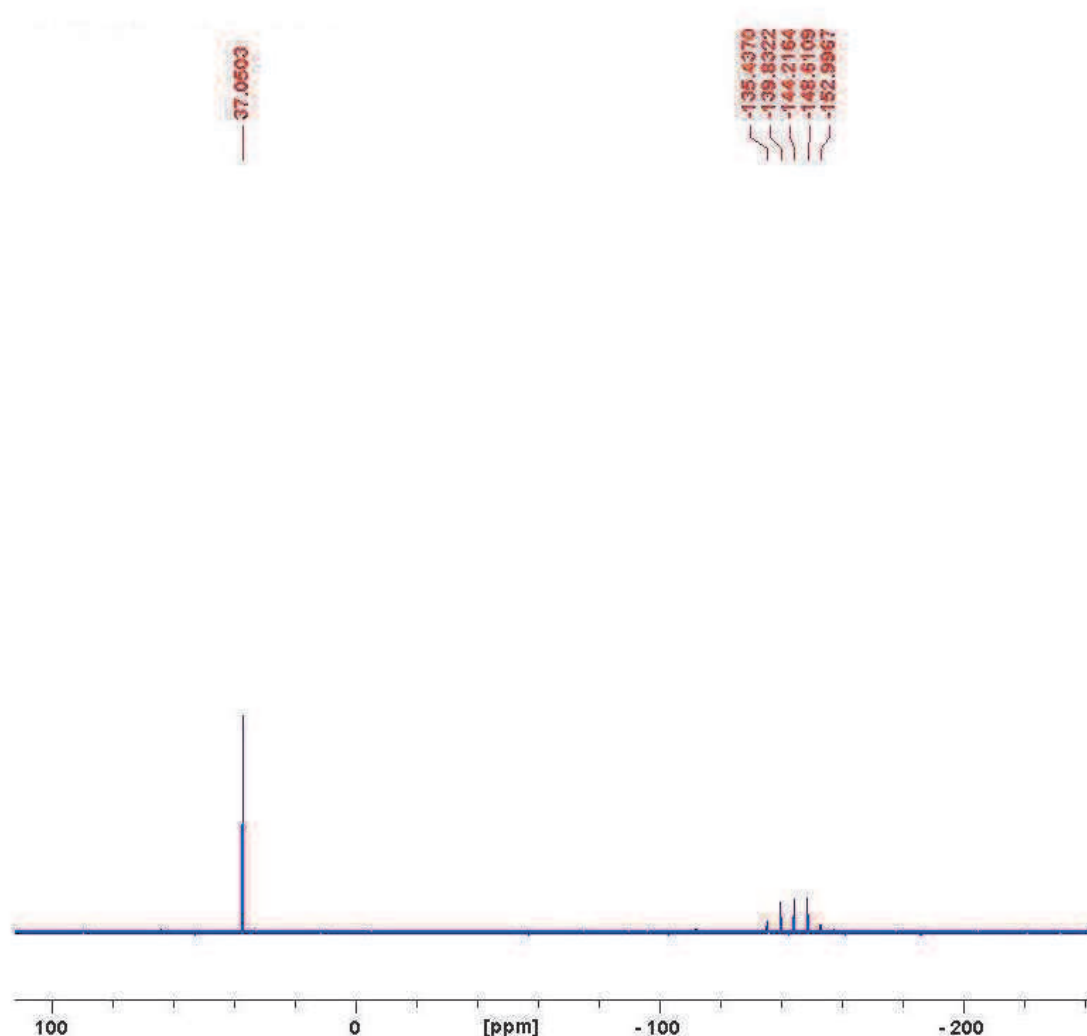


Figure B23. ^{31}P NMR of $[\text{Ph}_2\text{PN}(\text{C}_7\text{H}_7\text{O})\text{PPh}_2]\text{IrCp}^*(\text{Cl})]^+\text{PF}_6^-$ (**1f**).

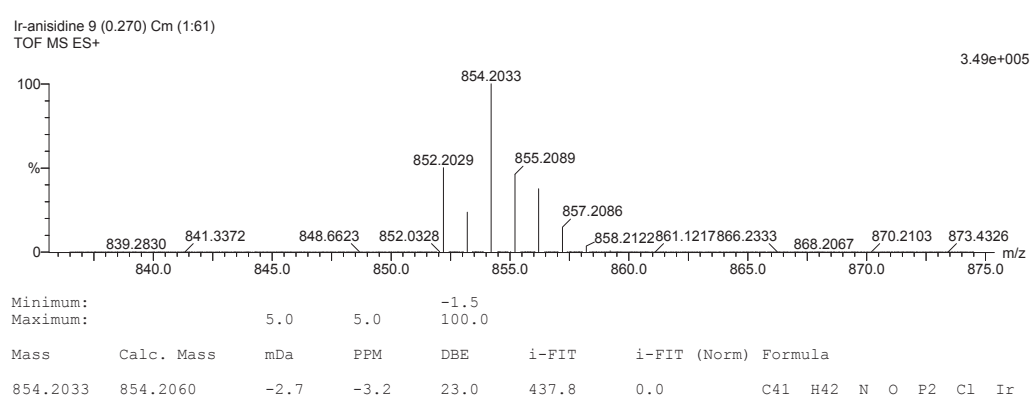


Figure B24. HRMS of $[\text{Ph}_2\text{PN}(\text{C}_7\text{H}_7\text{O})\text{PPh}_2]\text{IrCp}^*(\text{Cl})]^+\text{PF}_6^-$ (**1f**).

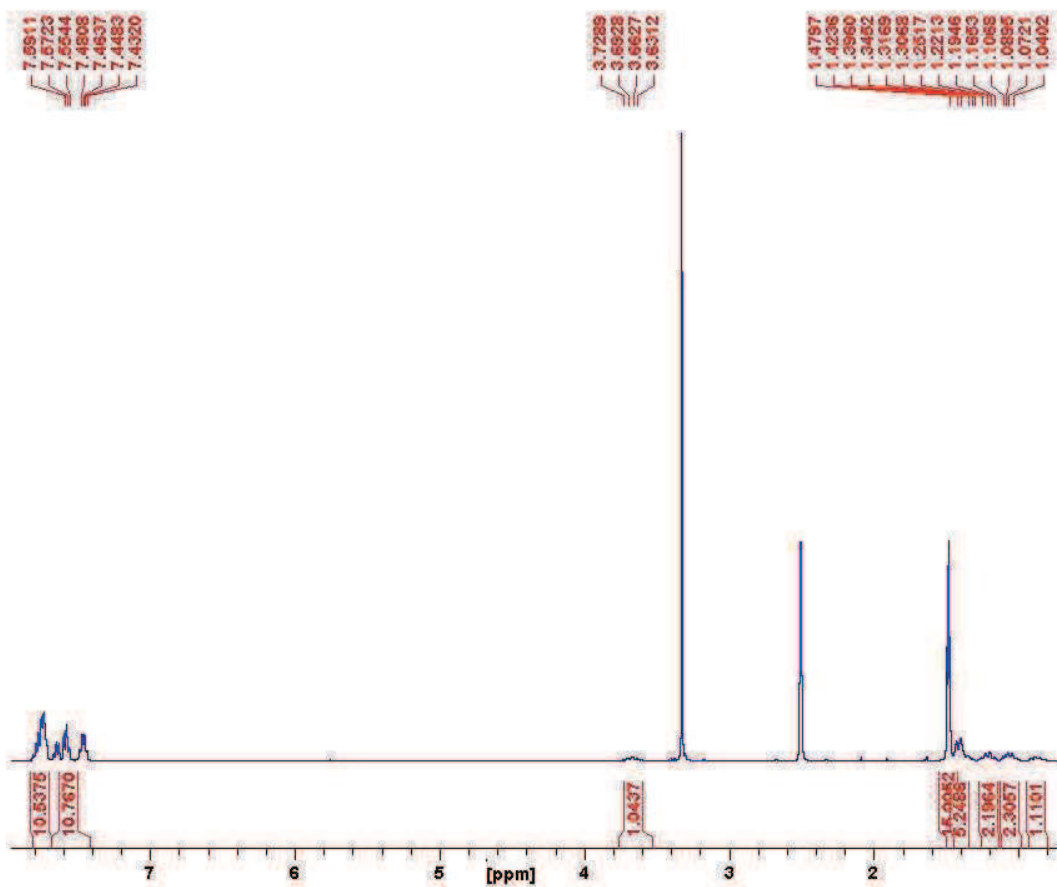


Figure B25. ^1H NMR of $[\text{Ph}_2\text{PN}(\text{C}_6\text{H}_{11})\text{PPh}_2]\text{RhCp}^*(\text{Cl})^+\text{PF}_6^-$ (**2a**).

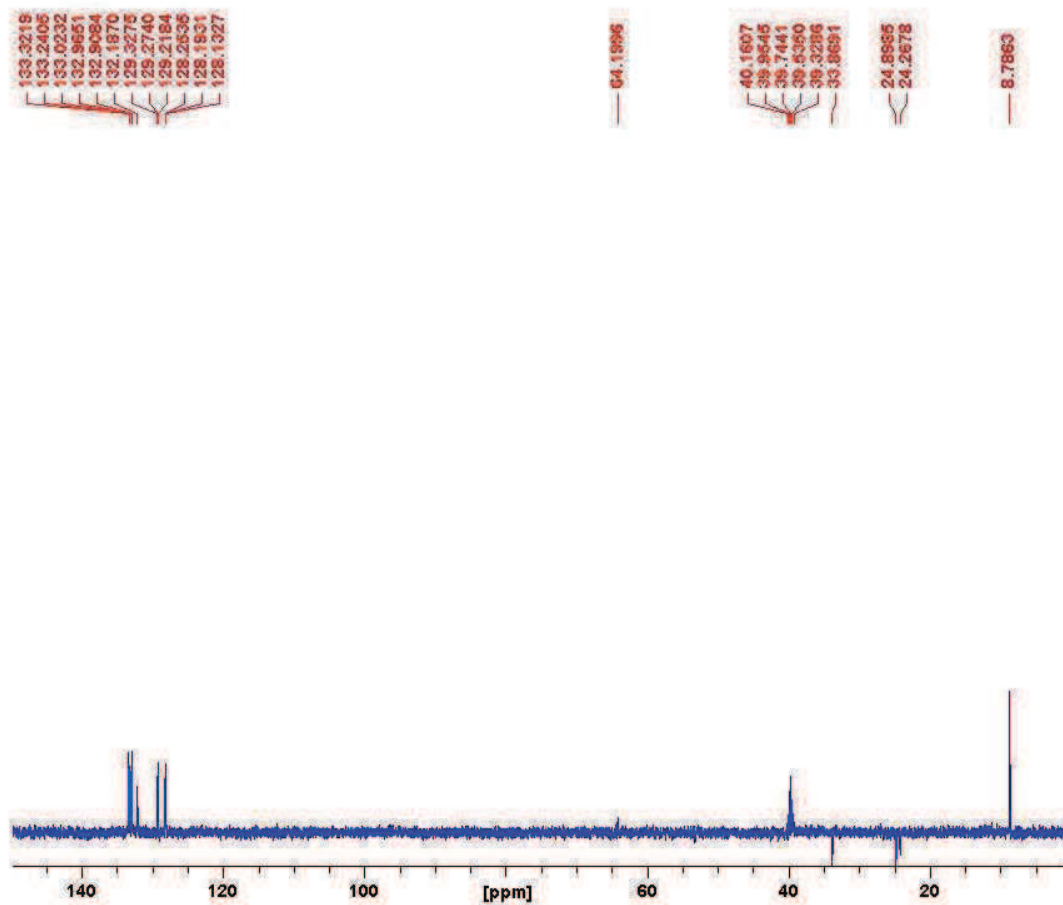


Figure B26. ^{13}C NMR of $[\text{Ph}_2\text{PN}(\text{C}_6\text{H}_{11})\text{PPh}_2]\text{RhCp}^*(\text{Cl})^+\text{PF}_6^-$ (**2a**).

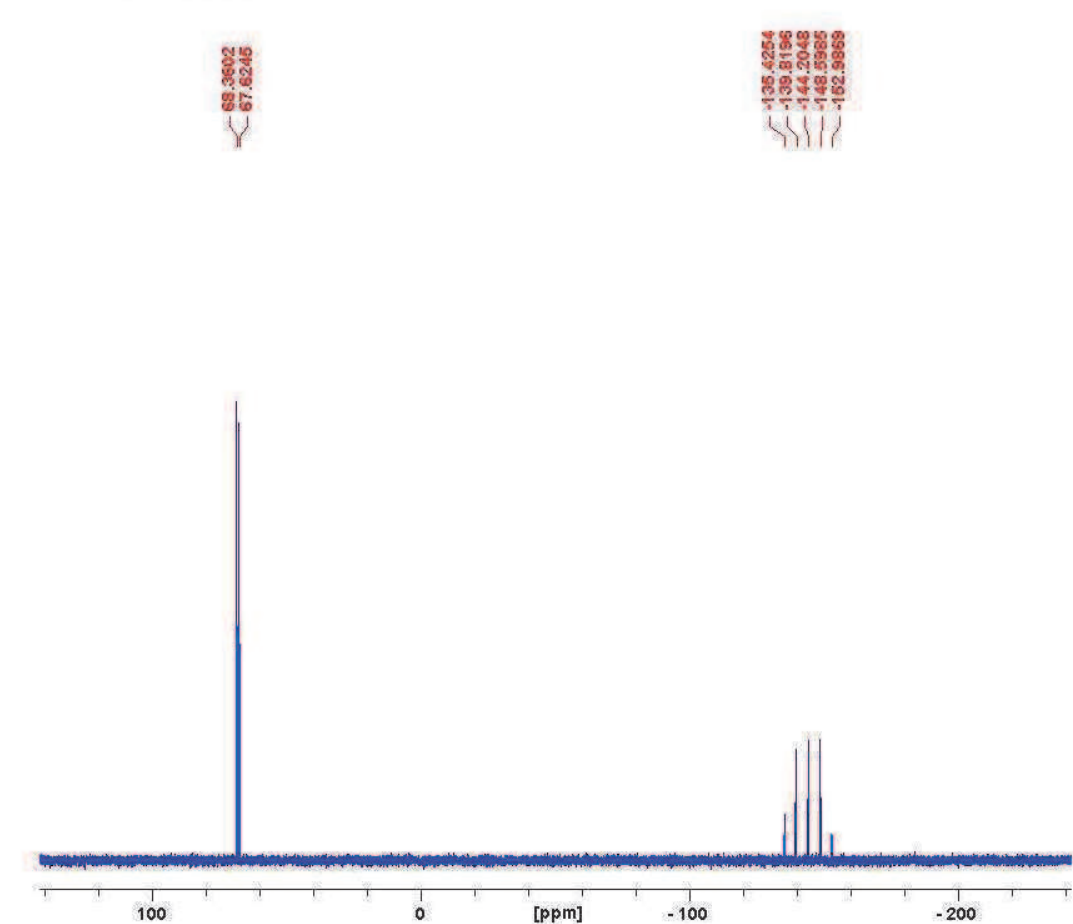


Figure B27. ^{31}P NMR of $[\text{Ph}_2\text{PN}(\text{C}_6\text{H}_{11})\text{PPh}_2]\text{RhCp}^*(\text{Cl})]^+\text{PF}_6^-$ (**2a**).

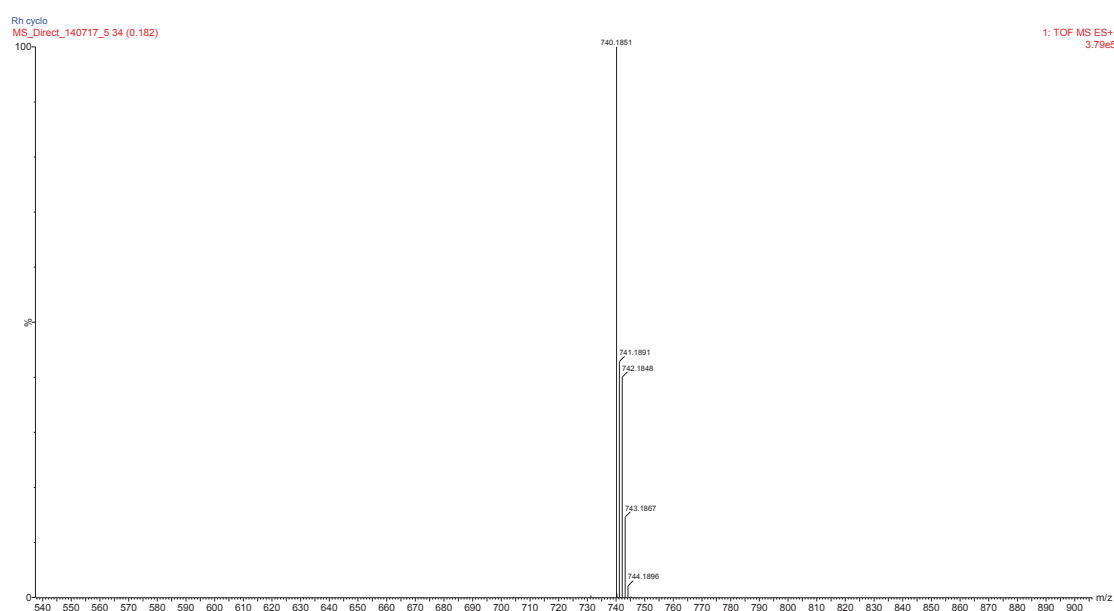


Figure B28. HRMS of $[\text{Ph}_2\text{PN}(\text{C}_6\text{H}_{11})\text{PPh}_2]\text{RhCp}^*(\text{Cl})]^+\text{PF}_6^-$ (**2a**).

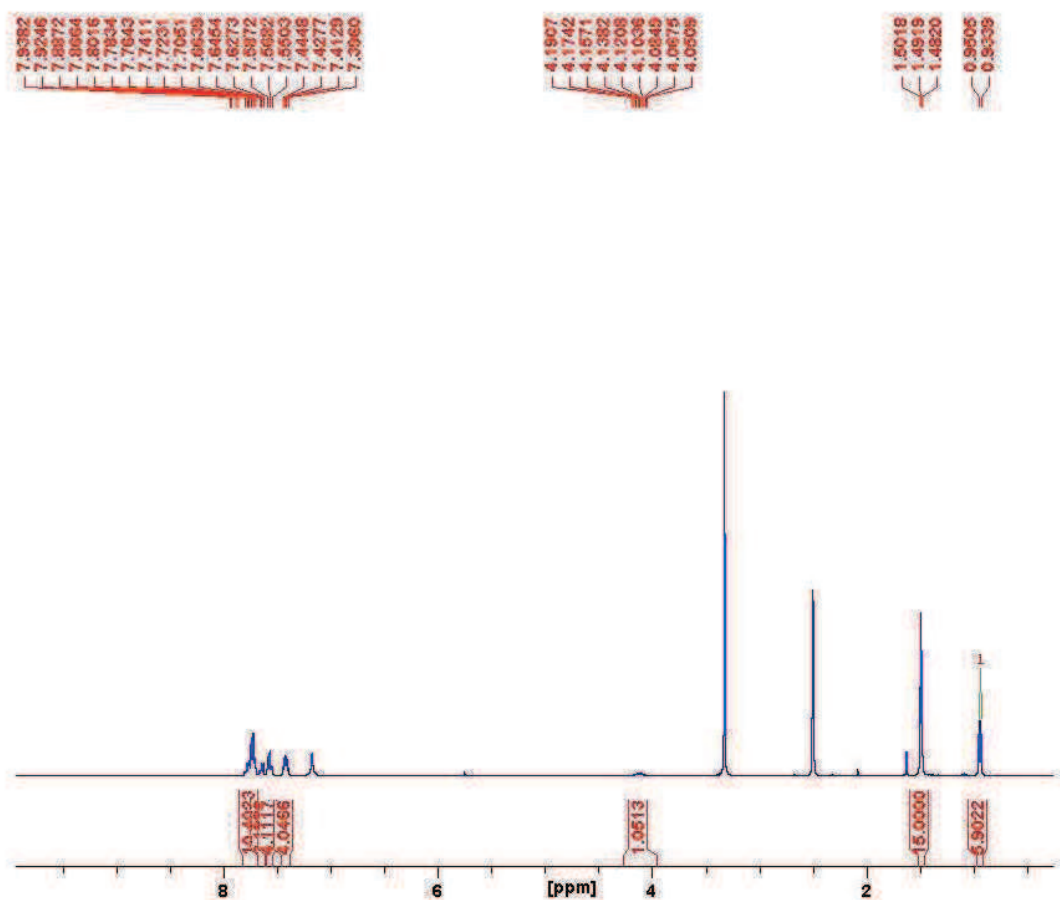


Figure B29. ¹H NMR of [Ph₂PN(C₃H₇)PPh₂]RhCp*(Cl)⁺PF₆⁻ (**2b**).

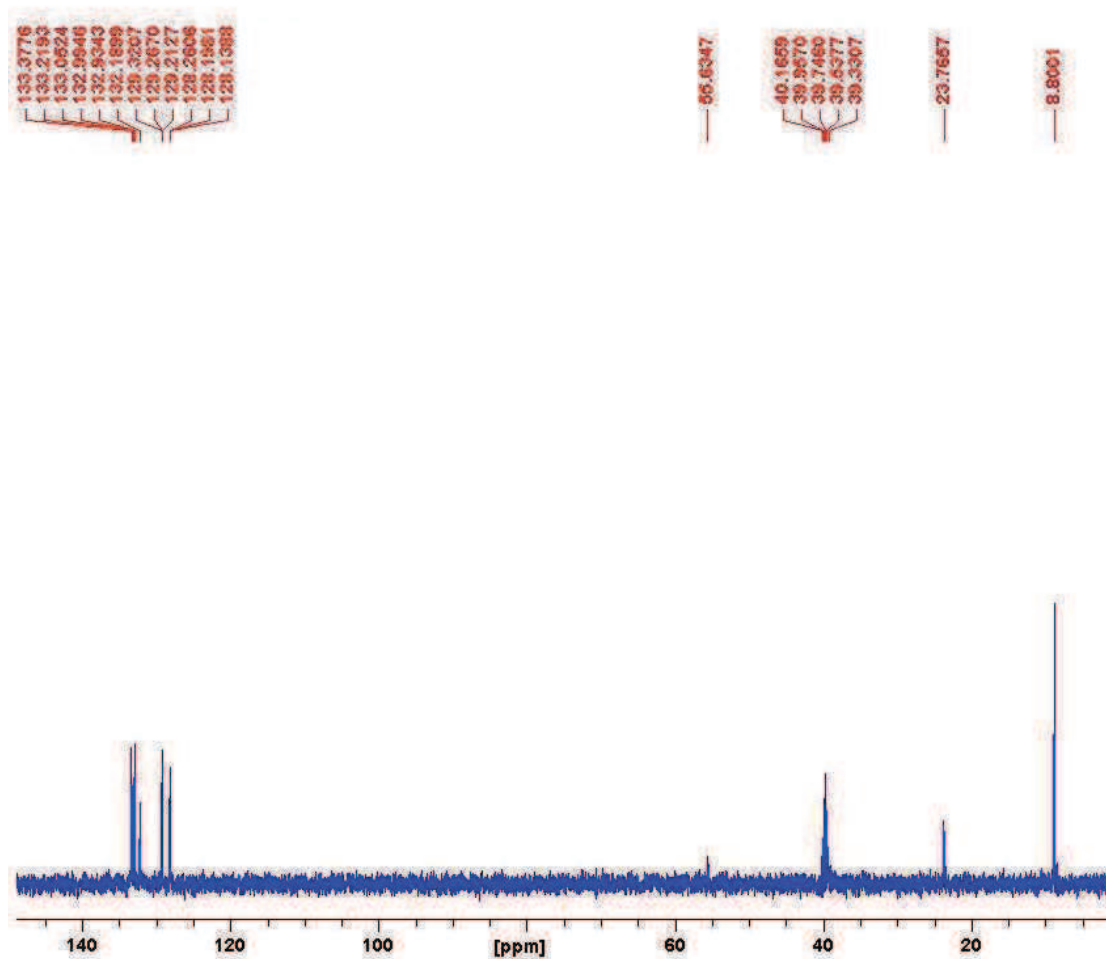


Figure B30. ^{13}C NMR of $[\text{Ph}_2\text{PN}(\text{C}_3\text{H}_7)\text{PPh}_2]\text{RhCp}^*(\text{Cl})^+\text{PF}_6^-$ (2b).

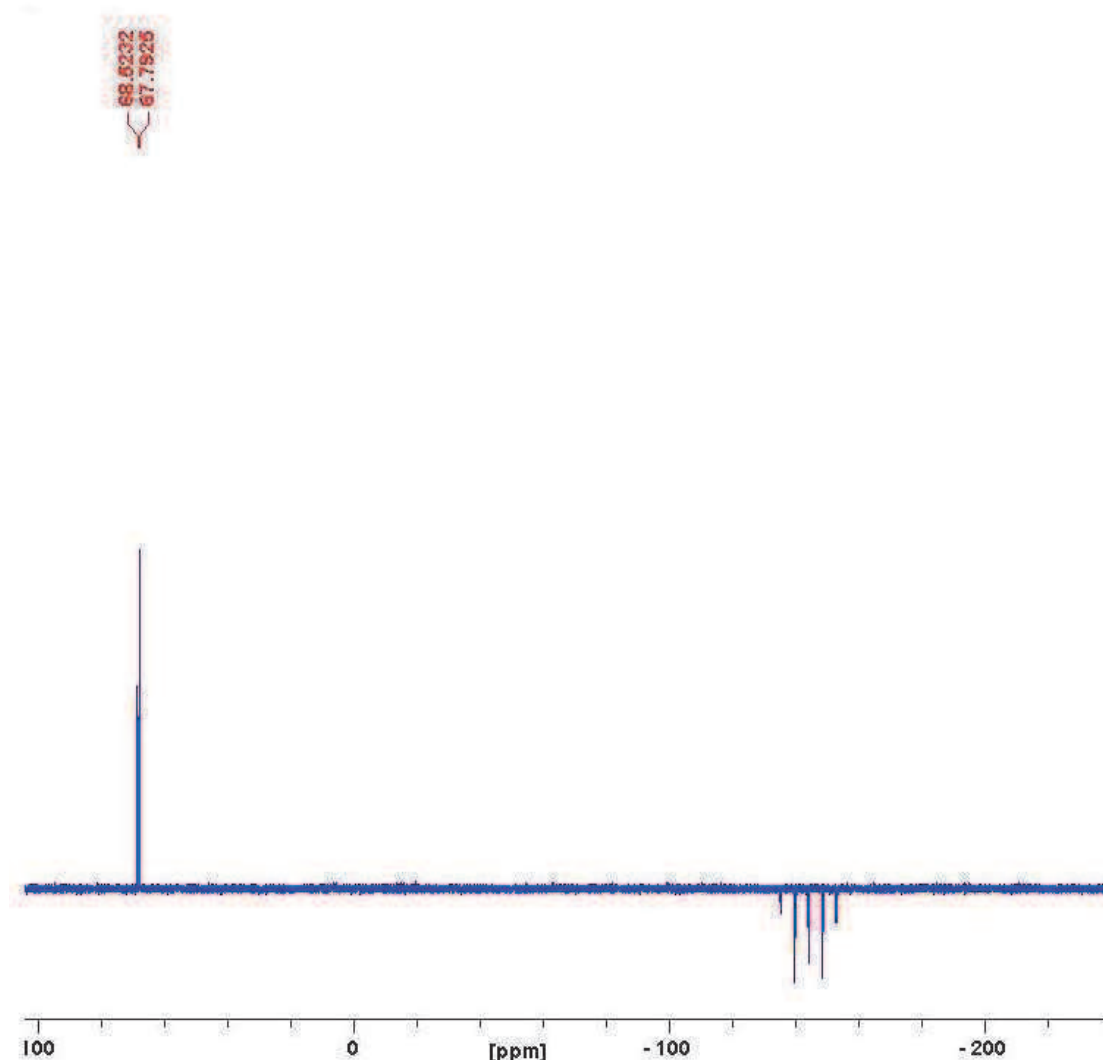


Figure B31. ^{31}P NMR of $[\text{Ph}_2\text{PN}(\text{C}_3\text{H}_7)\text{PPh}_2]\text{RhCp}^*(\text{Cl})]^+\text{PF}_6^-$ (**2b**).

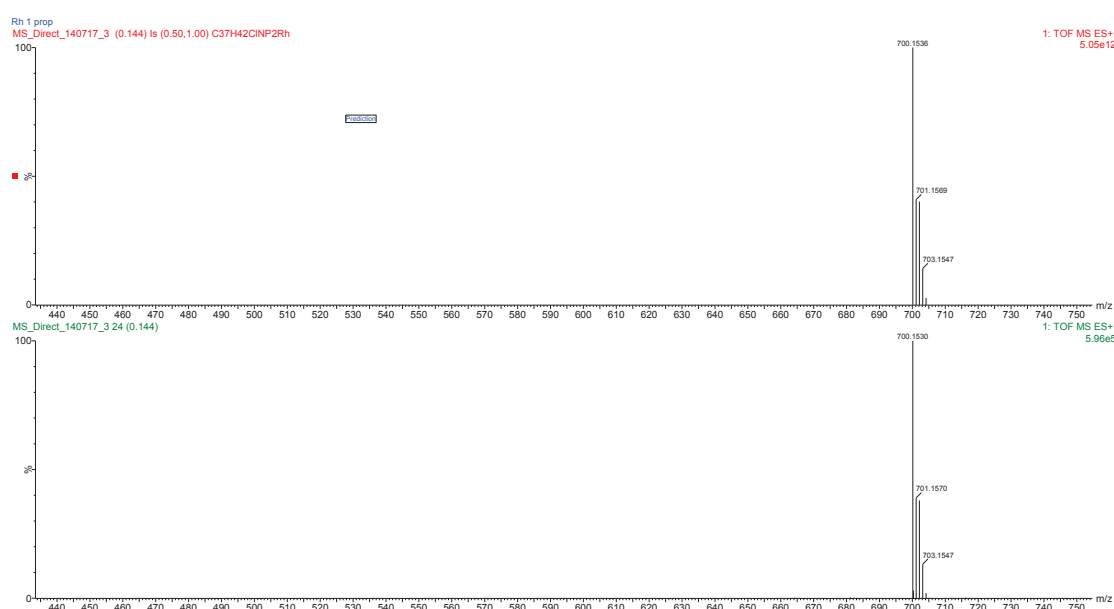


Figure B32. HRMS of $[\text{Ph}_2\text{PN}(\text{C}_3\text{H}_7)\text{PPh}_2]\text{RhCp}^*(\text{Cl})]^+\text{PF}_6^-$ (**2b**).

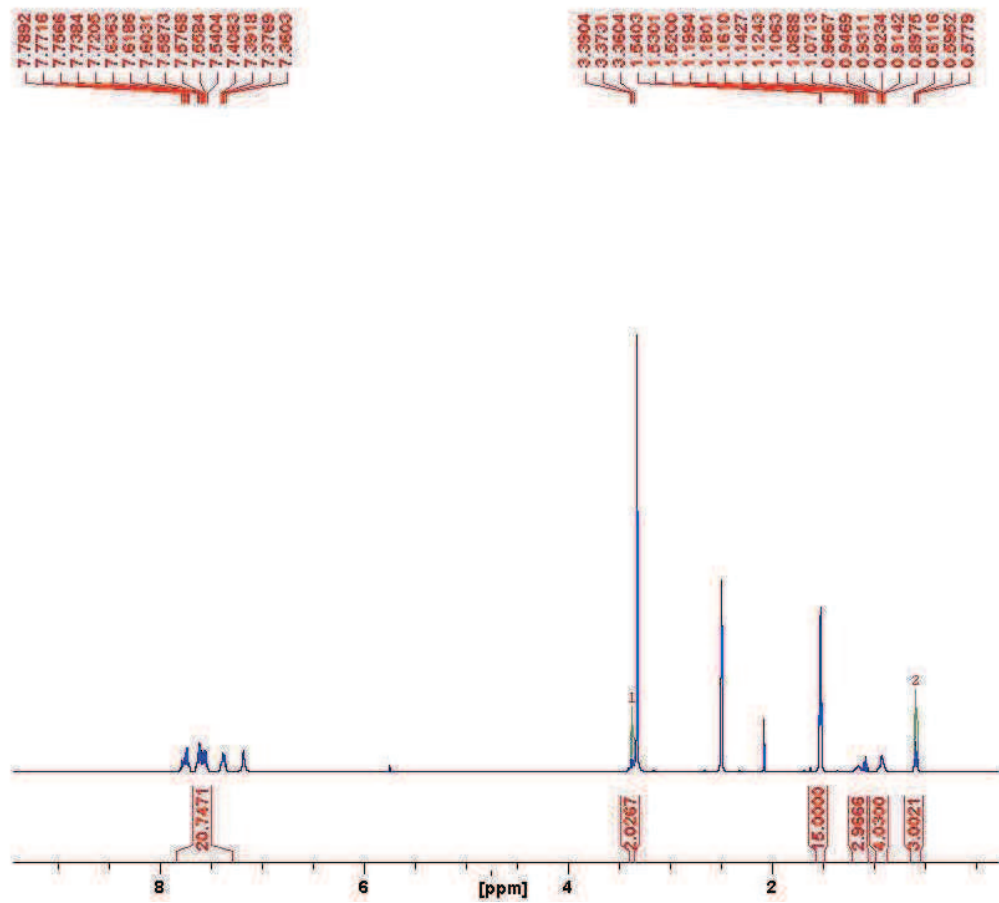


Figure B33. ¹H NMR of $[\text{Ph}_2\text{PN}(\text{C}_5\text{H}_{11})\text{PPh}_2]\text{RhCp}^*(\text{Cl})^+\text{PF}_6^-$ (**2c**).

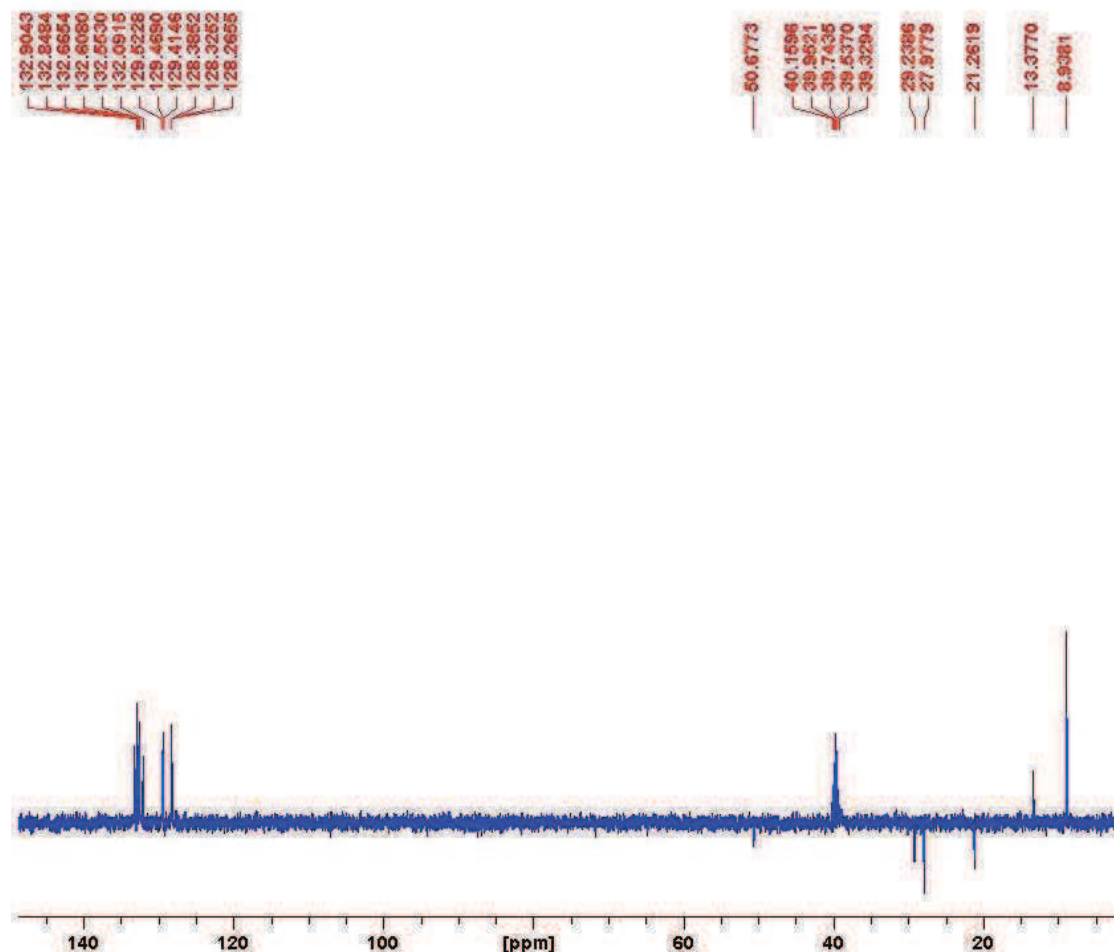


Figure B34. ^{13}C NMR of $[\text{Ph}_2\text{PN}(\text{C}_5\text{H}_{11})\text{PPh}_2]\text{RhCp}^*(\text{Cl})^+\text{PF}_6^-$ (**2c**).

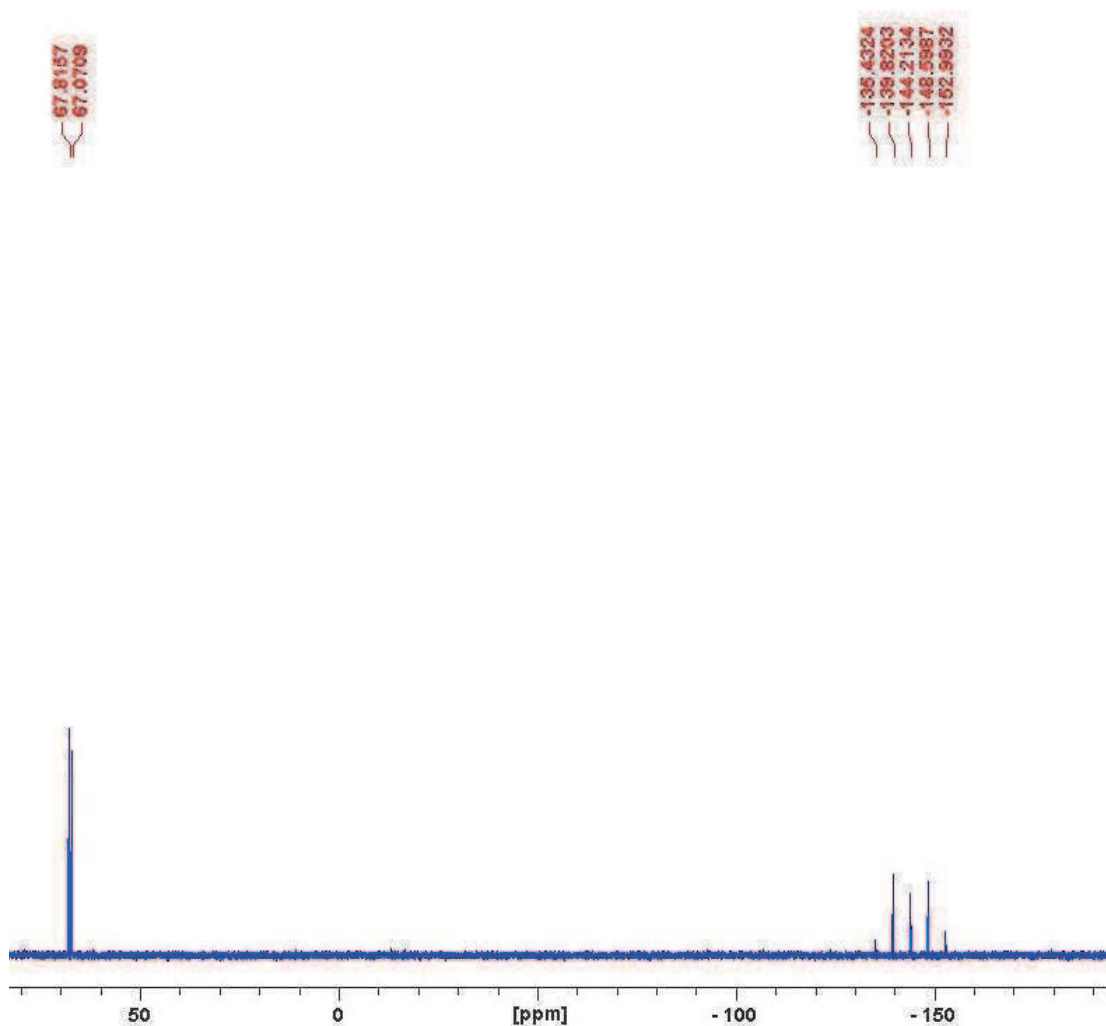


Figure B35. ^{31}P NMR of $[\text{Ph}_2\text{PN}(\text{C}_5\text{H}_{11})\text{PPh}_2]\text{RhCp}^*(\text{Cl})^+\text{PF}_6^-$ (**2c**).

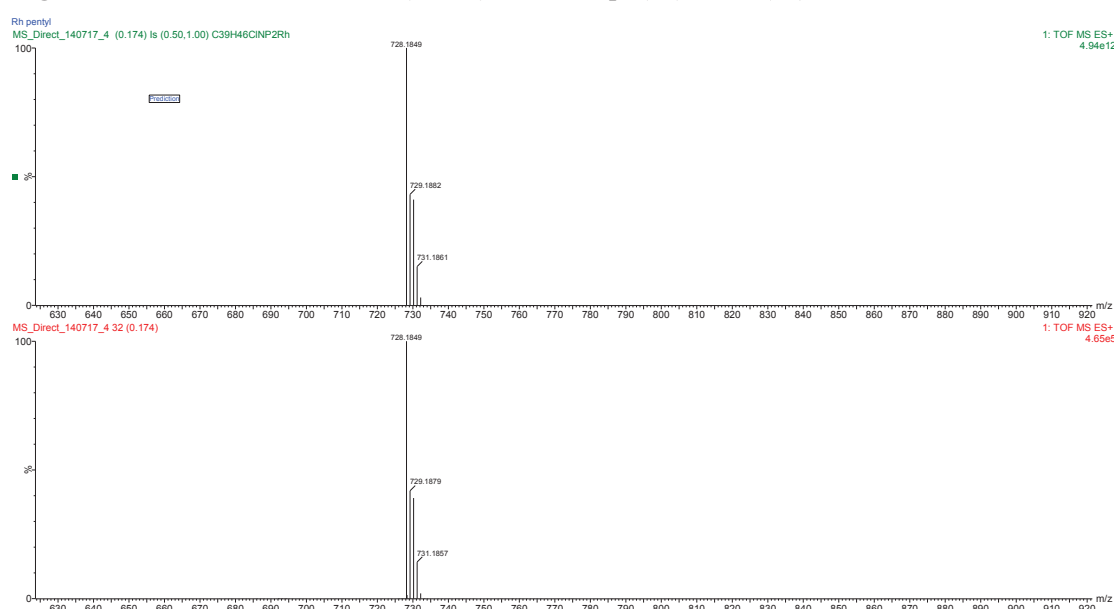


Figure B36. HRMS of $[\text{Ph}_2\text{PN}(\text{C}_5\text{H}_{11})\text{PPh}_2]\text{RhCp}^*(\text{Cl})^+\text{PF}_6^-$ (**2c**).

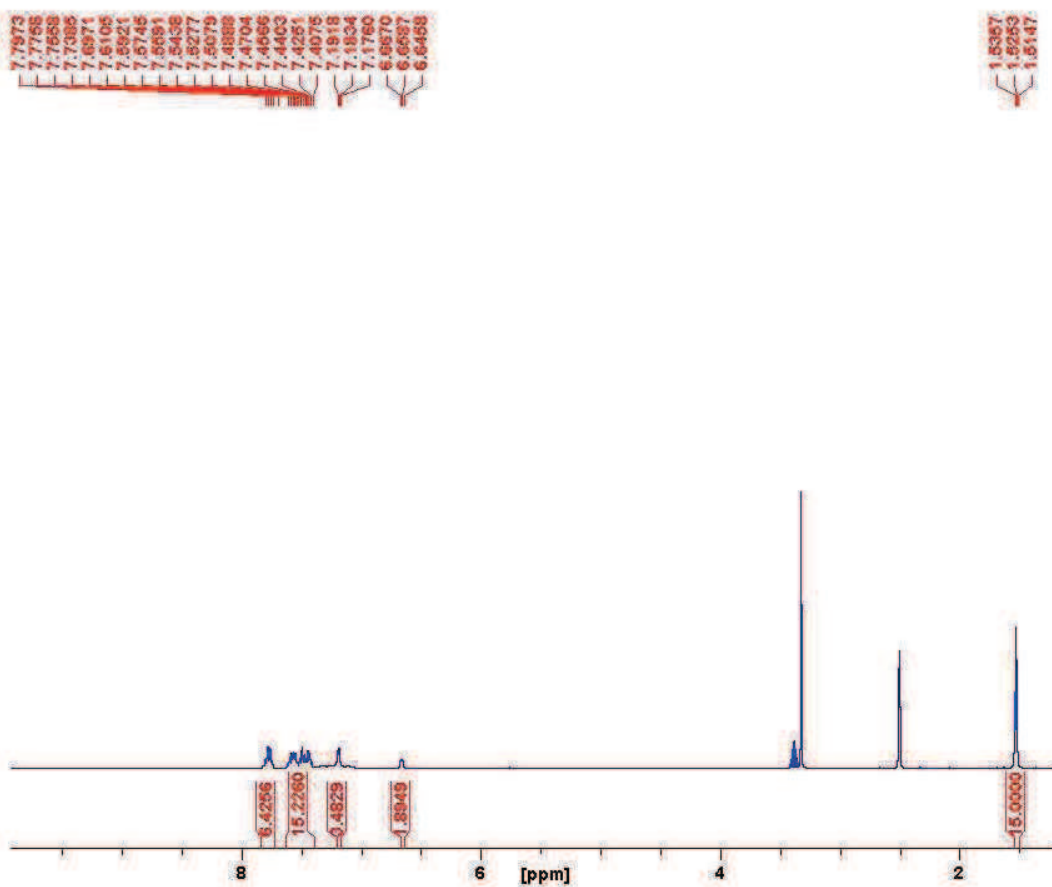


Figure B37. ¹H NMR of [Ph₂P(N(Ph)PPh₂)RhCp*(Cl)]⁺PF₆⁻ (**2d**).

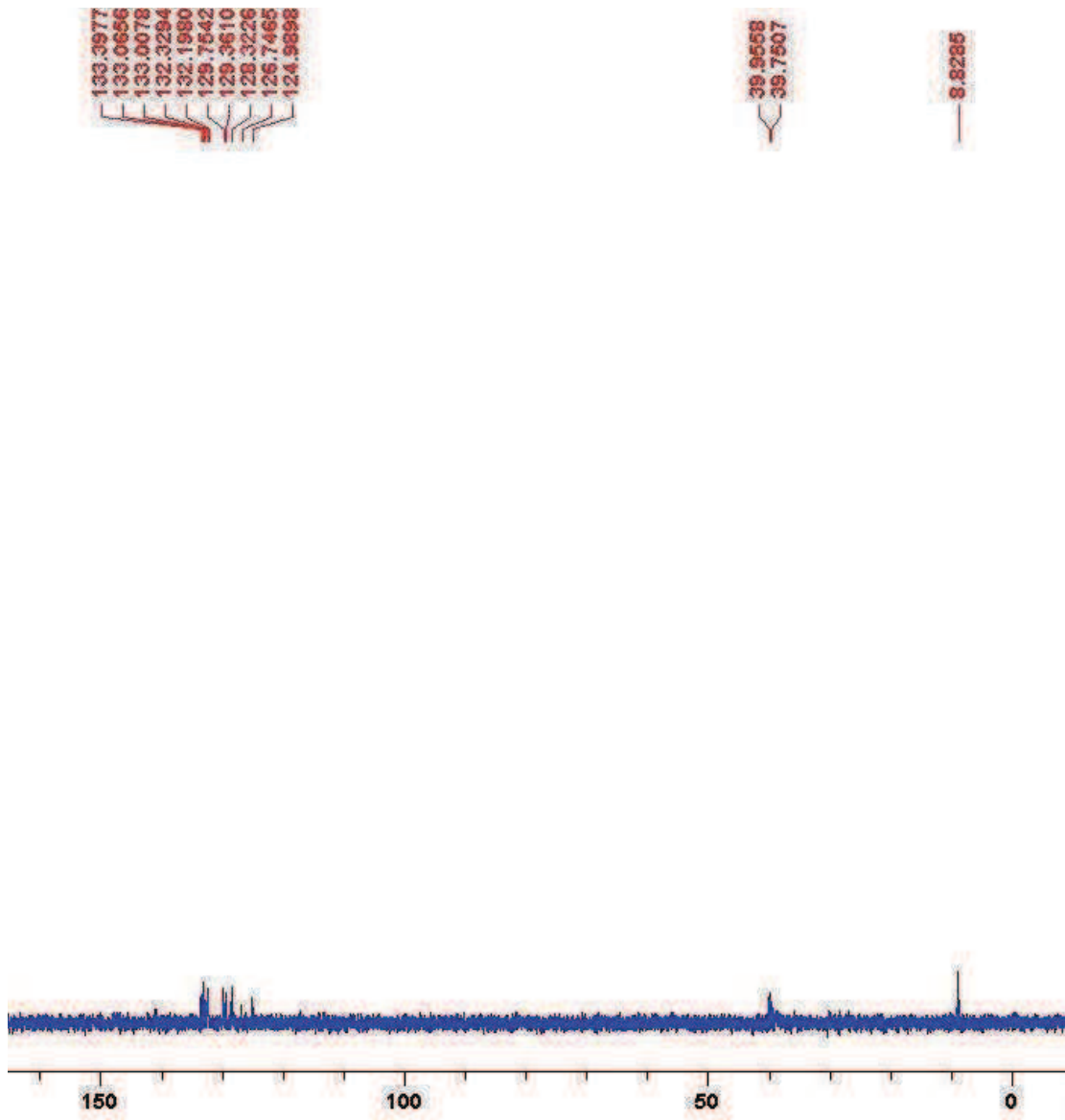


Figure B38. ^{13}C NMR of $[\text{Ph}_2\text{PN}(\text{Ph})\text{PPh}_2]\text{RhCp}^*(\text{Cl})^+\text{PF}_6^-$ (**2d**).

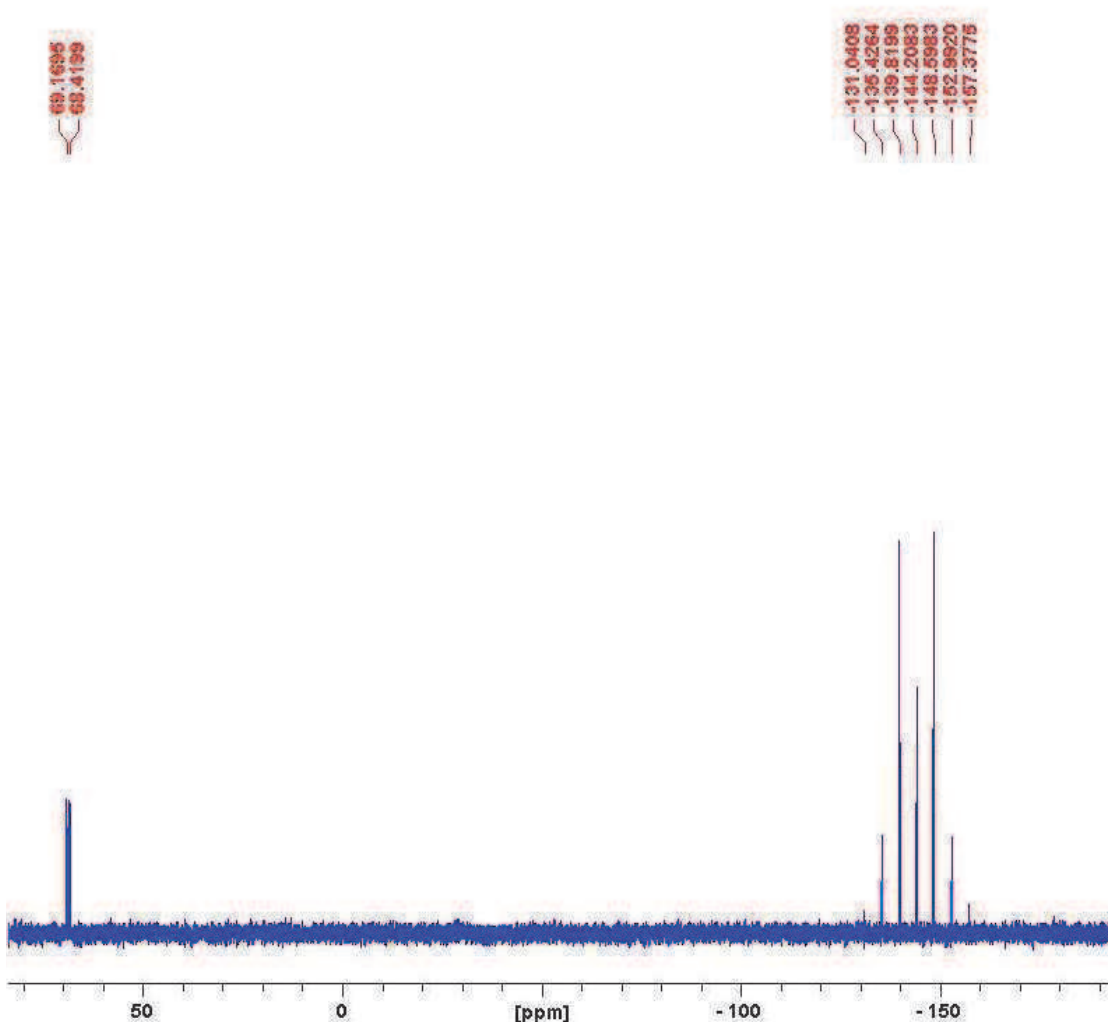


Figure B39. ^{31}P NMR of $[\text{Ph}_2\text{PN}(\text{Ph})\text{PPh}_2]\text{RhCp}^*(\text{Cl})]^+\text{PF}_6^-$ (**2d**).

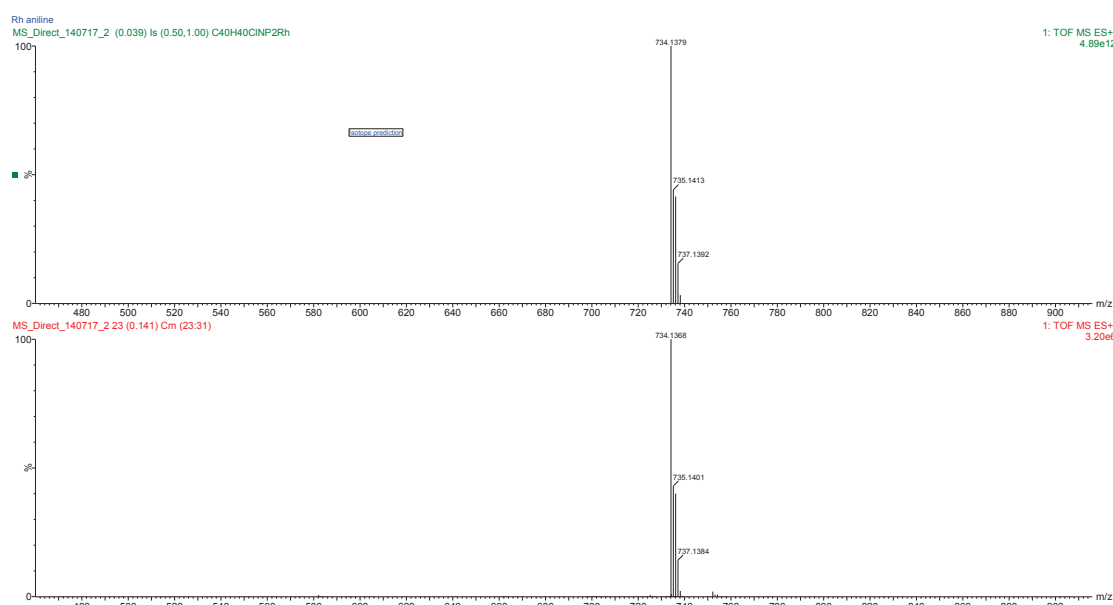


Figure B40. HRMS of $[\text{Ph}_2\text{PN}(\text{Ph})\text{PPh}_2]\text{RhCp}^*(\text{Cl})]^+\text{PF}_6^-$ (**2d**).

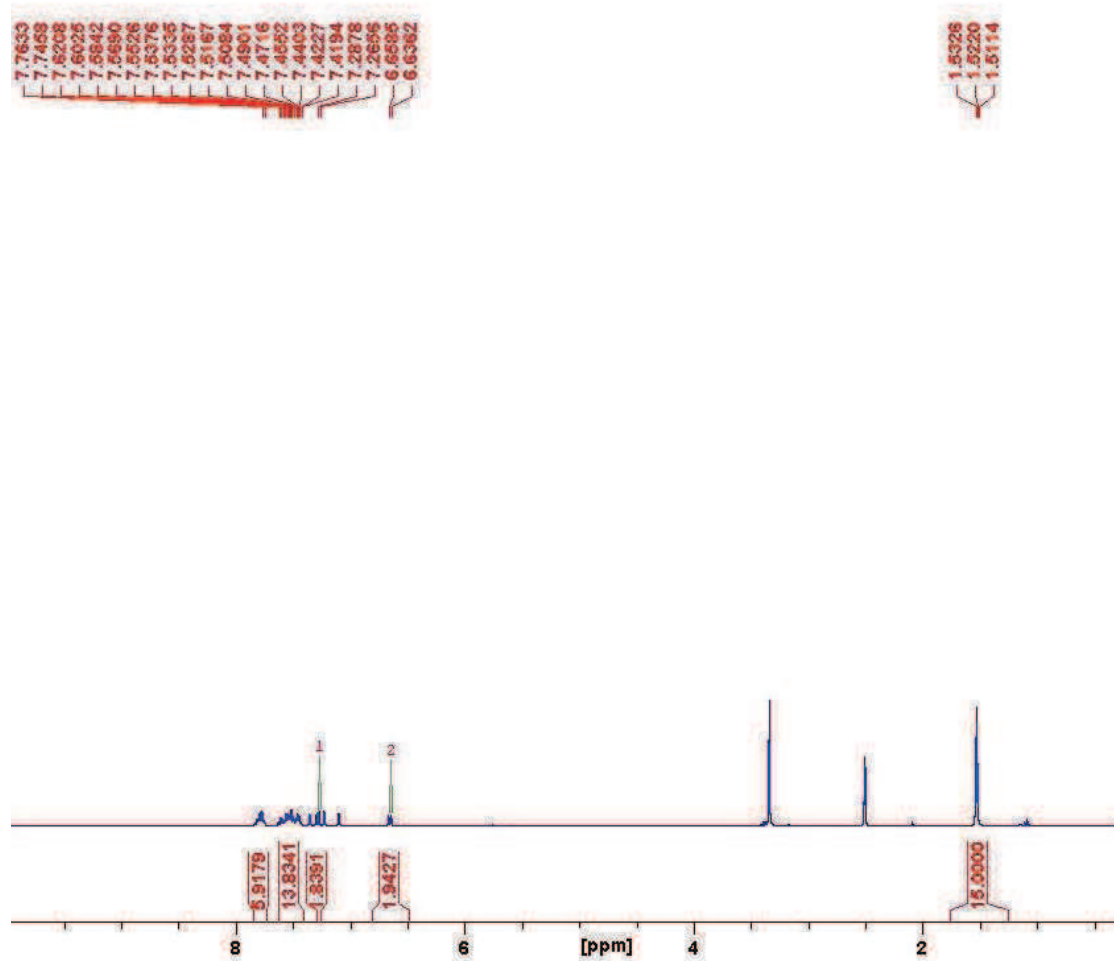


Figure B41. ¹H NMR of $[\text{Ph}_2\text{PN}(\text{C}_6\text{H}_4\text{Cl})\text{PPh}_2]\text{RhCp}^*(\text{Cl})^+\text{PF}_6^-$ (**2e**).

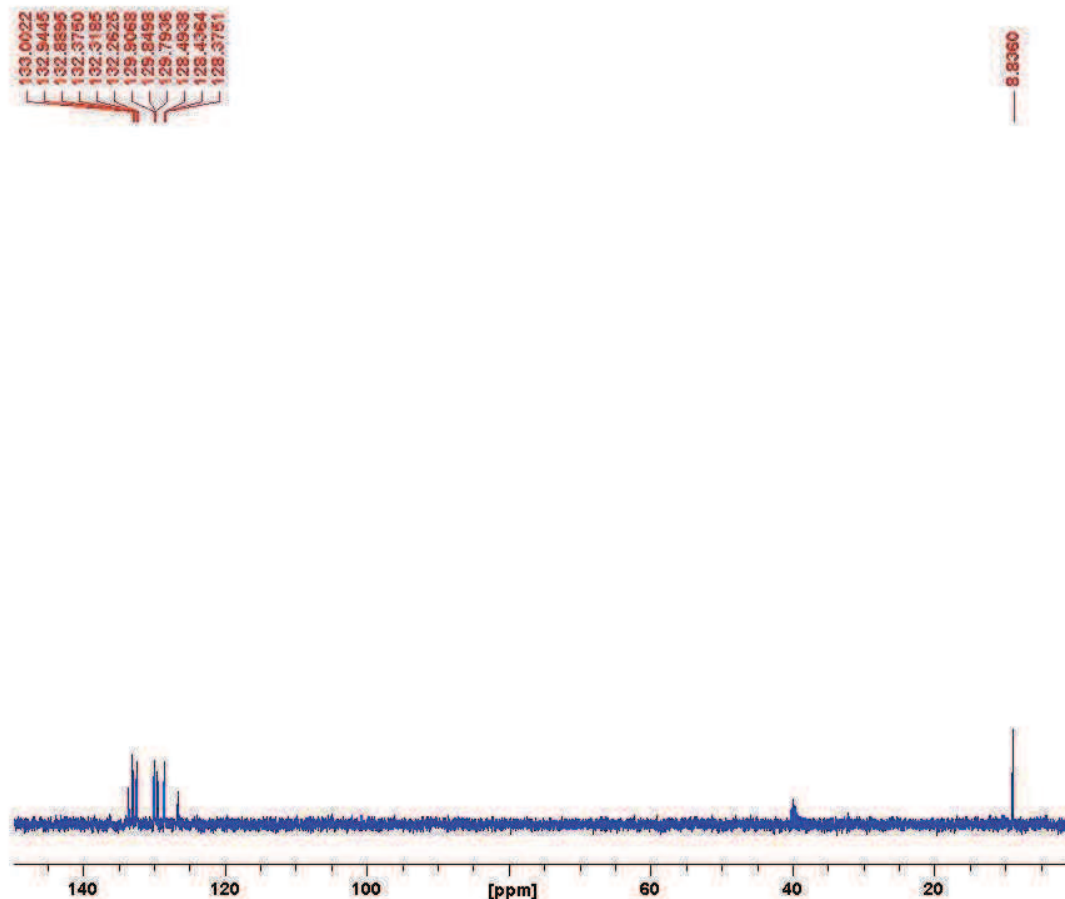


Figure B42. ^{13}C NMR of $[\text{Ph}_2\text{PN}(\text{C}_6\text{H}_4\text{Cl})\text{PPh}_2]\text{RhCp}^*(\text{Cl})^+\text{PF}_6^-$ (**2e**).

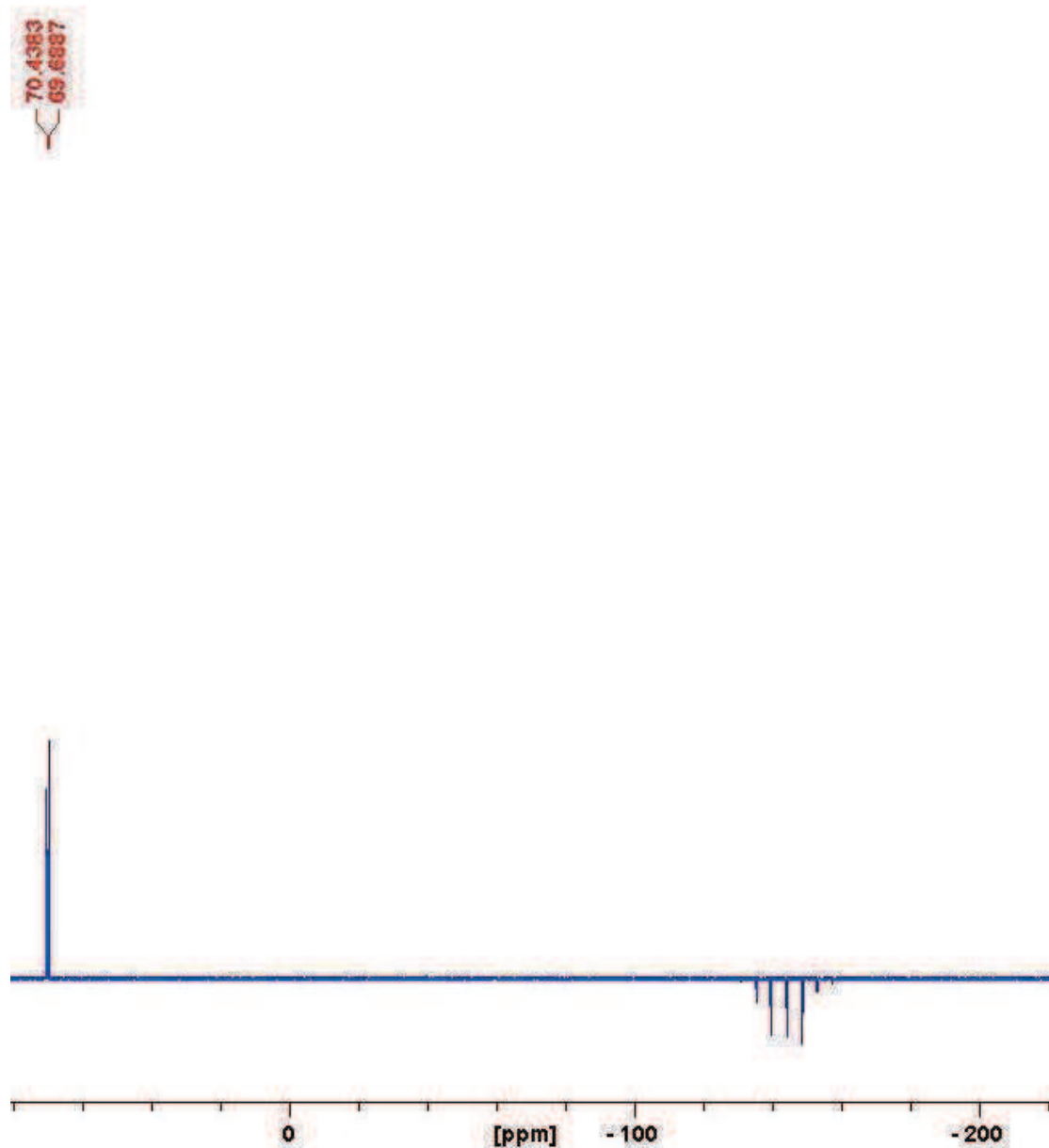


Figure B43. ^{31}P NMR of $[\text{Ph}_2\text{PN}(\text{C}_6\text{H}_4\text{Cl})\text{PPh}_2]\text{RhCp}^*(\text{Cl})^+\text{PF}_6^-$ (**2e**).

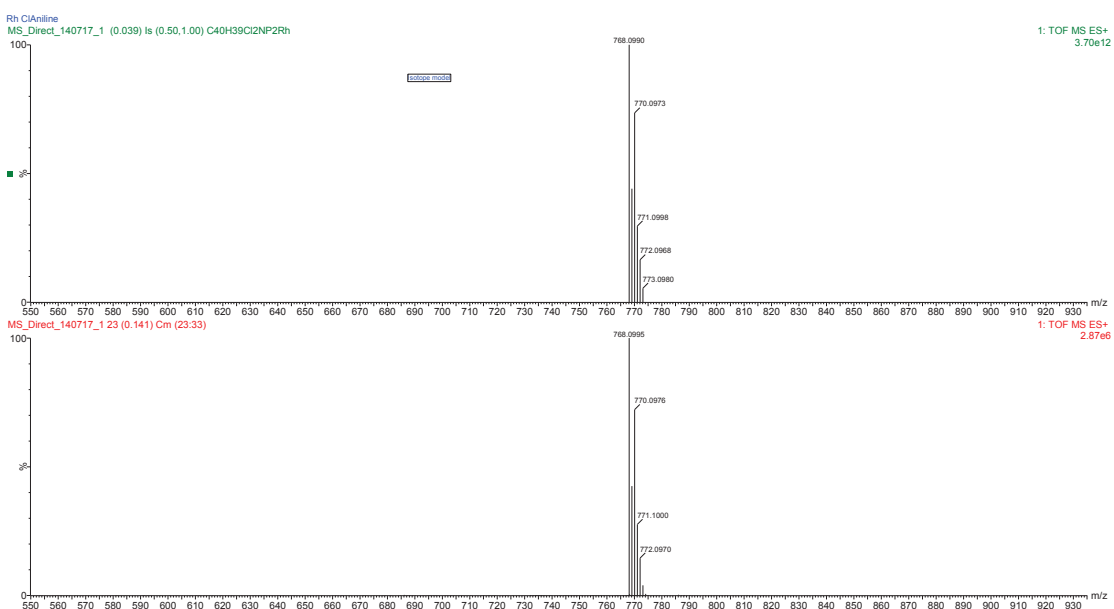


Figure B44. HRMS of $[\text{Ph}_2\text{PN}(\text{C}_6\text{H}_4\text{Cl})\text{PPh}_2]\text{RhCp}^*(\text{Cl})^+\text{PF}_6^-$ (**2e**).

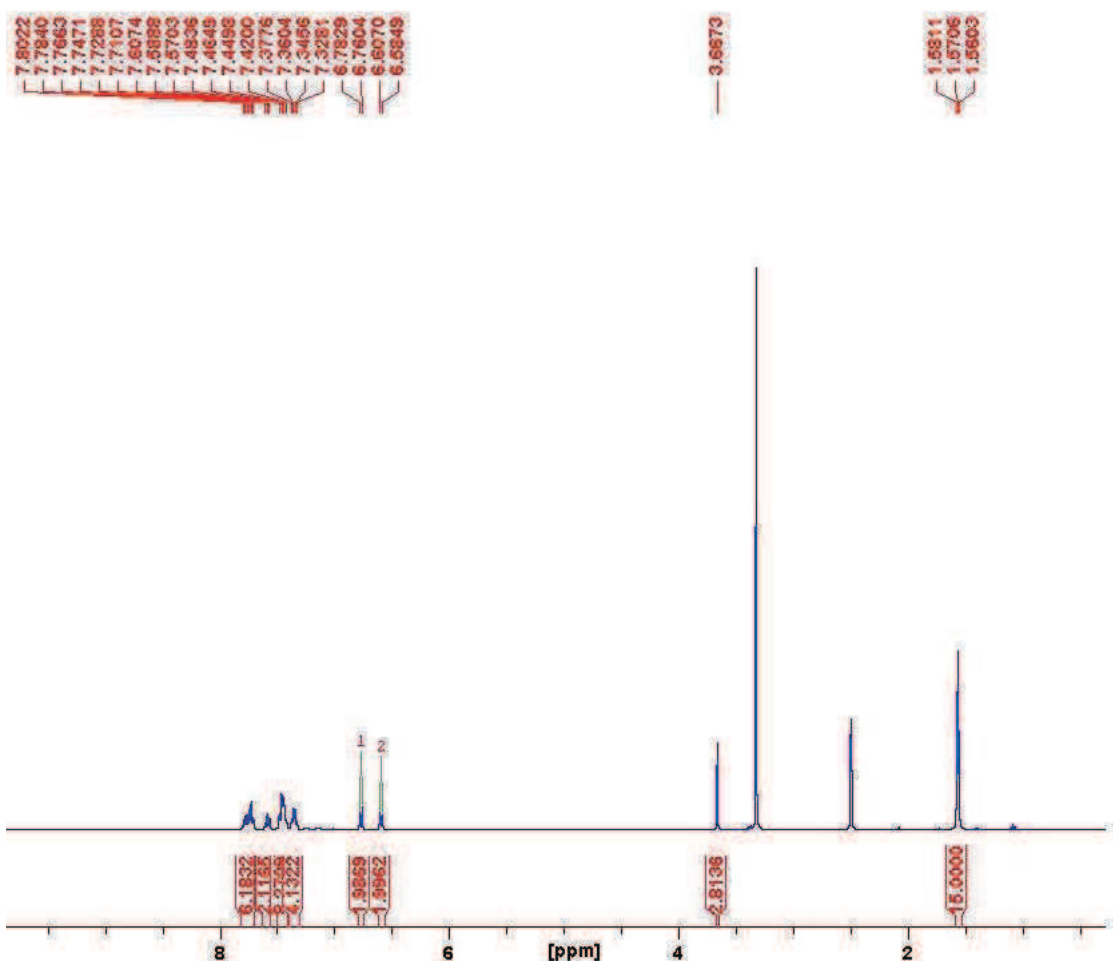


Figure B45. ¹H NMR of $[\text{Ph}_2\text{PN}(\text{C}_7\text{H}_7\text{O})\text{PPh}_2]\text{RhCp}^*(\text{Cl})^+\text{PF}_6^-$ (**2f**).

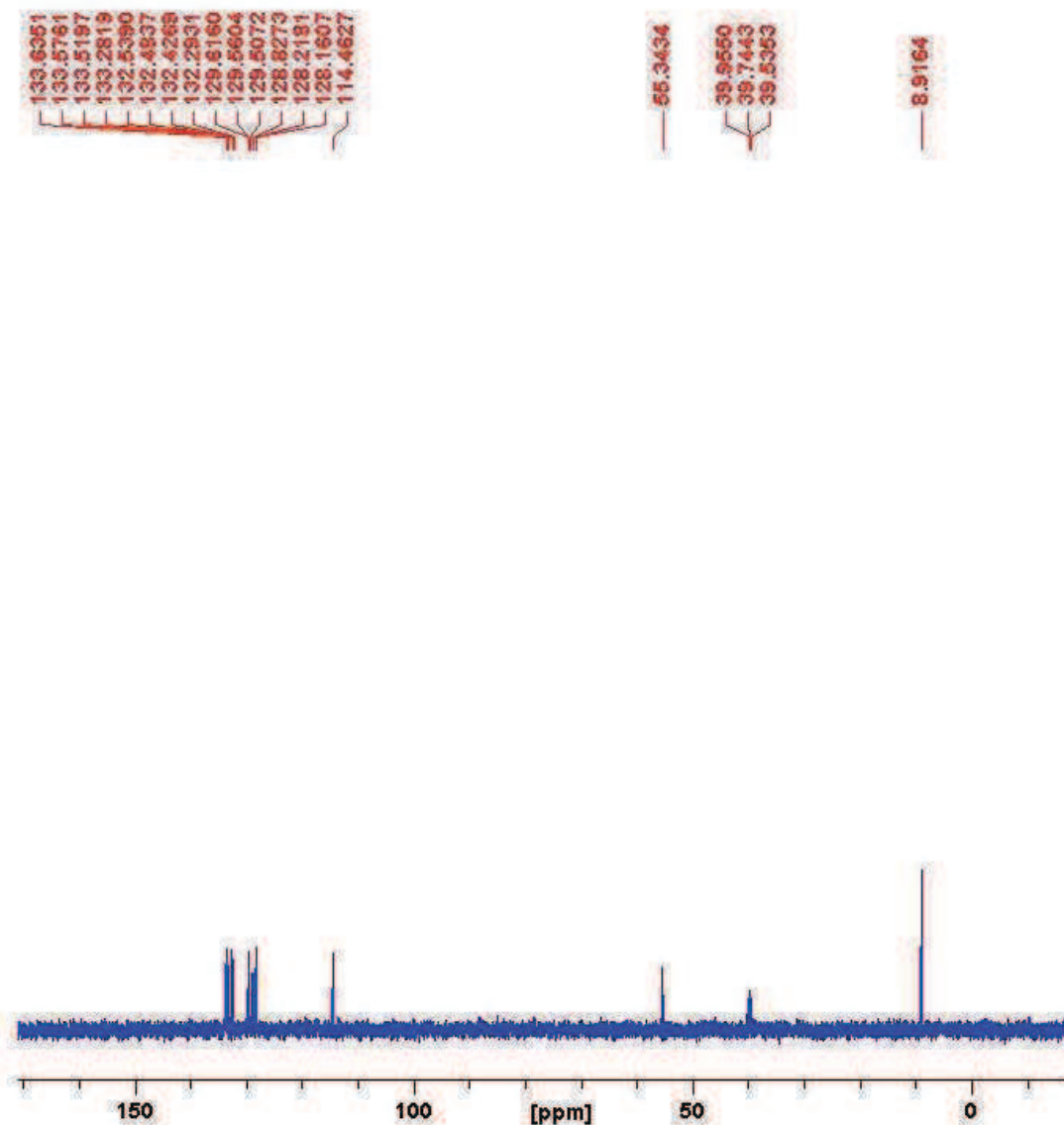


Figure B46. ^{13}C NMR of $[Ph_2PN(C_7H_7O)PPh_2]RhCp^*(Cl)^+PF_6^-$ (**2f**).

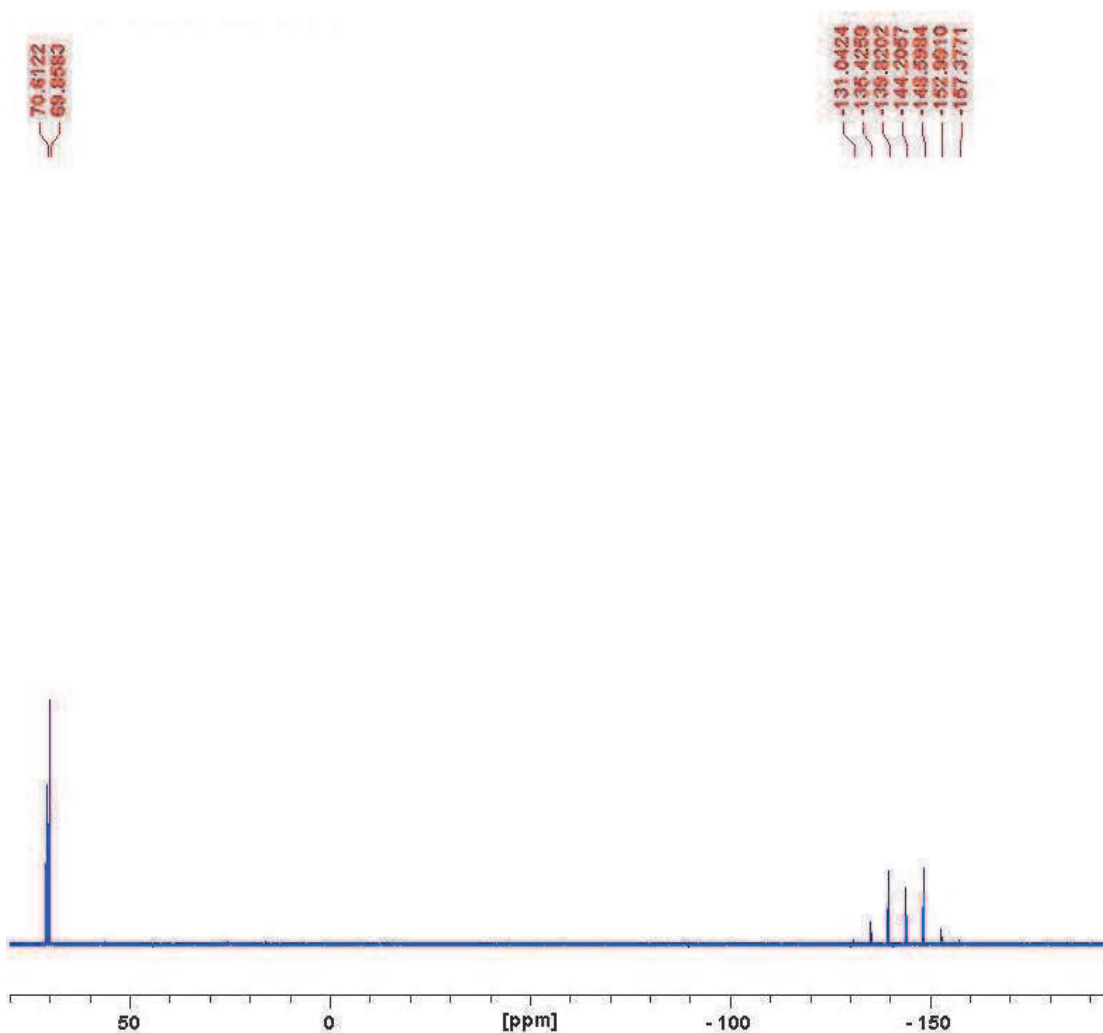


Figure B47. ^{31}P NMR of $[\text{Ph}_2\text{PN}(\text{C}_7\text{H}_7\text{O})\text{PPh}_2]\text{RhCp}^*(\text{Cl})]^+\text{PF}_6^-$ (**2f**).

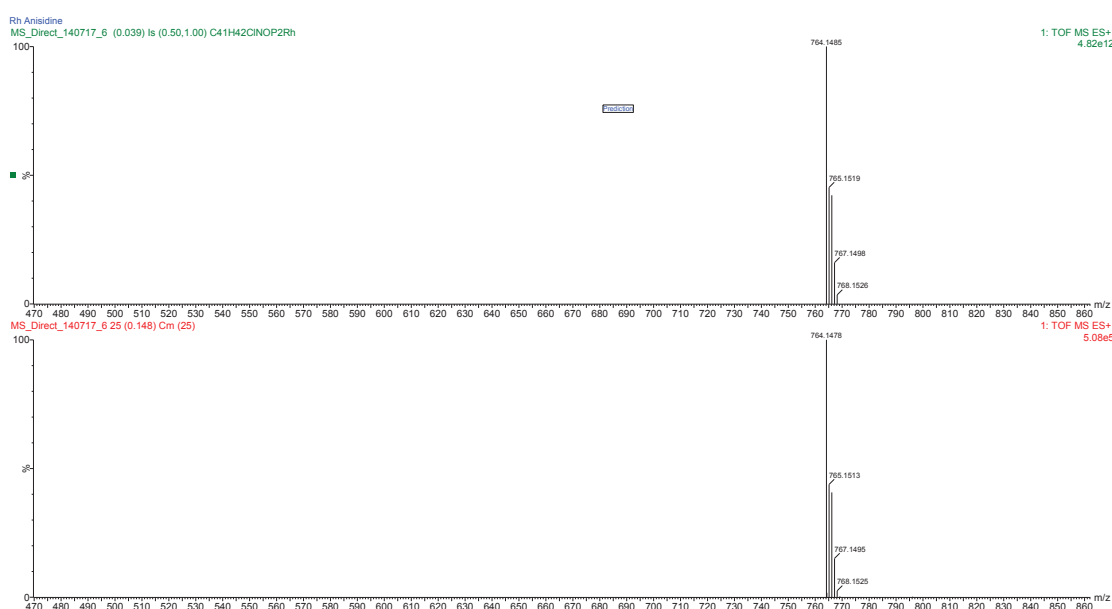


Figure B48. HRMS of $[\text{Ph}_2\text{PN}(\text{C}_7\text{H}_7\text{O})\text{PPh}_2]\text{RhCp}^*(\text{Cl})]^+\text{PF}_6^-$ (**2f**).

Crystal structure information for compound **1f**.

Table B1. Fractional Atomic Coordinates ($\times 10^4$) and Equivalent Isotropic Displacement Parameters ($\text{\AA}^2 \times 10^3$) for **1f** U_{eq} is defined as 1/3 of the trace of the orthogonalised U_{IJ} tensor.

Atom	x	y	z	$U(\text{eq})$
Ir1	1986.17(8)	2599.56(7)	1101.76(5)	18.18(4)
Cl1	3277.5(6)	2528.9(5)	2081.4(4)	31.45(18)
P1	3044.7(6)	3499.7(5)	689.5(4)	19.70(16)
P2	2983.9(6)	1581.8(5)	711.1(4)	20.11(16)
P3	-1453.6(8)	2617.6(7)	-2278.1(5)	42.9(2)
F1	-314.0(19)	2806(2)	-1924.6(13)	74.2(8)
F2	-2583(2)	2423(2)	-2621.3(15)	75.4(8)
F3	-1291(3)	1522(2)	-2100(3)	154(2)
F4	-1584(3)	3725(2)	-2462.9(16)	99.0(11)
F5	-1191(3)	2444(3)	-2936.6(16)	112.3(14)
F6	-1719(2)	2849(3)	-1641.2(14)	108.8(12)
O1	7384.6(17)	2352.4(16)	53.8(12)	35.5(6)
N1	3723.1(18)	2512.6(15)	590.8(12)	21.4(5)
C1	924(3)	3067(2)	1654.6(17)	30.8(7)
C2	721(2)	3594(2)	1072.3(17)	29.7(7)
C3	456(2)	2901(2)	543.5(16)	26.8(7)
C4	469(2)	1946(2)	827.5(15)	24.2(6)
C5	790(2)	2036(2)	1506.5(15)	26.6(7)
C6	1190(3)	3495(3)	2315.1(18)	45.8(10)
C7	703(3)	4676(2)	988(2)	45.8(10)
C8	32(3)	3172(3)	-146.5(17)	40.6(9)
C9	117(3)	1024(2)	471.9(17)	35.1(8)
C10	882(3)	1236(3)	1986.1(17)	39.8(9)
C11	2595(2)	4090(2)	-89.8(15)	23.2(6)
C12	2451(3)	3556(2)	-654.5(16)	32.8(8)
C13	2073(3)	4002(3)	-1242.7(18)	45.3(10)
C14	1829(3)	4978(3)	-1279.4(19)	43.2(9)
C15	1963(3)	5509(2)	-724.1(17)	35.0(8)
C16	2348(2)	5078(2)	-130.3(17)	29.7(7)
C17	3801(2)	4456(2)	1152.0(15)	26.5(7)

C18	3496(3)	4905(2)	1638.0(16)	35.8(8)
C19	3984(3)	5734(3)	1939.7(19)	49.7(12)
C20	4799(4)	6070(3)	1771(2)	61.6(15)
C21	5117(3)	5630(3)	1297(2)	54.7(13)
C22	4609(3)	4830(2)	968(2)	41.0(9)
C23	4650(2)	2471(2)	431.0(15)	24.2(6)
C24	5530(2)	2638(2)	912.5(15)	25.6(6)
C25	6425(2)	2598(2)	768.9(16)	28.7(7)
C26	6467(2)	2385(2)	147.0(17)	28.2(7)
C27	5601(3)	2203(2)	-328.1(16)	30.6(7)
C28	4696(2)	2246(2)	-181.5(16)	27.8(7)
C29	7441(3)	2112(3)	-581(2)	48.9(10)
C30	3707(2)	647(2)	1224.5(15)	25.1(7)
C31	4654(3)	369(2)	1216.6(17)	32.9(8)
C32	5122(3)	-396(2)	1606.2(18)	38.9(9)
C33	4646(3)	-882(2)	1991.3(18)	42.9(10)
C34	3703(3)	-614(2)	1999.4(17)	40.0(9)
C35	3229(3)	155(2)	1622.0(16)	31.6(8)
C36	2500(2)	971(2)	-56.1(14)	22.2(6)
C37	2968(3)	175(2)	-251.3(16)	33.5(8)
C38	2587(3)	-212(2)	-857.8(17)	40.1(9)
C39	1738(3)	157(2)	-1271.4(16)	37.4(9)
C40	1262(3)	939(2)	-1084.5(16)	31.9(8)
C41	1648(2)	1344(2)	-482.1(15)	26.1(7)

Table B2. Anisotropic Displacement Parameters ($\text{\AA}^2 \times 10^3$) for **1f**. The Anisotropic displacement factor exponent takes the form: $-2\pi^2[h^2a^*{}^2U_{11}+2hka^*b^*U_{12}+\dots]$.

Atom	U_{11}	U_{22}	U_{33}	U_{23}	U_{13}	U_{12}
Ir1	20.20(6)	16.73(6)	17.02(6)	-0.61(4)	4.09(4)	-0.46(4)
Cl1	35.3(4)	29.1(4)	22.7(4)	-0.6(3)	-4.3(3)	-0.5(3)
P1	20.3(4)	16.8(3)	21.3(4)	-0.1(3)	4.6(3)	-0.9(3)
P2	21.5(4)	16.6(3)	21.4(4)	0.0(3)	4.4(3)	1.0(3)
P3	41.5(6)	45.3(6)	44.5(6)	3.4(4)	16.3(5)	-3.3(4)
F1	45.8(16)	109(2)	66.0(19)	-8.2(16)	12.5(14)	-12.3(15)
F2	42.8(15)	101(2)	77(2)	14.9(15)	7.2(14)	-14.9(14)
F3	101(3)	53(2)	266(6)	45(3)	-22(3)	-0.1(18)

F4	124(3)	64.1(19)	104(3)	32.7(17)	23(2)	-2.3(18)
F5	72(2)	198(4)	75(2)	-63(2)	33.1(19)	-18(2)
F6	75(2)	216(4)	46.4(18)	12(2)	34.9(17)	0(2)
O1	27.4(13)	41.0(13)	42.8(15)	-7.9(11)	17.7(11)	-4.1(10)
N1	21.5(13)	17.8(12)	25.4(13)	-0.6(9)	7.3(10)	0.4(9)
C1	31.1(19)	31.5(17)	34.2(19)	-8.9(14)	16.1(16)	-3.4(13)
C2	21.9(17)	27.0(16)	43(2)	-2.0(14)	14.4(15)	3.0(12)
C3	21.0(16)	27.6(15)	33.1(18)	3.6(13)	9.7(14)	4.1(12)
C4	18.6(16)	29.8(16)	26.1(17)	-2.1(12)	9.1(13)	-4.9(12)
C5	27.3(18)	28.8(16)	26.3(17)	-3.6(12)	11.6(14)	-4.0(12)
C6	54(3)	51(2)	40(2)	-21.4(18)	25(2)	-10.1(19)
C7	35(2)	25.2(17)	81(3)	2.4(18)	22(2)	8.4(14)
C8	27(2)	52(2)	40(2)	17.9(17)	5.0(17)	10.3(16)
C9	37(2)	36.7(18)	30.8(19)	-5.2(14)	8.0(16)	-14.2(15)
C10	50(2)	42(2)	33(2)	6.1(15)	20.3(18)	-6.8(17)
C11	18.7(16)	23.3(14)	26.9(17)	4.3(12)	4.9(13)	-2.8(11)
C12	40(2)	26.5(16)	30.3(19)	3.3(13)	6.5(16)	0.9(14)
C13	64(3)	44(2)	24.2(19)	2.6(15)	6.0(19)	2.2(18)
C14	46(2)	44(2)	35(2)	17.4(16)	4.0(18)	-0.5(17)
C15	32(2)	29.6(17)	40(2)	13.5(15)	4.1(16)	0.9(14)
C16	29.7(19)	25.6(16)	33.5(19)	2.9(13)	8.4(15)	-0.6(13)
C17	24.3(17)	19.2(14)	29.8(18)	2.1(12)	-2.9(14)	-0.8(11)
C18	48(2)	24.4(16)	28.8(19)	-2.5(13)	0.4(16)	-2.4(14)
C19	72(3)	27.1(18)	35(2)	-5.9(15)	-11(2)	-1.0(18)
C20	65(3)	28(2)	64(3)	-0.6(19)	-29(3)	-13.2(19)
C21	33(2)	32(2)	87(4)	14(2)	-4(2)	-13.2(16)
C22	31(2)	28.4(17)	60(3)	7.0(16)	6.4(18)	-3.2(14)
C23	23.9(16)	21.0(14)	28.5(16)	1.0(12)	8.8(13)	1.3(11)
C24	25.9(16)	25.7(15)	26.2(16)	-2.6(12)	9.1(13)	0.6(12)
C25	24.2(16)	30.4(16)	29.8(17)	-4.5(13)	4.6(13)	-2.4(12)
C26	26.6(17)	23.5(15)	36.8(19)	-1.4(13)	12.8(14)	-1.3(12)
C27	34.8(19)	32.2(17)	28.3(18)	-3.9(13)	14.8(15)	-2.3(14)
C28	25.0(17)	29.4(16)	28.2(17)	-3.4(13)	5.9(13)	-2.4(12)
C29	41(2)	62(3)	54(3)	-7(2)	30(2)	-4.2(19)
C30	28.4(18)	19.8(14)	23.3(16)	-2.0(11)	0.7(14)	3.1(12)
C31	32(2)	25.8(16)	37(2)	-1.9(13)	3.3(16)	3.6(13)

C32	36(2)	27.3(17)	47(2)	-2.6(15)	-0.5(18)	8.8(14)
C33	59(3)	20.5(16)	35(2)	1.5(14)	-12.2(19)	5.5(15)
C34	56(3)	25.7(17)	32(2)	8.1(14)	3.0(18)	-3.7(16)
C35	36(2)	25.8(16)	29.9(19)	2.5(13)	4.0(15)	0.2(13)
C36	27.2(17)	19.0(14)	21.5(16)	-1.2(11)	8.7(13)	-1.1(11)
C37	43(2)	26.4(16)	30.3(19)	1.6(13)	9.3(16)	9.0(14)
C38	66(3)	25.9(17)	31(2)	-3.5(14)	17.0(19)	8.5(16)
C39	62(3)	27.9(17)	21.9(18)	-3.7(13)	11.8(18)	-8.6(16)
C40	38(2)	34.1(17)	22.6(17)	-0.2(13)	6.8(15)	-4.8(14)
C41	30.2(18)	25.2(15)	23.5(17)	0.0(12)	8.4(14)	0.9(12)

Table B3. Bond Lengths for **1f**.

Atom	Atom	Length/Å	Atom	Atom	Length/Å
Ir1	C3	2.197(3)	C4	C9	1.493(4)
Ir1	C2	2.226(3)	C5	C10	1.491(4)
Ir1	C5	2.233(3)	C11	C12	1.391(4)
Ir1	C4	2.236(3)	C11	C16	1.395(4)
Ir1	C1	2.244(3)	C12	C13	1.380(5)
Ir1	P1	2.2916(8)	C13	C14	1.379(5)
Ir1	P2	2.2958(8)	C14	C15	1.373(5)
Ir1	Cl1	2.3855(8)	C15	C16	1.383(4)
P1	N1	1.702(2)	C17	C18	1.383(5)
P1	C17	1.808(3)	C17	C22	1.398(5)
P1	C11	1.821(3)	C18	C19	1.395(5)
P1	P2	2.6325(10)	C19	C20	1.371(6)
P2	N1	1.709(2)	C20	C21	1.367(7)
P2	C30	1.815(3)	C21	C22	1.393(5)
P2	C36	1.818(3)	C23	C28	1.379(4)
P3	F3	1.553(3)	C23	C24	1.400(4)
P3	F6	1.555(3)	C24	C25	1.375(4)
P3	F4	1.568(3)	C25	C26	1.393(5)
P3	F2	1.579(3)	C26	C27	1.384(5)
P3	F5	1.584(3)	C27	C28	1.392(5)
P3	F1	1.595(3)	C30	C31	1.388(5)
O1	C26	1.358(4)	C30	C35	1.399(5)
O1	C29	1.435(4)	C31	C32	1.393(4)

N1	C23	1.436(4)		C32	C33	1.374(5)
C1	C2	1.412(5)		C33	C34	1.379(6)
C1	C5	1.450(4)		C34	C35	1.388(4)
C1	C6	1.495(5)		C36	C41	1.393(4)
C2	C3	1.455(4)		C36	C37	1.397(4)
C2	C7	1.495(4)		C37	C38	1.381(5)
C3	C4	1.444(4)		C38	C39	1.377(5)
C3	C8	1.496(5)		C39	C40	1.381(5)
C4	C5	1.419(4)		C40	C41	1.384(4)

Table B4. Bond Angles for **1f**.

Atom	Atom	Atom	Angle/ [°]	Atom	Atom	Atom	Angle/ [°]
C3	Ir1	C2	38.41(12)	C2	C1	Ir1	70.89(18)
C3	Ir1	C5	63.48(12)	C5	C1	Ir1	70.70(18)
C2	Ir1	C5	62.84(12)	C6	C1	Ir1	126.4(3)
C3	Ir1	C4	38.01(11)	C1	C2	C3	108.2(3)
C2	Ir1	C4	62.82(11)	C1	C2	C7	127.5(3)
C5	Ir1	C4	37.03(11)	C3	C2	C7	124.1(3)
C3	Ir1	C1	63.09(12)	C1	C2	Ir1	72.28(18)
C2	Ir1	C1	36.83(12)	C3	C2	Ir1	69.70(17)
C5	Ir1	C1	37.79(11)	C7	C2	Ir1	126.7(2)
C4	Ir1	C1	62.15(11)	C4	C3	C2	106.7(3)
C3	Ir1	P1	108.99(8)	C4	C3	C8	127.3(3)
C2	Ir1	P1	104.84(9)	C2	C3	C8	124.6(3)
C5	Ir1	P1	167.42(8)	C4	C3	Ir1	72.48(17)
C4	Ir1	P1	141.66(8)	C2	C3	Ir1	71.89(18)
C1	Ir1	P1	130.49(8)	C8	C3	Ir1	131.2(2)
C3	Ir1	P2	121.00(9)	C5	C4	C3	109.0(3)
C2	Ir1	P2	157.51(9)	C5	C4	C9	125.0(3)
C5	Ir1	P2	122.26(8)	C3	C4	C9	125.8(3)
C4	Ir1	P2	106.93(8)	C5	C4	Ir1	71.37(18)
C1	Ir1	P2	158.52(9)	C3	C4	Ir1	69.51(17)
P1	Ir1	P2	70.04(3)	C9	C4	Ir1	129.4(2)
C3	Ir1	Cl1	152.62(9)	C4	C5	C1	107.4(3)
C2	Ir1	Cl1	117.21(9)	C4	C5	C10	126.8(3)
C5	Ir1	Cl1	96.21(9)	C1	C5	C10	125.6(3)

C4	Ir1	Cl1	131.09(8)	C4	C5	Ir1	71.60(18)
C1	Ir1	Cl1	89.56(9)	C1	C5	Ir1	71.51(18)
P1	Ir1	Cl1	87.21(3)	C10	C5	Ir1	126.6(2)
P2	Ir1	Cl1	84.85(3)	C12	C11	C16	118.8(3)
N1	P1	C17	112.48(14)	C12	C11	P1	120.6(2)
N1	P1	C11	107.60(14)	C16	C11	P1	120.5(2)
C17	P1	C11	101.10(14)	C13	C12	C11	120.3(3)
N1	P1	Ir1	93.72(9)	C14	C13	C12	120.6(4)
C17	P1	Ir1	121.37(12)	C15	C14	C13	119.5(3)
C11	P1	Ir1	120.13(10)	C14	C15	C16	120.8(3)
N1	P1	P2	39.60(8)	C15	C16	C11	120.1(3)
C17	P1	P2	137.06(10)	C18	C17	C22	119.8(3)
C11	P1	P2	117.14(10)	C18	C17	P1	119.1(3)
Ir1	P1	P2	55.06(2)	C22	C17	P1	120.5(3)
N1	P2	C30	111.08(14)	C17	C18	C19	120.3(4)
N1	P2	C36	107.26(13)	C20	C19	C18	119.2(4)
C30	P2	C36	103.90(13)	C21	C20	C19	121.2(4)
N1	P2	Ir1	93.37(8)	C20	C21	C22	120.3(4)
C30	P2	Ir1	119.99(11)	C21	C22	C17	119.1(4)
C36	P2	Ir1	120.19(10)	C28	C23	C24	119.2(3)
N1	P2	P1	39.39(8)	C28	C23	N1	121.5(3)
C30	P2	P1	134.56(10)	C24	C23	N1	119.2(3)
C36	P2	P1	116.77(10)	C25	C24	C23	120.0(3)
Ir1	P2	P1	54.91(2)	C24	C25	C26	120.5(3)
F3	P3	F6	91.8(3)	O1	C26	C27	124.1(3)
F3	P3	F4	178.2(2)	O1	C26	C25	116.2(3)
F6	P3	F4	89.3(2)	C27	C26	C25	119.7(3)
F3	P3	F2	90.80(18)	C26	C27	C28	119.6(3)
F6	P3	F2	89.91(18)	C23	C28	C27	120.9(3)
F4	P3	F2	90.63(17)	C31	C30	C35	119.8(3)
F3	P3	F5	91.3(3)	C31	C30	P2	124.3(3)
F6	P3	F5	176.8(2)	C35	C30	P2	115.8(2)
F4	P3	F5	87.5(2)	C30	C31	C32	119.6(3)
F2	P3	F5	90.11(18)	C33	C32	C31	120.3(4)
F3	P3	F1	88.73(18)	C32	C33	C34	120.4(3)
F6	P3	F1	89.62(17)	C33	C34	C35	120.2(4)

F4	P3	F1	89.85(18)		C34	C35	C30	119.6(3)
F2	P3	F1	179.32(18)		C41	C36	C37	118.5(3)
F5	P3	F1	90.39(17)		C41	C36	P2	118.3(2)
C26	O1	C29	116.9(3)		C37	C36	P2	123.1(2)
C23	N1	P1	129.57(18)		C38	C37	C36	119.7(3)
C23	N1	P2	129.40(18)		C39	C38	C37	121.2(3)
P1	N1	P2	101.01(13)		C38	C39	C40	119.8(3)
C2	C1	C5	108.6(3)		C39	C40	C41	119.4(3)
C2	C1	C6	126.1(3)		C40	C41	C36	121.4(3)
C5	C1	C6	125.3(3)					

Table B5. Torsion Angles for **1f**.

A	B	C	D	Angle/ [°]	A	B	C	D	Angle/ [°]
C3	Ir	P			C5	Ir1	C3	C8	-160.5(3)
1	1		N1	-126.10(12)					
C2	Ir	P			C4	Ir1	C3	C8	-124.6(4)
1	1		N1	-166.10(13)					
C5	Ir	P			C1	Ir1	C3	C8	157.0(3)
1	1		N1	-177.4(4)					
C4	Ir	P			P1	Ir1	C3	C8	30.4(3)
1	1		N1	-101.38(15)					
C1	Ir	P			P2	Ir1	C3	C8	-47.2(3)
1	1		N1	163.50(15)					
P2	Ir	P			C11	Ir1	C3	C8	154.0(2)
1	1		N1	-9.07(9)					
C11	Ir	P			C2	C3	C4	C5	-3.5(4)
1	1		N1	76.46(9)					
C3	Ir	P	C1		C8	C3	C4	C5	-170.4(3)
1	1	7		114.65(15)					
C2	Ir	P	C1		Ir1	C3	C4	C5	60.7(2)
1	1	7		74.65(15)					
C5	Ir	P	C1		C2	C3	C4	C9	171.4(3)
1	1	7		63.4(4)					
C4	Ir	P	C1		C8	C3	C4	C9	4.5(5)
1	1	7		139.38(17)					
C1	Ir	P	C1	44.26(17)	Ir1	C3	C4	C9	-124.4(3)

	1	1	7						
P2	Ir	P	C1	-128.32(12)	C2	C3	C4	Ir1	-64.2(2)
	1	1	7						
Cl1	Ir	P	C1	-42.78(12)	C8	C3	C4	Ir1	128.9(3)
	1	1	7						
C3	Ir	P	C1	-13.26(15)	C3	Ir1	C4	C5	-119.5(3)
	1	1	1						
C2	Ir	P	C1	-53.26(15)	C2	Ir1	C4	C5	-80.1(2)
	1	1	1						
C5	Ir	P	C1	-64.5(4)	C1	Ir1	C4	C5	-38.41(19)
	1	1	1						
C4	Ir	P	C1	11.46(18)	P1	Ir1	C4	C5	-159.45(14)
	1	1	1						
C1	Ir	P	C1	-83.66(17)	P2	Ir1	C4	C5	121.52(17)
	1	1	1						
P2	Ir	P	C1	103.77(12)	Cl1	Ir1	C4	C5	23.4(2)
	1	1	1						
Cl1	Ir	P	C1	-170.70(12)	C2	Ir1	C4	C3	39.35(18)
	1	1	1						
C3	Ir	P	P2	-117.03(9)	C5	Ir1	C4	C3	119.5(3)
	1	1							
C2	Ir	P	P2	-157.03(10)	C1	Ir1	C4	C3	81.1(2)
	1	1							
C5	Ir	P	P2	-168.3(4)	P1	Ir1	C4	C3	-40.0(2)
	1	1							
C4	Ir	P	P2	-92.30(13)	P2	Ir1	C4	C3	-118.99(17)
	1	1							
C1	Ir	P	P2	172.58(12)	Cl1	Ir1	C4	C3	142.90(15)
	1	1							
Cl1	Ir	P	P2	85.53(3)	C3	Ir1	C4	C9	120.1(4)
	1	1							
C3	Ir	P	N1	109.72(13)	C2	Ir1	C4	C9	159.4(3)
	1	2							
C2	Ir	P	N1	89.5(2)	C5	Ir1	C4	C9	-120.5(4)
	1	2							
C5	Ir	P	N1	-173.97(13)	C1	Ir1	C4	C9	-158.9(3)

	1	2								
C4	Ir	P	N1	148.65(12)	P1	Ir1	C4	C9	80.1(3)	
1	2									
C1	Ir	P	N1	-155.4(3)	P2	Ir1	C4	C9	1.1(3)	
1	2									
P1	Ir	P	N1	9.03(9)	Cl1	Ir1	C4	C9	-97.1(3)	
1	2									
Cl1	Ir	P	N1	-79.87(9)	C3	C4	C5	C1	3.4(4)	
1	2									
C3	Ir	P	C3	-133.53(15)	C9	C4	C5	C1	-171.5(3)	
1	2	0								
C2	Ir	P	C3	-153.7(2)	Ir1	C4	C5	C1	63.0(2)	
1	2	0								
C5	Ir	P	C3	-57.22(16)	C3	C4	C5	C1 0	178.1(3)	
1	2	0								
C4	Ir	P	C3	-94.61(15)	C9	C4	C5	C1 0	3.2(5)	
1	2	0								
C1	Ir	P	C3	-38.7(3)	Ir1	C4	C5	C1 0	-122.4(3)	
1	2	0								
P1	Ir	P	C3	125.77(12)	C3	C4	C5	Ir1	-59.6(2)	
1	2	0								
Cl1	Ir	P	C3	36.88(12)	C9	C4	C5	Ir1	125.5(3)	
1	2	0								
C3	Ir	P	C3	-2.49(15)	C2	C1	C5	C4	-2.0(4)	
1	2	6								
C2	Ir	P	C3	-22.7(3)	C6	C1	C5	C4	175.5(3)	
1	2	6								
C5	Ir	P	C3	73.82(15)	Ir1	C1	C5	C4	-63.0(2)	
1	2	6								
C4	Ir	P	C3	36.43(14)	C2	C1	C5	C1 0	-176.7(3)	
1	2	6								
C1	Ir	P	C3	92.4(3)	C6	C1	C5	C1 0	0.8(6)	
1	2	6								
P1	Ir	P	C3	-103.18(11)	Ir1	C1	C5	C1 0	122.2(3)	
1	2	6								
Cl1	Ir	P	C3	167.92(11)	C2	C1	C5	Ir1	61.1(2)	

	1	2	6						
C3	Ir	P							
	1	2	P1	100.69(10)		C6	C1	C5	Ir1 -121.5(4)
C2	Ir	P							
	1	2	P1	80.5(2)		C3	Ir1	C5	C4 36.80(18)
C5	Ir	P							
	1	2	P1	177.00(10)		C2	Ir1	C5	C4 80.1(2)
C4	Ir	P							
	1	2	P1	139.62(9)		C1	Ir1	C5	C4 116.3(3)
C1	Ir	P							
	1	2	P1	-164.4(2)		P1	Ir1	C5	C4 92.3(4)
C11	Ir	P							
	1	2	P1	-88.90(3)		P2	Ir1	C5	C4 -74.65(19)
C1	P	P							
7	1	2	N1	-65.3(2)		C11	Ir1	C5	C4 -162.47(17)
C1	P	P							
1	1	2	N1	85.03(18)		C3	Ir1	C5	C1 -79.5(2)
Ir1	P	P							
	1	2	N1	-165.71(14)		C2	Ir1	C5	C1 -36.25(19)
N1	P	P	C3						
	1	2	0	66.2(2)		C4	Ir1	C5	C1 -116.3(3)
C1	P	P	C3						
7	1	2	0	0.9(2)		P1	Ir1	C5	C1 -24.0(5)
C1	P	P	C3						
1	1	2	0	151.22(19)		P2	Ir1	C5	C1 169.03(16)
Ir1	P	P	C3						
	1	2	0	-99.52(16)		C11	Ir1	C5	C1 81.22(18)
N1	P	P	C3						
	1	2	6	-84.79(18)		C3	Ir1	C5	C1 159.4(3)
C1	P	P	C3						
7	1	2	6	-150.1(2)		C2	Ir1	C5	C1 0 -157.3(3)
C1	P	P	C3						
1	1	2	6	0.24(17)		C4	Ir1	C5	C1 0 122.6(4)
Ir1	P	P	C3						
	1	2	6	109.51(12)		C1	Ir1	C5	C1 0 -121.1(4)
N1	P	P	Ir1	165.71(14)		P1	Ir1	C5	C1 -145.1(3)

	1	2				3	8		
C6	C	C	C3	-177.7(3)	P1	N1	C2 3	C2 4	79.4(3)
	1	2							
Ir1	C	C	C3	60.7(2)	P2	N1	C2 3	C2 4	-102.7(3)
	1	2							
C5	C	C	C7	175.9(3)	C2 8	C2 3	C2 4	C2 5	1.4(4)
	1	2							
C6	C	C	C7	-1.5(6)	N1	C2 3	C2 4	C2 5	179.8(3)
	1	2							
Ir1	C	C	C7	-123.1(3)	C2 3	C2 4	C2 5	C2 6	-0.5(4)
	1	2							
C5	C	C	Ir1	-60.9(2)	C2 9	O1	C2 6	C2 7	0.0(4)
	1	2							
C6	C	C	Ir1	121.6(4)	C2 9	O1	C2 6	C2 5	178.6(3)
	1	2							
C3	Ir	C	C1	118.0(3)	C2 4	C2 5	C2 6	O1	-179.4(3)
	1	2							
C5	Ir	C	C1	37.19(18)	C2 4	C2 5	C2 6	C2 7	-0.7(5)
	1	2							
C4	Ir	C	C1	79.0(2)	O1	C2 6	C2 7	C2 8	179.4(3)
	1	2							
P1	Ir	C	C1	-140.07(17)	C2 5	C2 6	C2 7	C2 8	0.8(5)
	1	2							
P2	Ir	C	C1	146.40(19)	C2 4	C2 3	C2 8	C2 7	-1.2(4)
	1	2							
Cl1	Ir	C	C1	-45.5(2)	N1	C2 3	C2 8	C2 7	-179.6(3)
	1	2							
C5	Ir	C	C3	-80.76(19)	C2 6	C2 7	C2 8	C2 3	0.1(5)
	1	2							
C4	Ir	C	C3	-38.93(17)	N1	P2 0	C3 1	C3 1	-36.0(3)
	1	2							
C1	Ir	C	C3	-118.0(3)	C3 6	P2 0	C3 1	C3 1	79.0(3)
	1	2							
P1	Ir	C	C3	101.98(17)	Ir1	P2 0	C3 1	C3 1	-143.1(2)
	1	2							
P2	Ir	C	C3	28.5(3)	P1	P2	C3 C3	C3 C3	-74.5(3)

	1	2				0	1
C11	Ir	C	C3	-163.45(15)	N1	P2	C3 C3 147.6(2)
	1	2			0	5	
C3	Ir	C	C7	-118.0(4)	C3	P2	C3 C3 -97.4(3)
	1	2			6	0	5
C5	Ir	C	C7	161.2(4)	Ir1	P2	C3 C3 40.4(3)
	1	2			0	5	
C4	Ir	C	C7	-157.0(4)	P1	P2	C3 C3 109.1(2)
	1	2			0	5	
C1	Ir	C	C7	124.0(4)	C3	C3	C3 C3 -0.1(5)
	1	2			5	0	1 2
P1	Ir	C	C7	-16.0(3)	P2	C3	C3 C3 -176.4(2)
	1	2			0	1	2
P2	Ir	C	C7	-89.6(4)	C3	C3	C3 C3 0.7(5)
	1	2			0	1	2 3
C11	Ir	C	C7	78.5(3)	C3	C3	C3 C3 -0.4(5)
	1	2			1	2	3 4
C1	C	C	C4	2.3(4)	C3	C3	C3 C3 -0.6(5)
	2	3			2	3	4 5
C7	C	C	C4	-174.1(3)	C3	C3	C3 C3 1.2(5)
	2	3			3	4	5 0
Ir1	C	C	C4	64.6(2)	C3	C3	C3 C3 -0.8(5)
	2	3			1	0	5 4
C1	C	C	C8	169.6(3)	P2	C3	C3 C3 175.8(3)
	2	3			0	5	4
C7	C	C	C8	-6.7(5)	N1	P2	C3 C4 -85.3(3)
	2	3			6	1	
Ir1	C	C	C8	-128.0(3)	C3	P2	C3 C4 157.0(2)
	2	3			0	6	1
C1	C	C	Ir1	-62.4(2)	Ir1	P2	C3 C4 19.3(3)
	2	3			6	1	
C7	C	C	Ir1	121.3(3)	P1	P2	C3 C4 -43.9(3)
	2	3			6	1	
C2	Ir	C	C4	-114.8(3)	N1	P2	C3 C3 91.4(3)
	1	3			6	7	
C5	Ir	C	C4	-35.87(17)	C3	P2	C3 C3 -26.3(3)

	1	3			0		6	7	
C1	Ir	C	C4	-78.38(19)	Ir1	P2	C3	C3	-164.0(2)
	1	3					6	7	
P1	Ir	C	C4	155.08(15)	P1	P2	C3	C3	132.8(2)
	1	3					6	7	
P2	Ir	C	C4	77.46(18)	C4	C3	C3	C3	0.7(5)
	1	3			1	6	7	8	
Cl1	Ir	C	C4	-81.4(2)	P2	C3	C3	C3	-176.0(3)
	1	3				6	7	8	
C5	Ir	C	C2	78.94(19)	C3	C3	C3	C3	-1.4(6)
	1	3			6	7	8	9	
C4	Ir	C	C2	114.8(3)	C3	C3	C3	C4	1.0(6)
	1	3			7	8	9	0	
C1	Ir	C	C2	36.43(18)	C3	C3	C4	C4	0.2(5)
	1	3			8	9	0	1	
P1	Ir	C	C2	-90.11(18)	C3	C4	C4	C3	-0.9(5)
	1	3			9	0	1	6	
P2	Ir	C	C2	-167.73(15)	C3	C3	C4	C4	0.5(5)
	1	3			7	6	1	0	
Cl1	Ir	C	C2	33.4(3)	P2	C3	C4	C4	177.4(2)
	1	3				6	1	0	
C2	Ir	C	C8	120.6(4)					
	1	3							

Table B6. Hydrogen Atom Coordinates ($\text{\AA} \times 10^4$) and Isotropic Displacement Parameters ($\text{\AA}^2 \times 10^3$) for **1f**.

Atom	x	y	z	U(eq)
H6A	1429	4163	2300	69
H6B	1710	3101	2600	69
H6C	604	3502	2478	69
H7A	27	4917	931	69
H7B	925	4841	609	69
H7C	1146	4979	1370	69
H8A	-56	2583	-413	61
H8B	485	3620	-278	61
H8C	-609	3492	-201	61

H9A	538	482	679	53
H9B	148	1088	27	53
H9C	-569	898	476	53
H10A	392	1332	2228	60
H10B	1549	1244	2283	60
H10C	765	608	1763	60
H12	2614	2883	-635	39
H13	1979	3632	-1626	54
H14	1571	5281	-1686	52
H15	1790	6180	-748	42
H16	2444	5455	250	36
H18	2952	4647	1767	43
H19	3755	6063	2258	60
H20	5150	6618	1989	74
H21	5687	5871	1190	66
H22	4809	4543	624	49
H24	5509	2779	1338	31
H25	7020	2717	1096	34
H27	5624	2048	-752	37
H28	4102	2119	-508	33
H29A	7133	1475	-706	73
H29B	8137	2088	-586	73
H29C	7092	2609	-884	73
H31	4982	699	947	40
H32	5774	-583	1606	47
H33	4969	-1405	2254	52
H34	3376	-958	2264	48
H35	2584	348	1634	38
H37	3546	-97	32	40
H38	2916	-744	-992	48
H39	1480	-126	-1684	45
H40	675	1196	-1367	38
H41	1325	1888	-357	31

Crystal structure information for compound **2f**.

Table B7. Fractional Atomic Coordinates ($\times 10^4$) and Equivalent Isotropic Displacement Parameters ($\text{\AA}^2 \times 10^3$) for **2f**. U_{eq} is defined as 1/3 of the trace of the orthogonalised U_{ij} tensor.

Atom	x	y	z	U(eq)
Rh1	3014.90(19)	7595.53(18)	3894.88(13)	23.75(10)
Cl1	1721.7(7)	7522.6(6)	2922.4(4)	36.1(2)
P1	1965.6(6)	8501.4(6)	4316.3(4)	24.4(2)
P2	2019.6(6)	6573.5(6)	4293.0(4)	24.3(2)
P3	6447.0(9)	7384.8(8)	2276.3(6)	47.1(3)
F1	5307(2)	7199(3)	1920.5(14)	81.0(9)
F2	7576(2)	7581(2)	2626.2(16)	83.3(10)
F3	6573(3)	6271(2)	2457.5(17)	107.5(12)
F4	6289(3)	8485(3)	2119(3)	169(2)
F5	6174(3)	7540(3)	2937.0(17)	116.3(15)
F6	6709(2)	7179(3)	1636.5(15)	115.4(14)
O2	-2385.1(18)	7371.4(18)	4941.4(13)	39.2(7)
N1	1291(2)	7509.7(18)	4413.2(14)	27.3(7)
C1	4065(3)	8073(3)	3349.5(19)	34.6(9)
C2	4268(3)	8594(3)	3932(2)	36.2(9)
C3	4538(3)	7895(3)	4451.2(19)	32.2(9)
C4	4527(2)	6942(3)	4170.9(18)	30.0(8)
C5	4201(3)	7031(3)	3493.2(17)	30.0(8)
C6	3800(3)	8495(3)	2688(2)	53.5(12)
C7	4286(3)	9671(3)	4014(2)	50.4(12)
C8	4961(3)	8168(3)	5137.8(19)	44.4(10)
C9	4891(3)	6017(3)	4523.1(19)	41.5(10)
C10	4110(3)	6242(3)	3011.3(19)	45.2(11)
C11	2414(2)	9088(3)	5095.5(17)	28.3(8)
C12	2556(3)	8554(3)	5661.4(18)	38.2(9)
C13	2934(3)	8995(3)	6246(2)	50.3(11)
C14	3186(3)	9969(3)	6294(2)	46.7(11)
C15	3047(3)	10508(3)	5735(2)	42.2(10)
C16	2659(3)	10077(3)	5143.0(19)	35.9(9)
C17	1203(3)	9465(2)	3854.3(18)	31.2(9)

C18	1497(3)	9900(3)	3363.8(19)	41.1(10)
C19	1001(4)	10724(3)	3059(2)	58.3(13)
C20	199(4)	11067(3)	3223(3)	68.2(16)
C21	-117(3)	10626(3)	3713(3)	65.2(15)
C22	398(3)	9835(3)	4041(2)	46.5(11)
C23	354(2)	7470(2)	4570.7(18)	27.3(8)
C24	-520(3)	7642(2)	4092.5(18)	29.5(8)
C25	-1420(3)	7610(2)	4226.6(18)	32.3(8)
C26	-1458(3)	7395(2)	4849.4(19)	31.3(8)
C27	-588(3)	7214(3)	5328.9(19)	33.5(9)
C28	308(3)	7252(3)	5183.1(18)	33.0(9)
C29	-2444(3)	7135(3)	5578(2)	52.0(12)
C30	1299(3)	5639(2)	3780.7(17)	28.6(8)
C31	344(3)	5367(3)	3788.8(19)	37.7(9)
C32	-126(3)	4602(3)	3399(2)	48.1(11)
C33	341(3)	4110(3)	3015(2)	48.2(11)
C34	1287(3)	4368(3)	3010(2)	46.3(11)
C35	1755(3)	5144(3)	3386.4(18)	36.2(9)
C36	2496(3)	5965(2)	5061.1(16)	27.1(8)
C37	2031(3)	5169(3)	5259.2(19)	39.3(10)
C38	2419(3)	4781(3)	5865.8(19)	44.8(11)
C39	3266(3)	5147(3)	6276.9(19)	40.6(10)
C40	3736(3)	5930(3)	6087.7(18)	37.1(9)
C41	3349(3)	6337(3)	5480.3(17)	32.0(9)

Table B8. Anisotropic Displacement Parameters ($\text{\AA}^2 \times 10^3$) for **2f**. The Anisotropic displacement factor exponent takes the form: $-2\pi^2[h^2a^*a^2U_{11} + 2hka^*b^*U_{12} + \dots]$.

Atom	U ₁₁	U ₂₂	U ₃₃	U ₂₃	U ₁₃	U ₁₂
Rh1	24.99(15)	24.17(16)	21.50(15)	0.59(12)	5.36(11)	0.45(12)
Cl1	40.1(5)	34.2(5)	26.4(5)	0.4(4)	-4.1(4)	-0.1(4)
P1	24.4(5)	22.8(5)	25.1(5)	-0.4(4)	5.1(4)	0.8(4)
P2	25.4(5)	22.4(5)	24.3(5)	-0.3(4)	5.2(4)	-0.7(4)
P3	44.3(6)	51.0(7)	48.9(7)	3.8(6)	17.5(6)	-4.1(5)
F1	50.6(17)	119(3)	70(2)	-5.7(18)	11.1(15)	-14.9(16)
F2	48.9(17)	113(3)	81(2)	13.5(17)	5.9(16)	-14.5(15)
F3	140(3)	65(2)	112(3)	30(2)	25(2)	-6(2)

F4	113(3)	57(2)	288(6)	44(3)	-26(3)	2(2)
F5	81(2)	198(4)	79(2)	-57(2)	38(2)	-23(2)
F6	83(2)	225(4)	50(2)	12(2)	36.2(18)	-9(3)
O2	29.3(14)	51.0(17)	41.9(16)	7.1(13)	17.5(13)	3.2(12)
N1	26.2(15)	23.0(16)	33.4(17)	-2.3(13)	9.5(13)	-0.8(12)
C1	32(2)	39(2)	38(2)	13.9(19)	18.1(19)	4.2(17)
C2	28(2)	32(2)	52(3)	-0.4(19)	17(2)	-5.6(16)
C3	22.0(19)	38(2)	37(2)	-2.7(18)	8.4(17)	-1.1(16)
C4	25.2(19)	33(2)	34(2)	2.2(17)	12.8(17)	6.5(16)
C5	26.5(19)	40(2)	27(2)	1.2(17)	13.6(17)	9.8(16)
C6	65(3)	54(3)	49(3)	22(2)	29(2)	12(2)
C7	45(3)	27(2)	82(4)	1(2)	22(2)	-5.1(18)
C8	35(2)	51(3)	45(3)	-13(2)	8(2)	-8.3(19)
C9	43(2)	43(2)	38(2)	8.7(19)	11(2)	16.8(19)
C10	60(3)	44(3)	36(3)	-8.2(19)	21(2)	4(2)
C11	23.1(19)	32(2)	29(2)	-5.6(16)	4.9(16)	2.4(15)
C12	45(2)	36(2)	32(2)	0.2(18)	6.7(19)	3.0(18)
C13	64(3)	52(3)	29(2)	-2(2)	4(2)	0(2)
C14	49(3)	52(3)	31(3)	-19(2)	-2(2)	1(2)
C15	44(2)	30(2)	49(3)	-13(2)	6(2)	0.1(18)
C16	39(2)	28(2)	40(2)	-4.6(17)	8.6(19)	-0.8(17)
C17	28(2)	21.8(19)	35(2)	-2.6(16)	-5.2(17)	2.0(15)
C18	54(3)	30(2)	33(2)	1.9(18)	0(2)	-1.9(19)
C19	87(4)	32(2)	40(3)	5(2)	-11(3)	3(2)
C20	73(4)	34(3)	69(4)	3(3)	-30(3)	12(3)
C21	39(3)	35(3)	106(5)	-19(3)	-6(3)	15(2)
C22	35(2)	32(2)	67(3)	-6(2)	6(2)	4.4(18)
C23	26.3(18)	22.6(18)	35(2)	0.5(16)	12.5(16)	-0.8(14)
C24	30.6(19)	29(2)	30(2)	3.2(16)	9.7(16)	1.3(15)
C25	28.3(19)	35(2)	33(2)	5.1(17)	6.1(16)	2.2(16)
C26	30.3(19)	25.0(19)	43(2)	2.3(17)	17.8(18)	3.2(15)
C27	40(2)	31(2)	34(2)	7.3(17)	18.3(19)	5.1(16)
C28	30(2)	37(2)	30(2)	2.8(17)	6.3(17)	0.5(16)
C29	42(3)	68(3)	55(3)	9(2)	27(2)	5(2)
C30	29(2)	21.4(18)	30(2)	1.1(15)	-0.6(17)	-1.8(15)
C31	36(2)	30(2)	43(3)	0.6(18)	3.9(19)	-6.3(17)

C32	39(2)	37(2)	58(3)	5(2)	-4(2)	-10.9(19)
C33	58(3)	26(2)	45(3)	-3.6(19)	-13(2)	-5(2)
C34	60(3)	37(2)	37(3)	-7.2(19)	4(2)	5(2)
C35	40(2)	31(2)	35(2)	-1.3(18)	7.5(19)	-0.5(17)
C36	33(2)	24.0(19)	25(2)	-2.1(15)	8.3(17)	0.3(15)
C37	53(3)	31(2)	34(2)	-1.6(18)	11(2)	-12.0(18)
C38	74(3)	26(2)	36(3)	3.1(18)	17(2)	-11(2)
C39	61(3)	34(2)	27(2)	2.2(18)	14(2)	6(2)
C40	44(2)	41(2)	25(2)	-0.4(18)	6.7(19)	4.4(18)
C41	35(2)	31(2)	32(2)	1.7(17)	12.5(18)	-0.6(16)

Table B9. Bond Lengths for **2f**.

Atom	Atom	Length/Å	Atom	Atom	Length/Å
Rh1	C3	2.188(4)	C4	C9	1.497(5)
Rh1	C2	2.214(3)	C5	C10	1.486(5)
Rh1	C5	2.220(3)	C11	C12	1.396(5)
Rh1	C1	2.226(3)	C11	C16	1.397(5)
Rh1	C4	2.230(3)	C12	C13	1.373(5)
Rh1	P1	2.2999(9)	C13	C14	1.380(6)
Rh1	P2	2.3078(9)	C14	C15	1.389(6)
Rh1	Cl1	2.3785(9)	C15	C16	1.382(5)
P1	N1	1.703(3)	C17	C18	1.377(5)
P1	C17	1.819(4)	C17	C22	1.397(5)
P1	C11	1.821(4)	C18	C19	1.394(5)
P1	P2	2.6463(13)	C19	C20	1.356(7)
P2	N1	1.706(3)	C20	C21	1.396(7)
P2	C30	1.813(3)	C21	C22	1.388(6)
P2	C36	1.819(4)	C23	C28	1.379(5)
P3	F4	1.549(4)	C23	C24	1.394(5)
P3	F6	1.555(3)	C24	C25	1.373(5)
P3	F3	1.575(3)	C25	C26	1.397(5)
P3	F2	1.583(3)	C26	C27	1.392(5)
P3	F5	1.595(3)	C27	C28	1.381(5)
P3	F1	1.596(3)	C30	C35	1.379(5)
O2	C26	1.372(4)	C30	C31	1.396(5)
O2	C29	1.442(5)	C31	C32	1.396(5)

N1	C23	1.448(4)		C32	C33	1.370(6)
C1	C2	1.411(5)		C33	C34	1.379(6)
C1	C5	1.463(5)		C34	C35	1.392(5)
C1	C6	1.496(5)		C36	C41	1.387(5)
C2	C3	1.448(5)		C36	C37	1.398(5)
C2	C7	1.488(5)		C37	C38	1.385(5)
C3	C4	1.439(5)		C38	C39	1.372(5)
C3	C8	1.491(5)		C39	C40	1.381(5)
C4	C5	1.419(5)		C40	C41	1.396(5)

Table B10. Bond Angles for **2f**.

Atom	Atom	Atom	Angle/ [°]	Atom	Atom	Atom	Angle/ [°]
C3	Rh1	C2	38.40(14)	C2	C1	Rh1	71.0(2)
C3	Rh1	C5	63.64(14)	C5	C1	Rh1	70.57(18)
C2	Rh1	C5	63.60(14)	C6	C1	Rh1	126.6(3)
C3	Rh1	C1	63.11(14)	C1	C2	C3	107.8(3)
C2	Rh1	C1	37.06(14)	C1	C2	C7	127.1(4)
C5	Rh1	C1	38.42(14)	C3	C2	C7	124.9(4)
C3	Rh1	C4	38.00(14)	C1	C2	Rh1	71.9(2)
C2	Rh1	C4	63.24(13)	C3	C2	Rh1	69.82(19)
C5	Rh1	C4	37.19(12)	C7	C2	Rh1	127.4(3)
C1	Rh1	C4	62.61(13)	C4	C3	C2	107.6(3)
C3	Rh1	P1	108.42(10)	C4	C3	C8	127.2(4)
C2	Rh1	P1	103.93(10)	C2	C3	C8	123.9(4)
C5	Rh1	P1	167.35(10)	C4	C3	Rh1	72.6(2)
C1	Rh1	P1	129.95(10)	C2	C3	Rh1	71.8(2)
C4	Rh1	P1	141.00(10)	C8	C3	Rh1	131.3(3)
C3	Rh1	P2	120.59(10)	C5	C4	C3	108.8(3)
C2	Rh1	P2	156.79(11)	C5	C4	C9	124.7(3)
C5	Rh1	P2	122.12(10)	C3	C4	C9	126.3(3)
C1	Rh1	P2	159.15(11)	C5	C4	Rh1	71.01(19)
C4	Rh1	P2	106.60(9)	C3	C4	Rh1	69.39(19)
P1	Rh1	P2	70.11(3)	C9	C4	Rh1	130.2(3)
C3	Rh1	Cl1	152.96(10)	C4	C5	C1	106.9(3)
C2	Rh1	Cl1	117.70(11)	C4	C5	C10	127.3(3)
C5	Rh1	Cl1	96.36(10)	C1	C5	C10	125.5(3)

C1	Rh1	Cl1	89.88(10)	C4	C5	Rh1	71.80(19)
C4	Rh1	Cl1	131.37(10)	C1	C5	Rh1	71.01(18)
P1	Rh1	Cl1	87.58(3)	C10	C5	Rh1	126.9(3)
P2	Rh1	Cl1	84.96(3)	C12	C11	C16	118.2(3)
N1	P1	C17	112.62(15)	C12	C11	P1	120.9(3)
N1	P1	C11	107.54(16)	C16	C11	P1	120.9(3)
C17	P1	C11	101.08(16)	C13	C12	C11	120.4(4)
N1	P1	Rh1	93.23(10)	C12	C13	C14	121.5(4)
C17	P1	Rh1	121.22(13)	C13	C14	C15	118.6(4)
C11	P1	Rh1	120.70(11)	C16	C15	C14	120.6(4)
N1	P1	P2	39.13(9)	C15	C16	C11	120.7(4)
C17	P1	P2	136.97(12)	C18	C17	C22	120.2(4)
C11	P1	P2	117.05(12)	C18	C17	P1	119.0(3)
Rh1	P1	P2	55.09(3)	C22	C17	P1	120.4(3)
N1	P2	C30	111.58(15)	C17	C18	C19	120.1(4)
N1	P2	C36	106.95(15)	C20	C19	C18	120.0(5)
C30	P2	C36	103.89(16)	C19	C20	C21	120.6(4)
N1	P2	Rh1	92.88(10)	C22	C21	C20	119.9(4)
C30	P2	Rh1	119.63(12)	C21	C22	C17	119.1(4)
C36	P2	Rh1	120.84(12)	C28	C23	C24	119.3(3)
N1	P2	P1	39.05(9)	C28	C23	N1	121.3(3)
C30	P2	P1	134.75(12)	C24	C23	N1	119.4(3)
C36	P2	P1	116.52(11)	C25	C24	C23	120.8(3)
Rh1	P2	P1	54.81(3)	C24	C25	C26	119.5(3)
F4	P3	F6	92.0(3)	O2	C26	C27	124.1(3)
F4	P3	F3	177.3(3)	O2	C26	C25	115.7(3)
F6	P3	F3	90.5(2)	C27	C26	C25	120.1(3)
F4	P3	F2	90.24(19)	C28	C27	C26	119.4(3)
F6	P3	F2	90.42(18)	C23	C28	C27	120.9(4)
F3	P3	F2	90.89(19)	C35	C30	C31	119.2(3)
F4	P3	F5	90.7(3)	C35	C30	P2	116.8(3)
F6	P3	F5	177.2(2)	C31	C30	P2	123.9(3)
F3	P3	F5	86.8(2)	C32	C31	C30	119.3(4)
F2	P3	F5	90.15(19)	C33	C32	C31	120.8(4)
F4	P3	F1	89.1(2)	C32	C33	C34	120.1(4)
F6	P3	F1	89.50(18)	C33	C34	C35	119.5(4)

F3	P3	F1	89.74(19)		C30	C35	C34	121.0(4)
F2	P3	F1	179.36(19)		C41	C36	C37	118.6(3)
F5	P3	F1	89.96(18)		C41	C36	P2	117.8(3)
C26	O2	C29	116.8(3)		C37	C36	P2	123.6(3)
C23	N1	P1	129.2(2)		C38	C37	C36	119.8(4)
C23	N1	P2	129.0(2)		C39	C38	C37	121.4(4)
P1	N1	P2	101.82(15)		C38	C39	C40	119.5(4)
C2	C1	C5	108.8(3)		C39	C40	C41	119.8(4)
C2	C1	C6	126.7(4)		C36	C41	C40	121.0(3)
C5	C1	C6	124.4(4)					

Table B11. Torsion Angles for **2f**.

A	B	C	D	Angle/ [°]	A	B	C	D	Angle/ [°]
C3	Rh	P			C5	Rh			
1	1		N1	-126.03(15)	1	C3	C8		-160.5(4)
C2	Rh	P			C1	Rh			
1	1		N1	-165.82(15)	1	C3	C8		156.3(4)
C5	Rh	P			C4	Rh			
1	1		N1	-175.2(4)	1	C3	C8		-124.6(5)
C1	Rh	P			P1	Rh			
1	1		N1	164.03(17)	1	C3	C8		30.1(4)
C4	Rh	P			P2	Rh			
1	1		N1	-101.34(18)	1	C3	C8		-47.2(4)
P2	Rh	P			Cl1	Rh			
1	1		N1	-9.29(11)	1	C3	C8		153.8(3)
Cl1	Rh	P			C2	C3	C4	C5	
1	1		N1	76.22(11)					-3.4(4)
C3	Rh	P	C1		C8	C3	C4	C5	
1	1	7		114.98(17)					-170.6(3)
C2	Rh	P	C1		Rh				
1	1	7		75.20(18)	1	C3	C4	C5	
C5	Rh	P	C1						60.3(2)
1	1	7		65.8(5)	C2	C3	C4	C9	
C1	Rh	P	C1						171.0(3)
1	1	7		45.05(19)	C8	C3	C4	C9	
C4	Rh	P	C1	139.7(2)					3.7(6)
					Rh	C3	C4	C9	-125.3(3)

	1	1	7		1				
P2	Rh	P	C1	-128.27(14)	C2	C3	C4	Rh	-63.7(2)
	1	1	7		1				
Cl1	Rh	P	C1	-42.77(14)	C8	C3	C4	Rh	129.0(4)
	1	1	7		1				
C3	Rh	P	C1	-13.41(18)	C3	Rh	C4	C5	-119.6(3)
	1	1	1		1				
C2	Rh	P	C1	-53.20(18)	C2	Rh	C4	C5	-80.8(2)
	1	1	1		1				
C5	Rh	P	C1	-62.6(5)	C1	Rh	C4	C5	-39.0(2)
	1	1	1		1				
C1	Rh	P	C1	-83.35(19)	P1	Rh	C4	C5	-159.64(17)
	1	1	1		1				
C4	Rh	P	C1	11.3(2)	P2	Rh	C4	C5	121.7(2)
	1	1	1		1				
P2	Rh	P	C1	103.33(14)	Cl1	Rh	C4	C5	23.6(3)
	1	1	1		1				
Cl1	Rh	P	C1	-171.16(14)	C2	Rh	C4	C3	38.7(2)
	1	1	1		1				
C3	Rh	P	P2	-116.74(11)	C5	Rh	C4	C3	119.6(3)
	1	1			1				
C2	Rh	P	P2	-156.53(11)	C1	Rh	C4	C3	80.5(2)
	1	1			1				
C5	Rh	P	P2	-165.9(4)	P1	Rh	C4	C3	-40.1(3)
	1	1			1				
C1	Rh	P	P2	173.32(14)	P2	Rh	C4	C3	-118.76(19)
	1	1			1				
C4	Rh	P	P2	-92.05(15)	Cl1	Rh	C4	C3	143.18(18)
	1	1			1				
Cl1	Rh	P	P2	85.51(3)	C3	Rh	C4	C9	120.6(4)
	1	1			1				
C3	Rh	P	N1	109.43(15)	C2	Rh	C4	C9	159.4(4)
	1	2			1				
C2	Rh	P	N1	88.1(3)	C5	Rh	C4	C9	-119.8(4)
	1	2			1				
C5	Rh	P	N1	-174.34(15)	C1	Rh	C4	C9	-158.8(4)

	1	2				1	
C1	Rh	P	N1	-156.2(3)	P1	Rh	
	1	2			1	C4	C9
C4	Rh	P	N1	148.26(14)	P2	Rh	
	1	2			1	C4	C9
P1	Rh	P	N1	9.27(11)	Cl1	Rh	
	1	2			1	C4	C9
Cl1	Rh	P	N1	-79.98(11)	C3	C4	C5
	1	2			C1	C1	3.4(4)
C3	Rh	P	C3	-133.68(17)	C9	C4	C5
	1	2	0		C1	C1	-171.0(3)
C2	Rh	P	C3	-155.0(3)	Rh	C4	C5
	1	2	0		1	C1	62.8(2)
C5	Rh	P	C3	-57.45(17)	C3	C4	C5
	1	2	0		C1	0	177.7(3)
C1	Rh	P	C3	-39.3(3)	C9	C4	C5
	1	2	0		C1	0	3.3(6)
C4	Rh	P	C3	-94.85(17)	Rh	C4	C5
	1	2	0		1	C1	-123.0(4)
P1	Rh	P	C3	126.16(13)	C3	C4	C5
	1	2	0		C1	Rh	
Cl1	Rh	P	C3	36.91(13)	C9	C4	C5
	1	2	0		Rh	1	126.2(3)
C3	Rh	P	C3	-2.28(17)	C2	C1	C5
	1	2	6		C4	C4	-2.2(4)
C2	Rh	P	C3	-23.6(3)	C6	C1	C5
	1	2	6		C4	C4	175.1(3)
C5	Rh	P	C3	73.95(17)	Rh	C1	C5
	1	2	6		1	C4	C4
C1	Rh	P	C3	92.1(3)	C2	C1	C5
	1	2	6		C1	0	-176.6(3)
C4	Rh	P	C3	36.55(16)	C6	C1	C5
	1	2	6		C1	0	0.7(6)
P1	Rh	P	C3	-102.44(13)	Rh	C1	C5
	1	2	6		1	C1	C1
Cl1	Rh	P	C3	168.31(13)	C2	C1	C5
					Rh	Rh	61.0(2)

	1	2	6						1	
C3	Rh	P								
	1	2	P1	100.16(12)						
					C6	C1	C5	Rh		-121.6(4)
								1		
C2	Rh	P								
	1	2	P1	78.8(2)						
					C3	Rh				
						1	C5	C4		36.7(2)
C5	Rh	P								
	1	2	P1	176.39(12)						
					C2	Rh				
						1	C5	C4		79.8(2)
C1	Rh	P								
	1	2	P1	-165.5(3)						
					C1	Rh				
						1	C5	C4		115.9(3)
C4	Rh	P								
	1	2	P1	138.99(10)						
					P1	Rh				
						1	C5	C4		90.0(5)
C11	Rh	P								
	1	2	P1	-89.25(3)						
					P2	Rh				
						1	C5	C4		-74.4(2)
C1	P1	P								
	7	2	N1	-64.9(2)						
					Cl1	Rh				
						1	C5	C4		-162.4(2)
C1	P1	P								
	1	2	N1	84.8(2)						
					C3	Rh				
						1	C5	C1		-79.2(2)
Rh	P1	P								
	1	2	N1	-165.20(17)						
					C2	Rh				
						1	C5	C1		-36.1(2)
N1	P1	P	C3							
	2	0		66.4(2)						
					C4	Rh				
						1	C5	C1		-115.9(3)
C1	P1	P	C3							
	7	2	0	1.5(3)						
					P1	Rh				
						1	C5	C1		-25.9(6)
C1	P1	P	C3							
	1	2	0	151.2(2)						
					P2	Rh				
						1	C5	C1		169.74(18)
Rh	P1	P	C3							
	1	2	0	-98.79(17)						
					Cl1	Rh				
						1	C5	C1		81.7(2)
N1	P1	P	C3							
	2	6		-84.4(2)						
					C3	Rh				
						1	C5	C1		160.2(4)
C1	P1	P	C3							
	7	2	6	-149.3(2)						
					C2	Rh				
						1	C5	C1		-156.8(4)
C1	P1	P	C3							
	1	2	6	0.39(18)						
					C1	Rh				
						1	C5	C1		-120.7(4)
Rh	P1	P	C3							
	1	2	6	110.43(13)						
					C4	Rh				
						1	C5	C1		123.5(4)
N1	P1	P	Rh	165.20(17)						
					P1	Rh				
							C5	C1		-146.6(4)

			2				3	8	
C6	C1	C	2	C3	-177.1(4)	P1	N1	C2	C2
		2				3	4		78.9(4)
Rh	C1	C	2	C3	60.9(2)	P2	N1	C2	C2
1		2				3	4		-102.7(4)
C5	C1	C	2	C7	175.6(3)	C2	C2	C2	C2
		2				8	3	4	5
C6	C1	C	2	C7	-1.6(6)	N1	C2	C2	C2
		2				3	4	5	
Rh	C1	C	2	C7	-123.6(4)	C2	C2	C2	C2
1		2				3	4	5	-0.4(5)
C5	C1	C	2	Rh	-60.8(2)	C2	O2	C2	C2
		2	1			9		6	7
C6	C1	C	2	Rh	122.0(4)	C2	O2	C2	C2
		2	1			9		6	5
C3	Rh	C	1	C1	117.5(3)	C2	C2	C2	O2
	1	2				4	5	6	
C5	Rh	C	1	C1	37.4(2)	C2	C2	C2	C2
	1	2				4	5	6	7
C4	Rh	C	1	C1	79.2(2)	O2	C2	C2	C2
	1	2				6	7	8	
P1	Rh	C	1	C1	-140.3(2)	C2	C2	C2	C2
	1	2				5	6	7	8
P2	Rh	C	1	C1	147.8(2)	C2	C2	C2	C2
	1	2				4	3	8	7
Cl1	Rh	C	1	C1	-45.6(2)	N1	C2	C2	C2
	1	2				3	8	7	
C5	Rh	C	1	C3	-80.1(2)	C2	C2	C2	C2
	1	2				6	7	8	3
C1	Rh	C	1	C3	-117.5(3)	N1	P2	C3	C3
	1	2				0		5	
C4	Rh	C	1	C3	-38.3(2)	C3	P2	C3	C3
	1	2				6		0	5
P1	Rh	C	1	C3	102.2(2)	Rh	P2	C3	C3
	1	2				1		0	
P2	Rh	C	C3	30.3(4)	P1	P2	C3	C3	109.0(3)

	1	2				0	5
C11	Rh	C	C3	-163.16(18)	N1	P2	C3 C3 -35.9(4)
	1	2			0	1	
C3	Rh	C	C7	-119.1(5)	C3	P2	C3 C3 79.0(3)
	1	2			6	0	1
C5	Rh	C	C7	160.8(4)	Rh	P2	C3 C3 -142.6(3)
	1	2			1	0	1
C1	Rh	C	C7	123.3(5)	P1	P2	C3 C3 -74.3(4)
	1	2			0	1	
C4	Rh	C	C7	-157.5(4)	C3	C3	C3 C3 0.1(6)
	1	2			5	0	1 2
P1	Rh	C	C7	-17.0(4)	P2	C3	C3 C3 -176.5(3)
	1	2			0	1	2
P2	Rh	C	C7	-88.8(4)	C3	C3	C3 C3 0.7(6)
	1	2			0	1	2 3
C11	Rh	C	C7	77.7(4)	C3	C3	C3 C3 -0.1(6)
	1	2			1	2	3 4
C1	C2	C	C4	1.9(4)	C3	C3	C3 C3 -1.3(6)
		3			2	3	4 5
C7	C2	C	C4	-173.6(3)	C3	C3	C3 C3 -1.4(6)
		3			1	0	5 4
Rh	C2	C	C4	64.2(2)	P2	C3	C3 C3 175.4(3)
1		3			0	5	4
C1	C2	C	C8	169.7(3)	C3	C3	C3 C3 2.1(6)
		3			3	4	5 0
C7	C2	C	C8	-5.8(6)	N1	P2	C3 C4 -85.5(3)
		3			6	1	
Rh	C2	C	C8	-128.0(3)	C3	P2	C3 C4 156.4(3)
1		3			0	6	1
C1	C2	C	Rh		Rh	P2	C3 C4 18.6(3)
		3	1	-62.3(2)	1	6	1
C7	C2	C	Rh		P1	P2	C3 C4 -44.5(3)
		3	1	122.1(4)	6	1	
C2	Rh	C	C4	-115.9(3)	N1	P2	C3 C3 92.0(3)
	1	3			6	7	
C5	Rh	C	C4	-35.9(2)	C3	P2	C3 C3 -26.1(3)

	1	3			0	6	7	
C1	Rh	C	C4	-79.1(2)	Rh	C3	C3	-163.9(3)
	1	3			1	P2	6	7
P1	Rh	C	C4	154.72(18)	P1	P2	C3	C3
	1	3					6	7
P2	Rh	C	C4	77.4(2)	C4	C3	C3	C3
	1	3			1	6	7	8
Cl1	Rh	C	C4	-81.6(3)	P2	C3	C3	C3
	1	3				6	7	8
C5	Rh	C	C2	80.0(2)	C3	C3	C3	C3
	1	3				6	7	9
C1	Rh	C	C2	36.8(2)	C3	C3	C3	C4
	1	3				7	8	9
C4	Rh	C	C2	115.9(3)	C3	C3	C4	C4
	1	3				8	9	0
P1	Rh	C	C2	-89.3(2)	C3	C3	C4	C4
	1	3				7	6	1
P2	Rh	C	C2	-166.65(18)	P2	C3	C4	C4
	1	3					6	0
Cl1	Rh	C	C2	34.3(3)	C3	C4	C4	C3
	1	3				9	0	1
C2	Rh	C	C8	119.5(5)				
	1	3						

Table B12. Hydrogen Atom Coordinates ($\text{\AA} \times 10^4$) and Isotropic Displacement Parameters ($\text{\AA}^2 \times 10^3$) for **2f**.

Atom	x	y	z	U(eq)
H6A	3525	9150	2696	80
H6B	3307	8078	2399	80
H6C	4394	8533	2535	80
H7A	4967	9908	4089	76
H7B	4040	9840	4382	76
H7C	3865	9976	3626	76
H8A	5070	7578	5403	67
H8B	4498	8599	5272	67
H8C	5592	8506	5189	67

H9A	4458	5477	4326	62
H9B	4888	6084	4973	62
H9C	5567	5885	4502	62
H10A	4611	6333	2779	68
H10B	3449	6262	2708	68
H10C	4210	5609	3229	68
H12	2389	7881	5642	46
H13	3024	8620	6626	60
H14	3449	10265	6702	56
H15	3221	11180	5759	51
H16	2556	10458	4764	43
H18	2037	9640	3233	49
H19	1226	11044	2736	70
H20	-152	11613	3002	82
H21	-684	10868	3821	78
H22	206	9549	4388	56
H24	-494	7783	3669	35
H25	-2012	7732	3898	39
H27	-612	7067	5753	40
H28	902	7126	5509	40
H29A	-2131	6500	5706	78
H29B	-3140	7106	5580	78
H29C	-2101	7636	5879	78
H31	18	5700	4057	45
H32	-778	4419	3400	58
H33	13	3590	2752	58
H34	1618	4020	2750	56
H35	2398	5336	3372	43
H37	1450	4897	4979	47
H38	2091	4249	6000	54
H39	3528	4863	6688	49
H40	4321	6192	6370	45
H41	3674	6876	5352	38

Appendix C

Crystal structure information for compound **1c**.

Table C1 Fractional Atomic Coordinates ($\times 10^4$) and Equivalent Isotropic Displacement Parameters ($\text{\AA}^2 \times 10^3$) for **1c**. U_{eq} is defined as 1/3 of the trace of the orthogonalised U_{IJ} tensor.

Atom	x	y	z	U(eq)
C1	9881.9(15)	1577(2)	3842.3(14)	22.5(6)
C2	9603.4(17)	458(2)	3806.2(17)	29.3(6)
C3	9439(2)	2500	3652(2)	21.6(8)
C4	8588(2)	2500	3516(2)	27.8(9)
C5	10594.8(15)	1923(2)	4120.2(14)	22.9(6)
C6	11223.2(17)	1252(3)	4418.7(16)	29.4(6)
C7	9645.7(16)	4341(2)	1745.5(15)	22.6(6)
C8	9713(2)	5265(3)	1351(2)	46.9(10)
C9	9058(2)	5788(4)	1118(3)	62.0(14)
C10	8337.1(19)	5413(3)	1282(2)	43.2(9)
C11	8267.0(17)	4509(3)	1678.9(19)	33.6(7)
C12	8917.0(17)	3979(3)	1913.2(17)	29.8(6)
C13	11281.3(15)	4380(2)	1800.9(15)	22.6(6)
C14	11406.9(18)	5233(2)	2260.1(17)	29.2(6)
C15	12042.6(19)	5881(3)	2159.3(19)	35.6(7)
C16	12543.3(18)	5692(3)	1600.9(19)	36.9(8)
C17	12421.0(18)	4846(3)	1145.8(19)	34.9(7)
C18	11795.1(17)	4183(3)	1248.9(17)	29.2(6)
N1	10484.4(19)	2500	1410.8(19)	24.0(7)
C20A	10371(13)	2500	653(12)	29(7)
C21A	9529(8)	2500	407(7)	34(4)
C22A	9376(8)	2500	-360(7)	26(4)
C23A	8620(7)	2500	-652(6)	28(4)
C24A	7916(7)	2500	-220(8)	21(3)
C20B	10336(11)	2675(14)	587(10)	14(5)
C21B	9589(7)	2875(16)	372(6)	17(3)
C22B	9358(9)	2819(18)	-351(8)	20(3)
C23B	8622(10)	2864(19)	-650(9)	32(4)

C24B	7949(10)	2773(18)	-100(10)	36(4)
P1	10467.0(4)	3537.4(6)	1985.1(4)	17.93(14)
P2	-1321.6(8)	2500	5780.3(6)	32.6(3)
Cl1	11861.9(5)	2500	2862.5(5)	24.08(19)
Ir1	10498.3(2)	2500	2991.8(2)	16.41(5)
F1	-510(2)	2500	5411(2)	90.8(16)
F2	-1598(2)	1613(2)	5237.0(14)	79.8(9)
F3	-1046.7(18)	1613(2)	6321.2(13)	72.8(8)
F4	-2132(2)	2500	6165(2)	66.6(11)
C1S	703(4)	2500	7090(4)	79(2)
O1S	873(3)	2500	6363(3)	68.8(13)

Table C2. Anisotropic Displacement Parameters ($\text{\AA}^2 \times 10^3$) for **1c**. The Anisotropic displacement factor exponent takes the form: $-2\pi^2[h^2a^{*2}U_{11} + 2hka^*b^*U_{12} + \dots]$.

Atom	U ₁₁	U ₂₂	U ₃₃	U ₂₃	U ₁₃	U ₁₂
C1	20.0(13)	24.7(14)	22.9(13)	1.7(11)	3.3(10)	0.6(11)
C2	28.5(15)	23.7(15)	35.8(16)	5.5(12)	2.2(12)	-4.4(12)
C3	20.7(18)	24(2)	19.8(17)	0	3.6(15)	0
C4	20.1(19)	39(2)	24.0(19)	0	4.2(16)	0
C5	20.5(13)	26.1(15)	22.2(13)	0.6(11)	0.5(10)	1.1(11)
C6	26.8(15)	31.7(16)	29.7(15)	6.5(13)	-4.1(12)	4.0(13)
C7	21.1(13)	22.5(14)	24.4(13)	1.1(11)	-0.8(10)	3.4(11)
C8	26.4(16)	45(2)	70(3)	30(2)	-0.8(17)	-1.7(15)
C9	30.7(18)	54(3)	101(4)	49(3)	-4(2)	3.9(18)
C10	25.6(16)	43(2)	61(2)	16.1(18)	-5.3(15)	6.9(15)
C11	19.1(14)	35.3(17)	46.5(19)	4.6(15)	1.7(13)	2.2(13)
C12	23.5(14)	27.2(16)	38.8(16)	6.4(13)	1.0(12)	3.1(12)
C13	19.0(13)	20.8(13)	27.9(13)	6.8(11)	-1.1(10)	-2.1(11)
C14	29.5(15)	27.6(15)	30.6(14)	1.3(12)	0.7(12)	-4.0(13)
C15	36.5(18)	27.0(16)	43.3(18)	2.7(14)	-7.3(14)	-8.7(14)
C16	25.5(15)	34.7(18)	50(2)	13.2(15)	-2.7(14)	-8.8(14)
C17	22.2(14)	36.0(18)	46.6(19)	9.3(15)	6.3(13)	-0.3(13)
C18	25.2(14)	27.1(15)	35.4(16)	1.8(13)	3.2(12)	0.2(12)
P1	16.2(3)	17.3(3)	20.3(3)	1.0(2)	0.5(2)	0.3(2)
P2	41.3(7)	29.4(6)	27.1(5)	0	2.2(5)	0
Cl1	14.8(4)	26.4(5)	31.0(5)	0	-0.8(3)	0

Ir1	14.26(7)	16.27(8)	18.68(8)	0	0.10(5)	0
F1	66(3)	151(5)	55(2)	0	35(2)	0
F2	137(3)	43.2(14)	58.7(16)	-16.6(12)	-16.9(17)	-8.8(17)
F3	100(2)	73.3(18)	45.4(13)	20.1(13)	9.9(14)	42.6(17)
F4	38.5(18)	63(2)	98(3)	0	14.6(19)	0
C1S	52(4)	101(7)	84(6)	0	-5(4)	0
O1S	45(2)	82(3)	79(3)	0	6(2)	0

Table C3. Bond Lengths for **1c**.

Atom	Atom	Length/Å	Atom	Atom	Length/Å
C1	C5	1.424(4)	C23A	C24A	1.476(17)
C1	C3	1.451(4)	C20B	C20B ¹	0.44(4)
C1	C2	1.505(4)	C20B	C21B	1.39(2)
C1	Ir1	2.254(3)	C20B	C21B ¹	1.54(2)
C3	C1 ¹	1.451(4)	C21B	C21B ¹	0.95(4)
C3	C4	1.515(5)	C21B	C22B	1.417(19)
C3	Ir1	2.231(4)	C21B	C20B ¹	1.54(2)
C5	C5 ¹	1.465(6)	C21B	C22B ¹	1.67(3)
C5	C6	1.502(4)	C22B	C22B ¹	0.81(5)
C5	Ir1	2.243(3)	C22B	C23B	1.41(2)
C7	C8	1.391(4)	C22B	C23B ¹	1.65(3)
C7	C12	1.394(4)	C22B	C21B ¹	1.67(3)
C7	P1	1.822(3)	C23B	C23B ¹	0.93(5)
C8	C9	1.398(5)	C23B	C24B	1.57(2)
C9	C10	1.385(5)	C23B	C22B ¹	1.65(3)
C10	C11	1.373(5)	C23B	C24B ¹	1.76(3)
C11	C12	1.395(4)	C24B	C24B ¹	0.69(5)
C13	C18	1.394(4)	C24B	C23B ¹	1.76(3)
C13	C14	1.401(4)	P1	Ir1	2.3011(8)
C13	P1	1.818(3)	P1	P1 ¹	2.6359(15)
C14	C15	1.399(4)	P2	F1	1.583(4)
C15	C16	1.387(5)	P2	F3	1.590(2)
C16	C17	1.388(5)	P2	F3 ¹	1.590(3)
C17	C18	1.397(4)	P2	F4	1.593(4)
N1	C20A	1.43(2)	P2	F2 ¹	1.594(3)
N1	C20B ¹	1.58(2)	P2	F2	1.594(3)

N1	C20B	1.58(2)		Cl1	Ir1	2.4038(10)
N1	P1	1.701(2)		Ir1	C5 ¹	2.243(3)
N1	P1 ¹	1.702(2)		Ir1	C1 ¹	2.254(3)
C20A	C21A	1.55(3)		Ir1	P1 ¹	2.3011(8)
C21A	C22A	1.462(19)		C1S	O1S	1.394(9)
C22A	C23A	1.435(18)				
¹ +X,1/2-Y,+Z						

Table C4. Bond Angles for **1c**.

Atom	Atom	Atom	Angle/ ^o	Atom	Atom	Atom	Angle/ ^o
C5	C1	C3	108.1(3)	C23B	C22B	C21B ¹	124.6(14)
C5	C1	C2	126.4(3)	C21B	C22B	C21B ¹	34.8(14)
C3	C1	C2	125.4(3)	C23B ¹	C22B	C21B ¹	100.8(18)
C5	C1	Ir1	71.12(16)	C23B ¹	C23B	C22B	87.6(10)
C3	C1	Ir1	70.26(18)	C23B ¹	C23B	C24B	85.8(9)
C2	C1	Ir1	128.0(2)	C22B	C23B	C24B	115.2(14)
C1	C3	C1 ¹	107.8(3)	C23B ¹	C23B	C22B ¹	58.3(13)
C1	C3	C4	124.67(17)	C22B	C23B	C22B ¹	29.3(16)
C1 ¹	C3	C4	124.67(17)	C24B	C23B	C22B ¹	109.0(14)
C1	C3	Ir1	71.99(18)	C23B ¹	C23B	C24B ¹	62.7(12)
C1 ¹	C3	Ir1	71.99(18)	C22B	C23B	C24B ¹	111.3(14)
C4	C3	Ir1	136.7(3)	C24B	C23B	C24B ¹	23.1(14)
C1	C5	C5 ¹	108.01(17)	C22B ¹	C23B	C24B ¹	94.8(18)
C1	C5	C6	127.2(3)	C24B ¹	C24B	C23B	94.2(9)
C5 ¹	C5	C6	124.63(17)	C24B ¹	C24B	C23B ¹	62.6(12)
C1	C5	Ir1	71.96(15)	C23B	C24B	C23B ¹	31.6(16)
C5 ¹	C5	Ir1	70.94(7)	N1	P1	C13	108.79(15)
C6	C5	Ir1	126.3(2)	N1	P1	C7	107.02(15)
C8	C7	C12	118.4(3)	C13	P1	C7	104.13(13)
C8	C7	P1	122.4(2)	N1	P1	Ir1	94.24(10)
C12	C7	P1	119.0(2)	C13	P1	Ir1	118.30(9)
C7	C8	C9	119.8(3)	C7	P1	Ir1	122.81(10)
C10	C9	C8	121.1(3)	N1	P1	P1 ¹	39.23(9)
C11	C10	C9	119.3(3)	C13	P1	P1 ¹	126.09(9)
C10	C11	C12	120.0(3)	C7	P1	P1 ¹	124.10(10)
C7	C12	C11	121.3(3)	Ir1	P1	P1 ¹	55.059(19)

C18	C13	C14	119.5(3)		F1	P2	F3	90.31(17)
C18	C13	P1	122.9(2)		F1	P2	F3 ¹	90.31(17)
C14	C13	P1	117.5(2)		F3	P2	F3 ¹	90.2(2)
C15	C14	C13	119.8(3)		F1	P2	F4	179.0(2)
C16	C15	C14	120.3(3)		F3	P2	F4	88.97(16)
C15	C16	C17	120.0(3)		F3 ¹	P2	F4	88.97(16)
C16	C17	C18	120.2(3)		F1	P2	F2 ¹	89.69(18)
C13	C18	C17	120.1(3)		F3	P2	F2 ¹	179.9(2)
C20B ¹	N1	C20B	16.2(12)		F3 ¹	P2	F2 ¹	89.87(16)
C20A	N1	P1	128.58(16)		F4	P2	F2 ¹	91.04(18)
C20B ¹	N1	P1	136.3(6)		F1	P2	F2	89.68(18)
C20B	N1	P1	120.3(6)		F3	P2	F2	89.87(16)
C20A	N1	P1 ¹	128.58(16)		F3 ¹	P2	F2	179.9(2)
C20B ¹	N1	P1 ¹	120.3(6)		F4	P2	F2	91.04(18)
C20B	N1	P1 ¹	136.3(6)		F2 ¹	P2	F2	90.0(2)
P1	N1	P1 ¹	101.53(19)		C3	Ir1	C5 ¹	62.67(12)
N1	C20A	C21A	115.3(15)		C3	Ir1	C5	62.67(12)
C22A	C21A	C20A	117.9(13)		C5 ¹	Ir1	C5	38.12(15)
C23A	C22A	C21A	123.0(12)		C3	Ir1	C1	37.75(9)
C22A	C23A	C24A	124.4(12)		C5 ¹	Ir1	C1	62.63(10)
C20B ¹	C20B	C21B	100.5(9)		C5	Ir1	C1	36.92(10)
C20B ¹	C20B	C21B ¹	63.0(12)		C3	Ir1	C1 ¹	37.75(9)
C21B	C20B	C21B ¹	37.5(16)		C5 ¹	Ir1	C1 ¹	36.92(10)
C20B ¹	C20B	N1	81.9(6)		C5	Ir1	C1 ¹	62.63(10)
C21B	C20B	N1	117.6(13)		C1	Ir1	C1 ¹	62.70(15)
C21B ¹	C20B	N1	109.4(13)		C3	Ir1	P1 ¹	115.72(8)
C21B ¹	C21B	C20B	79.5(9)		C5 ¹	Ir1	P1 ¹	163.91(8)
C21B ¹	C21B	C22B	87.1(10)		C5	Ir1	P1 ¹	125.93(8)
C20B	C21B	C22B	122.5(13)		C1	Ir1	P1 ¹	105.64(8)
C21B ¹	C21B	C20B ¹	63.0(11)		C1 ¹	Ir1	P1 ¹	149.94(7)
C20B	C21B	C20B ¹	16.5(14)		C3	Ir1	P1	115.73(8)
C22B	C21B	C20B ¹	118.2(13)		C5 ¹	Ir1	P1	125.93(8)
C21B ¹	C21B	C22B ¹	58.1(11)		C5	Ir1	P1	163.91(8)
C20B	C21B	C22B ¹	111.6(13)		C1	Ir1	P1	149.94(7)
C22B	C21B	C22B ¹	29.0(16)		C1 ¹	Ir1	P1	105.64(8)
C20B ¹	C21B	C22B ¹	100.4(16)		P1 ¹	Ir1	P1	69.88(4)

C22B ¹	C22B	C23B	92.4(10)	C3	Ir1	Cl1	152.14(11)
C22B ¹	C22B	C21B	92.9(10)	C5 ¹	Ir1	Cl1	91.14(7)
C23B	C22B	C21B	129.9(14)	C5	Ir1	Cl1	91.14(7)
C22B ¹	C22B	C23B ¹	58.3(13)	C1	Ir1	Cl1	123.25(7)
C23B	C22B	C23B ¹	34.0(17)	C1 ¹	Ir1	Cl1	123.25(7)
C21B	C22B	C23B ¹	125.0(14)	P1 ¹	Ir1	Cl1	86.63(3)
C22B ¹	C22B	C21B ¹	58.1(11)	P1	Ir1	Cl1	86.63(3)

¹+X,1/2-Y,+Z

Table C5. Hydrogen Bonds for **1c**.

D	H	A	d(D-H)/Å	d(H-A)/Å	d(D-A)/Å	D-H-A/°
C1 4	H1 4	F3 1	0.95	2.51	3.245(4)	134.7
C1 4	H1 4	F3 1	0.95	2.51	3.245(4)	134.7

¹1-X,1/2+Y,1-Z

Table C6. Torsion Angles for **1c**.

A	B	C	D	Angle/°	A	B	C	D	Angle/°
C5	C1	C3	C1 ¹	-2.1(4)	C21B ¹	C21B	C22B	C23B	95.5(19)
C2	C1	C3	C1 ¹	173.32(19)	C20B	C21B	C22B	C23B	171.1(18)
Ir1	C1	C3	C1 ¹	-63.5(2)	C20B ¹	C21B	C22B	C23B	152.6(19)
C5	C1	C3	C4	-163.7(3)	C22B ¹	C21B	C22B	C23B	95.5(19)
C2	C1	C3	C4	11.7(5)	C21B ¹	C21B	C22B	C23B ¹	52.6(18)
Ir1	C1	C3	C4	134.9(4)	C20B	C21B	C22B	C23B ¹	128(2)
C5	C1	C3	Ir1	61.4(2)	C20B ¹	C21B	C22B	C23B ¹	110(3)
C2	C1	C3	Ir1	-123.2(3)	C22B ¹	C21B	C22B	C23B ¹	52.6(18)
C3	C1	C5	C5 ¹	1.3(3)	C20B	C21B	C22B	C21B ¹	75.6(15)
C2	C1	C5	C5 ¹	-174.1(2)	C20B ¹	C21B	C22B	C21B ¹	57.1(14)
Ir1	C1	C5	C5 ¹	62.16(7)	C22B ¹	C21B	C22B	C21B ¹	-0.006(4)
C3	C1	C5	C6	176.9(3)	C22B ¹	C22B	C23B	C23B ¹	-0.010(3)
C2	C1	C5	C6	1.5(5)	C21B	C22B	C23B	C23B ¹	-95.8(19)
Ir1	C1	C5	C6	-122.3(3)	C21B ¹	C22B	C23B	C23B ¹	-52.1(16)
C3	C1	C5	Ir1	-60.9(2)	C22B ¹	C22B	C23B	C24B	84.2(13)
C2	C1	C5	Ir1	123.8(3)	C21B	C22B	C23B	C24B	-12(3)
C12	C7	C8	C9	-1.7(6)	C23B ¹	C22B	C23B	C24B	84.2(13)

P1	C7	C8	C9	173.1(4)	C21B ¹	C22B	C23B	C24B	32(2)
C7	C8	C9	C10	1.2(8)	C21B	C22B	C23B	C22B ¹	-95.7(19)
C8	C9	C10	C11	-0.4(7)	C23B ¹	C22B	C23B	C22B ¹	0.010(3)
C9	C10	C11	C12	0.2(6)	C21B ¹	C22B	C23B	C22B ¹	-52.1(16)
C8	C7	C12	C11	1.6(5)	C22B ¹	C22B	C23B	C24B ¹	59.4(14)
P1	C7	C12	C11	-173.4(3)	C21B	C22B	C23B	C24B ¹	-36(3)
C10	C11	C12	C7	-0.8(5)	C23B ¹	C22B	C23B	C24B ¹	59.4(14)
C18	C13	C14	C15	0.3(4)	C21B ¹	C22B	C23B	C24B ¹	7(2)
P1	C13	C14	C15	177.4(2)	C23B ¹	C23B	C24B	C24B ¹	0.000(3)
C13	C14	C15	C16	0.9(5)	C22B	C23B	C24B	C24B ¹	-85.4(14)
C14	C15	C16	C17	-1.0(5)	C22B ¹	C23B	C24B	C24B ¹	-54.4(14)
C15	C16	C17	C18	-0.1(5)	C22B	C23B	C24B	C23B ¹	-85.4(14)
C14	C13	C18	C17	-1.4(4)	C22B ¹	C23B	C24B	C23B ¹	-54.4(14)
P1	C13	C18	C17	-178.4(2)	C24B ¹	C23B	C24B	C23B ¹	0.000(4)
C16	C17	C18	C13	1.3(5)	C20A	N1	P1	C13	-67.7(12)
C20B ¹	N1	C20A	C21A	79(10)	C20B ¹	N1	P1	C13	-71.6(10)
C20B	N1	C20A	C21A	-79(10)	C20B	N1	P1	C13	-68.3(8)
P1	N1	C20A	C21A	-82.3(7)	P1 ¹	N1	P1	C13	124.54(15)
P1 ¹	N1	C20A	C21A	82.3(7)	C20A	N1	P1	C7	44.2(12)
N1	C20A	C21A	C22A	180.000(1)	C20B ¹	N1	P1	C7	40.3(10)
C20A	C21A	C22A	C23A	180.000(0)	C20B	N1	P1	C7	43.6(8)
C21A	C22A	C23A	C24A	0.000(0)	P1 ¹	N1	P1	C7	-123.51(16)
C20A	N1	C20B	C20B ¹	11(10)	C20A	N1	P1	Ir1	170.4(11)
P1	N1	C20B	C20B ¹	-171.8(5)	C20B ¹	N1	P1	Ir1	166.5(10)
P1 ¹	N1	C20B	C20B ¹	-10.3(7)	C20B	N1	P1	Ir1	169.8(8)
C20A	N1	C20B	C21B	109(11)	P1 ¹	N1	P1	Ir1	2.71(15)
C20B ¹	N1	C20B	C21B	97.7(12)	C20A	N1	P1	P1 ¹	167.7(12)
P1	N1	C20B	C21B	-74.1(14)	C20B ¹	N1	P1	P1 ¹	163.8(11)
P1 ¹	N1	C20B	C21B	87.4(15)	C20B	N1	P1	P1 ¹	167.1(8)
C20A	N1	C20B	C21B ¹	69(10)	C18	C13	P1	N1	2.5(3)
C20B ¹	N1	C20B	C21B ¹	57.6(14)	C14	C13	P1	N1	-174.5(2)
P1	N1	C20B	C21B ¹	-114.3(12)	C18	C13	P1	C7	-111.4(3)
P1 ¹	N1	C20B	C21B ¹	47.3(19)	C14	C13	P1	C7	71.6(3)
C20B ¹	C20B	C21B	C21B ¹	-0.006(3)	C18	C13	P1	Ir1	108.3(2)
N1	C20B	C21B	C21B ¹	-86.3(11)	C14	C13	P1	Ir1	-68.7(2)
C20B ¹	C20B	C21B	C22B	-79.7(15)	C18	C13	P1	P1 ¹	42.6(3)

C21B ¹	C20B	C21B	C22B	-79.7(15)	C14	C13	P1	P1 ¹	-134.4(2)
N1	C20B	C21B	C22B	-166.0(13)	C8	C7	P1	N1	-101.4(3)
C21B ¹	C20B	C21B	C20B ¹	0.006(3)	C12	C7	P1	N1	73.4(3)
N1	C20B	C21B	C20B ¹	-86.3(11)	C8	C7	P1	C13	13.7(3)
C20B ¹	C20B	C21B	C22B ¹	-49.4(13)	C12	C7	P1	C13	-171.5(2)
C21B ¹	C20B	C21B	C22B ¹	-49.3(13)	C8	C7	P1	Ir1	151.8(3)
N1	C20B	C21B	C22B ¹	-135.6(15)	C12	C7	P1	Ir1	-33.4(3)
C21B ¹	C21B	C22B	C22B ¹	0.006(3)	C8	C7	P1	P1 ¹	-140.9(3)
C20B	C21B	C22B	C22B ¹	75.6(15)	C12	C7	P1	P1 ¹	33.9(3)
C20B ¹	C21B	C22B	C22B ¹	57.1(14)					

¹+X,1/2-Y,+Z

Table C7. Hydrogen Atom Coordinates ($\text{\AA} \times 10^4$) and Isotropic Displacement Parameters ($\text{\AA}^2 \times 10^3$) for **1c**.

Atom	x	y	z	U(eq)
H2A	10041	-20	3778	44
H2B	9283	367	3382	44
H2C	9305	297	4235	44
H4A	8316	2415	3969	42
H4B	8457	1917	3196	42
H4C	8439	3168	3294	42
H6A	11148	520	4269	44
H6B	11216	1291	4941	44
H6C	11716	1505	4241	44
H8	10203	5539	1241	56
H9	9107	6411	841	74
H10	7896	5778	1123	52
H11	7775	4244	1794	40
H12	8862	3359	2192	36
H14	11061	5371	2639	35
H15	12132	6454	2475	43
H16	12970	6141	1530	44
H17	12764	4718	763	42
H18	11719	3597	942	35
H1S1	1135	2792	7357	118
H1S2	607	1777	7249	118

H1S3	249	2930	7176
			118

Table C8. Atomic Occupancy for **1c**.

Atom	Occupancy	Atom	Occupancy	Atom	Occupancy
H4A	0.5	H4B	0.5	H4C	0.5
C20A	0.49(4)	C21A	0.49(4)	C22A	0.49(4)
C23A	0.49(4)	C24A	0.49(4)	C20B	0.26(2)
C21B	0.26(2)	C22B	0.26(2)	C23B	0.26(2)
C24B	0.26(2)	H1S1	0.5	H1S2	0.5
H1S3	0.5				

Crystal structure information for compound **2c.****Table C9.** Fractional Atomic Coordinates ($\times 10^4$) and Equivalent Isotropic Displacement Parameters ($\text{\AA}^2 \times 10^3$) for **2c** U_{eq} is defined as 1/3 of the trace of the orthogonalised U_{ij} tensor.

Atom	x	y	z	U(eq)
Rh1	5652.5(2)	1327.9(2)	2520.7(2)	20.82(5)
Cl1	3865.7(6)	1176.1(2)	3316.8(4)	29.74(13)
P1	7069.1(6)	745.3(2)	3343.2(4)	21.06(12)
P2	7135.4(6)	1596.4(2)	3944.1(4)	20.85(12)
P3	9218.9(8)	1398.4(3)	8683.9(5)	38.18(17)
F1	9791.6(19)	1629.1(6)	9714.6(12)	55.8(5)
F2	8617(2)	1158.9(7)	7656.8(12)	63.9(5)
F3	7610.7(18)	1399.3(7)	8772.3(14)	60.3(5)
F4	10809(2)	1381.3(10)	8596.9(14)	84.2(8)
F5	8937(2)	1890.7(7)	8202.6(15)	84.2(7)
F6	9469(2)	904.6(6)	9174.1(14)	67.4(6)
N1	7963(2)	1081.1(6)	4283.2(13)	23.3(4)
C1	5451(3)	1170.4(8)	980.2(16)	32.0(5)
C2	4080(3)	1275.5(8)	1071.8(16)	31.0(5)
C3	4108(3)	1747.9(8)	1407.8(17)	30.6(5)
C4	5511(3)	1922.6(8)	1526.1(16)	30.1(5)
C5	6385(3)	1560.7(9)	1310.6(16)	30.9(5)
C6	5865(4)	752.1(10)	522(2)	52.4(8)
C7	2770(3)	975.3(10)	804(2)	49.5(8)

C8	2831(3)	2003.1(11)	1534(2)	46.8(7)
C9	5998(3)	2410.8(9)	1762.5(19)	45.3(7)
C10	7877(3)	1609.2(12)	1222(2)	50.9(8)
C11	6222(2)	249.8(7)	3718.4(17)	25.7(5)
C12	6928(3)	-14.4(8)	4513.3(18)	32.7(5)
C13	6297(3)	-412.0(9)	4733(2)	40.1(6)
C14	4985(3)	-553.4(9)	4154(2)	44.9(7)
C15	4277(3)	-301.4(9)	3352(2)	43.1(7)
C16	4889(3)	104.8(8)	3138(2)	32.7(5)
C17	8412(2)	470.3(7)	2878.7(16)	23.5(5)
C18	9820(3)	626.9(8)	3066.0(19)	33.0(6)
C19	10774(3)	417.2(10)	2650(2)	42.5(7)
C20	10328(3)	50.0(9)	2031(2)	40.8(6)
C21	8936(3)	-114.4(8)	1845.3(19)	34.8(6)
C22	7987(3)	91.4(8)	2271.1(17)	28.9(5)
C23	9047(2)	924.6(8)	5175.5(16)	26.1(5)
C24	10272(3)	1256.0(8)	5600.6(17)	28.7(5)
C25	11321(2)	1044.0(8)	6488.3(17)	27.2(5)
C26	12644(3)	1333.6(9)	6921.8(19)	35.5(6)
C27	13689(3)	1109.0(9)	7787.1(19)	36.9(6)
C28	8481(2)	2027.1(8)	3927.8(16)	25.3(5)
C29	9639(3)	1922.4(9)	3578.2(18)	33.4(5)
C30	10640(3)	2257(1)	3528(2)	42.1(7)
C31	10459(3)	2704(1)	3796.7(19)	43.8(7)
C32	9302(3)	2814.6(9)	4118.3(18)	41.5(7)
C33	8310(3)	2480.2(8)	4194.1(17)	32.8(5)
C34	6281(2)	1813.6(7)	4810.3(16)	23.5(4)
C35	6731(2)	1695.8(8)	5775.5(16)	26.6(5)
C36	6015(3)	1873.2(8)	6399.3(18)	32.1(5)
C37	4879(3)	2171.4(8)	6068.8(19)	33.0(5)
C38	4444(3)	2299.4(9)	5109.4(19)	35.1(6)
C39	5128(3)	2117.2(8)	4480.7(18)	31.3(5)

Table C10. Anisotropic Displacement Parameters ($\text{\AA}^2 \times 10^3$) for **2c**. The Anisotropic displacement factor exponent takes the form: $-2\pi^2[h^2a^{*2}U_{11}+2hka^{*}b^{*}U_{12}+\dots]$.

Atom	U ₁₁	U ₂₂	U ₃₃	U ₂₃	U ₁₃	U ₁₂
Rh1	22.21(9)	19.21(9)	20.01(9)	1.24(7)	4.41(6)	-0.43(7)
Cl1	27.1(3)	28.8(3)	35.6(3)	1.5(2)	12.6(2)	-3.6(2)
P1	22.2(3)	17.7(3)	22.8(3)	0.7(2)	5.8(2)	-0.7(2)
P2	24.0(3)	18.2(3)	19.9(3)	0.7(2)	5.5(2)	-0.9(2)
P3	33.5(4)	48.7(4)	29.9(3)	-5.7(3)	5.1(3)	12.0(3)
F1	59.3(11)	62.2(11)	39.7(9)	-19.0(8)	4.3(8)	11.7(9)
F2	60.8(12)	85.6(14)	36.5(9)	-17.4(9)	0.0(8)	15.8(10)
F3	37.5(9)	78.2(13)	64.2(12)	-7.2(10)	13.0(9)	11.1(9)
F4	39.4(10)	167(2)	48.6(11)	-10.6(13)	16.0(9)	7.8(12)
F5	91.7(16)	61.8(13)	73.3(14)	22.9(11)	-17.4(12)	-15.1(12)
F6	78.8(14)	49.5(11)	57.7(12)	0.1(9)	-6.6(10)	21.2(10)
N1	27.4(10)	19.1(9)	21.3(9)	1.1(7)	3.5(8)	-0.4(7)
C1	44.0(15)	31.9(12)	16.7(11)	1.7(9)	3.5(10)	7.4(11)
C2	34.5(13)	30.9(13)	20.2(11)	3.5(9)	-3.9(10)	-1.1(10)
C3	33.2(13)	30.4(12)	24.5(12)	12(1)	2.1(10)	8.1(10)
C4	40.6(14)	29.3(12)	18.0(11)	6.1(9)	4.8(10)	-0.2(10)
C5	35.4(13)	38.5(14)	19.1(11)	6.2(10)	8.5(10)	1.2(11)
C6	81(2)	42.9(16)	29.2(14)	-2.6(12)	9.8(15)	20.3(16)
C7	44.5(17)	48.6(17)	41.0(16)	3.1(13)	-11.1(13)	-11.8(14)
C8	44.5(17)	50.9(17)	44.2(16)	12.7(13)	11.5(13)	20.9(14)
C9	68(2)	29.5(14)	33.5(14)	6.9(11)	7.4(14)	-9.3(13)
C10	43.0(17)	77(2)	37.2(16)	11.6(15)	18.4(13)	0.7(15)
C11	28.9(12)	19.3(10)	32.5(12)	0.2(9)	14.4(10)	0.2(9)
C12	38.4(14)	26.0(12)	36.0(14)	2.6(10)	14.2(11)	0.1(10)
C13	56.0(18)	24.9(12)	47.6(16)	7.6(11)	27.8(14)	3.1(12)
C14	55.4(18)	21.1(12)	72(2)	0.9(13)	40.4(16)	-3.6(12)
C15	35.4(15)	28.5(13)	70(2)	-8.1(13)	22.3(14)	-9.0(11)
C16	29.8(13)	24.0(12)	45.7(15)	-1.6(10)	13.2(11)	-1.2(10)
C17	25.9(11)	20.1(10)	25.7(11)	2.5(9)	9.5(9)	1.5(9)
C18	30.8(13)	28.1(12)	41.1(14)	-8.9(11)	12.2(11)	-4.3(10)
C19	27.8(13)	40.7(15)	64.0(19)	-11.1(13)	21.2(13)	-5.3(11)
C20	36.8(15)	38.9(15)	53.9(18)	-5.9(13)	24.7(13)	3.9(12)

C21	41.1(15)	27.1(12)	37.9(14)	-6.4(10)	14.0(12)	0.8(11)
C22	27.5(12)	25.3(12)	34.0(13)	-1.8(10)	8.9(10)	-0.4(9)
C23	29.3(12)	23.1(11)	23.3(11)	3.6(9)	3.4(9)	2.7(9)
C24	26.8(12)	28.6(12)	27.5(12)	1.3(9)	2.5(10)	1.0(9)
C25	25.5(12)	25.5(11)	28.0(12)	0.7(9)	3.4(10)	3.5(9)
C26	30.8(13)	29.9(12)	40.8(14)	0.4(11)	2.0(11)	-2.1(10)
C27	26.8(13)	37.6(14)	39.8(14)	-5.0(12)	-0.9(11)	1.5(11)
C28	28.9(12)	24.5(11)	19.9(11)	2.2(9)	2.6(9)	-4.5(9)
C29	33.8(13)	32.7(13)	33.4(13)	3.9(10)	9.4(11)	-0.2(10)
C30	33.7(14)	53.2(17)	40.8(15)	10.9(13)	12.8(12)	-8.4(12)
C31	51.4(17)	45.0(16)	30.3(14)	6.1(12)	4.4(13)	-26.1(13)
C32	66.2(19)	30.4(13)	26.9(13)	-2.5(10)	11.7(13)	-18.5(13)
C33	45.3(15)	27.2(12)	26.0(12)	-1(1)	10.4(11)	-7.6(11)
C34	25.9(11)	20.5(10)	24.8(11)	-2.3(9)	8.2(9)	-3.6(9)
C35	27.6(12)	26.0(11)	26.9(12)	-0.6(9)	9(1)	-0.8(9)
C36	35.9(14)	36.2(13)	25.9(12)	-1.9(10)	11.4(10)	-2.9(11)
C37	32.5(13)	32.9(13)	38.2(14)	-10.2(11)	17.2(11)	-4.8(10)
C38	31.3(13)	31.2(13)	42.1(15)	-6.6(11)	9.4(11)	7.3(10)
C39	34.3(13)	29.6(12)	28.3(12)	0(1)	6(1)	5.3(10)

Table C11. Bond Lengths for **2c**.

Atom	Atom	Length/Å	Atom	Atom	Length/Å
Rh1	C5	2.188(2)	C4	C9	1.505(3)
Rh1	C2	2.226(2)	C5	C10	1.495(4)
Rh1	C3	2.229(2)	C11	C16	1.391(3)
Rh1	C4	2.235(2)	C11	C12	1.395(3)
Rh1	C1	2.243(2)	C12	C13	1.388(3)
Rh1	P1	2.2909(6)	C13	C14	1.372(4)
Rh1	P2	2.2945(6)	C14	C15	1.383(4)
Rh1	C11	2.3848(6)	C15	C16	1.397(3)
P1	N1	1.7027(18)	C17	C18	1.389(3)
P1	C17	1.815(2)	C17	C22	1.399(3)
P1	C11	1.818(2)	C18	C19	1.384(3)
P1	P2	2.6203(8)	C19	C20	1.384(4)
P2	N1	1.7046(18)	C20	C21	1.383(4)

P2	C34	1.810(2)		C21	C22	1.384(3)
P2	C28	1.813(2)		C23	C24	1.516(3)
P3	F4	1.582(2)		C24	C25	1.527(3)
P3	F5	1.583(2)		C25	C26	1.512(3)
P3	F6	1.591(2)		C26	C27	1.520(3)
P3	F1	1.5921(17)		C28	C29	1.392(3)
P3	F3	1.5998(19)		C28	C33	1.397(3)
P3	F2	1.6010(18)		C29	C30	1.390(4)
N1	C23	1.489(3)		C30	C31	1.383(4)
C1	C2	1.407(4)		C31	C32	1.371(4)
C1	C5	1.445(4)		C32	C33	1.394(3)
C1	C6	1.497(4)		C34	C35	1.390(3)
C2	C3	1.456(3)		C34	C39	1.396(3)
C2	C7	1.497(4)		C35	C36	1.391(3)
C3	C4	1.415(3)		C36	C37	1.376(4)
C3	C8	1.498(4)		C37	C38	1.390(4)
C4	C5	1.440(3)		C38	C39	1.381(3)

Table C12. Bond Angles for **2c**.

Atom	Atom	Atom	Angle/ [°]	Atom	Atom	Atom	Angle/ [°]	
C5	Rh1	C2	63.21(9)		C2	C1	C5	108.4(2)
C5	Rh1	C3	63.23(9)		C2	C1	C6	126.9(3)
C2	Rh1	C3	38.15(9)		C5	C1	C6	124.4(3)
C5	Rh1	C4	37.99(9)		C2	C1	Rh1	70.99(13)
C2	Rh1	C4	62.63(9)		C5	C1	Rh1	68.89(13)
C3	Rh1	C4	36.96(9)		C6	C1	Rh1	130.91(17)
C5	Rh1	C1	38.04(9)		C1	C2	C3	108.0(2)
C2	Rh1	C1	36.68(9)		C1	C2	C7	127.0(2)
C3	Rh1	C1	62.40(9)		C3	C2	C7	124.8(2)
C4	Rh1	C1	62.48(9)		C1	C2	Rh1	72.32(13)
C5	Rh1	P1	111.48(7)		C3	C2	Rh1	71.03(13)
C2	Rh1	P1	126.14(6)		C7	C2	Rh1	125.83(18)
C3	Rh1	P1	164.23(7)		C4	C3	C2	107.7(2)
C4	Rh1	P1	145.85(7)		C4	C3	C8	127.3(2)
C1	Rh1	P1	103.85(6)		C2	C3	C8	124.9(2)
C5	Rh1	P2	111.04(7)		C4	C3	Rh1	71.75(13)

C2	Rh1	P2	163.97(6)	C2	C3	Rh1	70.82(12)
C3	Rh1	P2	125.92(7)	C8	C3	Rh1	126.00(17)
C4	Rh1	P2	103.21(6)	C3	C4	C5	108.4(2)
C1	Rh1	P2	145.66(7)	C3	C4	C9	126.4(2)
P1	Rh1	P2	69.70(2)	C5	C4	C9	125.0(2)
C5	Rh1	Cl1	153.82(7)	C3	C4	Rh1	71.29(13)
C2	Rh1	Cl1	93.06(7)	C5	C4	Rh1	69.22(13)
C3	Rh1	Cl1	91.46(7)	C9	C4	Rh1	128.67(16)
C4	Rh1	Cl1	122.72(7)	C4	C5	C1	107.2(2)
C1	Rh1	Cl1	125.56(7)	C4	C5	C10	126.4(2)
P1	Rh1	Cl1	91.05(2)	C1	C5	C10	125.0(2)
P2	Rh1	Cl1	88.71(2)	C4	C5	Rh1	72.78(13)
N1	P1	C17	107.39(10)	C1	C5	Rh1	73.07(13)
N1	P1	C11	112.47(10)	C10	C5	Rh1	130.12(18)
C17	P1	C11	101.33(10)	C16	C11	C12	119.1(2)
N1	P1	Rh1	94.97(6)	C16	C11	P1	118.55(18)
C17	P1	Rh1	121.12(7)	C12	C11	P1	122.01(18)
C11	P1	Rh1	119.28(8)	C13	C12	C11	120.5(2)
N1	P1	P2	39.76(6)	C14	C13	C12	120.0(3)
C17	P1	P2	126.10(7)	C13	C14	C15	120.6(2)
C11	P1	P2	128.19(8)	C14	C15	C16	119.8(3)
Rh1	P1	P2	55.214(17)	C11	C16	C15	120.0(2)
N1	P2	C34	112.08(10)	C18	C17	C22	118.5(2)
N1	P2	C28	109.33(10)	C18	C17	P1	123.43(17)
C34	P2	C28	104.03(10)	C22	C17	P1	118.04(17)
N1	P2	Rh1	94.78(6)	C19	C18	C17	120.7(2)
C34	P2	Rh1	117.10(7)	C18	C19	C20	120.2(2)
C28	P2	Rh1	119.32(7)	C21	C20	C19	119.9(2)
N1	P2	P1	39.71(6)	C20	C21	C22	119.9(2)
C34	P2	P1	126.17(7)	C21	C22	C17	120.7(2)
C28	P2	P1	126.67(8)	N1	C23	C24	115.85(18)
Rh1	P2	P1	55.085(17)	C23	C24	C25	110.01(19)
F4	P3	F5	92.37(14)	C26	C25	C24	114.1(2)
F4	P3	F6	88.93(13)	C25	C26	C27	113.0(2)
F5	P3	F6	178.68(14)	C29	C28	C33	118.7(2)
F4	P3	F1	90.27(11)	C29	C28	P2	120.77(18)

F5	P3	F1	90.32(11)		C33	C28	P2	120.34(19)
F6	P3	F1	89.43(10)		C30	C29	C28	120.9(2)
F4	P3	F3	178.30(13)		C31	C30	C29	119.8(3)
F5	P3	F3	89.18(12)		C32	C31	C30	120.0(2)
F6	P3	F3	89.52(11)		C31	C32	C33	120.9(3)
F1	P3	F3	90.43(10)		C32	C33	C28	119.8(3)
F4	P3	F2	90.80(11)		C35	C34	C39	119.5(2)
F5	P3	F2	90.53(12)		C35	C34	P2	123.06(17)
F6	P3	F2	89.70(11)		C39	C34	P2	117.49(17)
F1	P3	F2	178.61(13)		C34	C35	C36	119.9(2)
F3	P3	F2	88.48(11)		C37	C36	C35	120.3(2)
C23	N1	P1	126.55(14)		C36	C37	C38	120.2(2)
C23	N1	P2	132.63(15)		C39	C38	C37	119.9(2)
P1	N1	P2	100.53(9)		C38	C39	C34	120.2(2)

Table C13. Hydrogen Atom Coordinates ($\text{\AA} \times 10^4$) and Isotropic Displacement Parameters ($\text{\AA}^2 \times 10^3$) for **2c**.

Atom	x	y	z	U(eq)
H6A	5288	489	617	79
H6B	6889	686	814	79
H6C	5689	807	-166	79
H7A	2189	1049	151	74
H7B	2199	1028	1251	74
H7C	3065	652	836	74
H8A	3151	2294	1866	70
H8B	2356	1816	1915	70
H8C	2152	2066	905	70
H9A	5897	2583	1168	68
H9B	7010	2413	2148	68
H9C	5405	2555	2126	68
H10A	7829	1693	561	76
H10B	8392	1317	1386	76
H10C	8389	1850	1659	76
H12	7848	78	4907	39
H13	6773	-586	5285	48
H14	4560	-827	4305	54

H15	3376	-404	2949	52
H16	4395	282	2595	39
H18	10132	881	3485	40
H19	11737	526	2788	51
H20	10978	-89	1735	49
H21	8631	-368	1426	42
H22	7036	-26	2150	35
H23A	9465	631	5038	31
H23B	8543	861	5664	31
H24A	9881	1547	5777	34
H24B	10784	1327	5120	34
H25A	10809	993	6978	33
H25B	11631	740	6315	33
H26A	12340	1634	7116	43
H26B	13146	1391	6429	43
H27A	13231	1079	8303	55
H27B	14556	1300	8008	55
H27C	13956	804	7609	55
H29	9747	1618	3371	40
H30	11444	2179	3310	51
H31	11136	2934	3759	53
H32	9175	3123	4292	50
H33	7520	2560	4426	39
H35	7527	1494	6009	32
H36	6312	1788	7056	39
H37	4390	2290	6497	40
H38	3676	2512	4886	42
H39	4814	2199	3822	38

Crystal structure information for compound 2d.

Table C14. Fractional Atomic Coordinates ($\times 10^4$) and Equivalent Isotropic Displacement Parameters ($\text{\AA}^2 \times 10^3$) for **2d**. U_{eq} is defined as 1/3 of the trace of the orthogonalised U_{IJ} tensor.

Atom	x	y	z	U(eq)
Rh1	7442.1(2)	2991.1(2)	5119.6(2)	19.37(5)
Cl1	7326.1(4)	3117.6(4)	6438.9(3)	32.77(13)
Cl2	7086.6(10)	-717.0(6)	2680.5(8)	102.5(4)
Cl3	6766.0(8)	-1740.7(7)	1274.9(6)	87.0(3)
P1	8387.5(3)	1896.2(3)	5555.0(3)	18.84(10)
P2	6579.2(3)	1838.8(3)	5009.8(3)	20.66(11)
P3	12078.4(4)	3449.2(4)	5910.2(4)	34.16(14)
F1	11356.0(11)	3150.3(11)	6320.5(10)	56.2(4)
F2	12806.9(11)	3757.1(12)	5506.2(11)	61.9(5)
F3	11305.6(12)	3435.9(14)	5055.7(10)	69.5(6)
F4	12849.0(12)	3426.5(11)	6765.1(10)	60.7(5)
F5	11841.0(13)	4359.9(10)	6048.4(11)	62.2(5)
F6	12316.5(12)	2526.4(11)	5782.2(12)	66.9(5)
N5	7503.5(11)	1244.2(10)	5469.4(10)	20.4(3)
C1	7805.1(16)	4293.5(14)	5110.2(14)	30.7(5)
C2	8278.5(16)	3861.7(14)	4685.4(15)	33.6(5)
C3	7622.2(19)	3457.6(14)	4019.2(14)	36.4(6)
C4	6730.6(17)	3698.8(14)	4017.2(14)	35.9(6)
C5	6835.3(16)	4192.2(14)	4702.5(14)	31.6(5)
C6	8215(2)	4808.7(16)	5835.4(17)	51.6(8)
C7	9289.8(19)	3868.7(19)	4840(2)	58.1(9)
C8	7864(3)	3023.9(19)	3359.6(19)	66.6(10)
C9	5847(2)	3501.3(19)	3373.0(19)	65.3(10)
C10	6104(2)	4605.4(17)	4938(2)	54.2(8)
C11	9065.2(13)	1454.7(12)	4988.5(12)	21.3(4)
C12	8743.8(15)	840.4(13)	4424.2(13)	26.6(4)
C13	9306.2(17)	520.8(14)	4022.0(14)	33.5(5)
C14	10180.4(16)	813.4(14)	4176.3(15)	33.2(5)
C15	10503.3(16)	1426.1(14)	4729.5(15)	32.8(5)
C16	9952.5(14)	1744.8(14)	5137.9(14)	27.4(5)
C17	9221.3(14)	1904.5(13)	6559.7(12)	24.4(4)

C18	9455.1(16)	2625.6(17)	6977.8(15)	37.8(6)
C19	10135.2(19)	2638(2)	7720.3(17)	56.6(8)
C20	10571(2)	1933(2)	8058.1(16)	58.9(9)
C21	10356(2)	1220(2)	7635.6(18)	57.5(8)
C22	9694.1(17)	1205.1(16)	6883.7(15)	39.8(6)
C23	7530.2(13)	435.0(13)	5786.2(12)	22.3(4)
C24	7796.7(17)	333.5(16)	6615.3(14)	36.2(5)
C25	7851(2)	-436.4(18)	6938.5(17)	49.4(7)
C26	7609.0(18)	-1094.7(17)	6439.0(19)	46.7(7)
C27	7315.2(17)	-998.9(15)	5615.8(18)	40.0(6)
C28	7282.0(15)	-228.5(14)	5282.3(14)	28.8(5)
C29	5750.0(14)	1778.3(14)	5533.2(13)	26.3(4)
C30	5530.6(15)	1064.0(16)	5847.2(14)	33.9(5)
C31	4835.7(16)	1062.2(19)	6187.2(15)	42.6(6)
C32	4354.8(17)	1758(2)	6203.6(16)	46.5(7)
C33	4560.7(17)	2464.4(19)	5884.6(18)	47.6(7)
C34	5258.8(16)	2478.0(16)	5555.8(16)	37.6(6)
C35	5967.6(14)	1425.8(13)	4023.0(12)	23.9(4)
C36	5042.5(15)	1233.4(15)	3797.0(14)	33.2(5)
C37	4582.8(17)	978.8(18)	3017.9(15)	43.4(6)
C38	5029.3(18)	915.1(16)	2455.6(14)	41.0(6)
C39	5946.5(18)	1110.2(16)	2668.2(14)	37.4(6)
C40	6410.7(16)	1365.0(15)	3448.2(13)	31.3(5)
C41	7184(3)	-1695(2)	2325(2)	68.5(10)

Table C15. Anisotropic Displacement Parameters ($\text{\AA}^2 \times 10^3$) for **2d**. The Anisotropic displacement factor exponent takes the form: $-2\pi^2[h^2a^*{}^2U_{11} + 2hka^*b^*U_{12} + \dots]$.

Atom	U ₁₁	U ₂₂	U ₃₃	U ₂₃	U ₁₃	U ₁₂
Rh1	20.58(8)	16.89(8)	19.81(8)	0.00(6)	5.39(6)	2.20(6)
Cl1	35.4(3)	40.3(3)	24.8(3)	-5.6(2)	12.9(2)	3.1(2)
Cl2	156.9(12)	50.4(6)	131.3(10)	-14.6(6)	89.7(9)	-10.2(6)
Cl3	113.2(8)	69.5(6)	74.6(6)	14.1(5)	25.5(6)	25.7(6)
P1	18.9(2)	17.8(3)	19.4(2)	-0.54(19)	5.57(18)	1.15(19)
P2	18.7(2)	20.4(3)	23.3(2)	0.6(2)	7.46(19)	1.50(19)
P3	27.8(3)	42.3(4)	29.2(3)	-4.7(3)	4.8(2)	1.0(3)
F1	50.9(10)	67.4(12)	57(1)	2.9(9)	26.9(8)	-4.5(8)

F2	42.6(9)	83.1(14)	67.5(11)	16.6(10)	28.3(9)	8.3(9)
F3	43.3(9)	119.3(17)	35.6(9)	-4.7(10)	-1.5(7)	7.5(10)
F4	54(1)	60.2(12)	45.9(9)	4.8(8)	-14.1(8)	-12.4(9)
F5	86.8(13)	38.8(10)	70.1(12)	5.7(8)	38(1)	12.8(9)
F6	64.3(12)	48.5(11)	85.8(14)	-25.1(10)	21.8(10)	1.9(9)
N5	19.5(8)	17.3(9)	24.2(8)	1.1(7)	6.6(6)	0.1(6)
C1	32.5(12)	18.8(11)	34.7(12)	3.9(9)	2.5(9)	0.5(9)
C2	32.9(12)	22.2(12)	46.4(14)	12.9(10)	13.8(10)	0.4(9)
C3	58.8(16)	22.8(12)	31.7(12)	8.0(9)	20.2(11)	1.8(11)
C4	42.6(14)	24.3(12)	29.9(12)	10.0(9)	-3.4(10)	-0.1(10)
C5	30.7(11)	20.0(11)	40.2(13)	6.2(9)	5.9(10)	5.7(9)
C6	62.7(19)	26.5(14)	49.5(16)	-6.8(12)	-3.8(14)	-6.1(13)
C7	39.2(15)	41.8(17)	99(3)	25.4(17)	30.1(16)	1.6(13)
C8	126(3)	47.0(18)	46.7(17)	7.3(14)	55(2)	-1.1(19)
C9	68(2)	45.0(18)	49.5(17)	12.2(14)	-27.3(15)	-4.5(15)
C10	48.4(17)	32.1(15)	85(2)	9.4(15)	26.3(16)	17.8(13)
C11	22.9(10)	19.7(10)	22.3(9)	1.9(8)	8.7(8)	1.8(8)
C12	27.3(11)	25.0(12)	28.5(11)	-4.2(9)	10.3(9)	-3.3(9)
C13	42.7(13)	27.3(13)	36.4(12)	-9.7(10)	20.9(11)	-3.8(10)
C14	39.0(13)	28.2(13)	42.0(13)	-3.7(10)	26.2(11)	2.4(10)
C15	28.5(11)	30.3(13)	45.2(13)	-3.5(10)	19.8(10)	-3.4(9)
C16	24.7(10)	23.5(11)	35.0(12)	-5.3(9)	11.2(9)	-1.6(8)
C17	23.3(10)	28.4(12)	20.0(9)	0.3(8)	5.0(8)	1.2(8)
C18	30.4(12)	39.9(15)	37.6(13)	-12.0(11)	3.2(10)	2.3(11)
C19	42.6(16)	78(2)	40.0(15)	-30.7(15)	0.7(12)	-1.2(15)
C20	41.3(15)	102(3)	23.1(12)	-0.3(15)	-3.7(11)	4.6(17)
C21	47.4(17)	67(2)	43.1(16)	23.6(15)	-6.1(13)	9.0(15)
C22	38.0(13)	32.2(14)	39.6(14)	6.5(11)	-0.7(11)	3.7(11)
C23	19.9(9)	20.1(11)	27.8(10)	3.5(8)	8.8(8)	1.0(8)
C24	45.9(14)	35.1(14)	29.5(12)	3.2(10)	14.9(10)	-6.1(11)
C25	54.2(17)	48.7(18)	42.2(15)	21.3(13)	11.7(13)	-9.8(14)
C26	37.9(14)	31.8(15)	69.2(19)	24.8(14)	15.8(13)	-1.1(11)
C27	34.1(13)	22.0(12)	68.4(18)	-1.1(12)	22.7(12)	-4.8(10)
C28	27.0(11)	24.9(12)	35.3(12)	-1.0(9)	11.2(9)	-2.6(9)
C29	21.2(10)	32.3(12)	27.2(10)	-1.8(9)	10.2(8)	1.1(8)
C30	26.4(11)	40.6(14)	37.6(13)	8.6(11)	14.4(10)	4(1)

C31	30.5(12)	60.8(18)	40.6(14)	13.5(13)	17.2(11)	0.2(12)
C32	29.6(13)	75(2)	42.1(14)	-5.9(14)	21.4(11)	1.4(13)
C33	32.4(13)	51.2(18)	65.4(18)	-15.8(14)	24.3(13)	4.9(12)
C34	30.8(12)	33.4(14)	53.1(15)	-5.0(11)	19.8(11)	2.5(10)
C35	24.2(10)	20.7(11)	25.3(10)	3.5(8)	6.1(8)	2.1(8)
C36	25.7(11)	41.7(14)	29.6(11)	4.8(10)	5.4(9)	-0.2(10)
C37	28.6(12)	57.1(18)	35.1(13)	6.4(12)	-2.6(10)	-8.8(12)
C38	48.2(15)	40.4(15)	24.2(11)	1.9(10)	-2.1(10)	-8.2(12)
C39	45.9(14)	38.7(15)	27.5(11)	-0.3(10)	11.8(10)	-2.5(11)
C40	29.0(11)	34.9(13)	30.2(11)	-1.8(10)	9.7(9)	-2.4(10)
C41	101(3)	46.0(19)	76(2)	11.9(17)	53(2)	17.8(18)

Table C16. Bond Lengths for **2d**.

Atom	Atom	Length/Å	Atom	Atom	Length/Å
Rh1	C3	2.177(2)	C4	C9	1.500(3)
Rh1	C5	2.217(2)	C5	C10	1.490(3)
Rh1	C4	2.221(2)	C11	C12	1.392(3)
Rh1	C1	2.228(2)	C11	C16	1.398(3)
Rh1	C2	2.229(2)	C12	C13	1.390(3)
Rh1	P1	2.2977(5)	C13	C14	1.379(3)
Rh1	P2	2.2996(6)	C14	C15	1.379(3)
Rh1	Cl1	2.3850(5)	C15	C16	1.383(3)
Cl2	C41	1.757(3)	C17	C18	1.385(3)
Cl3	C41	1.743(4)	C17	C22	1.388(3)
P1	N5	1.7105(17)	C18	C19	1.383(3)
P1	C17	1.814(2)	C19	C20	1.380(5)
P1	C11	1.815(2)	C20	C21	1.375(5)
P1	P2	2.6508(7)	C21	C22	1.382(4)
P2	N5	1.7076(17)	C23	C28	1.382(3)
P2	C29	1.807(2)	C23	C24	1.385(3)
P2	C35	1.813(2)	C24	C25	1.385(4)
P3	F4	1.5836(16)	C25	C26	1.371(4)
P3	F3	1.5844(17)	C26	C27	1.373(4)
P3	F5	1.5876(18)	C27	C28	1.396(3)
P3	F1	1.5920(17)	C29	C30	1.391(3)
P3	F2	1.5974(17)	C29	C34	1.392(3)

P3	F6	1.6029(19)	C30	C31	1.389(3)
N5	C23	1.444(3)	C31	C32	1.376(4)
C1	C2	1.398(3)	C32	C33	1.376(4)
C1	C5	1.448(3)	C33	C34	1.380(3)
C1	C6	1.490(3)	C35	C36	1.394(3)
C2	C3	1.439(4)	C35	C40	1.394(3)
C2	C7	1.500(3)	C36	C37	1.384(3)
C3	C4	1.436(4)	C37	C38	1.379(4)
C3	C8	1.507(4)	C38	C39	1.385(4)
C4	C5	1.417(3)	C39	C40	1.387(3)

Table C17. Bond Angles for **2d**.

Atom	Atom	Atom	Angle/ ^o	Atom	Atom	Atom	Angle/ ^o
C3	Rh1	C5	63.46(9)	C2	C1	Rh1	71.78(13)
C3	Rh1	C4	38.10(10)	C5	C1	Rh1	70.61(12)
C5	Rh1	C4	37.23(9)	C6	C1	Rh1	125.83(17)
C3	Rh1	C1	62.97(9)	C1	C2	C3	108.3(2)
C5	Rh1	C1	38.03(8)	C1	C2	C7	126.6(3)
C4	Rh1	C1	62.55(9)	C3	C2	C7	124.8(3)
C3	Rh1	C2	38.11(9)	C1	C2	Rh1	71.65(13)
C5	Rh1	C2	62.61(9)	C3	C2	Rh1	68.97(13)
C4	Rh1	C2	62.74(9)	C7	C2	Rh1	129.16(17)
C1	Rh1	C2	36.57(9)	C4	C3	C2	107.4(2)
C3	Rh1	P1	108.80(7)	C4	C3	C8	127.5(3)
C5	Rh1	P1	166.31(6)	C2	C3	C8	123.9(3)
C4	Rh1	P1	141.89(7)	C4	C3	Rh1	72.60(13)
C1	Rh1	P1	129.01(6)	C2	C3	Rh1	72.92(13)
C2	Rh1	P1	104.13(6)	C8	C3	Rh1	130.21(18)
C3	Rh1	P2	117.24(7)	C5	C4	C3	108.2(2)
C5	Rh1	P2	122.84(6)	C5	C4	C9	126.1(3)
C4	Rh1	P2	104.67(7)	C3	C4	C9	125.6(3)
C1	Rh1	P2	160.39(6)	C5	C4	Rh1	71.26(13)
C2	Rh1	P2	153.26(7)	C3	C4	Rh1	69.29(12)
P1	Rh1	P2	70.424(19)	C9	C4	Rh1	127.84(18)
C3	Rh1	Cl1	154.00(7)	C4	C5	C1	107.4(2)
C5	Rh1	Cl1	94.79(7)	C4	C5	C10	127.6(2)

C4	Rh1	Cl1	128.63(7)		C1	C5	C10	124.7(2)
C1	Rh1	Cl1	91.20(6)		C4	C5	Rh1	71.51(13)
C2	Rh1	Cl1	120.60(7)		C1	C5	Rh1	71.36(12)
P1	Rh1	Cl1	89.30(2)		C10	C5	Rh1	126.76(18)
P2	Rh1	Cl1	85.94(2)		C12	C11	C16	119.11(19)
N5	P1	C17	112.78(9)		C12	C11	P1	123.02(16)
N5	P1	C11	106.67(9)		C16	C11	P1	117.86(16)
C17	P1	C11	100.24(9)		C13	C12	C11	119.9(2)
N5	P1	Rh1	93.56(6)		C14	C13	C12	120.3(2)
C17	P1	Rh1	119.49(7)		C15	C14	C13	120.3(2)
C11	P1	Rh1	123.69(7)		C14	C15	C16	120.0(2)
N5	P1	P2	39.11(6)		C15	C16	C11	120.4(2)
C17	P1	P2	133.31(7)		C18	C17	C22	119.3(2)
C11	P1	P2	121.28(7)		C18	C17	P1	120.09(17)
Rh1	P1	P2	54.821(16)		C22	C17	P1	120.36(17)
N5	P2	C29	110.73(9)		C19	C18	C17	119.9(3)
N5	P2	C35	109.33(9)		C20	C19	C18	120.5(3)
C29	P2	C35	103.04(10)		C21	C20	C19	119.6(2)
N5	P2	Rh1	93.58(6)		C20	C21	C22	120.2(3)
C29	P2	Rh1	119.53(8)		C21	C22	C17	120.3(3)
C35	P2	Rh1	120.09(7)		C28	C23	C24	120.0(2)
N5	P2	P1	39.19(6)		C28	C23	N5	121.52(18)
C29	P2	P1	131.37(7)		C24	C23	N5	118.5(2)
C35	P2	P1	121.37(7)		C25	C24	C23	119.9(2)
Rh1	P2	P1	54.755(16)		C26	C25	C24	120.1(3)
F4	P3	F3	177.85(12)		C25	C26	C27	120.5(2)
F4	P3	F5	91.09(10)		C26	C27	C28	120.0(2)
F3	P3	F5	90.91(11)		C23	C28	C27	119.5(2)
F4	P3	F1	89.43(10)		C30	C29	C34	119.3(2)
F3	P3	F1	89.79(10)		C30	C29	P2	123.55(17)
F5	P3	F1	89.67(10)		C34	C29	P2	116.96(18)
F4	P3	F2	90.16(10)		C31	C30	C29	119.6(2)
F3	P3	F2	90.64(10)		C32	C31	C30	120.5(3)
F5	P3	F2	89.82(10)		C31	C32	C33	120.2(2)
F1	P3	F2	179.34(11)		C32	C33	C34	119.9(3)
F4	P3	F6	88.45(10)		C33	C34	C29	120.5(3)

F3	P3	F6	89.55(11)	C36	C35	C40	118.7(2)
F5	P3	F6	179.23(11)	C36	C35	P2	121.83(17)
F1	P3	F6	89.71(10)	C40	C35	P2	119.24(16)
F2	P3	F6	90.79(10)	C37	C36	C35	120.1(2)
C23	N5	P2	129.04(13)	C38	C37	C36	120.7(2)
C23	N5	P1	128.92(13)	C37	C38	C39	119.9(2)
P2	N5	P1	101.70(9)	C38	C39	C40	119.6(2)
C2	C1	C5	108.5(2)	C39	C40	C35	121.0(2)
C2	C1	C6	126.5(2)	Cl3	C41	Cl2	111.61(19)
C5	C1	C6	125.0(2)				

Table C18. Torsion Angles for **2d**.

A	B	C	D	Angle/ [°]	A	B	C	D	Angle/ [°]
C2 9	P2	N5	C2 3	42.8(2)	C1 2	C1 3	C1 4	C1 5	-0.1(4)
C3 5	P2	N5	C2 3	-70.04(19)	C1 3	C1 4	C1 5	C1 6	0.6(4)
Rh 1	P2	N5	C2 3	166.31(16)	C1 4	C1 5	C1 6	C1 1	-0.6(4)
P1	P2	N5	C2 3	173.7(2)	C1 2	C1 1	C1 6	C1 5	0.1(3)
C2 9	P2	N5	P1	-130.85(10)	P1 1	C1 6	C1 5		179.41(18)
C3 5	P2	N5	P1	116.29(10)	N5	P1 7	C1 8		-125.16(19)
Rh 1	P2	N5	P1	-7.37(8)	C1 1	P1 7	C1 8		121.76(19)
C1 7	P1	N5	C2 3	-42.2(2)	Rh 1	P1 7	C1 8		-16.8(2)
C1 1	P1	N5	C2 3	66.91(19)	P2	P1 7	C1 8		-84.7(2)
Rh 1	P1	N5	C2 3	-166.31(16)	N5	P1 7	C1 2		61.1(2)
P2	P1	N5	C2 3	-173.7(2)	C1 1	P1 7	C1 2		-52.0(2)
C1	P1	N5	P2	131.51(10)	Rh	P1	C1	C2	169.48(17)

					0	9	4	3	
Rh 1	C1	C5	C4	-62.83(16)	P2	C2 9	C3 4	C3 3	174.6(2)
C2	C1	C5	C1 0	-175.5(2)	N5	P2 5	C3 6	C3 6	124.57(19)
C6	C1	C5	C1 0	1.6(4)	C2 9	P2 5	C3 6	C3 6	6.8(2)
Rh 1	C1	C5	C1 0	122.3(2)	Rh 1	P2 5	C3 6	C3 6	-129.19(17)
C2	C1	C5	Rh 1	62.13(16)	P1	P2 5	C3 6	C3 6	166.14(16)
C6	C1	C5	Rh 1	-120.7(2)	N5	P2 5	C3 0	C4 0	-61.2(2)
N5	P1	C1 1	C1 2	16.5(2)	C2 9	P2 5	C3 0	C4 0	-179.01(18)
C1 7	P1	C1 1	C1 2	134.24(18)	Rh 1	P2 5	C3 0	C4 0	45.0(2)
Rh 1	P1	C1 1	C1 2	-89.58(18)	P1	P2 5	C3 0	C4 0	-19.6(2)
P2	P1	C1 1	C1 2	-23.5(2)	C4 0	C3 5	C3 6	C3 7	0.7(4)
N5	P1	C1 1	C1 6	-162.78(16)	P2	C3 5	C3 6	C3 7	175.0(2)
C1 7	P1	C1 1	C1 6	-45.09(19)	C3 5	C3 6	C3 7	C3 8	-0.3(4)
Rh 1	P1	C1 1	C1 6	91.10(17)	C3 6	C3 7	C3 8	C3 9	-0.3(4)
P2	P1	C1 1	C1 6	157.20(14)	C3 7	C3 8	C3 9	C4 0	0.3(4)
C1 6	C1 1	C1 2	C1 3	0.4(3)	C3 8	C3 9	C4 0	C3 5	0.2(4)
P1	C1 1	C1 2	C1 3	-178.90(18)	C3 6	C3 5	C4 0	C3 9	-0.7(4)
C1 1	C1 2	C1 3	C1 4	-0.4(4)	P2	C3 5	C4 0	C3 9	-175.07(19)

Table C19. Hydrogen Atom Coordinates ($\text{\AA} \times 10^4$) and Isotropic Displacement Parameters ($\text{\AA}^2 \times 10^3$) for **2d**.

Atom	x	y	z	U(eq)
H6A	8859	4665	6087	77
H6B	7887	4722	6222	77
H6C	8167	5379	5674	77
H7A	9450	4333	4565	87
H7B	9471	3368	4634	87
H7C	9609	3910	5422	87
H8A	7307	2808	2965	100
H8B	8284	2579	3594	100
H8C	8157	3403	3091	100
H9A	5349	3512	3604	98
H9B	5887	2961	3156	98
H9C	5728	3901	2938	98
H10A	6107	5184	4819	81
H10B	6216	4529	5517	81
H10C	5510	4374	4632	81
H12	8141	640	4314	32
H13	9088	99	3640	40
H14	10562	592	3900	40
H15	11104	1629	4830	39
H16	10179	2164	5522	33
H18	9149	3111	6755	45
H19	10304	3135	8000	68
H20	11018	1941	8579	71
H21	10663	736	7862	69
H22	9562	714	6587	48
H24	7942	791	6961	43
H25	8057	-508	7507	59
H26	7645	-1621	6664	56
H27	7135	-1457	5274	48
H28	7090	-161	4713	35
H30	5854	580	5829	41
H31	4691	577	6410	51
H32	3879	1751	6436	56

H33	4223	2942	5891	57
H34	5405	2968	5343	45
H36	4727	1277	4178	40
H37	3953	847	2869	52
H38	4708	738	1923	49
H39	6256	1070	2282	45
H40	7040	1500	3593	38
H41A	7833	-1861	2515	82
H41B	6840	-2079	2551	82

Appendix D

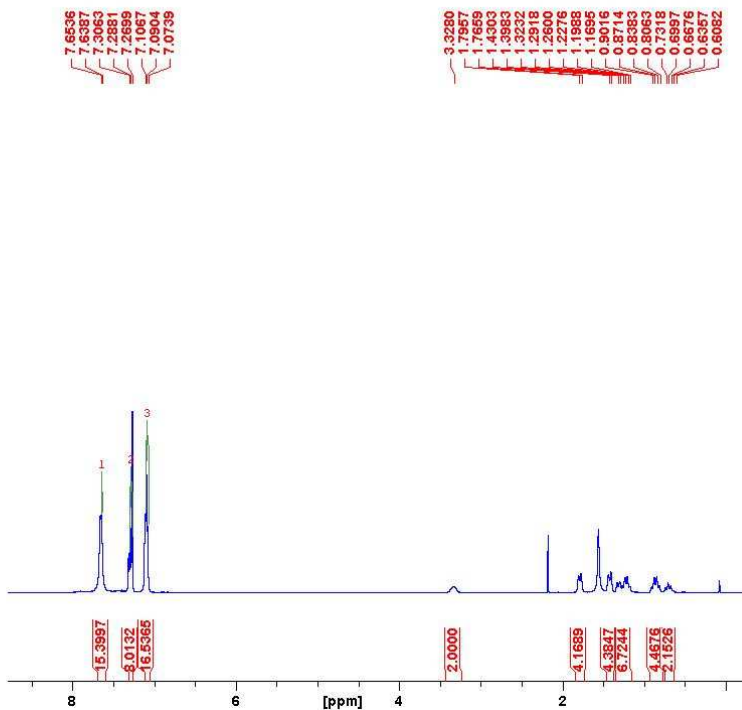


Figure D1. ¹H NMR of $[(\text{Ph}_2\text{PN}(\text{C}_6\text{H}_{11})\text{PPh}_2)_2\text{Ru}(\text{Cl})_2]$ (a).

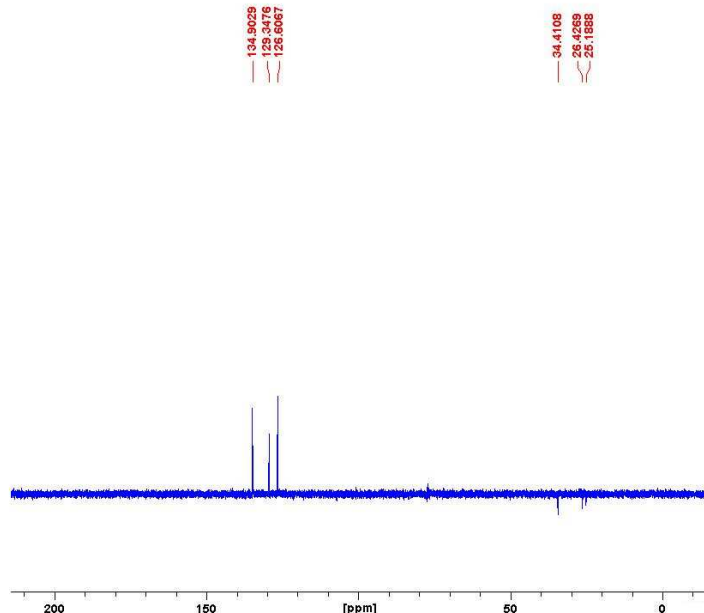


Figure D2. ¹³C NMR $[(\text{Ph}_2\text{PN}(\text{C}_6\text{H}_{11})\text{PPh}_2)_2\text{Ru}(\text{Cl})_2]$ (a).



Figure D3. ^{31}P NMR of $[(\text{Ph}_2\text{PN}(\text{C}_6\text{H}_{11})\text{PPh}_2)_2\text{Ru}(\text{Cl})_2]$ (a).

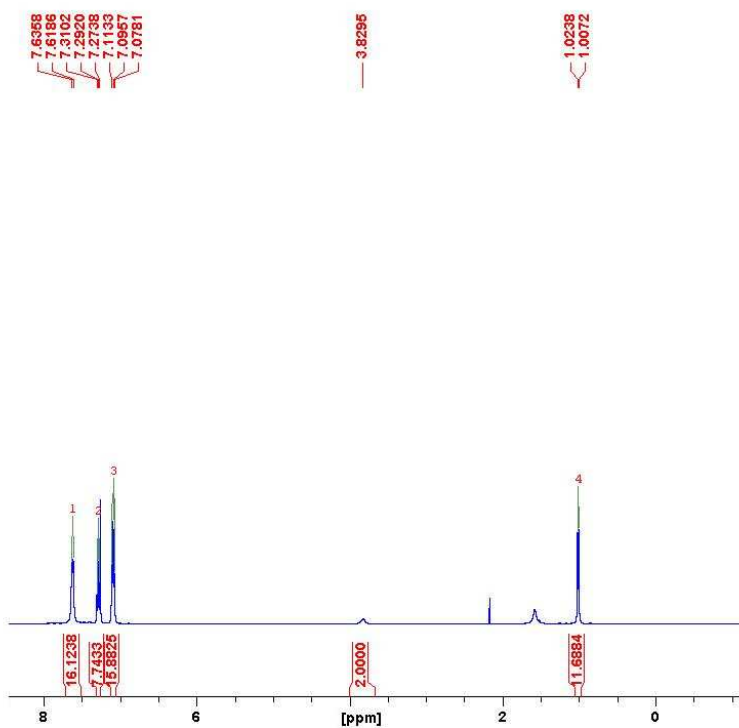


Figure D4. ¹H NMR of $[(\text{Ph}_2\text{PN}(\text{C}_3\text{H}_7)\text{PPh}_2)_2\text{Ru}(\text{Cl})_2]$ (**b**).

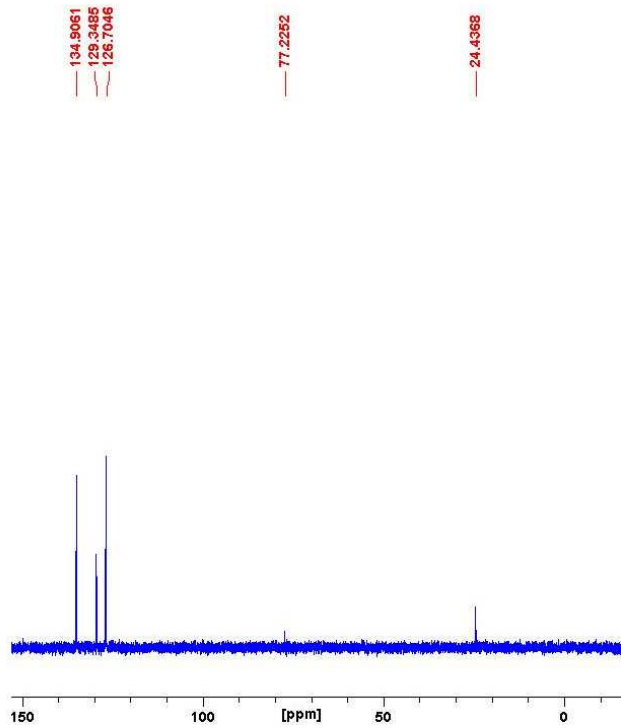


Figure D5. ¹³C NMR $[(\text{Ph}_2\text{PN}(\text{C}_3\text{H}_7)\text{PPh}_2)_2\text{Ru}(\text{Cl})_2]$ (**b**).

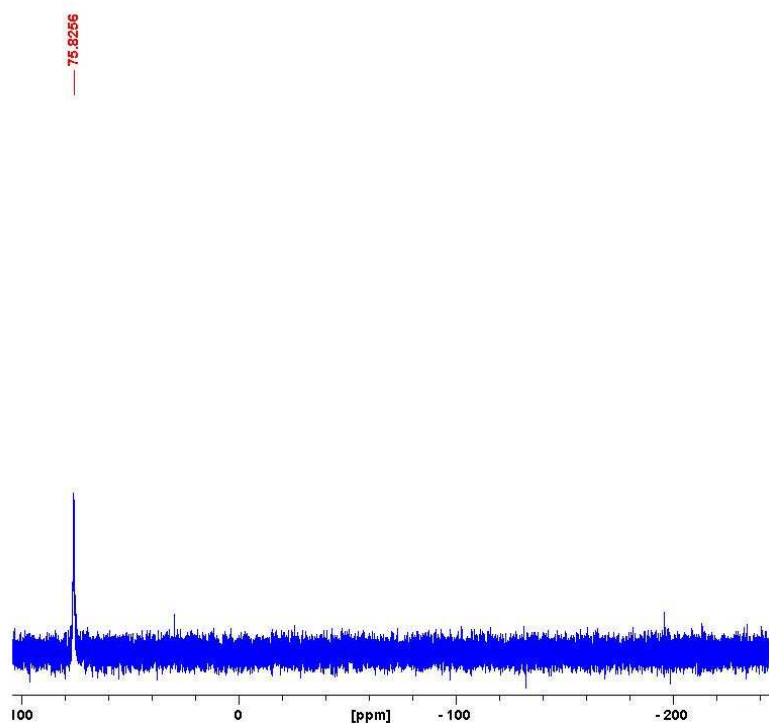


Figure D6. ^{31}P NMR of $[(\text{Ph}_2\text{PN}(\text{C}_3\text{H}_7)\text{PPh}_2)_2\text{Ru}(\text{Cl})_2]$ (b).

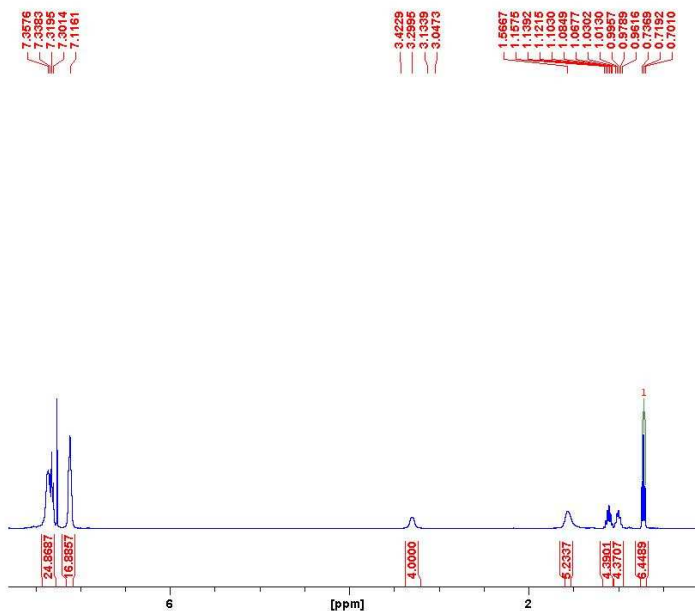


Figure D7. ^1H NMR of $[(\text{Ph}_2\text{PN}(\text{C}_3\text{H}_7)\text{PPh}_2)_2\text{Ru}(\text{Cl})_2]$ (c).

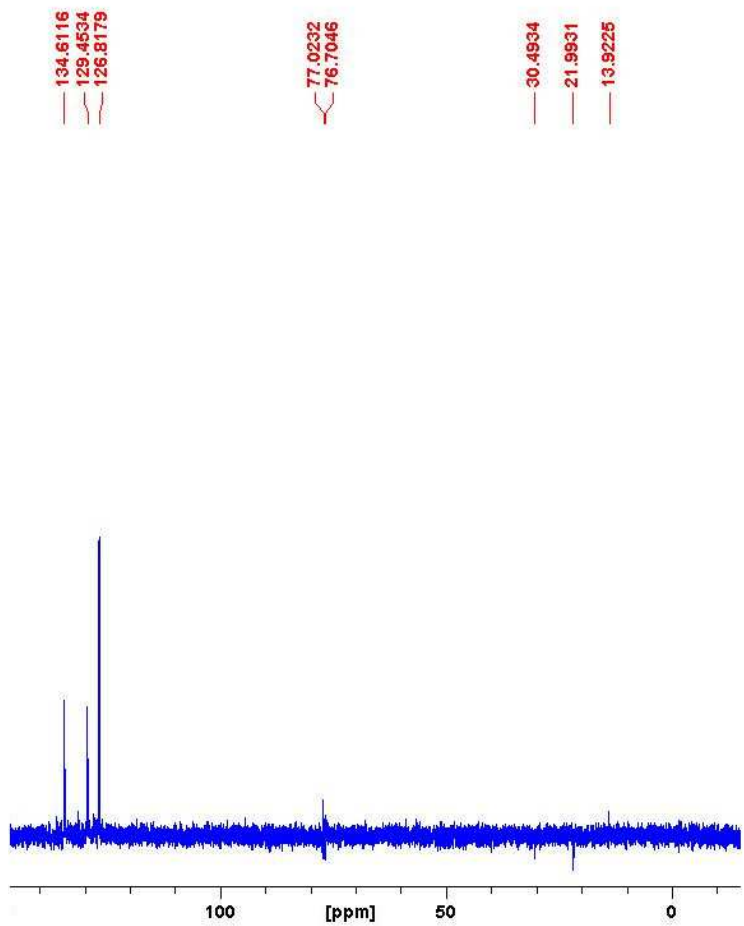


Figure D8. ^{13}C NMR $[(\text{Ph}_2\text{PN}(\text{C}_3\text{H}_7)\text{PPh}_2)_2\text{Ru}(\text{Cl})_2]$ (c).

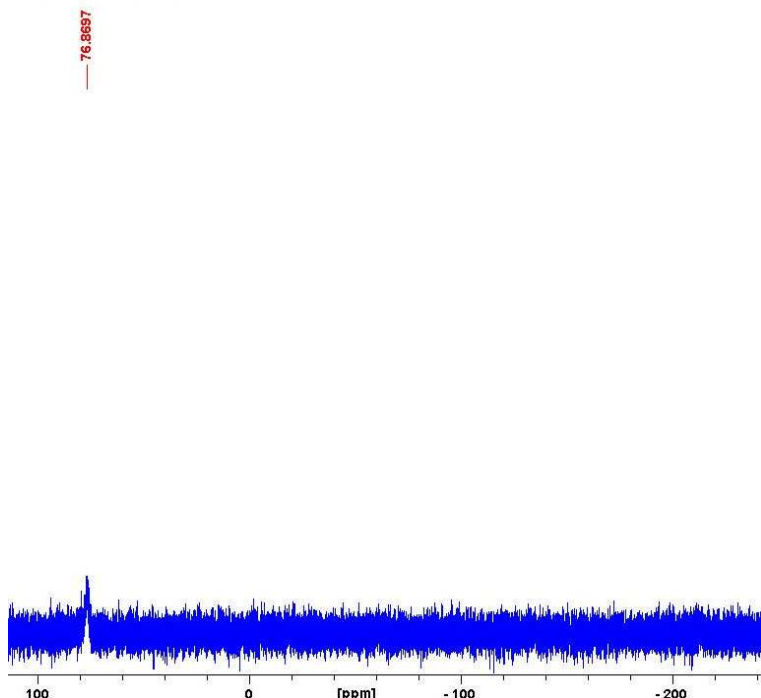
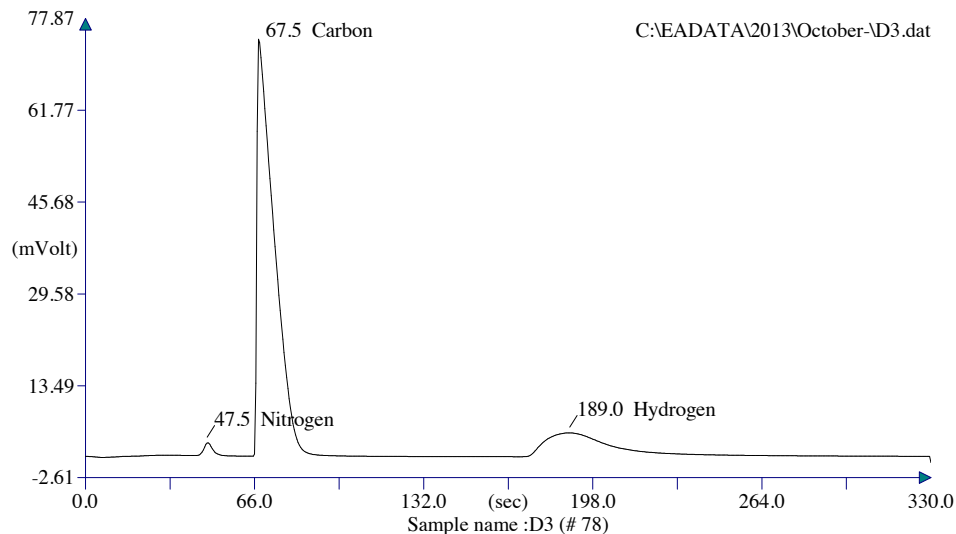
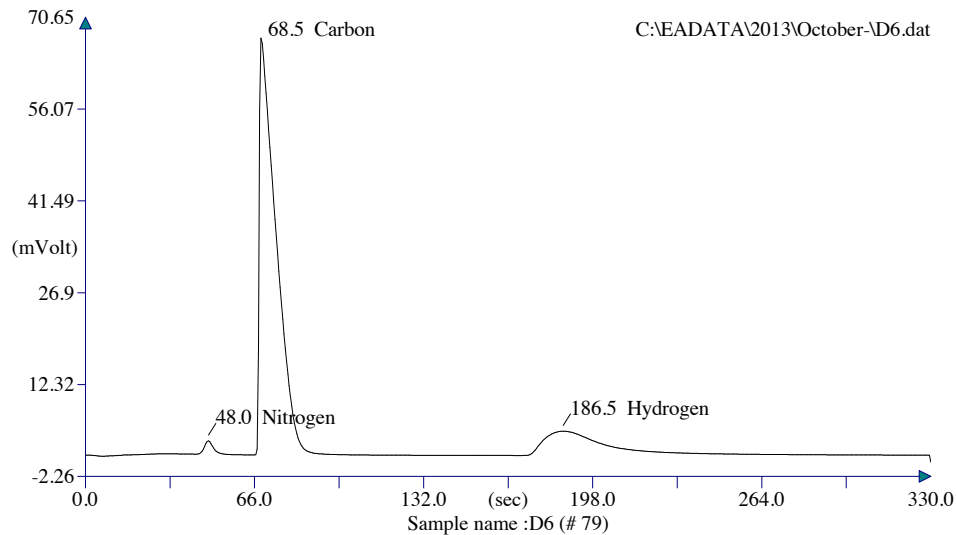


Figure D9. ^{31}P NMR of $[(\text{Ph}_2\text{PN}(\text{C}_3\text{H}_7)\text{PPh}_2)_2\text{Ru}(\text{Cl})_2]$ (c).



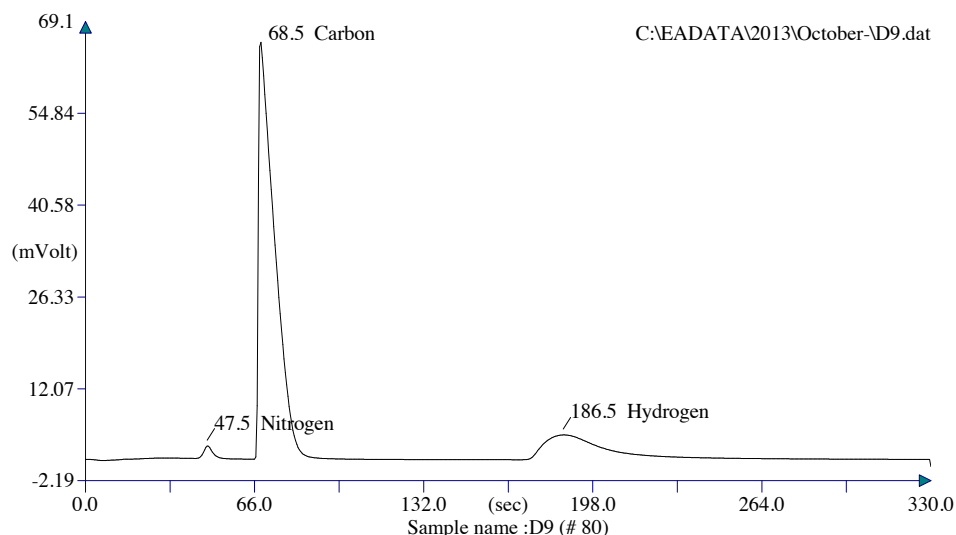
Retention Time (min)	Element Name	Element %
0 . 792	Nitrogen	2 . 497
1 . 125	Carbon	64 . 979
3 . 150	Hydrogen	5 . 192
		72 . 667

Figure D10. Elemental Analyses of $[(\text{Ph}_2\text{PN}(\text{C}_6\text{H}_{11})\text{PPh}_2)_2\text{Ru}(\text{Cl})_2]$ (a).



Retention Time (min)	Element Name	Element %
0 . 800	Nitrogen	2 . 664
1 . 142	Carbon	63 . 309
3 . 108	Hydrogen	4 . 974
		70 . 948

Figure D11. Elemental Analyses of $[(\text{Ph}_2\text{PN}(\text{C}_3\text{H}_7)\text{PPh}_2)_2\text{Ru}(\text{Cl})_2]$ (b).



Retention Time (min)	Element Name	Element %
0.792	Nitrogen	2.557
1.142	Carbon	64.210
3.108	Hydrogen	5.354
<hr/>		
<hr/> <hr/> <hr/> 72.120		

Figure D12. Elemental Analyses of $[(\text{Ph}_2\text{PN}(\text{C}_3\text{H}_7)\text{PPh}_2)_2\text{Ru}(\text{Cl})_2]$ (c).

Crystal structure information for compound a.

Table D1. Fractional Atomic Coordinates ($\times 10^4$) and Equivalent Isotropic Displacement Parameters ($\text{\AA}^2 \times 10^3$) for 1. U_{eq} is defined as 1/3 of the trace of the orthogonalised U_{II} tensor.

Atom	x	y	z	U(eq)
C1	9232(9)	982(7)	2472(6)	33.2(17)
C2	9161(11)	3111(9)	8095(8)	45(2)
C3	10763(14)	2722(13)	1438(11)	71(4)
C4	9989(9)	2517(7)	6751(6)	27.6(15)
C5	8801(10)	2629(9)	5931(7)	40.8(19)
C6	10160(14)	3099(11)	2087(13)	73(4)
C7	10134(10)	2739(8)	7828(7)	34.9(17)
C8	3721(11)	220(9)	2351(8)	44(2)
C9	4503(11)	133(10)	3362(9)	46(2)
C10	9917(11)	659(10)	1851(8)	42(2)
C11	5901(10)	45(8)	3630(7)	37.3(18)

C12	5719(10)	214(9)	1824(7)	37.7(18)
C13	6515(8)	88(7)	2852(6)	27.4(15)
C14	7830(12)	3017(10)	6194(9)	50(2)
C15	10655(11)	1496(11)	1327(8)	52(2)
C16	9392(12)	2238(9)	2602(10)	52(2)
C17	8017(12)	3244(9)	7278(9)	48(2)
C18	4315(11)	265(10)	1563(8)	49(2)
C19	14038(10)	3841(8)	6211(7)	36.8(18)
C20	12482(11)	4798(8)	6392(7)	38.0(18)
C21	13608(12)	6005(8)	6393(8)	47(2)
C22	15177(11)	5051(10)	6244(7)	47(2)
C23	14986(12)	6152(9)	6350(8)	53(3)
C24	6308(9)	-2694(8)	1477(6)	30.4(16)
C25	4643(9)	-3124(9)	1399(7)	36.3(18)
C26	6496(11)	-2206(8)	485(6)	36.2(18)
C27	12655(8)	3685(7)	6297(6)	28.2(15)
C28	5093(11)	-3219(9)	-636(7)	43(2)
C29	3294(11)	-4095(9)	256(8)	45(2)
C30	3460(11)	-3563(10)	-705(8)	47(2)
Cl1	12068(2)	841.8(18)	4362.8(15)	28.5(4)
N1	7674(7)	-1705(6)	2594(5)	24.1(12)
P1	8308(2)	-75.7(17)	3222.4(15)	23.2(4)
P2	11221(2)	2064.3(17)	6317.3(14)	21.9(4)
Ru1	10000	0	5000	21.8(2)

Table D2. Anisotropic Displacement Parameters ($\text{\AA}^2 \times 10^3$) for 1. The Anisotropic displacement factor exponent takes the form: $-2\pi^2[h^2a^{*2}U_{11} + 2hka^{*}b^{*}U_{12} + \dots]$.

Atom	U ₁₁	U ₂₂	U ₃₃	U ₁₂	U ₁₃	U ₂₃
C1	33(4)	30(4)	29(4)	10(3)	13(3)	10(3)
C2	45(5)	48(5)	43(5)	19(4)	28(4)	8(4)
C3	52(6)	77(8)	79(8)	21(6)	31(6)	57(7)
C4	25(3)	25(3)	33(4)	13(3)	15(3)	2(3)
C5	37(5)	49(5)	34(5)	25(4)	10(4)	9(4)
C6	48(6)	39(6)	127(12)	16(5)	37(7)	46(7)
C7	33(4)	35(4)	28(4)	16(3)	8(3)	3(3)
C8	32(4)	44(5)	58(6)	21(4)	16(4)	21(4)
C9	38(5)	57(6)	61(6)	32(4)	29(5)	26(5)
C10	36(5)	43(5)	36(5)	15(4)	13(4)	9(4)
C11	33(4)	46(5)	38(5)	24(4)	16(4)	13(4)
C12	33(4)	47(5)	37(4)	23(4)	14(4)	14(4)
C13	20(3)	27(3)	35(4)	15(3)	8(3)	7(3)
C14	46(5)	69(6)	51(6)	46(5)	17(5)	19(5)
C15	35(5)	73(7)	46(6)	21(5)	23(4)	27(5)
C16	40(5)	41(5)	81(7)	21(4)	31(5)	23(5)
C17	45(5)	46(5)	63(6)	27(4)	30(5)	11(4)
C18	38(5)	49(5)	45(5)	24(4)	0(4)	11(4)
C19	40(5)	28(4)	26(4)	11(4)	8(3)	3(3)
C20	48(5)	37(4)	32(4)	21(4)	20(4)	16(5)
C21	55(6)	26(4)	41(5)	9(4)	15(4)	10(4)
C22	32(4)	53(5)	34(5)	6(4)	13(4)	13(4)
C23	54(6)	36(5)	33(5)	-3(4)	16(4)	10(4)
C24	26(4)	36(4)	23(4)	14(3)	8(3)	7(3)
C25	26(4)	41(5)	32(4)	14(3)	8(3)	5(3)
C26	43(5)	39(4)	23(4)	21(4)	11(3)	8(3)
C27	22(3)	31(4)	20(3)	11(3)	4(3)	2(3)
C28	43(5)	40(5)	31(4)	18(4)	8(4)	3(4)
C29	30(4)	44(5)	42(5)	14(4)	3(4)	2(4)
C30	37(5)	50(5)	31(4)	16(4)	1(4)	4(4)
Cl1	19.2(8)	38.0(9)	29.3(9)	14.0(7)	12.9(7)	9.0(7)
N1	20(3)	28(3)	21(3)	13(2)	6(2)	6(2)
P1	19.5(8)	24.9(8)	23.6(9)	11.4(7)	8.2(7)	6.0(7)

P2	19.5(8)	25.1(8)	21.6(9)	12.9(7)	7.9(7)	5.6(
Ru1	16.3(4)	27.7(4)	22.2(4)	11.9(3)	8.9(3)	5.8(

Table D3. Bond lengths for a.

Atom	Atom	Length/ \AA	Atom	Atom	Length/ \AA
C1	C10	1.388(12)	C19	C22	1.370(12)
C1	C16	1.392(12)	C19	C27	1.406(11)
C1	P1	1.825(8)	C20	C21	1.377(12)
C2	C7	1.392(12)	C20	C27	1.391(11)
C2	C17	1.380(14)	C21	C23	1.380(15)
C3	C6	1.374(19)	C22	C23	1.388(15)
C3	C15	1.378(17)	C24	C25	1.524(11)
C4	C5	1.397(11)	C24	C26	1.537(11)
C4	C7	1.385(11)	C24	N1	1.521(9)
C4	P2	1.814(7)	C25	C29	1.531(11)
C5	C14	1.398(12)	C26	C28	1.541(11)
C6	C16	1.393(15)	C27	P2	1.832(8)
C8	C9	1.352(13)	C28	C30	1.516(14)
C8	C18	1.390(14)	C29	C30	1.515(14)
C9	C11	1.413(11)	Cl1	Ru1	2.4204(18)
C10	C15	1.374(13)	N1	P1	1.724(6)
C11	C13	1.393(11)	N1	P2 ¹	1.726(6)
C12	C13	1.395(11)	P1	P2 ¹	2.665(3)
C12	C18	1.397(12)	P1	Ru1 ¹	2.373(2)
C13	P1	1.843(7)	P2	Ru1	2.338(2)
C14	C17	1.379(14)			
¹ 2-X,-Y,1-Z					

Table D4. Bond Angles for a.

Atom	Atom	Atom	Angle/°	Atom	Atom	Atom	Angle/°
C16	C1	C10	117.3(8)	C29	C30	C28	108.6(8)
P1	C1	C10	123.9(7)	P1	N1	C24	131.6(5)
P1	C1	C16	118.6(7)	P2 ¹	N1	C24	126.4(5)
C17	C2	C7	120.0(9)	P2 ¹	N1	P1	101.1(3)
C15	C3	C6	119.6(10)	C13	P1	C1	98.8(4)
C7	C4	C5	118.2(7)	N1	P1	C1	108.8(3)
P2	C4	C5	117.2(6)	N1	P1	C13	107.9(3)
P2	C4	C7	124.5(6)	P2 ¹	P1	C1	123.1(3)
C14	C5	C4	121.3(8)	P2 ¹	P1	C13	131.1(2)
C16	C6	C3	120.7(11)	P2 ¹	P1	N1	39.46(19)
C4	C7	C2	120.8(8)	Ru1 ¹	P1	C1	118.5(3)
C18	C8	C9	120.1(9)	Ru1 ¹	P1	C13	127.5(3)
C11	C9	C8	121.2(9)	Ru1 ¹	P1	N1	94.4(2)
C15	C10	C1	122.6(10)	Ru1 ¹	P1	P2 ¹	54.94(5)
C13	C11	C9	119.5(8)	C27	P2	C4	100.4(3)
C18	C12	C13	121.1(8)	N1 ¹	P2	C4	107.9(3)
C12	C13	C11	118.5(7)	N1 ¹	P2	C27	105.5(3)
P1	C13	C11	118.0(6)	P1 ¹	P2	C4	123.0(3)
P1	C13	C12	123.4(6)	P1 ¹	P2	C27	128.4(2)
C17	C14	C5	118.9(9)	P1 ¹	P2	N1 ¹	39.41(19)
C10	C15	C3	119.4(11)	Ru1	P2	C4	119.2(2)
C6	C16	C1	120.3(11)	Ru1	P2	C27	126.5(2)
C14	C17	C2	120.6(8)	Ru1	P2	N1 ¹	95.6(2)
C12	C18	C8	119.4(9)	Ru1	P2	P1 ¹	56.18(5)
C27	C19	C22	120.9(9)	Cl1 ¹	Ru1	Cl1	180.0
C27	C20	C21	121.7(9)	P1 ¹	Ru1	Cl1	95.41(6)
C23	C21	C20	120.2(9)	P1 ¹	Ru1	Cl1 ¹	84.59(6)
C23	C22	C19	120.8(9)	P1	Ru1	Cl1	84.59(6)
C22	C23	C21	119.0(8)	P1	Ru1	Cl1 ¹	95.41(6)
C26	C24	C25	111.6(7)	P1	Ru1	P1 ¹	180.0
N1	C24	C25	113.7(6)	P2	Ru1	Cl1	91.74(6)
N1	C24	C26	112.3(6)	P2	Ru1	Cl1 ¹	88.26(6)
C29	C25	C24	112.5(7)	P2 ¹	Ru1	Cl1 ¹	91.74(6)
C28	C26	C24	111.3(7)	P2 ¹	Ru1	Cl1	88.26(6)

C20	C27	C19	117.2(7)	P2 ¹	Ru1	P1 ¹	111.12(6)
P2	C27	C19	119.0(6)	P2	Ru1	P1 ¹	68.88(6)
P2	C27	C20	123.7(6)	P2	Ru1	P1	111.12(6)
C30	C28	C26	113.1(8)	P2 ¹	Ru1	P1	68.88(6)
C30	C29	C25	113.0(8)	P2 ¹	Ru1	P2	180.0

¹2-X,-Y,1-Z

Table D5. Hydrogen Atom Coordinates ($\text{\AA} \times 10^4$) and Isotropic Displacement Parameters ($\text{\AA}^2 \times 10^3$) for a.

Atom	x	y	z	U(eq)
H2	9250(110)	3210(90)	8810(80)	40(30)
H3	11290(140)	3270(120)	1020(100)	90(40)
H5	8660(90)	2480(70)	5140(70)	25(19)
H6	10190(140)	3850(120)	2130(90)	70(40)
H7	10860(90)	2710(70)	8430(60)	30(20)
H8	2740(130)	230(100)	2140(90)	60(30)
H9	4060(130)	110(110)	3920(90)	70(30)
H10	9810(100)	40(80)	1800(70)	20(20)
H11	6500(100)	-30(80)	4390(70)	40(20)
H12	6110(130)	260(100)	1260(90)	70(30)
H14	7050(140)	3100(110)	5600(90)	80(40)
H15	11130(140)	1220(110)	900(100)	80(40)
H16	8950(100)	2500(80)	3020(70)	40(20)
H17	7360(120)	3590(90)	7450(80)	50(30)
H18	3740(110)	200(90)	880(80)	40(30)
H19	14050(90)	3150(70)	6080(60)	19(19)
H20	11590(110)	4740(90)	6490(70)	40(30)
H21	13550(130)	6790(110)	6510(90)	70(30)
H22	16080(100)	5120(70)	6150(60)	30(20)
H23	15730(110)	6990(90)	6300(70)	40(20)
H24	6480(90)	-3490(70)	1430(60)	30(20)
H25a	4590(80)	-3590(70)	2070(60)	17(17)
H25b	4590(90)	-2350(70)	1550(60)	20(18)
H26a	6390(100)	-1500(80)	620(60)	30(20)
H26b	7620(130)	-2020(100)	480(80)	60(30)

H28a	5290(110)	-2830(90)	-1220(80)	40(20)
H28b	5100(120)	-4010(110)	-790(80)	60(30)
H29a	3320(120)	-4980(100)	120(80)	50(30)
H29b	2390(130)	-4220(100)	200(80)	60(30)
H30a	3410(120)	-2670(100)	-670(80)	60(30)
H30b	2550(130)	-4160(110)	-1500(90)	70(30)